UNIVERSITY OF LONDON

Dual-fuel Combustion Phenomena

by

Muhammad Osman Khan,
M.Sc.(Eng.), D.I.C., B.E., G.I.Mech.E., A.M.Inst.F.

A Thesis submitted for the Degree of
Doctor of Philosophy in the Faculty of Engineering

Department of Mechanical Engineering
IMPERIAL COLLEGE OF SCIENCE AND TECHNOLOGY
London, S.W. 7

November 1969

ACKNOWLEDGEMENTS

I wish to express my deepest gratitude to my supervisor, Mr. N.P.W. Moore, for his guidance, help and encouragement.

My sincere thanks go also to Professor G.A. Karim of the University of Calgary for his supervision in the initial stages of this investigation.

The financial assistance offered by the Burmah Oil Company (Pakistan Trading) Ltd., in the form of an external scholarship, is gratefully acknowledged.

My thanks to Mr. George Lewis and his colleagues of the Internal Combustion Engines Laboratories for their technical assistance.

I would like to express my sincere thanks to all my research colleagues who made my stage in this College most pleasant.

I am indebted to my parents for their extra-ordinary patience and encouragement throughout my career, particularly during my stay in this country.

M.O.K.

A B S T R A C T

The combustion processes in a dual-fuel engine are at first examined through the computation and analysis of effective rates of combustion heat release. An examination of a large number of heat release records, covering a wide range of pilot and gaseous fuelling rates, suggests that in dual-fuel engines the combustion generally appears to undergo two distinct phases; the first is associated with the consumption of the pilot and some gaseous fuel, while the second is dependent on the concentration and quality of the gaseous fuel employed. Under light audible knock the rates of burning are excessively high and project well over the second phase. This is indirectly indicative of the autoignition nature of knock and the simultaneous rapid burning of the pilot together with a substantial fraction of the gaseous charge.

Details are provided of a generalised computer programme developed in Fortran IV, which is workable for the computations of rates of heat release for dual-fuel, diesel, gas and motored autoigniting engine. Errors normally associated with the computations of apparent rates of combustion heat release are examined systematically and suggestions for their improvement are made. A comparative study of dual-fuel engine combustion processes is made by collating heat release records of various principles of reciprocating engine operation.

It is shown that the thermodynamic analysis of the autoignition processes in a motored engine of propane-, n-heptane-air mixtures and the blends of propane and methane with n-heptane yields quantitative information which provides better understanding of the dual-fuel combustion phenomena as encountered in engines. The implications and significance of these findings are fully discussed with direct reference to knock reactions.

It is demonstrated that gross chemical kinetic data of the self-ignition of n-heptane and propane in air together with the role of the presence of a higher hydrocarbon vapour such as n-heptane with methane and propane

can be obtained using a motored engine. These data are shown to characterise the dual-fuel combustion phenomena.

Finally, a possibility is explored for a simplified model to explain on a qualitative basis the mechanisms in dual-fuel engines under normal and knocking combustion.

C O N T E N T S

		PAGE
TITLE		1
ACKNOWLEDGEMENTS		2
ABSTRACT		3
CHAPTER 0: INTRODUCTION		10
0.1	Dual-fuel Engine as a Prime Mover	10
0.2	The Development of Dual-fuel Engines	11
0.3	Scope of Present Work	15
	0.3-1 Objectives	15
	0.3-2 Approach	15
0.4	Outline of the Thesis	16
CHAPTER A0: INTRODUCTION TO PART A		18
A0.1	Motivation	18
A0.2	Present Contribution	19
A0.3	Outline of Part A	20
CHAPTER A1: APPARATUS AND EXPERIMENTAL PROCEDURE FOR DUAL-FUEL ENGINE TRIALS		21
A1.1	Introduction	21
A1.2	Apparatus	21
	A1.2-1 The engine and the test bed	21
	A1.2-2 Air and fuel flow measuring system	23
	A1.2-3 Electronic measuring instruments	24
	A1.2-3a Pressure transducer	24
	A1.2-3b Injector needle lift indicator	25
	A1.2-3c Electromagnetic pick-up for crank rotation	26
	A1.2-3d The Cathode Ray Oscilloscope	26
A1.3	Experimental Procedure	27

		PAGE
CHAPTER A2: COMPUTING PROCEDURE AND RESULTS		45
A2.1	Purpose of the Chapter	45
A2.2	Computing Procedure	45
	A2.2-1 Introduction	45
	A2.2-2 The calculation of effective rate of heat release, etc.	46
	A2.2-3 The computer programme	48
A2.3	Presentation of Results	51
	A2.3-1 Rate of heat release records of a dual-fuel engine	51
	A2.3-2 Typical heat release records of diesel, gas and motored engine operation	52
	A2.3-3 Heat release records of stratified charge combustion	53
CHAPTER A3: ERROR ANALYSIS OF HEAT RELEASE COMPUTATIONS		79
A3.0	Introduction	79
A3.1	Purpose of the Chapter	79
A3.2	The Type of Errors Considered	80
A3.3	Presentation of Error Analysis	81
	A3.3-1 Methodical errors	81
	A3.3-1a Method of derivation of rate of heat release equation	81
	A3.3-1b Calculation of gas temperature	82
	A3.3-1c Rate of heat transfer calculation	83
	A3.3-1d Assessment of progress of reactions	85
	A3.3-1e Variability of thermodynamic properties of the working system	87
	A3.3-1f Accounting for dissociation	88
	A3.3-1g Step length	89
	A3.3-1h Initial and boundary conditions	89
	A3.3-2 Instrumental errors	91
	A3.3-2a Pressure measuring instruments	91
	A3.3-2b Recording of crank rotation	93
	A3.3-2c Air and fuel flow measurement	94
	A3.3-2d Speed measurement	95

		PAGE
	A3.3-3 Computational errors	95
	A3.3-3a Data smoothing	96
	A3.3-3b Computation of rate of pressure rise	96
	A3.3-3c Smoothing of rate of pressure rise	97
	A3.3-4 Observational errors	97
	A3.3-5 Reliance on design parameters	98
	A3.3-5a Compression ratio	98
	A3.3-5b Connecting rod - crank throw ratio	98
	A3.3-5c Angular twist	99
A3.4	Discussion	99
A3.5	Conclusions	101
CHAPTER A4: DISCUSSION OF RESULTS AND CONCLUSIONS		126
A4.1	Introduction	126
A4.2	Discussion of Results	126
A4.3	Conclusions	132
CHAPTER B0: INTRODUCTION TO PART B		134
B0	Introduction	134
B0.1	Motivation	134
B0.2	Literature Survey	136
B0.3	Present Contribution	141
B0.4	Outline of Part B	142
CHAPTER B1: APPARATUS AND EXPERIMENTAL PROCEDURE		144
B1.1	Apparatus	144
	B1.1-1 The engine	144
	B1.1-2 Air and fuel flow measuring system	145
	B1.1-3 Electronic measuring instruments	145
	B1.1-3a Cylinder gas pressure measurement	145
	B1.1-3b Recording of crank rotation	148
	B1.1-3c The Cathode Ray Oscilloscope	148
B1.2	Experimental procedure	149

		PAGE
CHAPTER B2: COMPUTING PROCEDURE AND RESULTS		169
B2.1	Introduction	169
B2.2	Computing Procedure	169
	B2.2-1 Introduction	169
	B2.2-2 The derivation of overall combustion kinetic data from combustion heat release	171
B2.3	Presentation of Results	173
	B2.3-1 Results of the computed rates of heat release during autoignition	173
	B2.3-2 Results of the computed overall combustion kinetics of autoignition	175
CHAPTER B3: DISCUSSION AND CONCLUSIONS		217
B3.1	Discussion on heat release variation due to autoignition	217
	B3.1-1 Propane as a fuel	217
	B3.1-2 n-heptane as a fuel	220
	B3.1-3 Propane-n-heptane mixtures as a fuel	223
	B3.1-4 Methane-n-heptane mixtures as a fuel	224
B3.2	Discussion on Overall Combustion Kinetics	225
B3.3	Conclusions	229
CHAPTER C1: GENERAL DISCUSSION AND CONCLUSIONS		231
C1.0	Introduction	231
C1.1	Dual-fuel combustion phenomena in engines	232
	C1.1-1 'Normal' combustion processes	232
	C1.1-2 Knocking combustion processes	235
C1.2	Consideration of a Simplified Model	236
C1.3	Recommendations for Future Work	241
APPENDICES		245
I	Theory of Viscous Flow Air Meter	245
II	Theory of choked nozzle flow	246
III	Typical composition of fuels and diluent used	248
IV	Derivation of differential form of rate of heat release equation	250
V	Derivation of finite difference form of rate of heat release equation	252

		PAGE
VI	The computer programme	254
VII	Theory of smoothing of data scatter	272
VIII	The Simpson's rule of integration for evaluating cumulative heat release	274
IX	Evaluation of composition of products	275
X	Evaluation of pressure-rate by empirical differentiation	277
XI	List of symbols and abbreviations	278
XII	References	280
XIII	Publications	290

0. INTRODUCTION

0.1 Dual-fuel Engine as a Prime Mover

Any emphasis on the efficient utilisation of gaseous fuels, whether from natural or industrial sources, for power production in relatively small units, will focus attention on the dual-fuel engine as a prime mover. Under dual-fuel operation the primary fuel is normally gaseous at atmospheric temperatures and pressures, and in the case of Liquified Natural Gas ought to be evaporated with exhaust heat. In the four-stroke engines it is either inducted with the air charge or, in the case of large engines, introduced into the engine cylinder under positive pressure during ~~compression~~ induction stroke. Also, during this stroke at some point near to top-dead-centre position, a small charge of liquid fuel is injected through the conventional diesel fuel system to act as a source of ignition for the main charge. Power output is controlled by changing the amount of the primary gaseous fuel added to the air, whilst the quantity of the pilot charge per injection is usually kept constant for a given engine, regardless of the engine output and it normally contributes ~~to~~ less than ten per cent of the total heat release at full load. Engines of this type are usually capable of operating in this manner or purely on the diesel principle. Such a system is assuming a particular significance with the increased exploitation of natural gas reserves in various parts of the globe and the prospects of increased availability of natural gas from sources located in and around the North Sea (9).

In recent years dual-fuel engines have been used for thermal power production; in industry for electricity, in process plants like sewage treatment plants, in refineries and for pumping bulk water supply; and in transport for automotive (8), locomotive and marine purposes (55). The transportation of indigenous fuels like Liquified Petroleum Gases (LPG) and Liquified Natural Gas (LNG) from Alaska, Libya, the Middle East and Algeria

to various parts of the globe, otherwise deficient in energy sources, calls upon the development of transmission and/or transportation techniques in both of which cases dual-fuel engines are promising in fulfilling the power requirements. Another important use of dual-fuel engines has been found in reducing the atmospheric pollution by converting the diesel transport into dual-fuel operation utilising L.P.G.(8). Dual-fuel engines possess the unparallel flexibility of operation on diesel or dual-fuel principle which makes them ideal for use in sewage treatment plants where the availability of the sewage gas varies in accordance with the progress of sewage treatment process.

0.2 The Development of Dual-fuel Engines - A survey of historical background

Although one comes across occasional references about the dual-fuel principle of operation in the early part of the present century, extensive investigations on this system only took place during the Second World War (1939-1945) when the operability of the prime movers on gaseous fuels was a pressing need to get round the scarcity of liquid fuel supplies. Early efforts in the development of dual-fuel engines were mainly directed towards operating techniques so that satisfactory running conditions could be obtained. However, after the War was over, investigators could afford to look with more detail into the problems posed by the wartime efforts.

Notable investigations during and before the War were made by Sir Alfred Egerton and collaborators (18), whose underlying theme of engineering interest was to understand the slow oxidation processes and to run the automotive engines on L.N.G. Whilst the former problem bore, and still bears, the significance of utilising lean gaseous fuel mixtures in Internal Combustion Engine, the latter was spurred on in the quest to provide alternative fuels, other than 'conventional' liquid fuels, for the production of motive power. Perhaps the first 'status'

report presented in dual-fuel engine combustion was that by Boyer (14) in 1949. His treatment was, however, generalised and contained certain remarks which may now be regarded as extraordinary with the present state of our knowledge. For example, Boyer thought that these engines do not 'knock'. In a rather elaborate study Elliot and Davis (20) investigated the loss of efficiency under part-load performance. They found that at light loads when the mixture strength of the gaseous fuel is below a certain critical value, part of the charge escapes the combustion processes unreacted, thus imposing a toll on the engine efficiency.

At Imperial College an extensive research programme for looking in detail into the Combustion processes in dual-fuel engines had started in the early fifties. Moore and Lewis (72) have, in agreement with the findings of Elliot and Davis, established by direct exhaust gas analyses that under part-load performance, unburnt fuel was present in the exhaust and partial oxidation products were formed. They suggested that this poor performance of the dual-fuel engine could be improved either by increasing the pilot quantity or by pre-heating the intake charge. Moore and Simonson (75), in addition to conducting spectroscopic studies of blue flames in the autoignition of methane using a motored engine, demonstrated the influence of injection timings and pilot fuelling rate on the dual-fuel engine performance. In an exhaustive study of combustion processes in dual-fuel engines, Moore and Mitchell (74) presented clearly the nature of the problem and demonstrated that an improvement in the combustion efficiency at low loads can be effected by any of the following: air restriction; increase in pilot quantity; advancing in pilot injection; and increasing the inlet charge temperature. They found that air restriction is the most effective means of controlling the engine part-load efficiency. They also observed that the values of preignition and knock resistance for spark ignition can be applied qualitatively under dual-fuel engine conditions. These studies, as may be noticed, were mostly confined to lean mixtures whose limiting strength used was around 70%

of Chemically Correct value beyond which knock ensues. The autoignition and knock studies of propane as a fuel by Moore and Roy (73) will be discussed in the introduction to Part B. In an interesting exercise Karim and Moore studied the proposition of simultaneous production of power and synthesis gas by running a dual-fuel engine on rich mixtures (45). Azouz (10) repeated some of Simonson's work with an extended range of pilot injection timings. He analysed exhaust gases to assess incompleteness of combustion processes as indicated by the presence of carbon monoxide and unreacted methane. Rogers (47) extended Klat's (51) and Moore and Roy's work (73) by using butane as an engine fuel and comparing its performance with that of propane. He experimented systematically in defining the knock-limited performance on these fuels utilising three pilot fuelling rates. He attempted to construct approximately heat release diagram from the experimentally obtained pressure variations, which was later extended by the present investigator (49).

The development of dual-fuel engines for higher ratings has brought the problem of avoiding knock to the fore. When this type of engine is required to utilise richer mixtures of gaseous fuels, as warranted by the increased load conditions, there occurs a loss of combustion control with subsequently higher rates of pressure rise, increase in heat transfer and consequent loss in thermal efficiency. In some cases such abnormal phenomena, usually termed as knock, entail mechanical failures, in addition to imparting structural vibrations.

In their studies of knocking combustion processes in dual-fuel engines, Felt and Steele (22) noticed that the phenomena of knock in these engines are akin to those of end-gas autoignition in a spark-ignition engine. They found that pressure development patterns for knocking in both types of engines are similar, and the addition of Lead Alkyls has the same effect in knock suppression. In their efforts to develop large dual-fuel engines above 1500 B.H.P., Hopkins et al. (30) experienced that they had to derate the power output by 4% for every $10^{o}F$ intake temperature rise when using sludge gas to avoid knock.

The recent studies of the combustion mechanisms in dual-fuel engines by Karim, Klat and Moore (43) have shown that there exists a linear relation between the knock Limited Power Output of a dual-fuel engine to the inverse of the intake temperature. They have also ascertained the knock-free operating limits for propane, methane, hydrogen, ethylene, acetylene and their blends over a wide range of mixture strengths, intake temperatures and compression ratios. In an exhaustive survey of dual-fuel and gas engine development, Leiker (55, 56) describes most of the German efforts and concludes the inability, up to the present time, of predicting the behaviour of large engines on the basis of the findings over relatively small units. He also points out the necessity of a standardised procedure for knock-rating of gaseous fuels which lie beyond the usual Octane ratings.

Most of the studies referred to above helped in bringing out the effects of various parameters, such as pilot quantity, injection timing, injection pressure, ignition quality of pilot fuel, speed and turbulence in the combustion space, on the performance of dual-fuel engines. These investigations looked into the useful output, exhaust analysis, spectroscopic studies of the combustion processes. Because of an empirical nature, they lack generality and cannot even provide a basis for a broad analysis which could be formulated as a guide to engine designers who, in the absence of any such guide, resort to guesswork. This is why efforts for extending these findings, which are mostly confined to small research engines, fall short because of lack of correspondence between the small engines and those used in the industry. Analytical approaches to prescribe these complex processes, on the other hand, are limited in their applications because of oversimplifications which cannot however be avoided.

0.3 Scope of Present Work

0.3-1 Objectives

A survey of literature indicated that, although the nature of the limitations in dual-fuel engine operation associated with the use of lean gaseous fuel mixtures and that of knock in richer ones, has been the subject of several investigations, the exact nature of the combustion processes in such a relatively complex system is far from being completely understood. With this in mind, the present investigation set out with the following objectives:

(i) to develop experimental procedures to establish experimentally the nature of underlying combustion processes that limit the useful output of dual-fuel engines;

(ii) to develop analytical and computing procedures to aid the interpretation of such processes on a more broad and generalised basis; and

(iii) to attempt to look into the possibility of providing a simplified analytical model towards predicting the onset of these limits with the help of the understanding developed.

0.3-2 Approach

The present approach to above objectives consisted of the following steps:

(i) Development of a computer programme in Fortran IV workable for I.B.M. 7094, to compute rates of heat release and heat transfer from experimentally obtained cylinder gas pressure records;

(ii) Analysis and examination of computed variations of gross rates of heat release under a wide range of pilot and gaseous fuelling rates with particular emphasis on the part-load and light knocking performance of dual-fuel engines;

(iii) Comparison and confirmation of the salient features of dual-fuel combustion processes as against

various other modes of operation by collating heat release records computable with the generalised programme developed and other records available in literature;

(iv) Examination of the errors normally associated with the calculation of apparent rates of combustion heat release in these engines and suggestion of the means to improve their accuracy;

(v) Development of experimental procedures for the 'end-gas' simulated autoignition studies of the following fuels in a motored engine:

(a) propane-air,
(b) n-heptane-air,
(c) propane-n-heptane-air,
(d) methane-n-heptane-air,
(e) rich mixtures of (b)-(d) with carbon dioxide as a diluent;

(vi) Examination of rates of heat release and confirmation as to the nature of the processes leading to autoignition;

(vii) Characterisation of the chemical nature of the autoignition processes by deriving gross chemical kinetic data based on the accurate calculation of the rates of heat release; and

(viii) Exploring the possibility of making use of the information yielded by the preceding steps in developing a simplified model capable of predicting the engine behaviour under normal and knocking conditions.

0.4 Outline of the Thesis

This thesis has been divided into three main parts. The chapters belonging to each part form an array such as A1, A2, ... while the subscript zero signifies that it forms the introduction, e.g. (A0) is the introduction to Part A.

Part A deals with the development of the computer programme, analysis and examination of combustion heat

release in dual-fuel engines and examines critically most of the errors normally associated with the computations of heat release. Discussions and conclusions are appended whenever necessary, instead of keeping the reader away from the immediate significance as pertinent to this part of our present investigation. In order to demonstrate the implications of the results, records have been some times superimposed to depict relative differences at a glance.

Part B covers the autoignition studies in a motored engine, as a logical sequence to part A which underlines the knock reactions through heat release analysis in dual-fuel engines. It can be subdivided into two parts; part one examines the heat release due to auto-ignition reactions, while the second part derives the combustion kinetic data. In keeping with the format of Part A, discussions and conclusions related to the chemical aspects of autoignition reactions with particular reference to knock in dual-fuel engines are presented within Part B.

In Part C, it is attempted to conjoin Parts A and B so as to demonstrate the adequacy or otherwise of the available data in presenting a simplified model. It contains general conclusions and recommendations for future work.

List of symbols used in the text and references are arranged in alphabetical order and follow Part C.

Listing of the computer programme and the description of the numerical procedures adopted appear in Appendix form, together with the analysis of fuels used, theory of calibration of viscous flow air meter and choked nozzle meters.

C H A P T E R AO

INTRODUCTION TO PART A

DUAL-FUEL ENGINE TRIALS

AO.1 Motivation

The method of calculating rates of heat release from experimentally obtained pressure-time records was first conceived by Schweitzer (86), which he named as 'Tangent-method', as pressure rates were obtained graphically by drawing tangents to the pressure diagram. This method was not adopted for being cumbersome and inaccurate. Moreover, the pressure measuring techniques in those days were in their infancy. Recently, the use of fast electronic computers for engine cycle simulation brought the technique of heat release analysis to the fore. Recent attempts in this direction can be divided into two groups; the first group synthesised the heat release diagrams from the fundamental considerations of the combustion of diesel fuel droplets under quasi-steady conditions, while the second group analysed experimentally obtained pressure records so as to interpret indirectly the combustion processes through heat release analyses in diesel and gasolene engines.

Original studies by Lyn (62, 63) are a classical example of the first group. He established the relation between the heat release diagram, pressure development and cycle efficiency. Later Gee and Karim (27), and more recently Shipinski, Myers and Uyehara (87), synthesised the heat release diagram with the 'droplet-model' technique while assuming that the atomised spray of the diesel fuel undergoes combustion on the pattern of various droplets being burnt under quasi-steady conditions. The second group is formed by Whitehouse et al. (104), Krieger and Borman (52), Patterson and Van Wylen (83) and McAulay (67) who analysed the pressure-time records to obtain heat release diagrams. Their studies have demonstrated that

heat release analysis is an effective means of interpreting indirectly the combustion processes in internal combustion engines. No efforts, however, seem to have been directed in the past towards employing such an analysis to the more complex combustion processes of the dual-fuel type of engines.

AO.2 Present Contribution

The present work was undertaken making use of the technique of heat release analysis to establish better understanding and providing solutions to the problems related to dual-fuel engine combustion. It sets out with the analysis of pressure-time records obtained experimentally over a wide range of operating conditions from light-load to that of onset of knock. Methane was adopted as the primary fuel in view of its extensive abundance in natural gas sources, its comparatively high calorific value on mass basis among other common fuels and the large information available about its combustion characteristics in general (71) and those in dual-fuel engines in particular (74). A wide range of methane concentrations and that of pilot fuelling rate was covered for the analysis. The effect of deliberately introducing carbon dioxide along with methane was also examined to simulate operation on methane sources containing CO_2 as a major contaminant, as commonly is the case with sludge gas.

The generalised character of the computer programme developed is demonstrated by analysing the heat release rates of diesel, gas and motored autoigniting engine cycles. It is shown that the numerical procedures adopted in the programme depict effectively the characterising features of combustion processes under these modes of operation.

A comparison is then made of the heat release rates in dual-fuel engine combustion with all other possible modes of operation as presently computed together with the ones reported in the literature. This is thought to be of

value in bringing out the relative differences which characterise dual-fuel systems into perspective.

AO.3 Outline of Part A

Part A presents the heat release analysis of a single cylinder naturally aspirated dual-fuel engine. It consists of four chapters.

In chapter A1 is described the apparatus used and the experimental procedure adopted.

Chapter A2 describes the computing procedure in detail and presents the results of heat release analysis of dual-fuel engine trials. It also presents some typical heat-release plots of diesel, gas and motored engine operation, which serve to illustrate the generality of the computing programme developed. Some heat release records depicting special configurations of reciprocating engines such as stratified charge engines as available in the literature, have been reproduced to complete the picture.

Chapter A3 analyses, at length, all possible errors which have a bearing on the accuracy of the present heat release analysis. The errors are discussed and conclusions drawn as to the reliability of the present analysis in presenting the dual-fuel engine combustion phenomena.

In chapter A4 are discussed the dual-fuel engine combustion processes in the light of the detailed heat release analyses. It conclusively demonstrates the capability of heat release techniques in characterising the combustion processes, while purporting the experimental evidence available in the literature thus far.

C H A P T E R A1

APPARATUS AND EXPERIMENTAL PROCEDURE

A1.1 Introduction

One of the main objectives of the present investigation is to develop better understanding, through heat release analysis, of the underlying processes in dual-fuel engines and particularly those pertaining to part-load and knocking performance. An engine is therefore required which can be operated on a wide range of load conditions, while suitable instrumentation is needed to record important parameters such as cylinder pressure, intake temperature and pressure, air and fuel flow rates and brake horse power.

A vertical single cylinder National Oil and Gas Engine was used for this purpose. As common with the dual-fuel engines, in general, it was a conventional diesel engine incorporating the facility of introducing metered quantity of gaseous fuel in the intake. This feature had an added advantage of comparing the dual-fuel engine performance with that of 'pure' diesel operation. The single cylinder construction rendered the formation of mixture consistent and the effect of residuals could be computed reliably.

A1.2 Apparatus

A1.2-1 The Engines and the Test-Bed

The engine used was a standard vertical, single cylinder National Oil and Gas Engine conforming to the following particulars:

Bore	4.125"
Stroke	6.0"
Compression ratio	14.7 : 1
Injector Type	Conventional spring loaded needle valve with 5 holes

Injection Pressure	100 - 200 atmos.
Maximum Speed	1500 Rev.
Combustion Chamber	Open, direct injection type
Con-rod to crank-throw ratio	4 : 1.

The engine was coupled to a D.C. compound wound swinging field dynamometer which had the facility of being operated as a motor or generator depending on the performance of the engine. The motoring could afford the engine to be started from cold and to measure the Frictional Horse Power, if need be. The voltage generated by the dynamometer under normal conditions was dissipated through immersion heaters, while the same heaters could serve as a starting resistor at the beginning of engine operation.

A dial type spring balance hung with the load arm across the dynamometer registered the brake torque whose calibration gave:

$$BHP = \frac{WN}{2600}$$

where, BHP is the brake horse power, W the net brake load and N the engine speed. Plates (A1.1 - A1.5) show general views of the engine installation, the control panels and the housing of pressure pick-up and injector needle lift indicator.

Fig. A1.1 presents schematically the engine cooling water and lubricating oil circuit. A closed circulating cooling water system was adopted whose circulation was maintained by an electrically driven pump. The cooling water was, in turn, cooled by a supply of mains water in the heat exchanger which received thermostatically controlled quantity of mains water to keep the cylinder jacket water outlet temperature at $70^{\circ}C$ within set limits of $\pm 2^{\circ}C$.

Shown in Fig. A1.1 is also the lubricant circuit. The engine has a dry sump forced lubricating system. An electrically driven scavenge pump maintained the flow through the sealed tank, the filter and finally to the internally located lubricating oil pump. The mains cooling water in the intercooler was controlled thermostatically via a solenoid valve.

A1.2-2 Air and Fuel Flow-Measuring System

A viscous flow air meter was used for measuring air flow to the engine because of its effective smoothed characteristics to pulsating flow measurements, its independence from the introduction of gaseous fuel downstream and being least prone to hazardous back-firing. It consisted of a matrix of metallic triangular arrays offering triangular passages of equal area to air flow and rendering the flow 'viscous', whereby there occurred a pressure drop in linear proportion to volume rate as shown in Appendix I. The viscous flow air meter was calibrated by a 7/8" Ø orifice plate with D/2 and D pressure tappings across in accordance with the B.S.S. 1042,(7).Fig. A1.2 shows the calibration curve obtained.

Methane and carbon dioxide flows were metered with AMAL Jets which are commercially meant for carburettors. Under choked conditions these nozzle-jets render the flow rates linear to the upstream pressure and temperature ratio and they are independent of the pulsating flow downstream (44). Shown in Appendix II is the underlying theory behind the choked nozzle flow measurements. The nozzles were calibrated against a B.S.S. 1042, 5/16" Ø orifice plate. Fig. A1.3 shows the calibrated linear relationship of methane and carbon dioxide flow through various jets used.

Fig. A1.4 shows a general layout of the apparatus used. It can be seen that methane and carbon dioxide were used in bottles containing about 200 s.cft. at 2000 psig. Both methane and CO_2 flow circuits were essentially the same except a portable electric heater was mounted on the CO_2 bottle, whereas methane was heated in the heat exchanger by the engine coolant. This heating was necessary to avoid freezing of moisture in lines because of the Joule-Thomson effect due to sudden expansion across the regulating valve. Facility was also available to pre-heat the intake, if need be, with a Variac heater situated in the intake.

Commercial gas oil was used as a pilot fuel. It was supplied to the fuel pump through an auxiliary reservoir at a head maintained constant by transferring oil by auto-

matically operated D.C. pump from a six-gallon can. The pilot fuel oil consumption was recorded volumetrically by a graded burette having a range of 10, 50 and 100 c.c. The fuel pump was a C.A.V. variable stroke plunger type. Pilot fuel could easily be varied by adjusting the plunger stroke against a rack. The fuel pump was driven through a cam shaft ~~by~~ through helical splines at half the engine speed. The driving mechanism of the fuel pump could afford the variations in the actuating time of the plunger and hence the injector lift timings by changing the relative position of the pump shaft to that of the engine. Thus the injection timings could be varied over about 30° of crank movement.

Methane, gas oil and carbondioxide used for the trials belonged to commercial grades whose composition was checked regularly with the suppliers. Appendix III presents their typical composition.

A1.2-3 Electronic Measuring Instruments

Arrangements, as shown schematically in Fig. A1.4, were made for recording cylinder pressure, crank timings and injector needle lift. The variations of these parameters were displayed on a Cathode Ray Oscilloscope (C.R.O.) and preserved for computer analysis on a film by a camera.

A1.2-3a Pressure Transducer

A Kistler piezo-electric transducer of type 410W was used for recording cylinder gas pressure. It conformed to the following particulars:

Type	Kistler 410W, quartz crystal
Cooling System	Water cooled, internally
Pressure Range	0 - 3500 p.s.i.
Sensitivity	8.5 pc/p.s.i.
Response	10μ Sec, rise Time
Natural frequency	50 KC/sec.
Resolution	.0003 atmos.

The transducer was found particularly suitable for its wide pressure range, fast response and fine resolution, while its natural frequency was exceptionally high as compared to the frequency of working cycle at a rate of 8½ c/s.

The transducer was screwed in a 14mm Ø tapped hole at the end of a short passage leading to the combustion chamber through the cylinder head. This arrangement was the only way out as the atomiser occupied the central position, leaving no space for the transducer to be flush-mounted. The effect of such a passage has been found to be insignificant on pressure response (51). Fig. A1.5 presents the drawing of the pick-up while Fig. A1.6 is its static calibration carried out with a Budenberg dead-weight tester. It can be seen that the charge-pressure relationship is linear over a wide range.

A Kistler 220 Volts A/C mains operated universal eléctrostatic charge amplifier Model 568 was used for pre-amplification of the pressure pick-up output before it is displayed on to C.R.O. This compact unit was kept in a glass wool pads' enclosure for isolation from the noise. It was selected for its matching high input impedence, high frequency response, low linearity error and wide range of operation.

A1.2-3b Injector Needle-Lift Indicator

A photo-electric cell was used to record the injector needle movement. The duration of injector lift, in proportion to the amount of pilot fuel being injected, causes proportionate interruption of the light reaching the photo cell which, in turn, develops a charge across the cell. In construction, the indicator consisted principally of a miniature Mullard type BPY 10 Silicon photovoltaic cell mounted on a tufnol block. It received light from a 2.5 W pre-focussed bulb energised by a 6V steady D.C. supply obtained by stepping down the 220V Mains supply and filtering after rectifying. The light from the bulb passed through a narrow aperture of .012" x .125"

formed by two sharp-edged blades. The extension rod welded to the injector needle was situated in between the cell and the bulb. The assembly of the cell and the light source were clamped to the engine casing. Except for very small pilot fuelling rates, the photo-cell was sufficiently strong to produce signals on the oscilloscope without pre-amplification. For the pilot fuelling rates of 0.35 lb/h, it was found necessary to introduce an amplifier in addition to the amplification done by the built-in operational amplifier in the oscilloscope. Such arrangement was thought to be necessary to eliminate the mechanical vibrations of the injector assembly together with those of the engine, which otherwise make it difficult to reckon the duration of injection. The injector lift traces displayed on the oscilloscope could represent well the dynamic injection timings. Shown in Fig. A1.4 is the position of the photo-cell in the general layout, wile its mounting in close-up appears in Plate A1.4.

A1.2-3c Electromagnetic Pick-up for Crank Rotation

Crank shaft rotation was sensed by an electro-magnetic pick-up mounted just above the fly wheel. The peripheral equi-angular slots inscribed on the rim of the fly wheel for positions 90^{o} before and after T.D.C. caused changes in the permeability to the magnetic flux produced by the permanent magnet of the pick-up. This, in turn, gave rise to a change in the inductance of the coils wound round the pick-up. The electromotive force thus produced was displayed on the oscilloscope which recorded the crank shaft movement in terms of 5 and 10^{o} intervals.

A1.2-3d The Cathode Ray Oscilloscope

A dual-beam Tektronix Cathode Ray Oscilloscope (C.R.O.) type 502A was used for its high input sensitivity, trace stability, good frequency response, effective and reliable trigger operation and relative freedom from noise. The pressure transducer output was displayed via a Kistler

568 pre-amplifier. The second beam was permanently used for crank angle display, while injector needle lift diagram could be accommodated in place of cylinder gas pressure. The triggering facility of the oscilloscope could scan a cycle out of the continuous display of recurrent cycles.

Permanent photographic records of cylinder gas pressure and injector lift together with crank angle were obtained on a 35 mm fine grain black and white ILFORD FP4 film of ASA 125. The camera used was a Cossor Model 1428 MK II A. Its large aperture with f1.5 could resolve finely the traces displayed on the oscilloscope screen. The film could either be exposed by manually operating the shutter or it could be moved at a speed of .05" - 25"/sec while keeping the shutter open. Continuous recording of a few cycles in combed records could be effected with the latter arrangement and was found to be extremely suitable for studying cyclic dispersion (50).

A1.3 Experimental Procedure

At first all the air, fuel and pressure measuring instruments were calibrated. Stabilised operating conditions conforming to the following particulars, were attained while running the engine on diesel operation.

Speed	1000 $\pm$ 5 r.p.m.
Injection Timings	20^{o} BTDC
Injection Pressure	150 atmos.
Pilot Oil	.35, .5, .75, 1.0 lb/h
Methane in Intake	Varied from lean to knocking
Cylinder jacket water outlet temperature	70 $\pm$ 2^{o}C
Lubricant temperature	40 $\pm$ 2^{o}C.

The above operating conditions were selected on the basis of initial trials conducted to familiarise with the comparative diesel and dual-fuel engine performances. The injection timings and the injection pressure were found

to be satisfactory over the wide range of pilot fuelling rates, while the selection of a constant medium speed, in effect, kept the residence time of the charge in the engine cylinder constant. Under lean concentration of gaseous fuel in the intake with relatively small pilot rate of 0.35 lb/h, it was found difficult for the engine to develop sufficient power to overcome frictional losses. Such marginal operating conditions were obtained starting from the rich boundary-line knocking operation and reducing the gaseous fuel concentration discretely until the unsatisfactory conditions of negative output were reached.

Knocking was reckoned by virtue of its audibility and roughness of engine performance which was also manifested by the oscillations in the pressure traces due to excessive pressure rates. Violent knocking was not reached essentially for avoiding excessive thermal and mechanical loading of engine parts and also for the fact that excessive pressure oscillations on the pressure diagrams render the results void of certainty. However, a few knocking records were obtained to analyse heat release under these abnormal conditions.

Before procuring the pressure record on film pertaining to a particular trial, it was ensured that steady conditions were reached. In order to obtain a representative cycle, five separate records were obtained at random. Mean cycle could, therefore, be selected out of five during enlarging. However, it can be recalled that steady conditions with comparatively less cyclic dispersions were easily attainable under medium to full-load operation. Under part-load performance with smaller pilot fuelling rates, it was found that cyclic dispersion gets pronounced. While dealing with rich mixtures it was noticeable that although conditions were stabilised, there occurred advancing in ignition if violent knocking ensued. Similar experience has been reported by earlier workers (43).

The traces obtained on the film were projected by an enlarger on a sectional scale, wherefrom pressure readings could be scaled out with reference to crank angle.

The effects of crude traces and eventual difficulty in finding the actual pressure and the sub-division of crank-time markings on the accuracy of results shall be discussed at length under 'error analysis'. This, in fact, led to the development of a digitaliser which was later used in the autoignition studies and will be described in the relevant section.

In the absence of a reliable dynamic reference pressure the scavenging pressure line displayed 'simultaneously' with the triggering arrangement could serve to indicate the inlet valve closure at which instant the cylinder gas pressure was assumed to be 1 p.s.i. less than the ambient intake pressure. An improvement in reference pressure recording was later effected in motored-engine studies by using a Kistler adapter pick-up, to be discussed in the description of apparatus of motored-engine trials.

A specimen set of photographed pressure-time traces and needle lift indicator diagrams are shown on Plates A1.6 to A1.8.

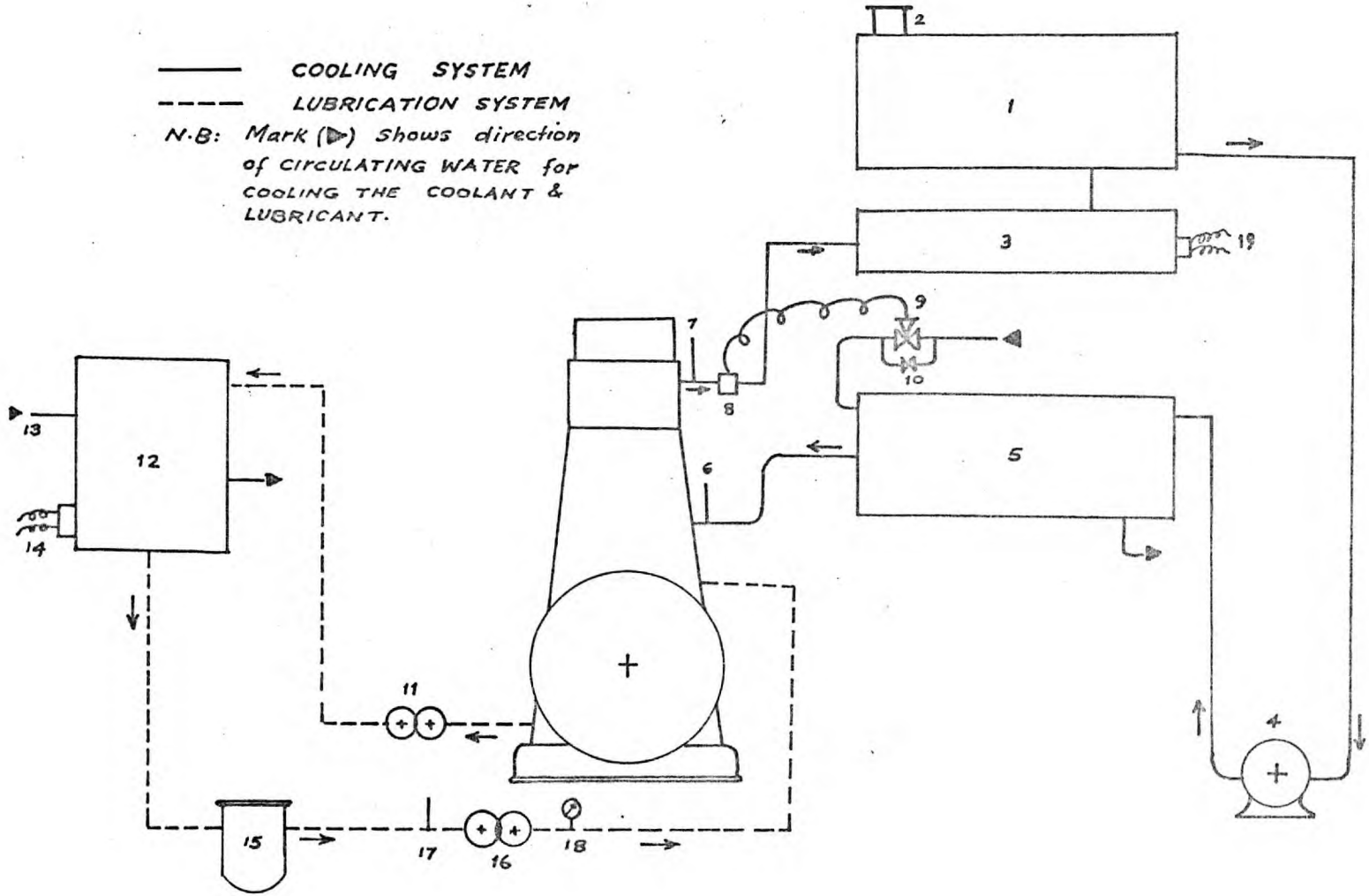


FIG. (A1·1) : ENGINE COOLANT AND LUBRICANT FLOW CIRCUIT.

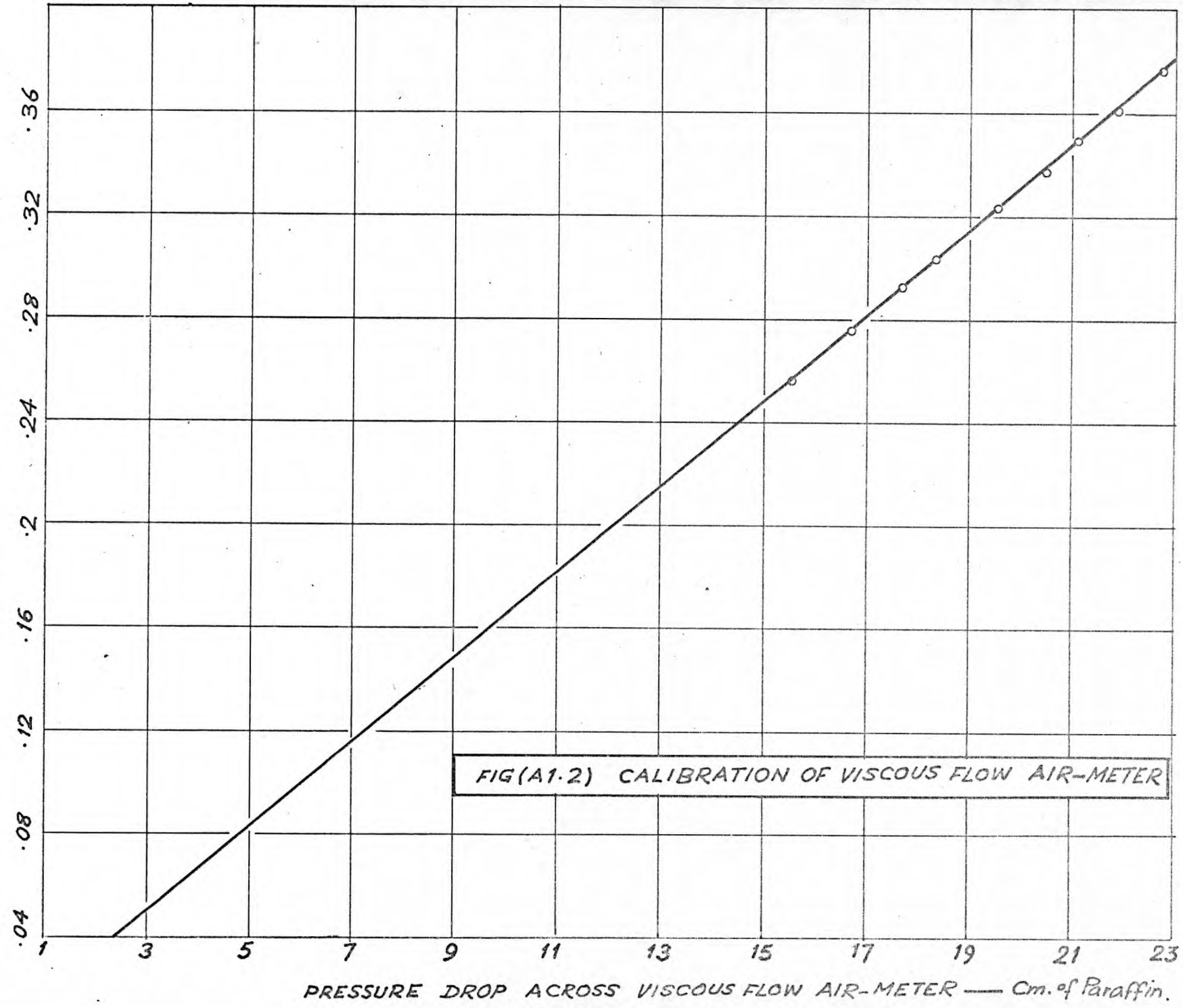
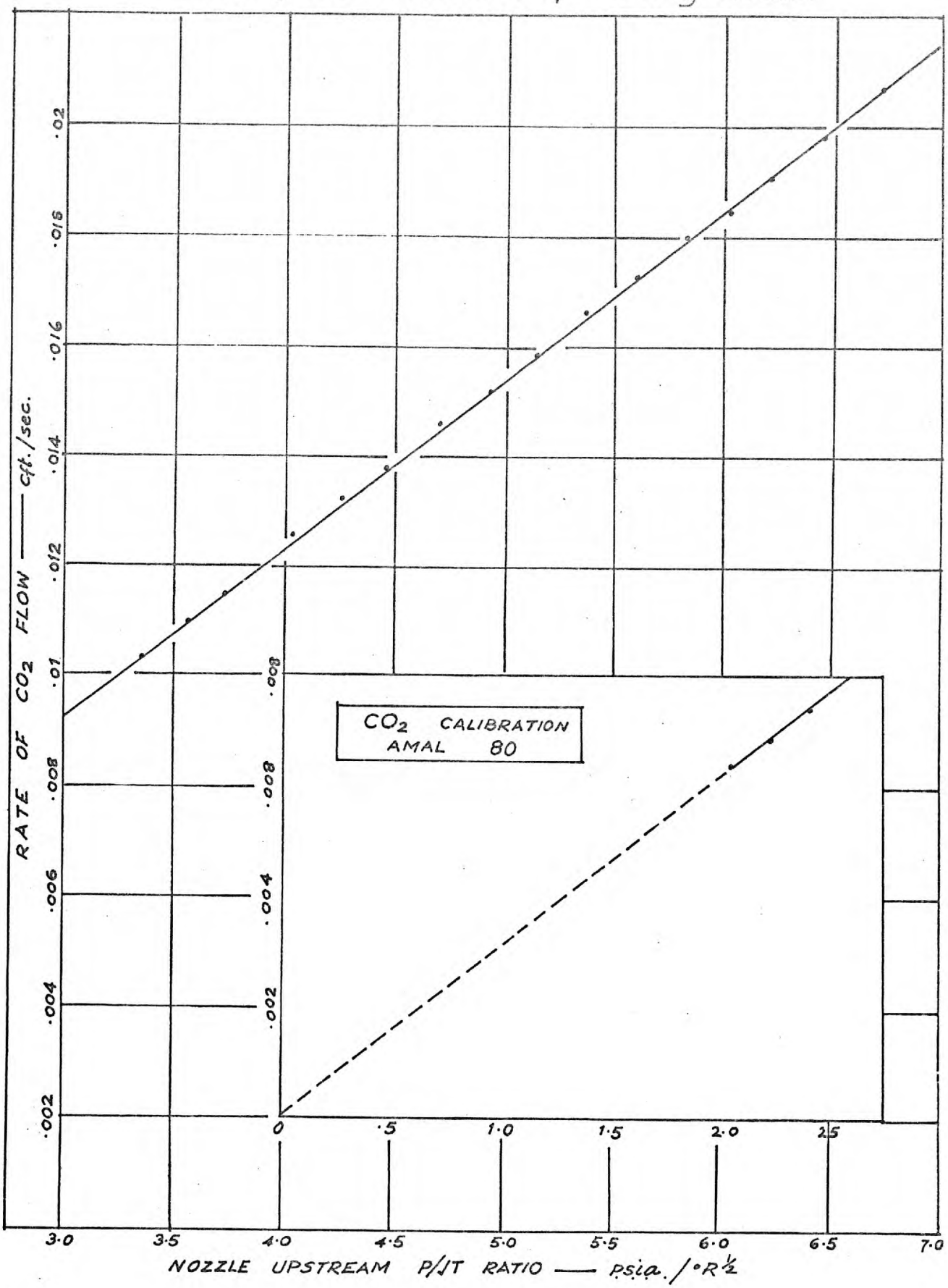


FIG (A1·2) CALIBRATION OF VISCOUS FLOW AIR-METER

FIG. (A1·3) CO_2 Calibration of Metering Nozzle.



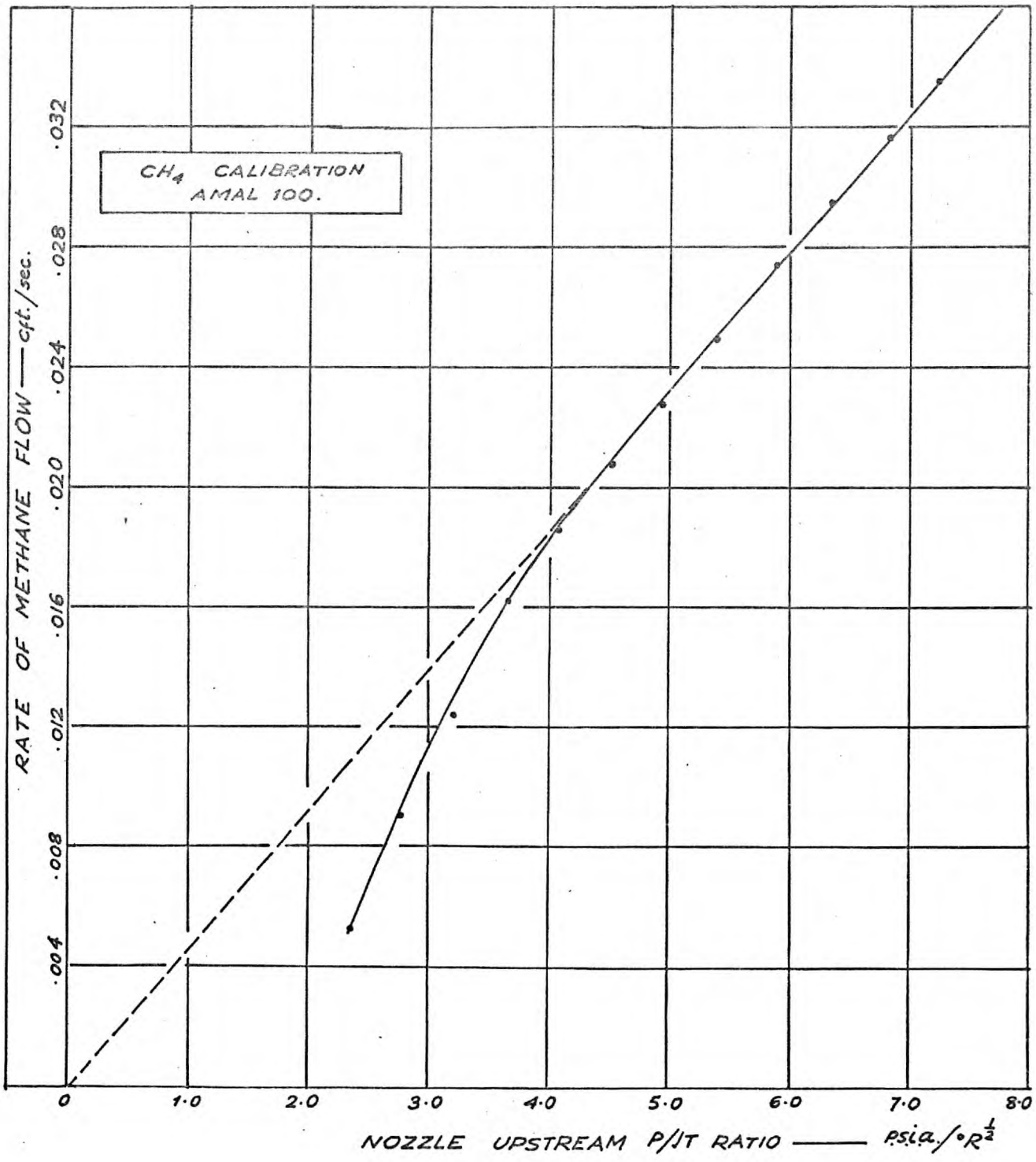
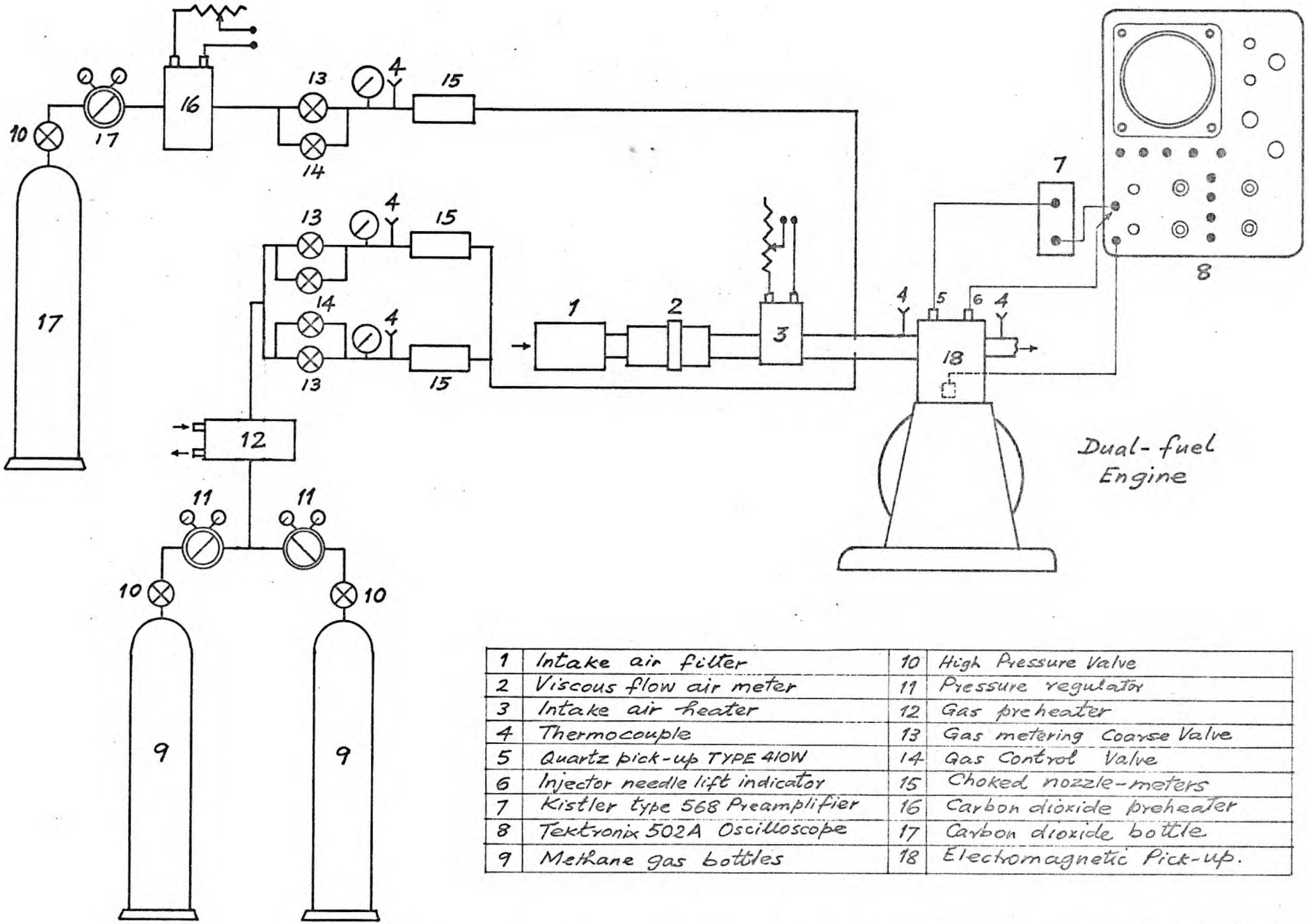


FIG. A1.3a CALIBRATION CURVE FOR METHANE. FLOW.



1	Intake air filter	10	High Pressure Valve
2	Viscous flow air meter	11	Pressure regulator
3	Intake air heater	12	Gas preheater
4	Thermocouple	13	Gas metering Coarse Valve
5	Quartz pick-up TYPE 410W	14	Gas Control Valve
6	Injector needle lift indicator	15	Choked nozzle-meters
7	Kistler type 568 Preamplifier	16	Carbon dioxide preheater
8	Tektronix 502A Oscilloscope	17	Carbon dioxide bottle
9	Methane gas bottles	18	Electromagnetic Pick-up.

FIG. (A1.4) A Schematic Layout of the Apparatus used in Dual-fuel Engine Trials

Fig. A1.5:
QUARTZ PRESSURE TRANSDUCER, SCREW-IN-TYPE, WATER-COOLED

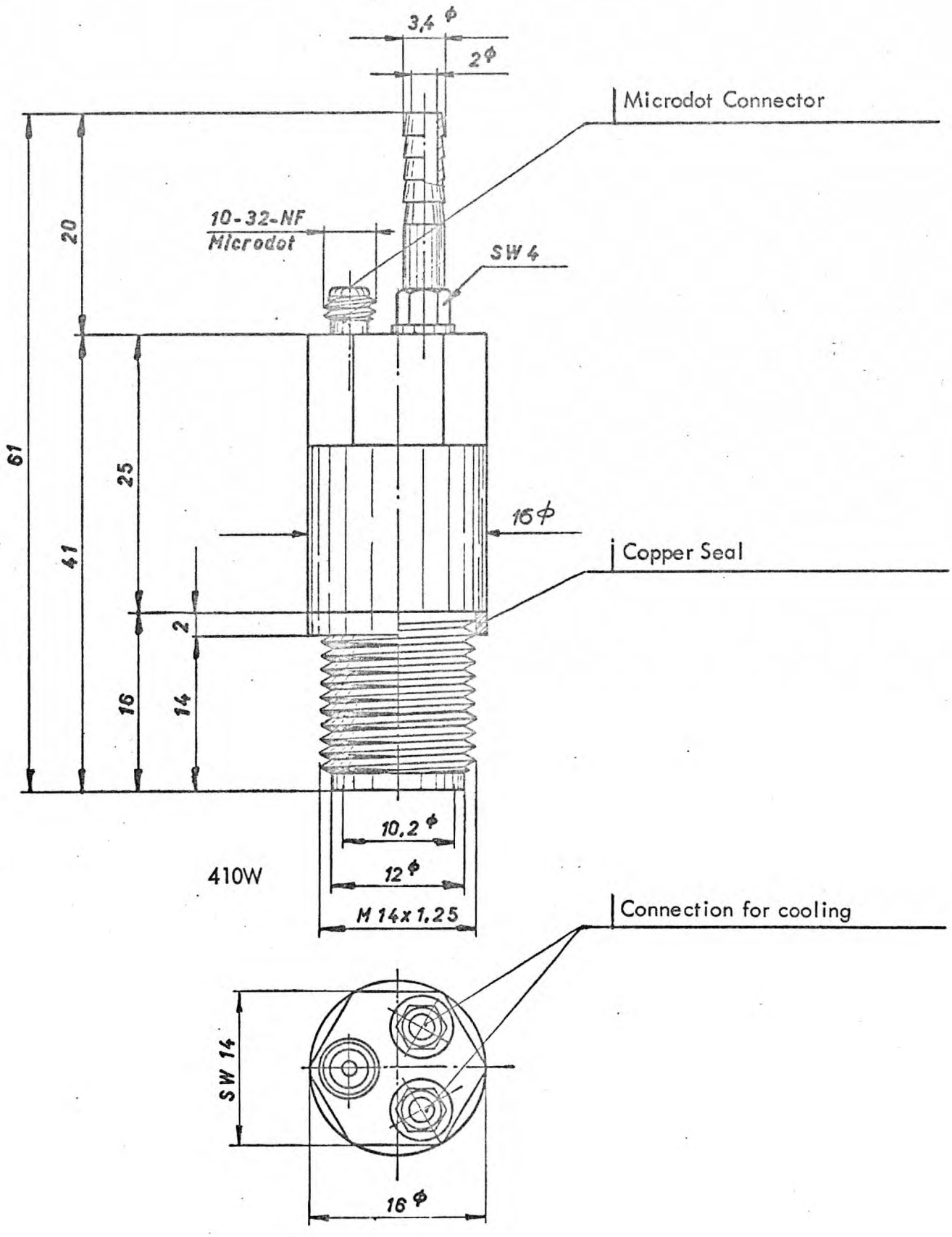
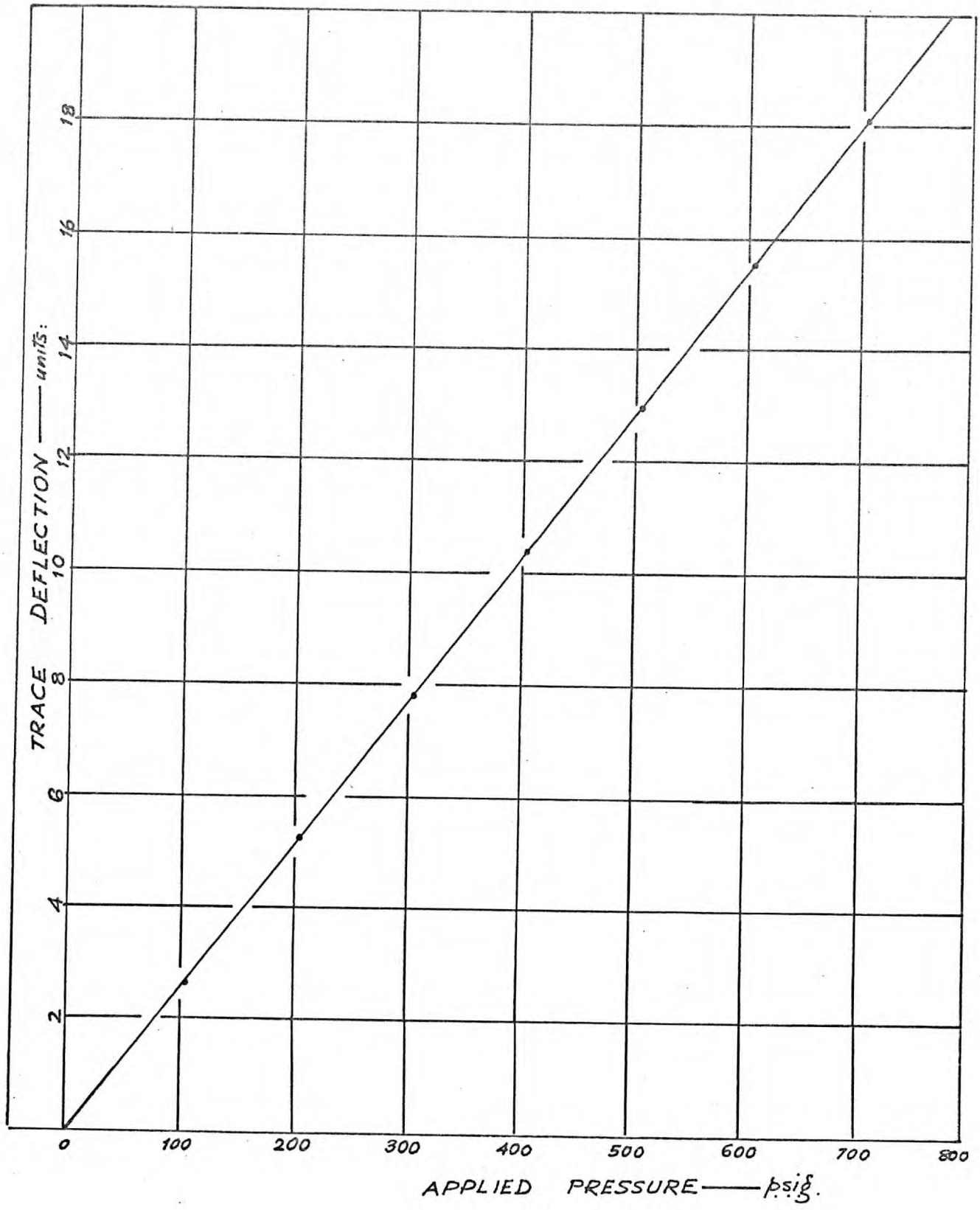


FIG: (A1.6) TRANSDUCER STATIC CALIBRATION.



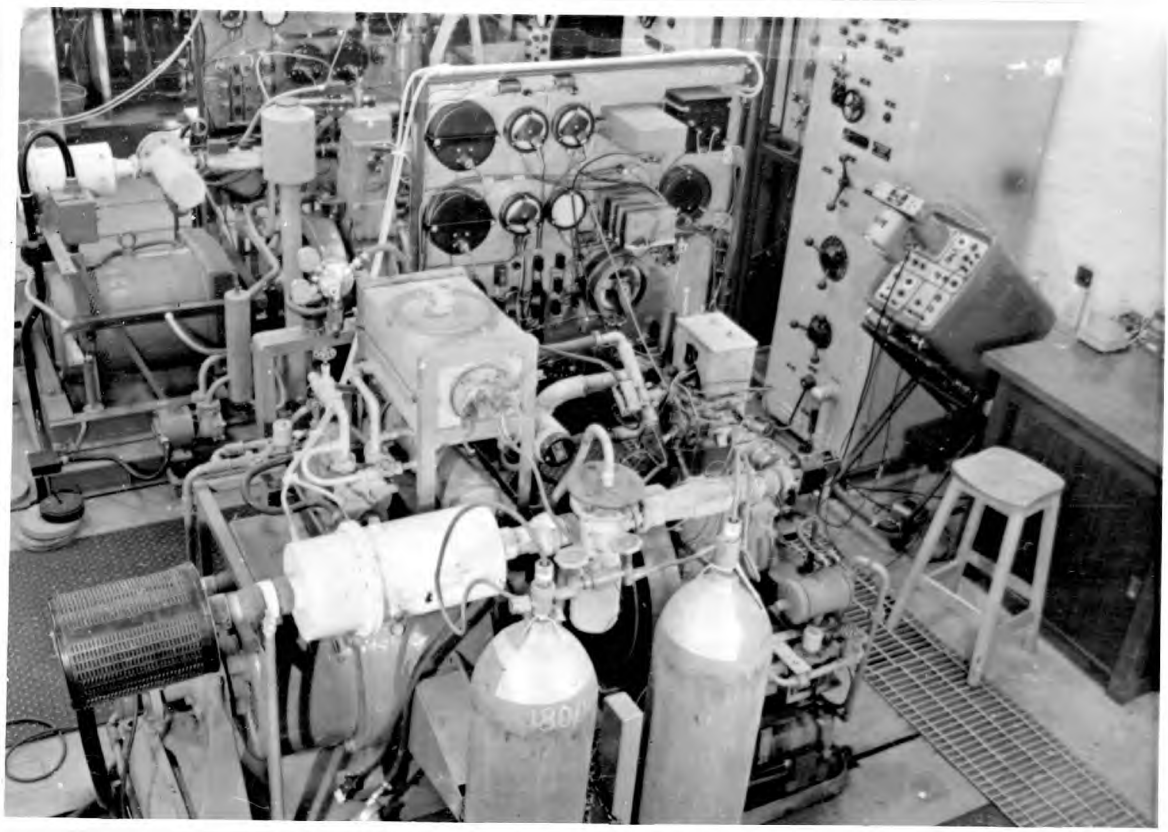


PLATE A1.1: A GENERAL VIEW OF THE DUAL-FUEL ENGINE TEST RIG

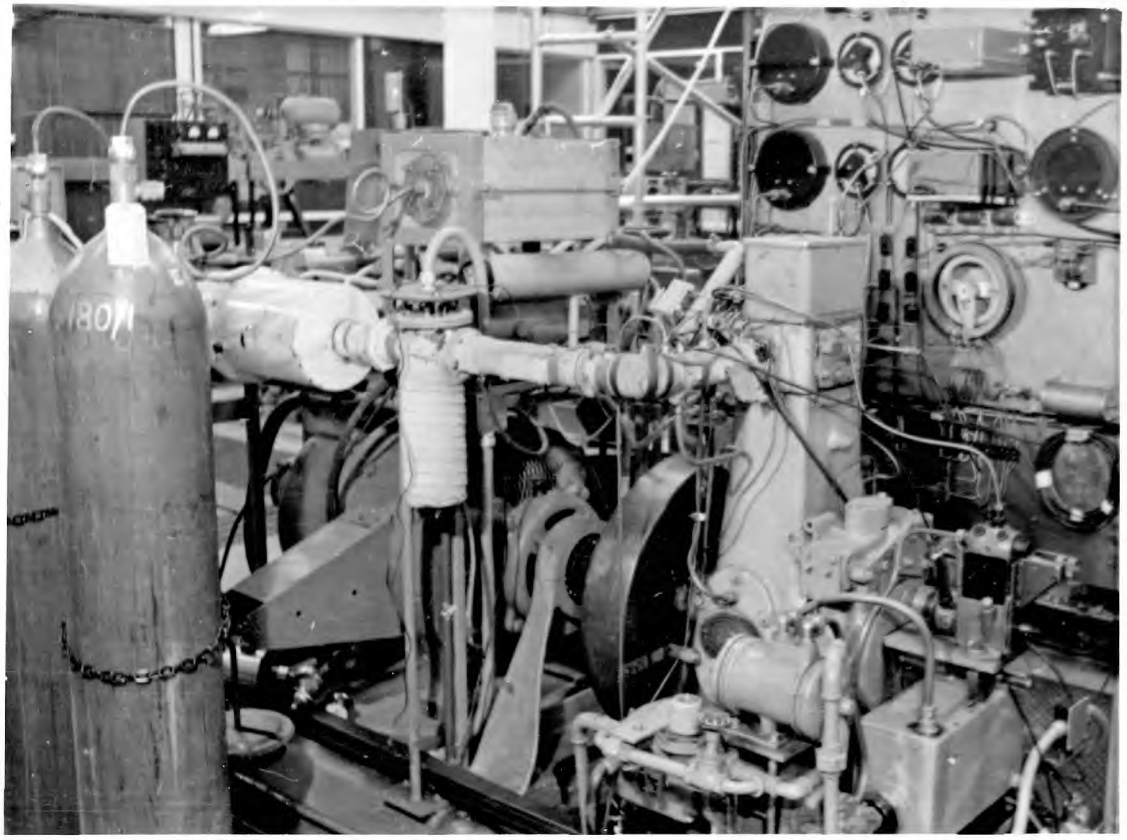


PLATE A1.2: ANOTHER VIEW OF THE DUAL-FUEL ENGINE TEST RIG

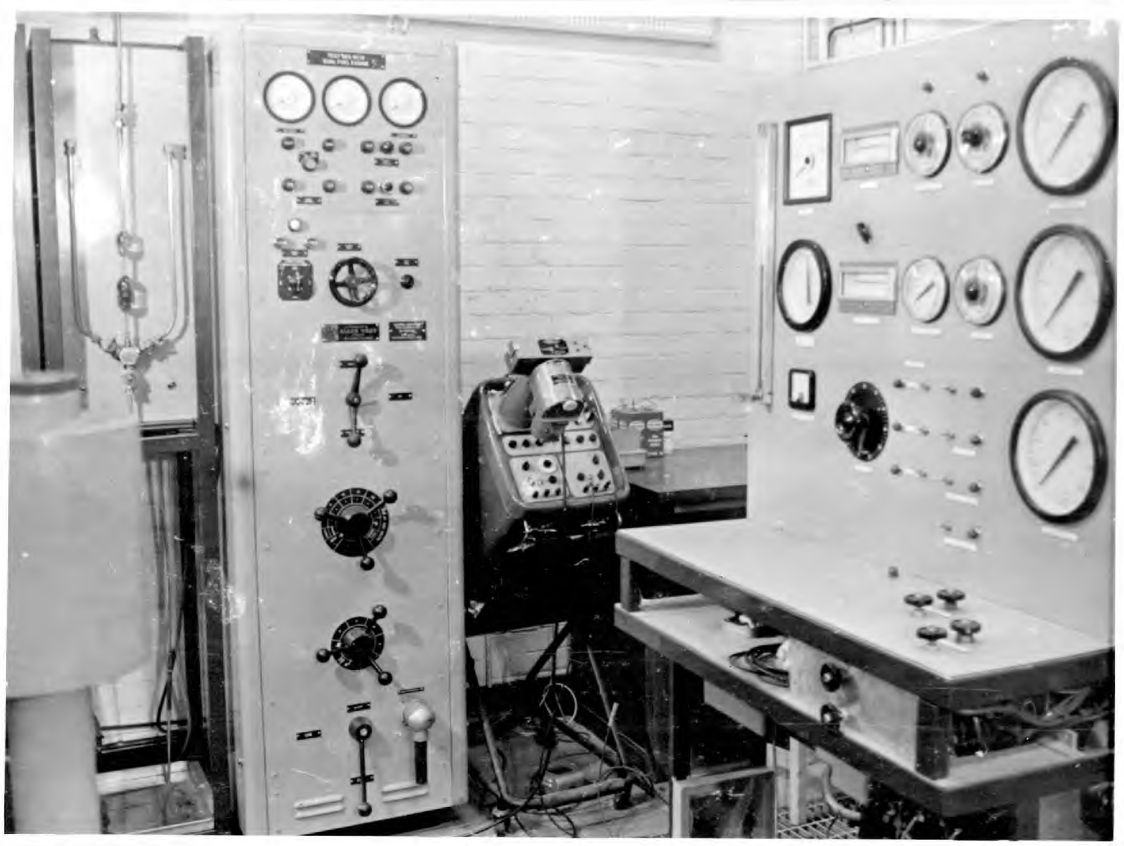


PLATE A1.3: A VIEW OF THE CONTROL PANELS AND THE OSCILLOSCOPE

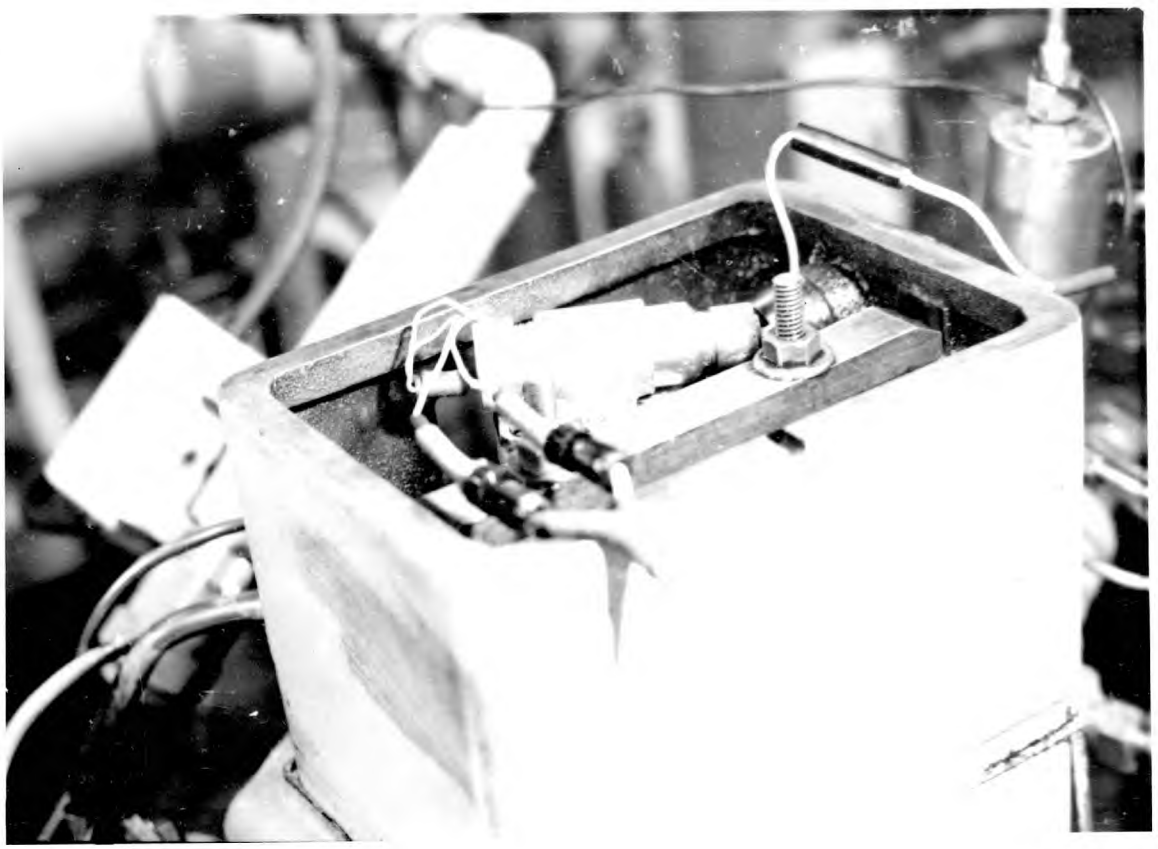
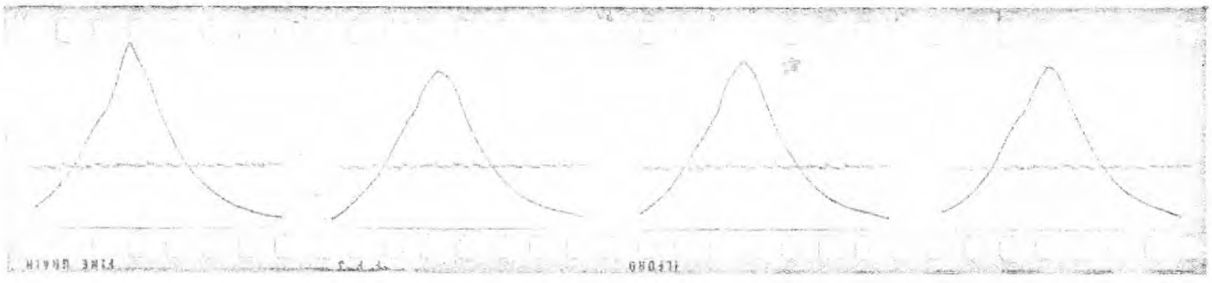


PLATE A1.4: A CLOSE-UP OF INJECTOR NEEDLE LIFT INDICATING PHOTO CELL MOUNTING

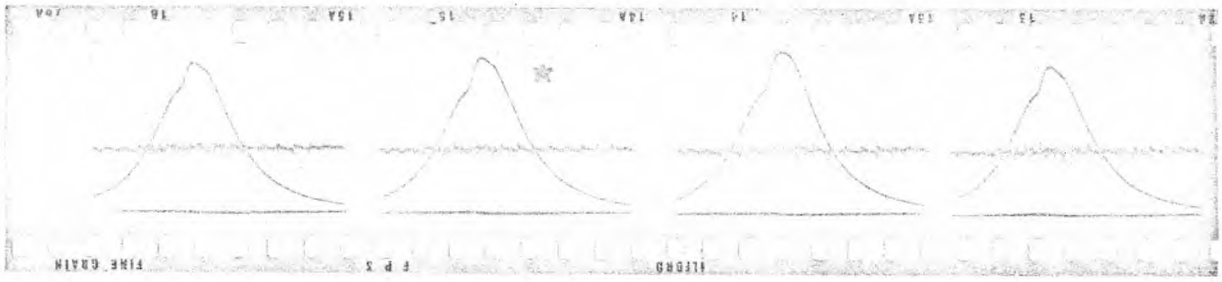


PLATE A1.5: A CLOSE-UP OF ELECTROMAGNETIC PICK-UP FOR CRANK ROTATION

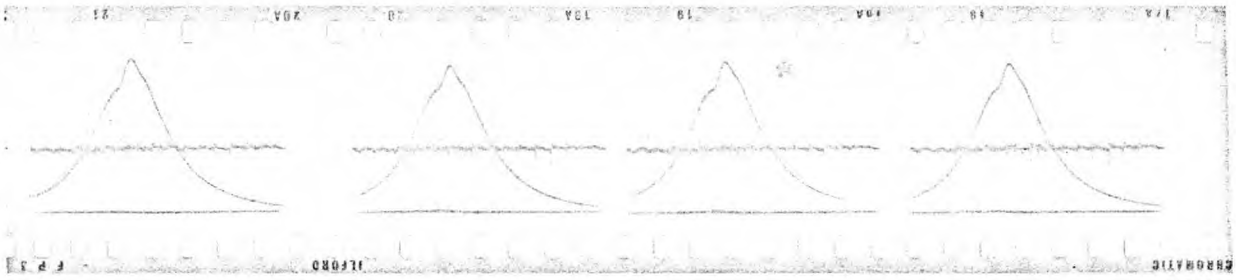
BMEP = 70 p.s.i., 77.5 % C.C.M., Methane in Intake 7.04%



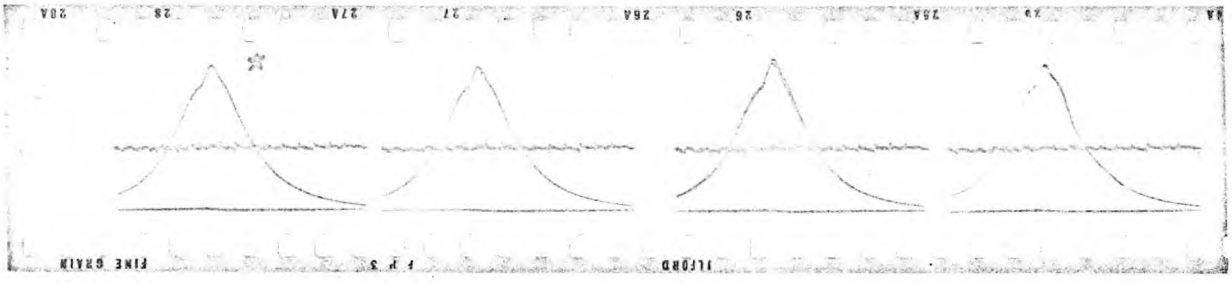
BMEP = 66.8, 66.8% C.C.M., Methane in Intake 5.82 %



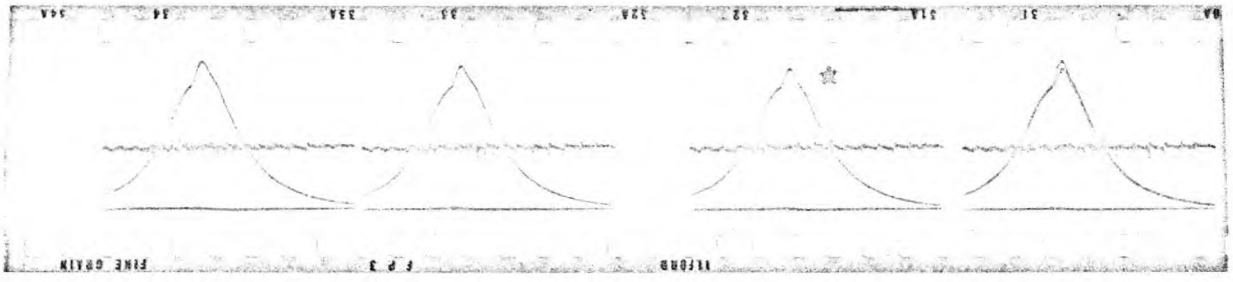
BMEP = 21.35, 63.1 % C.C.M., Methane in Intake = 5.48 %



BMEP = 11.4 p.s.i., 55.2 % C.C.M., Methane in Intake = 4.73 %



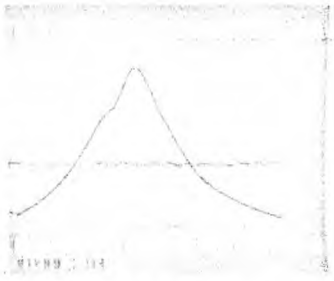
BMEP = 10.0 p.s.i., 43.6 % C.C.M., Methane in Intake = 3.63%



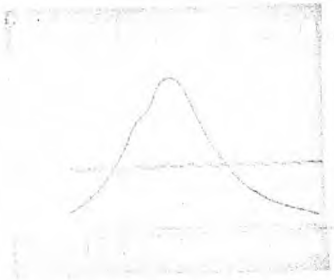
Engine Speed = 1000 Rev., Pilot felling Rate 0.5 lb/h
Coolant outlet Temperature = 70°C

Plate (A1.6). A Set of Pressure Records.

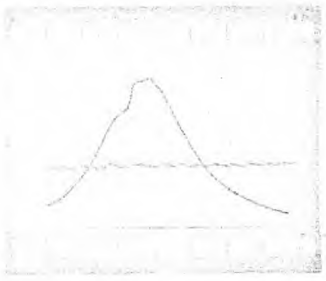
BMEP = 67·5 p.s.i., 78·3% CCM
% CO_2 in Intake 17·5



BMEP = 65·6 p.s.i., 79·3% CCM
% CO_2 in Intake 25



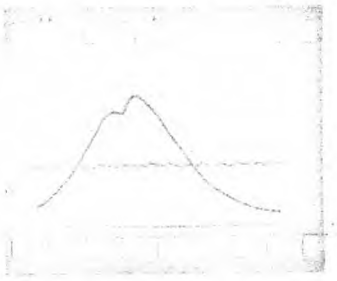
BMEP = 65 p.s.i., 80·3% CCM
% CO_2 in Intake 31



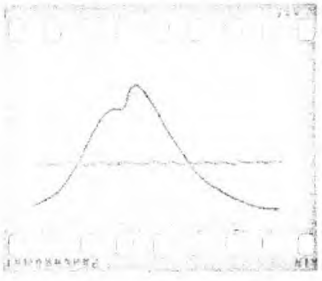
BMEP = 54 p.s.i., 80% CCM.
CO_2 in Intake 36%



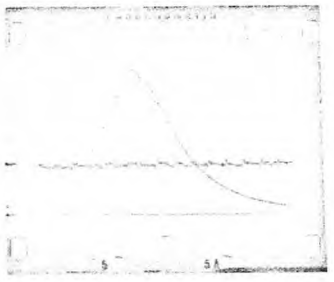
BMEP = 52·5 p.s.i., 80% CCM
CO_2 in Intake 40·5%



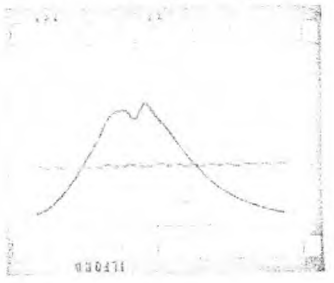
BMEP = 49 p.s.i., 81·4% CCM
CO_2 in Intake 45%



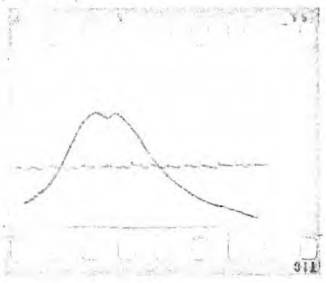
BMEP = 43·8 p.s.i., 82·3% CCM
CO_2 in Intake 48%



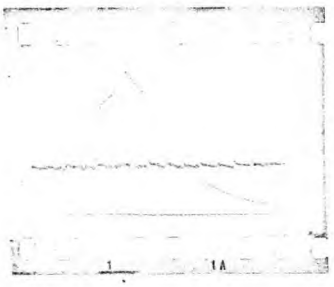
BMEP = 41 p.s.i., 82% C.C.M.,
CO_2 in Intake 50%



BMEP = 30, 65% C.C.M.
CO_2 in Intake 19%



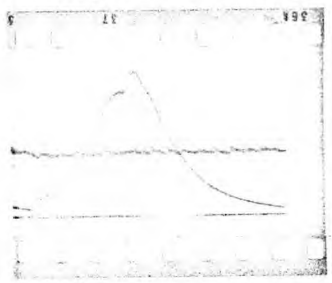
BMEP = 25·7, 65·6% CCM
CO_2 in Intake 25%



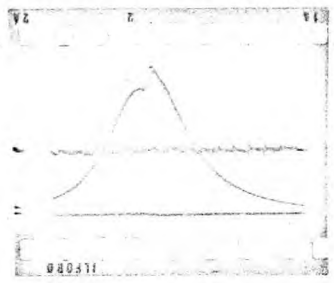
BMEP = 24·7, 66·2% CCM.
CO_2 in Intake 27%



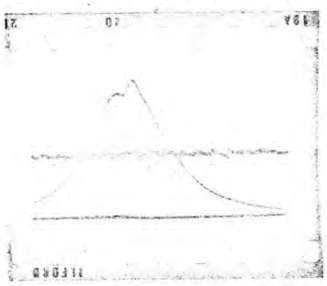
BMEP = 23·7, 66·8% CCM
CO_2 in Intake 31%



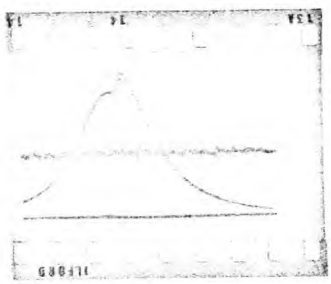
BMEP = 22·8, 67·7% CCM
CO_2 in Intake 35%



BMEP = 21 p.s.i., 68·3% CCM
CO_2 in Intake 37%



BMEP = 32 p.s.i., 63·4% CCM



Engine Speed = 1000 Rev, Pilot fuel = 0·5 lb/h, Injection Timing = 20° BTDC,
Cooling Water Temperature = 70°C.

PLATE (A1.7). A Set of Cylinder Pressure Records.



Pilot Fuelling Rate 0·35 lb/h



Pilot Fuelling Rate 0·5 lb/h



Pilot Fuelling Rate 1·0 lb/h

Injection Timings 20° B.T.D.C., Engine Speed 1000 Rev.

PLATE (A1.8). C.R.O. TRACES OF INJECTOR NEEDLE – LIFT.

C H A P T E R A2

COMPUTING PROCEDURE AND RESULTS

A2.1 Purpose of the Chapter

The calculation of rates of heat release and heat transfer in dual-fuel engines from experimentally obtained pressure-time records is a well-known simple thermodynamic exercise. Recent use of fast computers enabled us to look into the details of the combustion processes, which was hitherto not possible. The essential features of any heat-release analysis ought to be its effectiveness in characterising the combustion processes under study with minimum of simplifying assumptions and economy in computer time.

It is the purpose of this chapter to describe the computing procedures together with the underlying assumptions and to discuss their limitations to present accurately the combustion processes. Results are then presented to illustrate the output of the computer programme.

A2.2 Computing Procedure

A2.2-1 Introduction

Despite various computing procedures which have been referred to in many recent engine research publications (67, 87, 104), it still remains relatively difficult to conduct readily a heat release analysis of a dual-fuel engine from cylinder pressure development records, due mainly to lack of information on the thermodynamic and combustion behaviour of the mixtures of two vastly different fuels which render the analysis complex. This is why, perhaps, there is a dearth of computing procedures in the literature for dual-fuel engines.

With the above context in mind, the present section is set out to provide details of the generalised

computer programme developed in Fortran IV and is workable for dual-fuel, diesel and gas engine operation and also in the event of the absence of spark timings in the latter motored autoignition is implied. The programme computes the rates of heat release on the basis of known pressure-time records. It incorporates iterative smoothing of experimental data scatter and it accounts for dissociation, variability of thermodynamic and transport properties of the system, while a subroutine executes the computation of rates of heat transfer on the basis of either Eichelberg's or Annand's formulations (5).

The benefit of heat release analysis, in addition to being indicative of the characteristic combustion processes, is that it offers the research engineers and designers an effective guide towards thermal and mechanical loading of the engine assembly. The latter aim can be achieved by the help of rational prediction of the cylinder pressure development with the knowledge of heat release pattern. A computing procedure for the prediction of pressure development from a statement of the heat release pattern is also described. Results then follow to illustrate the computations of rates of heat release, rates of heat transfer and the prediction of pressure-time development for dual-fuel, diesel and gas engine operations (46).

A2.2-2 The Calculation of Effective Rates of Heat Release, Heat Transfer and Pressure-time Development Records

Due to the complex and relatively unknown nature of the combustion processes in reciprocating engines, the problem of determining the gross heat release is normally idealised to the extent that the cylinder charge is assumed to be homogeneous. Moreover, the energy as a result of combustion is assumed for simplicity to be released throughout the entire charge at all stages of the working cycle. The application of the first law of thermodynamics to the cylinder charge over an infinitesimally small increment of time will lead to the following

working equation, as shown in Appendix IV:

$$\dot{q} = \frac{1}{J(\bar{\gamma}-1)} \left[\bar{\gamma} P \frac{dv}{d\theta} + V \frac{dP}{d\theta}\right] \frac{d\theta}{dt}$$

where ($\dot{q}$) is the net heat release rate, (P) cylinder pressure, (V) cylinder volume, (θ) crank angle, (t) time and ($\bar{\gamma}$) is the ratio of specific heats of the charge.

An account for any heat loss or gain to the system per unit area can be made with reference to a generalised correlation for the heat transfer proposed by Annand (5), following a survey of heat transfer literature, of the type:

$$Q''_{HT} = a \frac{K}{D} (\overline{Re})^{b} (T-T_w) + c(T^4-T_w^4)$$

where (Q''_{HT}) is the rate of heat transfer per unit area, (a), (b) and (c) are constants, ($\overline{Re}$) Reynolds number, (T) absolute charge temperature, (T_w) is the corresponding temperature of the wall, (K) thermal conductivity and (D) is the engine bore. It is up to the investigator to decide from a knowledge of the relative importance of the radiative to convective heat transfer components and that of the design of his engine, reasonable values for these constants.

Another widely used correlation for the estimation of heat transfer is that due to Eichelberg (19) which is the following:

$$Q''_{HT} = 8.06 \times 10^{-5} (V_p)^{1/3} (PT)^{\frac{1}{2}} (T-T_w)$$

where (V_p) is mean piston speed in ft/s and (P) is the pressure in atmospheres. This empirically based formulation has been adopted by many workers despite its shortcomings mainly because of its simple form.

When an account for heat transfer is made, the gross heat release rate may be determined from a knowledge of p, V, $\frac{dv}{d\theta}$, $\frac{dP}{d\theta}$ and $\frac{d\theta}{dt}$ together with an assumed knowledge of the corresponding variation of the effective thermodynamic and transport properties of the charge.

With this in mind the following simplifying assumptions were incorporated in the computer programme:

(i) Purely for the evaluation of the thermodynamic properties of the system, combustion is assumed initially to take place simultaneously after a significant pressure rise from the normal compression curve. Means are provided to refine these calculations, if need be, on the assumption that the extent of conversion of reactants to products at any instant is directly proportional to the energy released by combustion thus far.

(ii) The reaction is homogeneous with no effective temperature, concentration or pressure gradients within the charge.

(iii) The effects of leakage and residuals, unless otherwise stated are negligible.

(iv) The charge behaves as an ideal gas.

(v) The rate of heat transfer when accounted for can follow either Eichelberg's or Annand's formulations. The working surface temperatures remain unaltered throughout the cycle.

Similar procedures can be followed for the synthesis of pressure-time diagrams based on heat release equation when a knowledge of the pattern of heat release and initial conditions are known.

It is to be expected of course that the relative success of these assumptions will depend on the combustion system being considered and the ultimate use of the data gathered.

A2.2-3 The Computer Programme

The main programme which is written in Fortran IV was used to work with an IBM 7094 computer. Initially, the programme was developed for the determination of heat release rates for a dual-fuel engine operating on methane or propane. It was modified later and used extensively as a generalised programme to handle diesel and gas engine operations equally well.

Fig. A2.1 shows a schematic layout of the programming procedure for the evaluation of rate of heat

release, heat transfer and allied operational parameters such as cylinder charge temperature, rate of pressure rise and cumulative heat release. The listing of this programme appears verbatimly in Appendix VI.

To facilitate effective control the input data are divided into two parts. The first part deals with mainly those data which remain unaltered for a given engine configuration such as engine bore, stroke, the number of steps to be considered, functions for evaluating the thermodynamic properties of the charge constituents etc. While the second group deals mainly with variable parameters such as fuel and air consumption, injection timing, start of ignition and details of pressure development with crank angle.

The programme is controlled sequentially in such a way that its execution is carried out in accordance with the input information available. In the absence of diesel fuel flow rate, for example, control is carried over to gas operation and the composition of the charge is then assumed to remain constant until ignition takes place. Similarly, the control is switched over to diesel operation when the gaseous fuel is found absent, otherwise dual-fuel operation is normally assumed.

A sub-routine is provided for the smoothing of cylinder pressure input data. This smoothing of data was found to be necessary in view of the errors involved in the processing of pressure-time records and the sensitivity of the heat release rate to any pressure variations. The theory of smoothing data scatter, on the principle of least square fit, is given in Appendix VII.

The mean cylinder charge temperature is calculated on the basis of the smoothed pressure values and cylinder volume as supplied by the respective sub-routines and employing the ideal gas relationship. When combustion is taking place, the cylinder charge is assumed initially, for a small increment of crank angle rotation, to be the product of complete combustion. This assumption is then modified iteratively to account for dissociation and variable specific heats employing special sub-routines.

The extent of consideration of dissociation can be varied depending on the accuracy required and the charge temperature. Dissociation can be ignored, for example, when the molar fraction of the dissociated species falls below a certain specified percentage (in our case 5%) of their respective parent products. This procedure can be improved upon, if need be, by the facility of repeating the calculations on the assumption of finite rate of conversion of the reactants to products in a manner depending on the extent of cumulative heat release. This latter procedure, although perhaps lengthy, is desirable in applications where heat is released gradually over a wide range of crank angle rotation such as in spark ignition engines. In diesel engine applications, however, the assumption of a step change from reactants to products appears to be normally of sufficient accuracy.

The net heat release over the small increment of crank angle $\Delta\theta$ is calculated using the heat release equation and thermodynamic properties defined as polynomials in temperature based on data reported in the J.A.N.A.F. Tables (31). The associated heat transfer is then calculated by a sub-routine based on Annand's formulation. Facilities are provided for the computation of the transport properties of the cylinder charge for any temperature together with the computation of the heat transfer coefficient if need be, on the basis of Eichelberg's formulation. The extent of heat transfer is then calculated taking into consideration the working temperature of the cylinder liner and head and that of the piston together with their respective areas.

The gross heat release is then found by the summation of the net heat release rate and that of heat loss. Cumulative heat release up to that point is then calculated by numerical integration employing Simpson's Rule (see Appendix VIII).

A progressive iterative execution of the above calculations over consecutive small increments of crank angle rotation is then carried out for the range specified at the outset of the programme.

For many design and theoretical considerations the gross heat release pattern may be assumed from a theoretical or experimental evaluation of the system. The pressure-time development record will then be required probably as a part of a complete synthesis of an engine cycle incorporating the processes of induction and exhaust. For this sort of application essentially a reversed procedure to that indicated for the main programme, is followed and is shown schematically in Fig. A2.2. It incorporates iterative procedures for the calculation of the pressure for each increment over the time interval considered.

A2.3 Presentation of Results

The results of heat release analyses are presented in three parts; the first part deals with a detailed examination of combustion porcesses in dual-fuel engines, the second demonstrates the generality of the computer programme by presenting the heat release diagrams of diesel, gas and motored autoigniting engine cycles, while the third brings together, for the sake of comparison, heat release records of various other important configurations of reciprocating engines reported in the literature.

A2.3-1 Rate of Heat Release Records of a Dual-fuel Engine

A large number of pressure-time records were obtained over a wide range of operating conditions of the dual-fuel engine. These records were then processed and analysed using computing methods as outlined in the preceding section. Fig. A2.3 is a typical example of the diagrams constructed directly from the computer results. The parameters considered are cylinder gas pressure, rate of pressure rise, the gross rate of heat release and heat transfer, cumulative heat release and cylinder gas temperature. Their values were calculated with reference to each degree of crank rotation over a normal range of 150°

crank rotation and the charge drawn in per cycle. Figs. A2.4 to A2.7 show a cross-section of superimposed rate of heat release diagrams computed for four ranges of pilot fuelling and for different concentrations of methane in intake under constant pilot injection timings and engine speed. The concentration of primary fuel covered a wide range from the case when sufficient power was produced just to overcome the frictional losses to that when knock was detected. Fig. A2.8 presents the cumulative heat release of the rates shown in Fig. A2.4. Figs. A2.9 to A2.11 show the effect of varying pilot fuel on cylinder pressure, rate of heat release and cumulative heat release, respectively, with a constant methane concentration. Similarly, another set with a different constant methane concentration is covered in Figs. A2.12 to A2.14 which present cylinder gas pressure, pressure rates and rate of heat release superimposed. Shown in Fig. A2.15 is a typical record of violent knocking combustion. It may be noted that the pressure oscillations have been smoothed out during the data processing and iterative smoothing.

The effect of carbon dioxide addition to methane in intake is depicted by Figs. A2.16 and A2.17. A wide range of CO_2 was added from pure methane operation under knocking to that of almost 50% methane used when further addition was responsible for sporadic combustion rendering the results irreproducible. Fig. A2.25 presents the effect of CO_2 addition on engine performance. Fig. A2.18 illustrates the pressure prediction with the known rates of heat release as described in the computing procedure shown in Fig. A2.2.

A2.3-2 Typical Heat Release Records of Diesel, Gas and Motored-Engine Operation

Figs. A2.19 to A2.21 explain the main features of combustion heat release in diesel, gas and motored auto-ignition cycles respectively. It is illustrated that the present computer programme, because of its generalised nature, can effectively be employed for heat release analyses of other modes of piston engine operation.

A2.3-3 Heat Release Records of Stratified Charge Combustion

In order to bring the combustion processes in dual-fuel engines into real perspective, it is endeavoured to gather some more configurations of engine operation in addition to what has been computed by the present computer programme. Figs. A2.22 to A2.24 serve this purpose. Whereas Fig. A2.22 is a typical example of compression ignition of diesel fuel under 'M' system, the spark-ignition of stratified gasolene combustion is presented by Fig. A2.23. Fig. A2.24 explains the essential features of spark-ignition of carburetted gasolene. It is pointed out that the heat release records presented in Figs. A2.22 to A2.24 belong to comparable conditions, as far as possible, to that of the dual-fuel combustion processes presently examined. The relevant references for these figures are affixed to the respective diagrams.

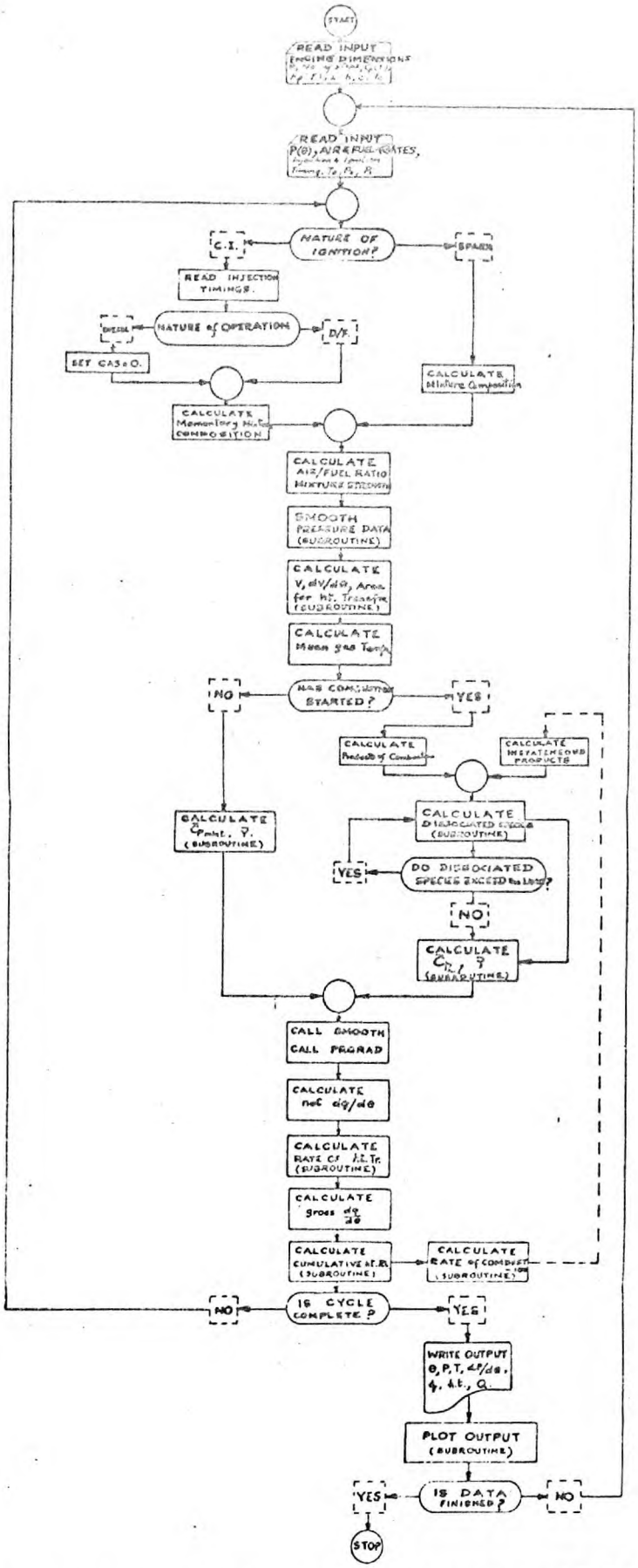


Fig. A2.1: BLOCK DIAGRAM OF THE COMPUTER PROGRAM
—ANALYSIS OF HEAT RELEASE—

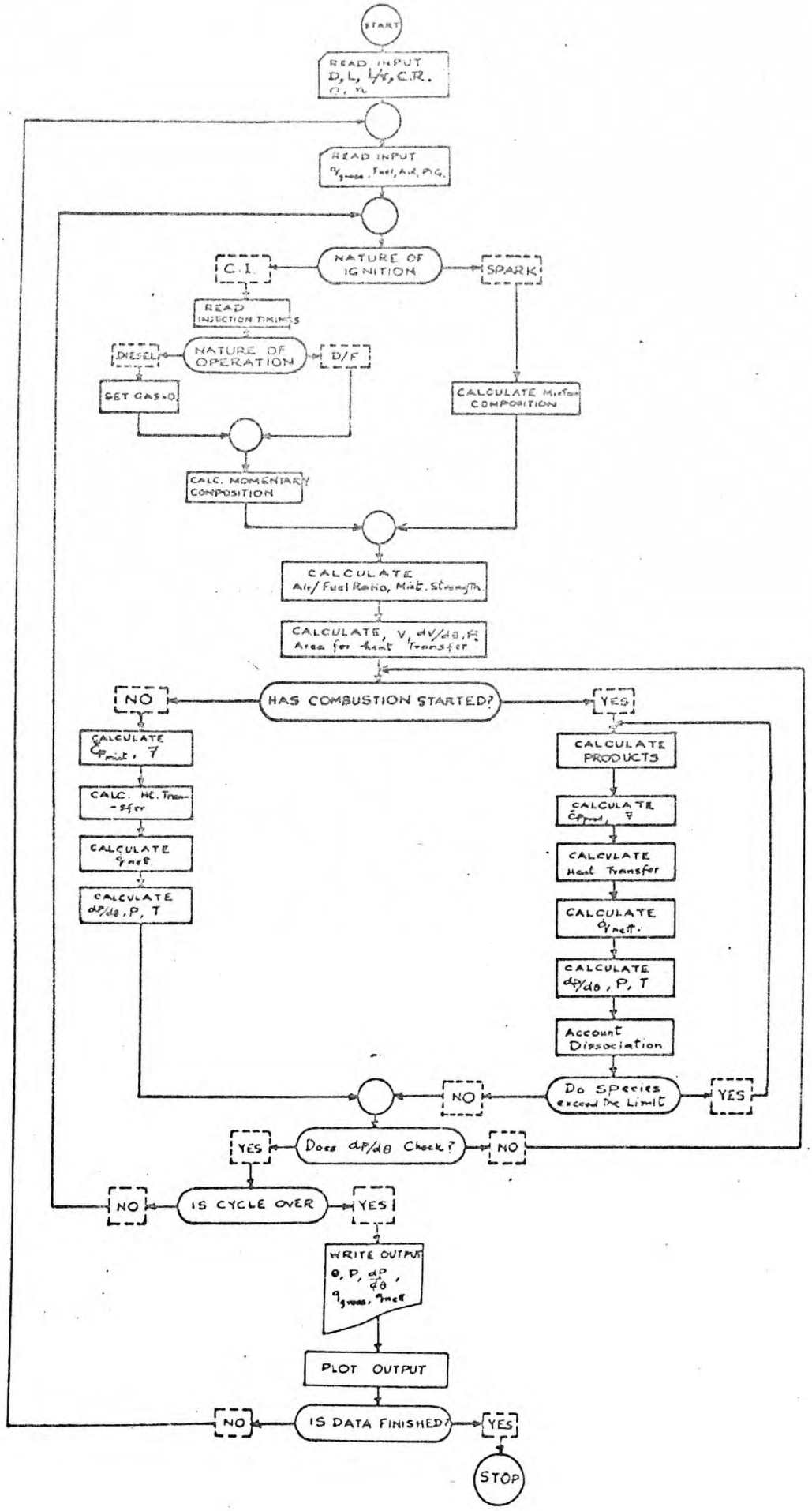


Fig. A2.2: Block Diagram of the Computer Programme — Prediction of pressure from known heat release pattern.

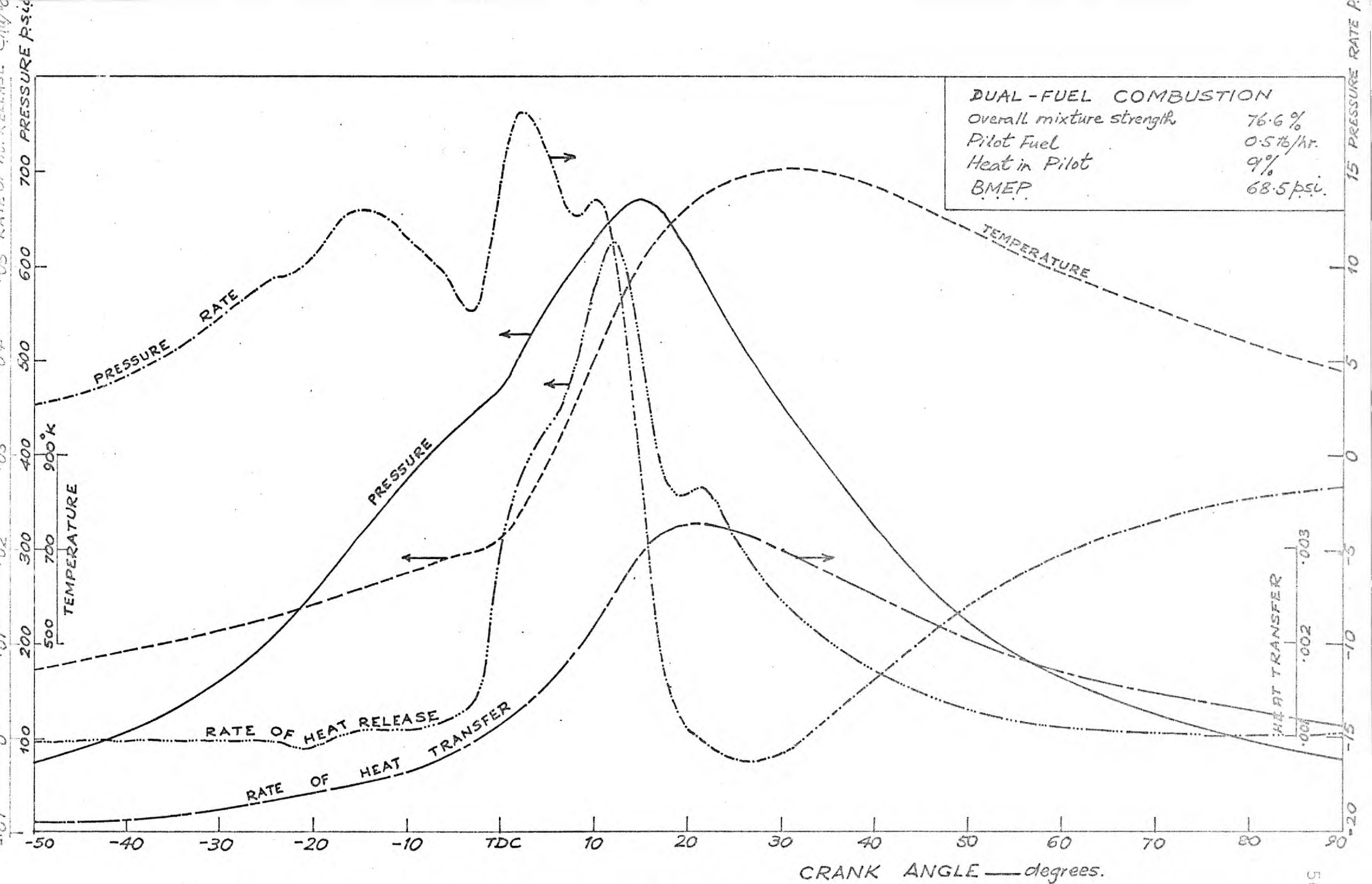


Fig. (A2.3) Typical output plots from IBM 7094 computer.

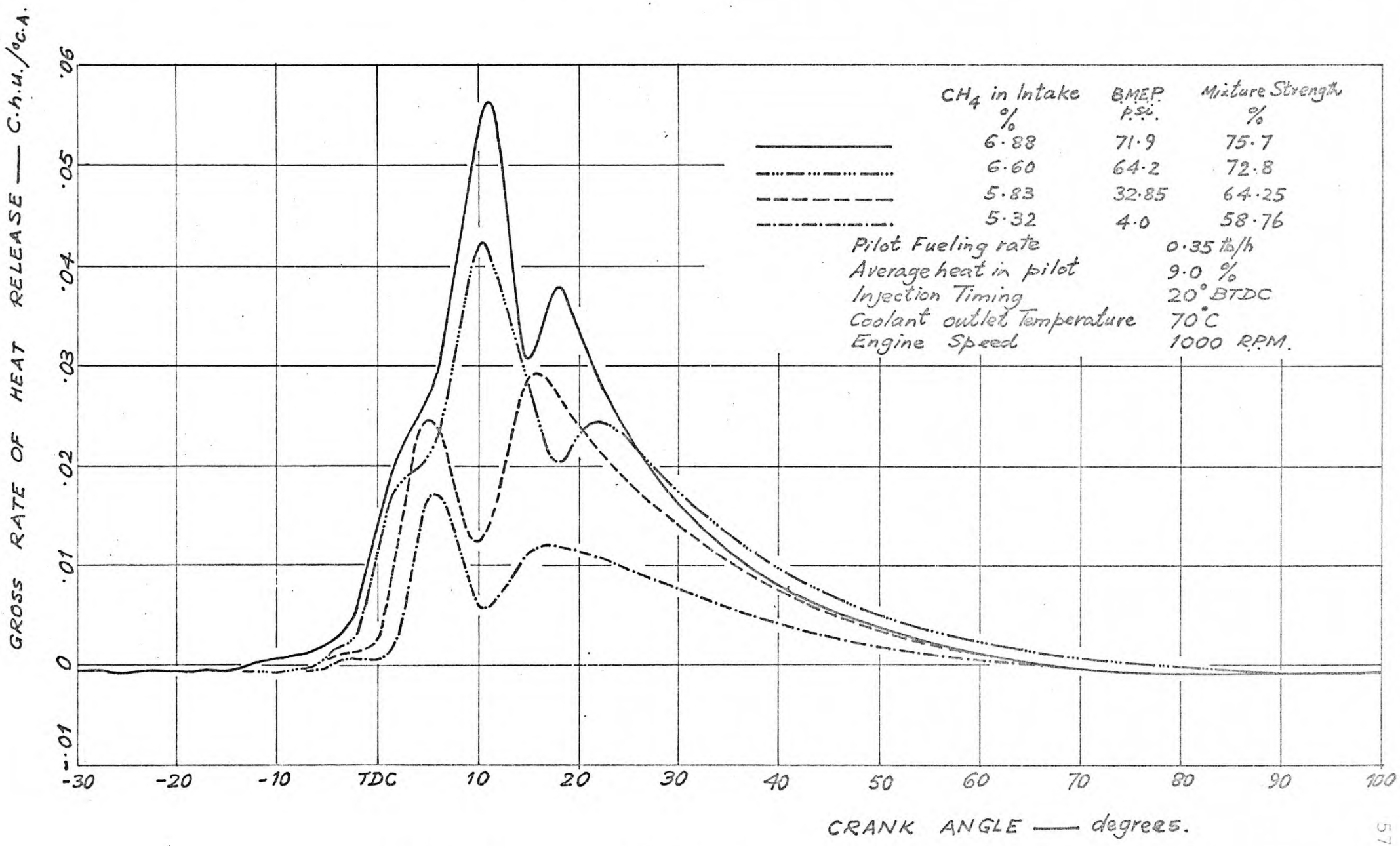


Fig. A2·4: Analysis of heat release – effect of varying gaseous fuel concentration with a constant pilot fuelling rate of 0·35 lb/h.

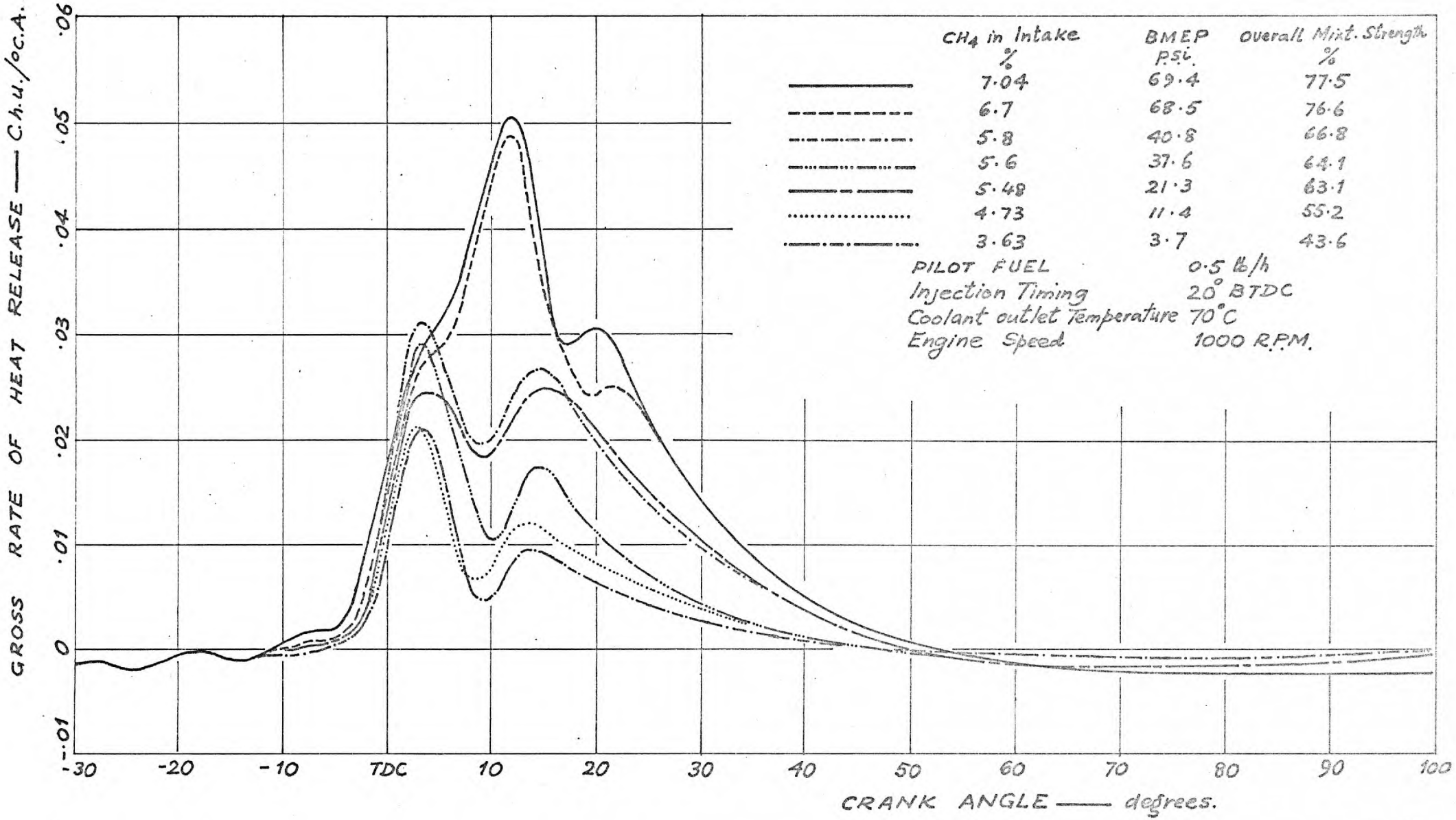


Fig A2·5: Effect on rates of heat release due to variation of gaseous fuel concentration in a dual-fuel engine running on a constant pilot rate of 0·5 lb/h.

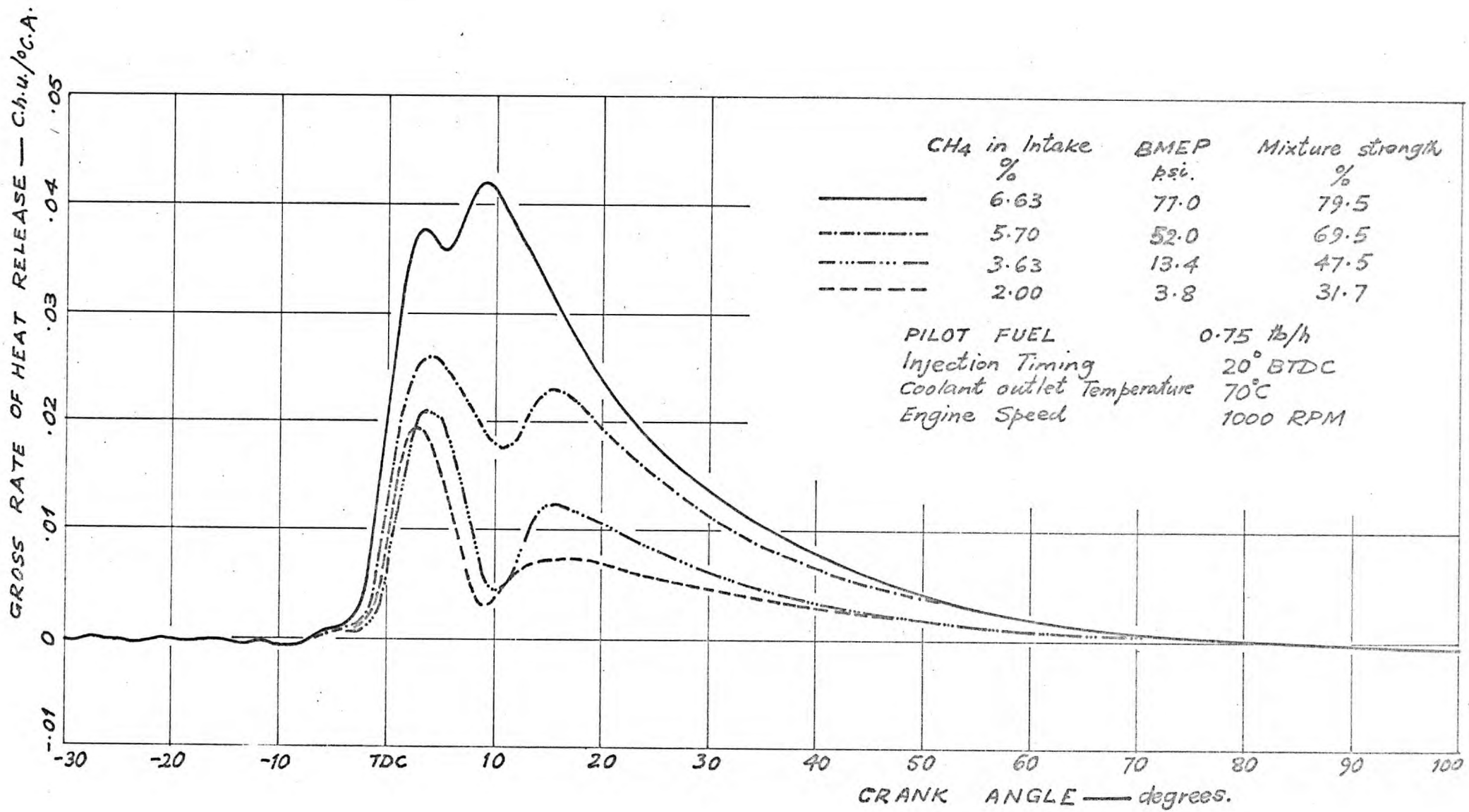


Fig. (A2.6) Analysis of rate of heat release — effect of varying methane concentration with a constant pilot fuelling rate of 0·75 lb/h.

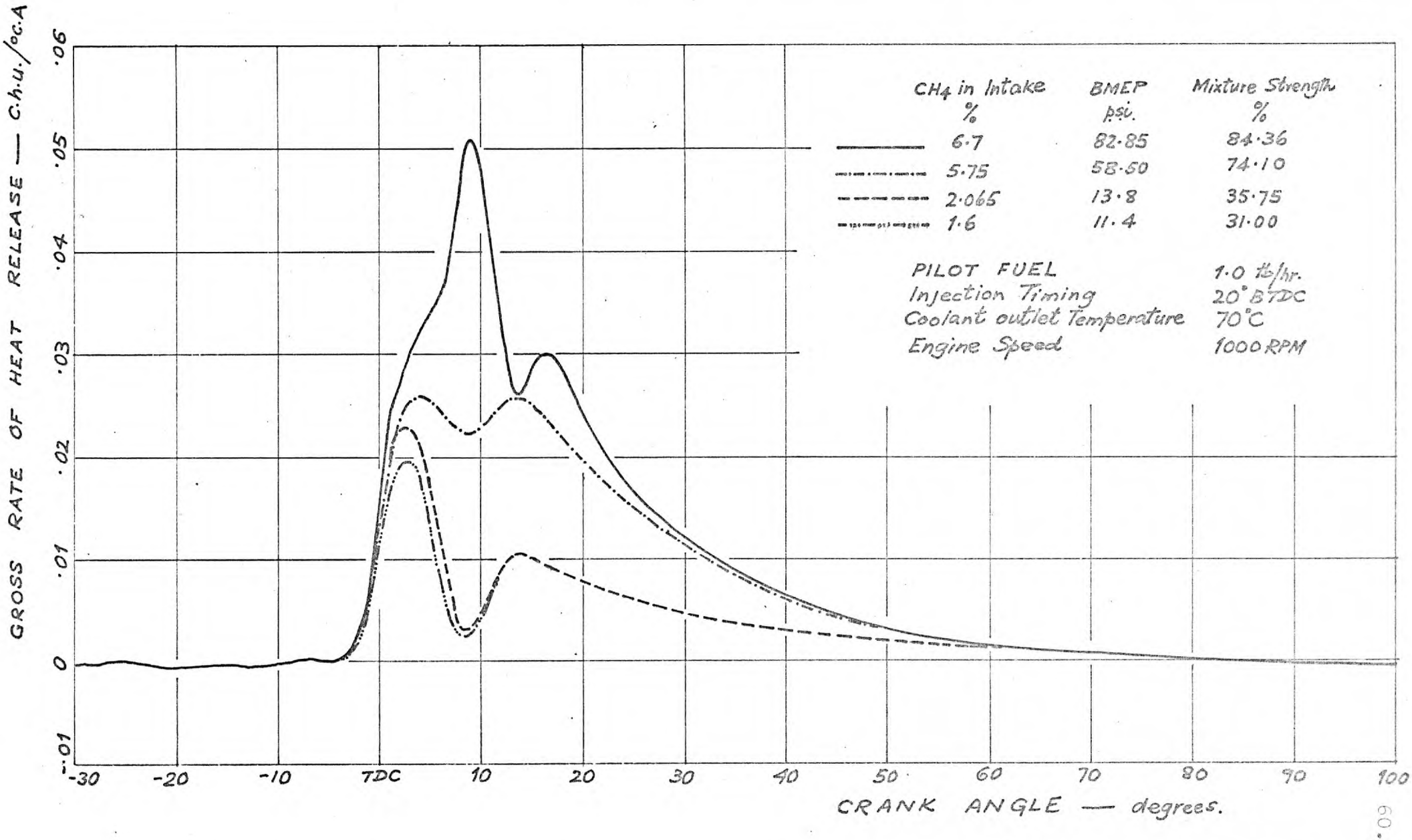


Fig. A2·7: Analysis of rates of heat release — effect of varying methane in intake with a constant pilot rate of 1·0 lb/h.

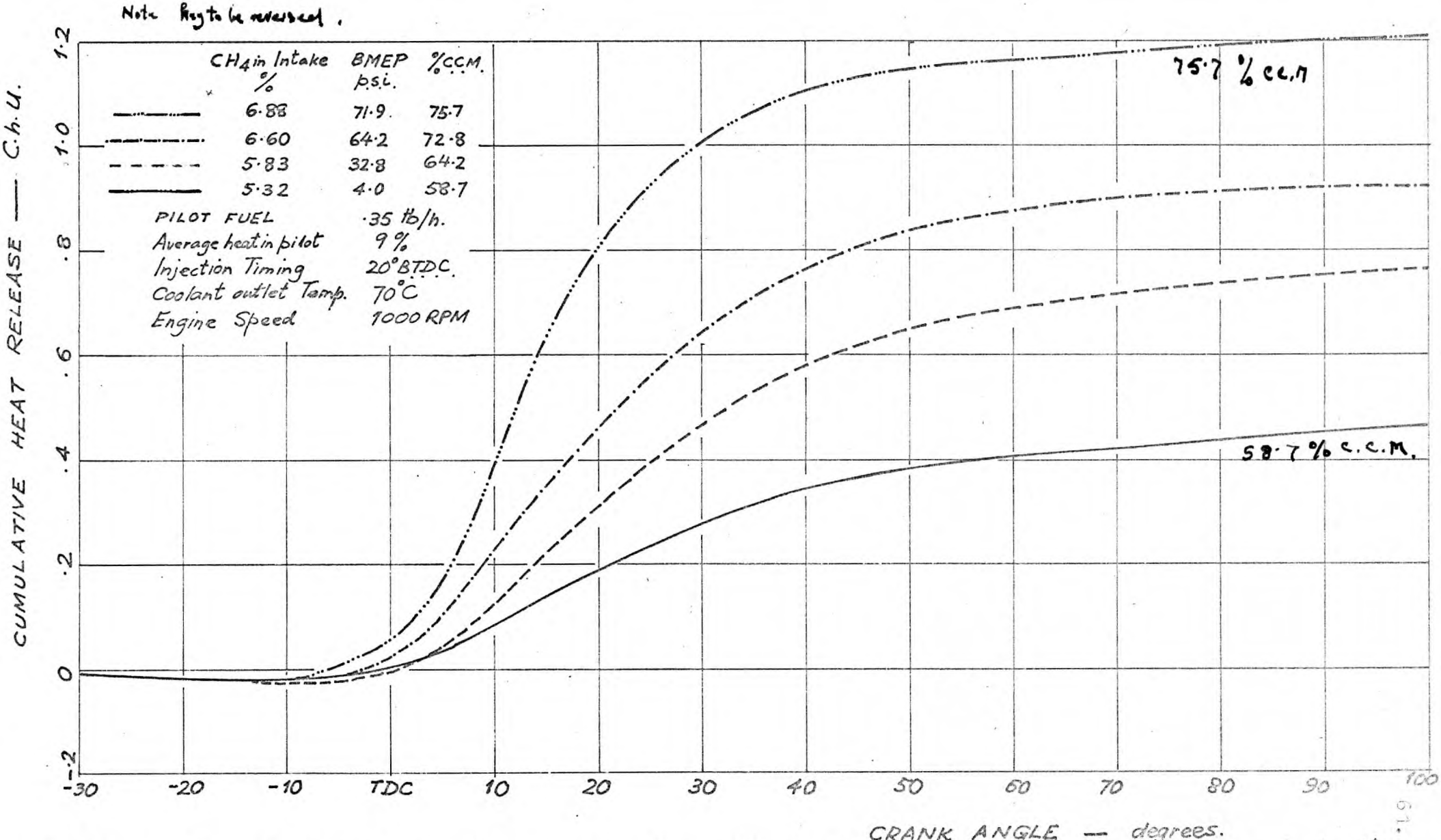


Fig. A2.8: Cumulative heat release records - effect of varying gaseous fuel concentration with constant 0.35 lb/h pilot rate.

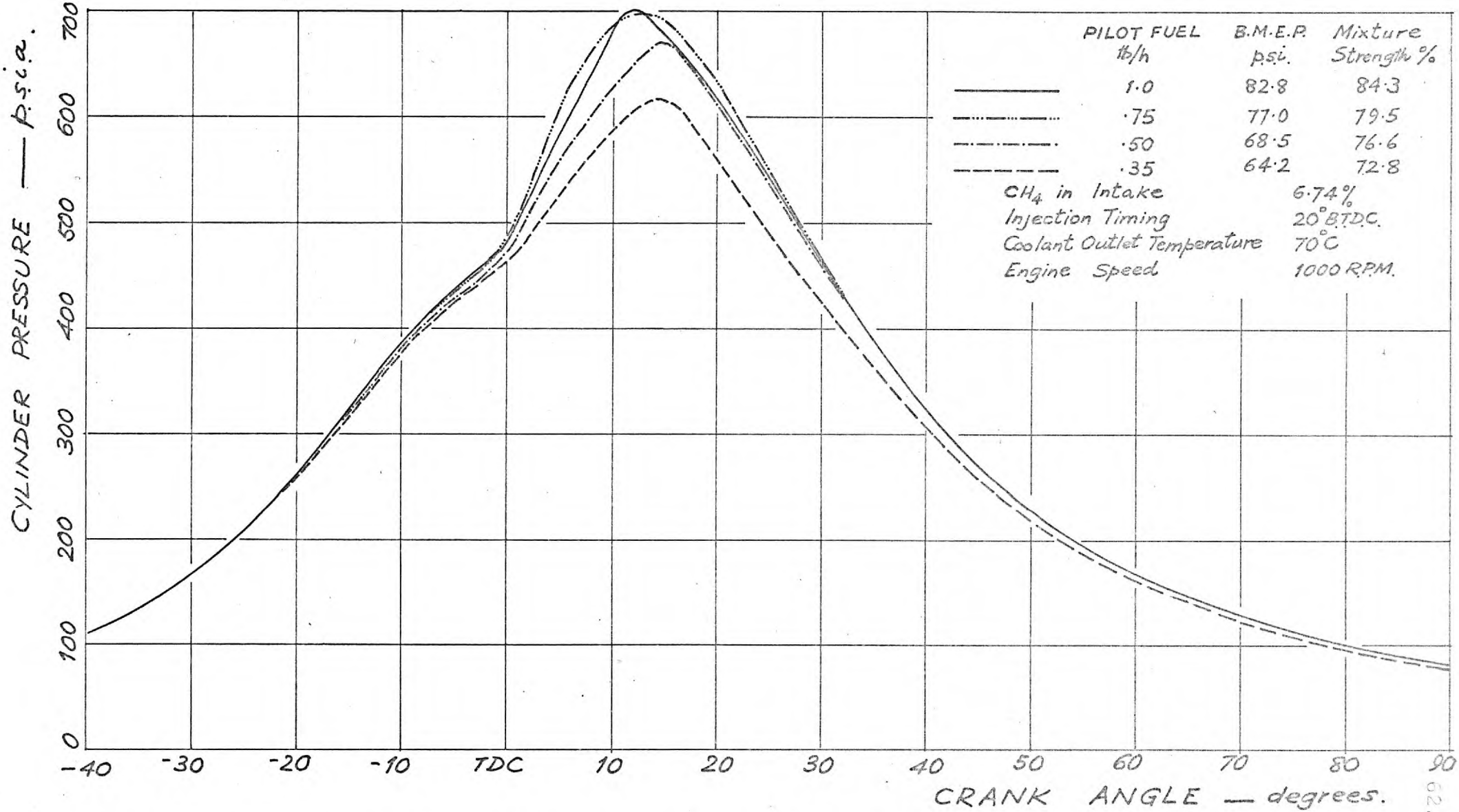


Fig. A2.9: Cylinder gas pressure records: effects of varying pilot fuel with a constant methane concentration in intake.

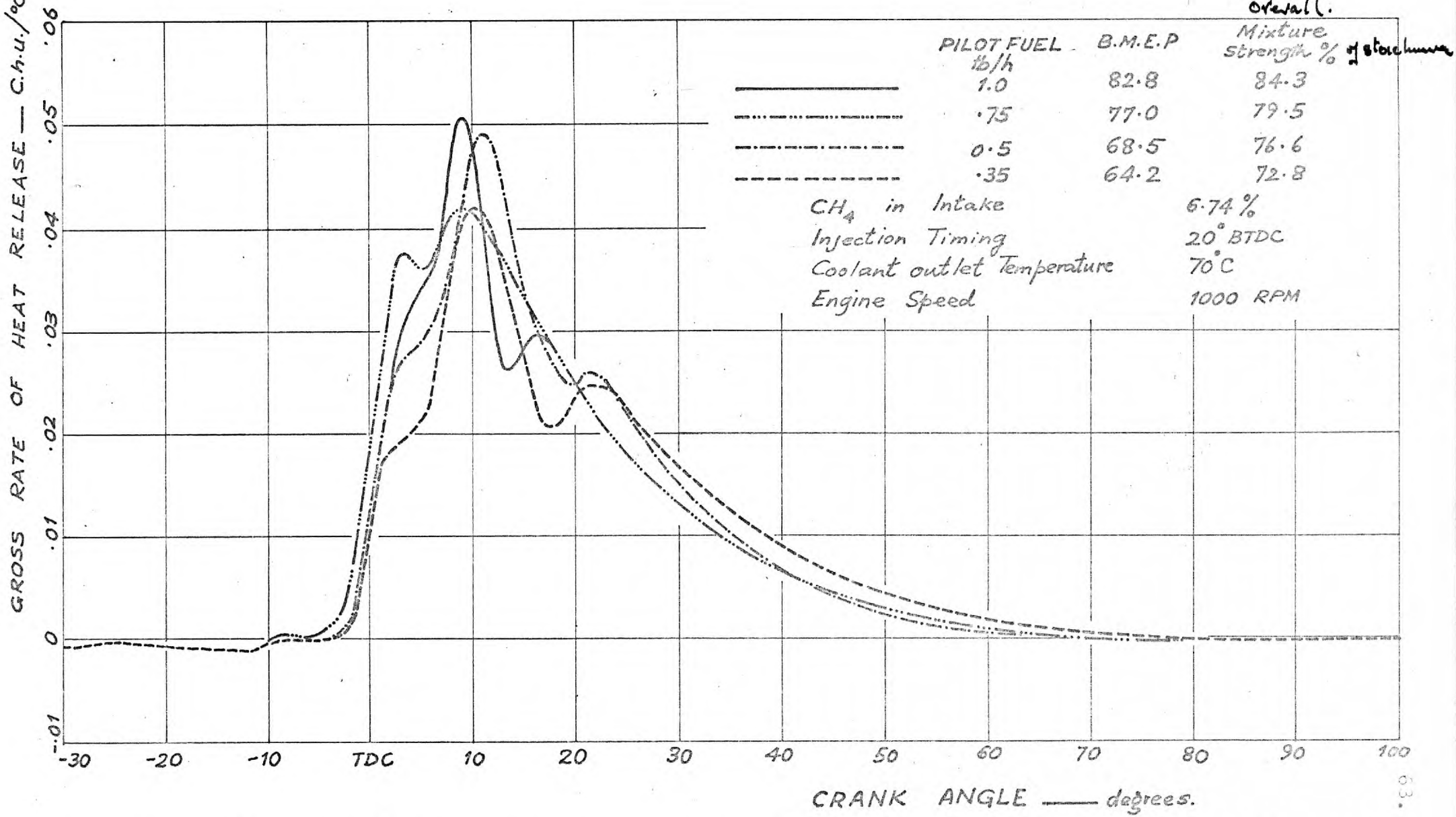


Fig. A2.10: Analysis of heat release variations for a dual-fuel engine - effects of varying pilot fuel with a constant methane concentration in intake.

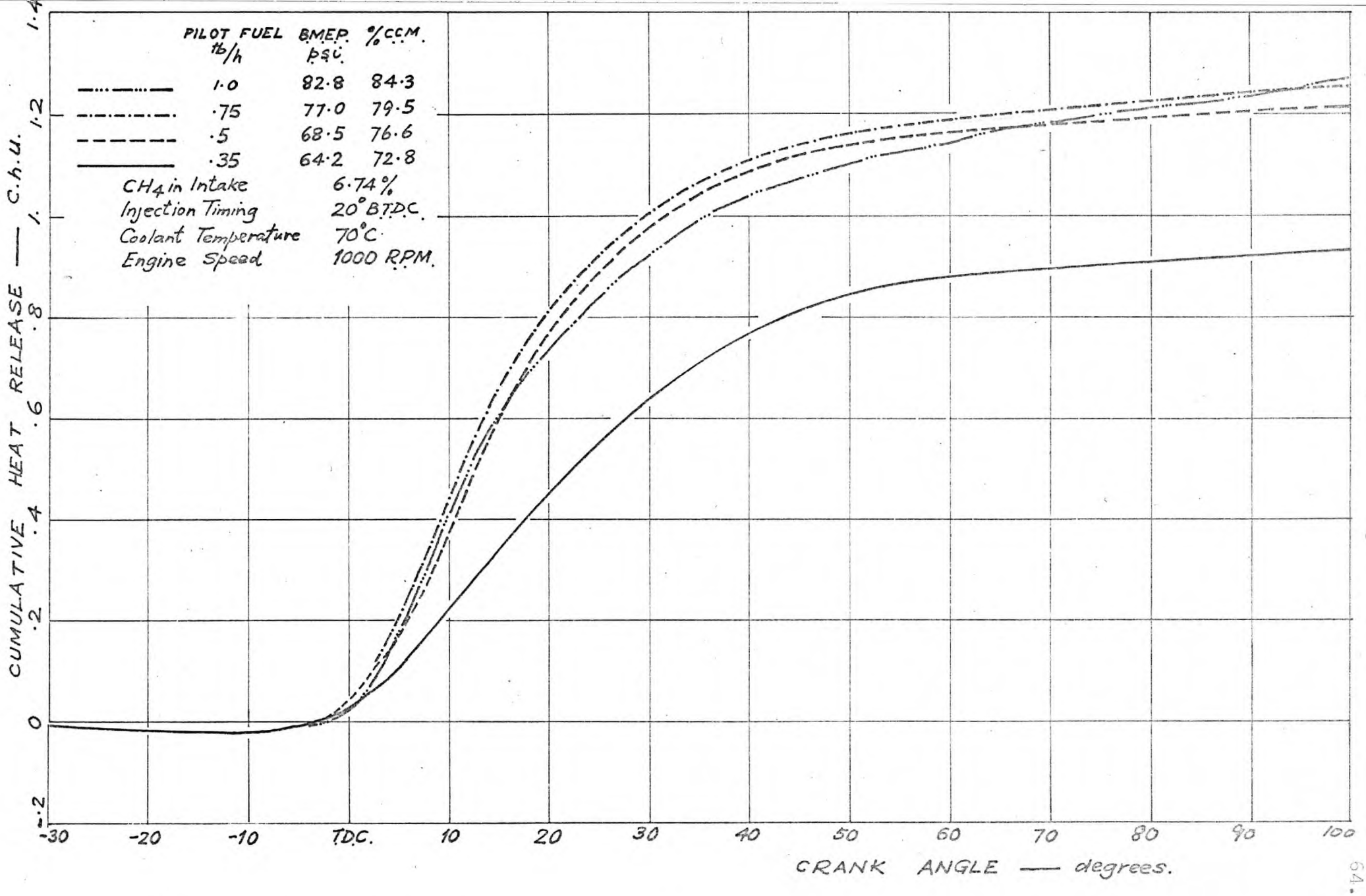


Fig. A2.11: Cumulative heat release records for a dual-fuel engine – effects of varying pilot with a constant gaseous fuel in intake.

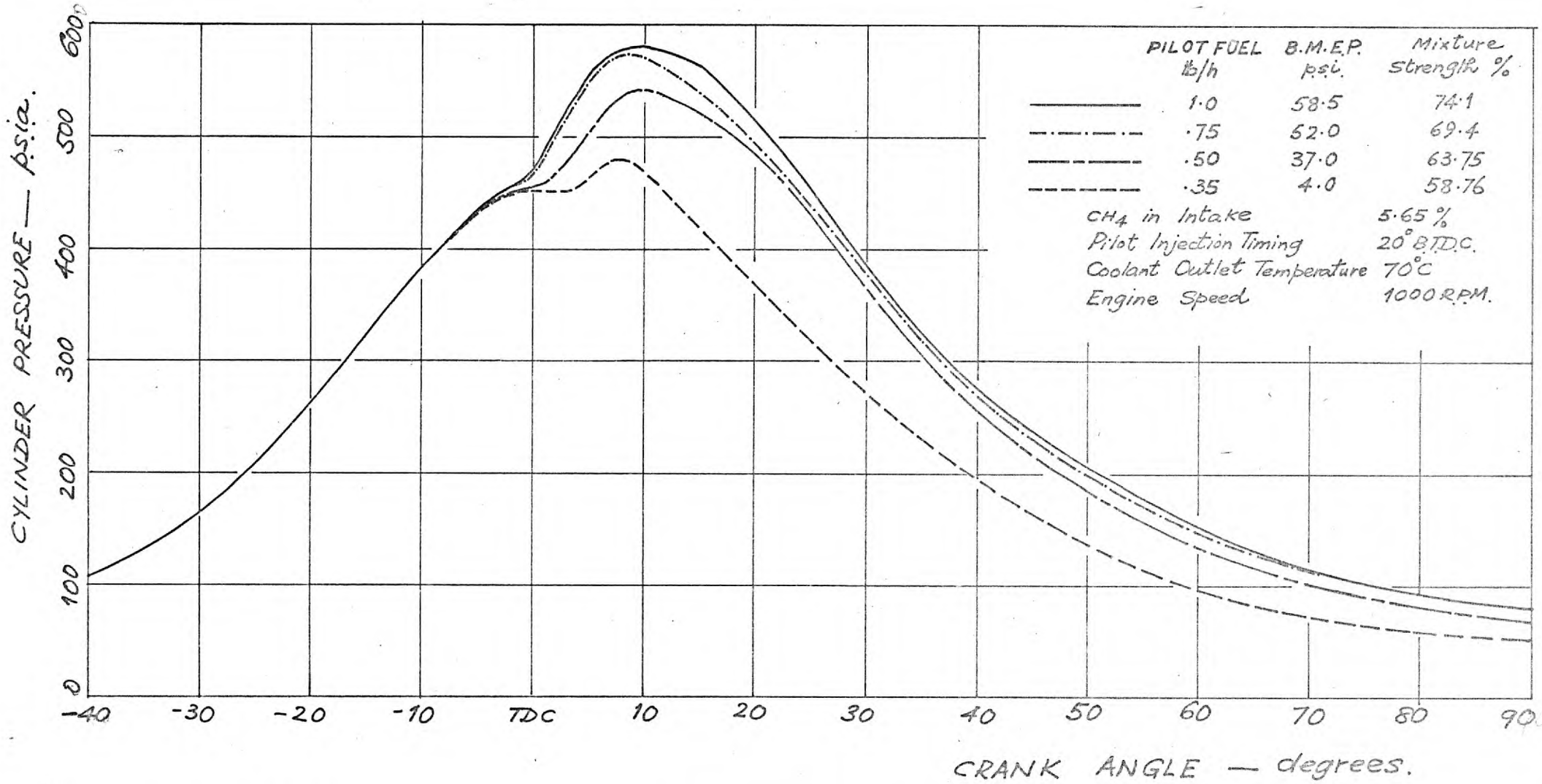


Fig. A2.12: Cylinder gas pressure records: effect of varying pilot fuel with a constant CH4 flow rate.

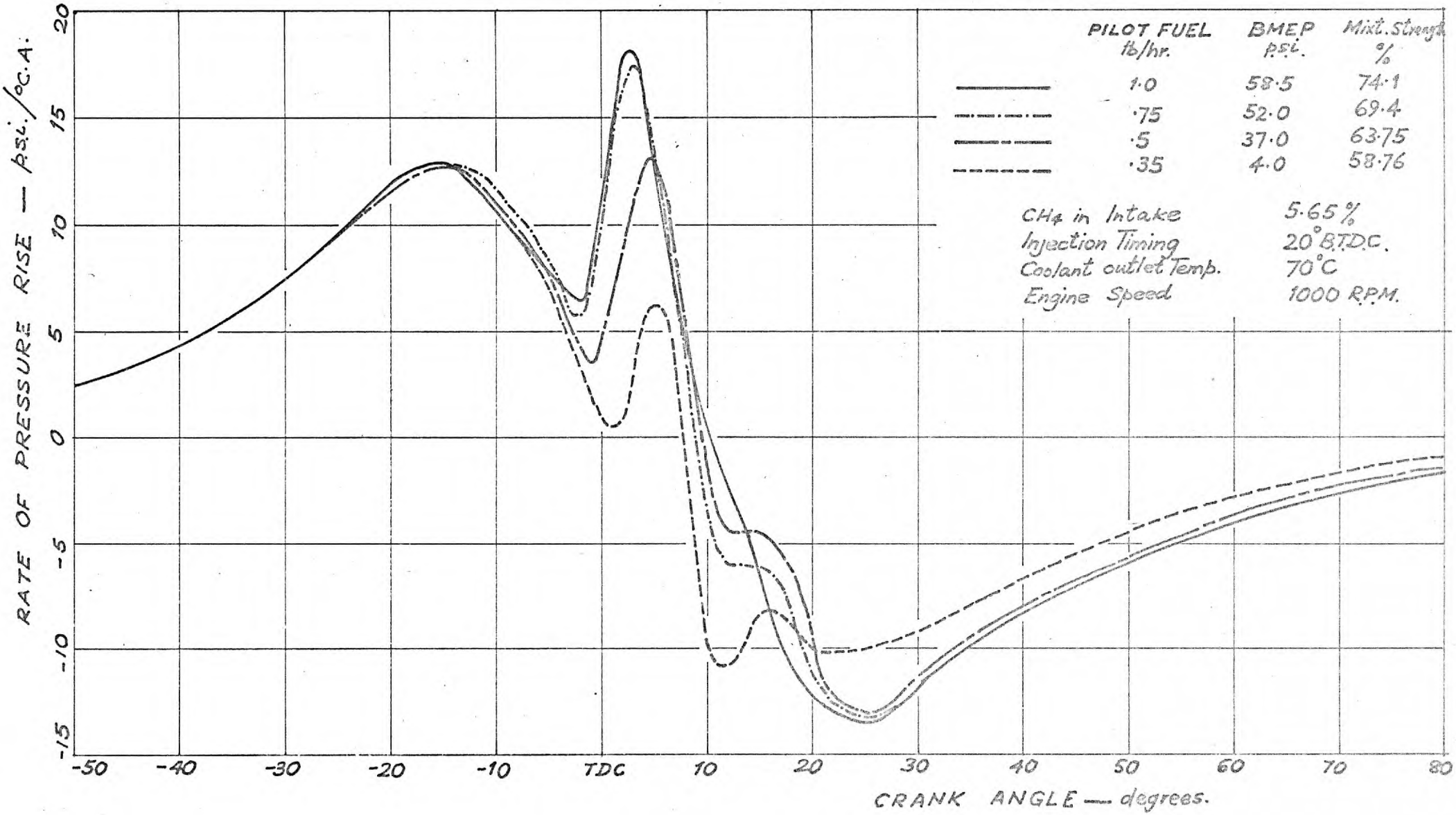


Fig. A2.13: Pressure-rate records – effects of varying pilot fuel with a constant methane concentration in intake.

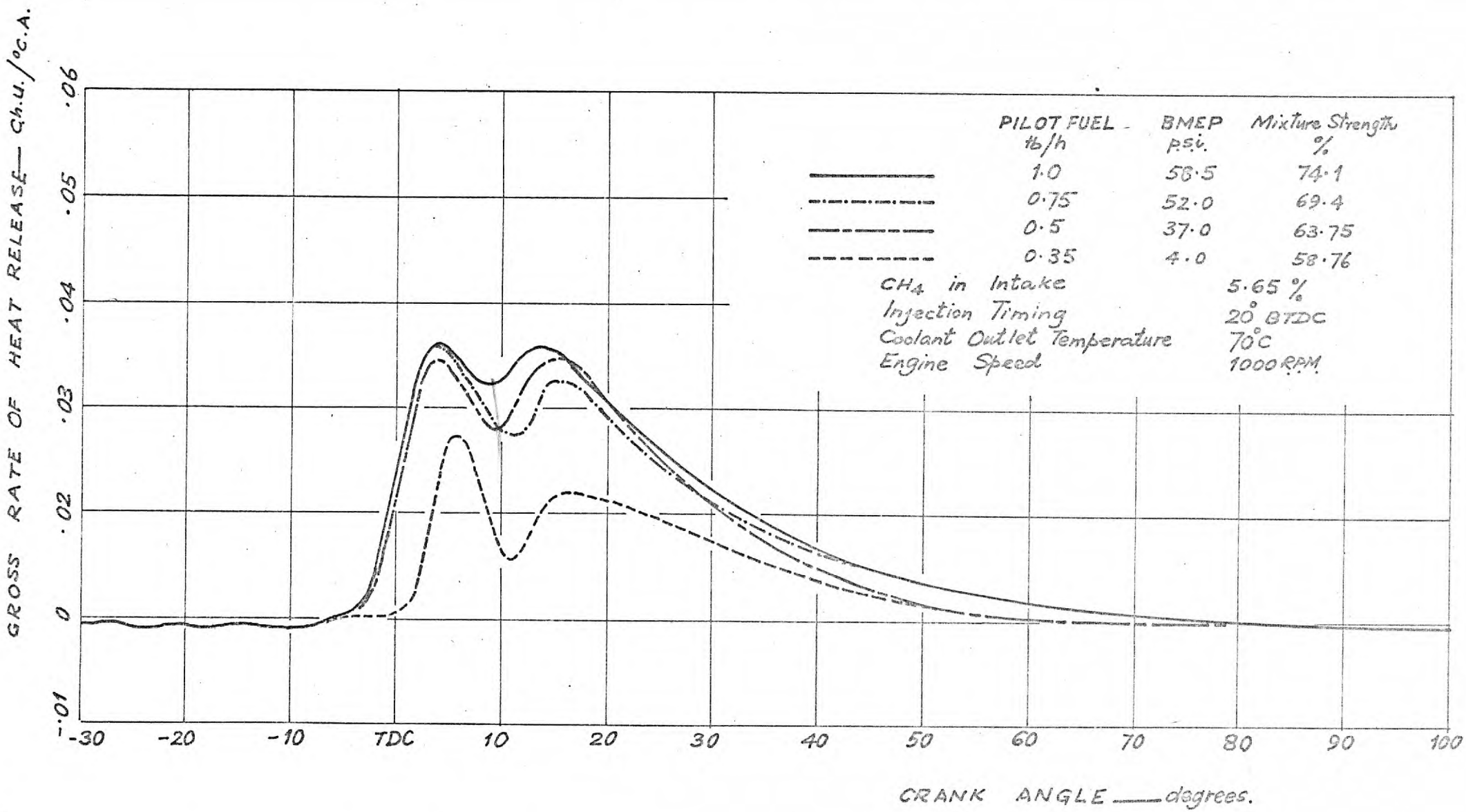


Fig. A2.14: Analysis of heat release variations - effect of varying pilot fuel with a constant methane concentration in intake.

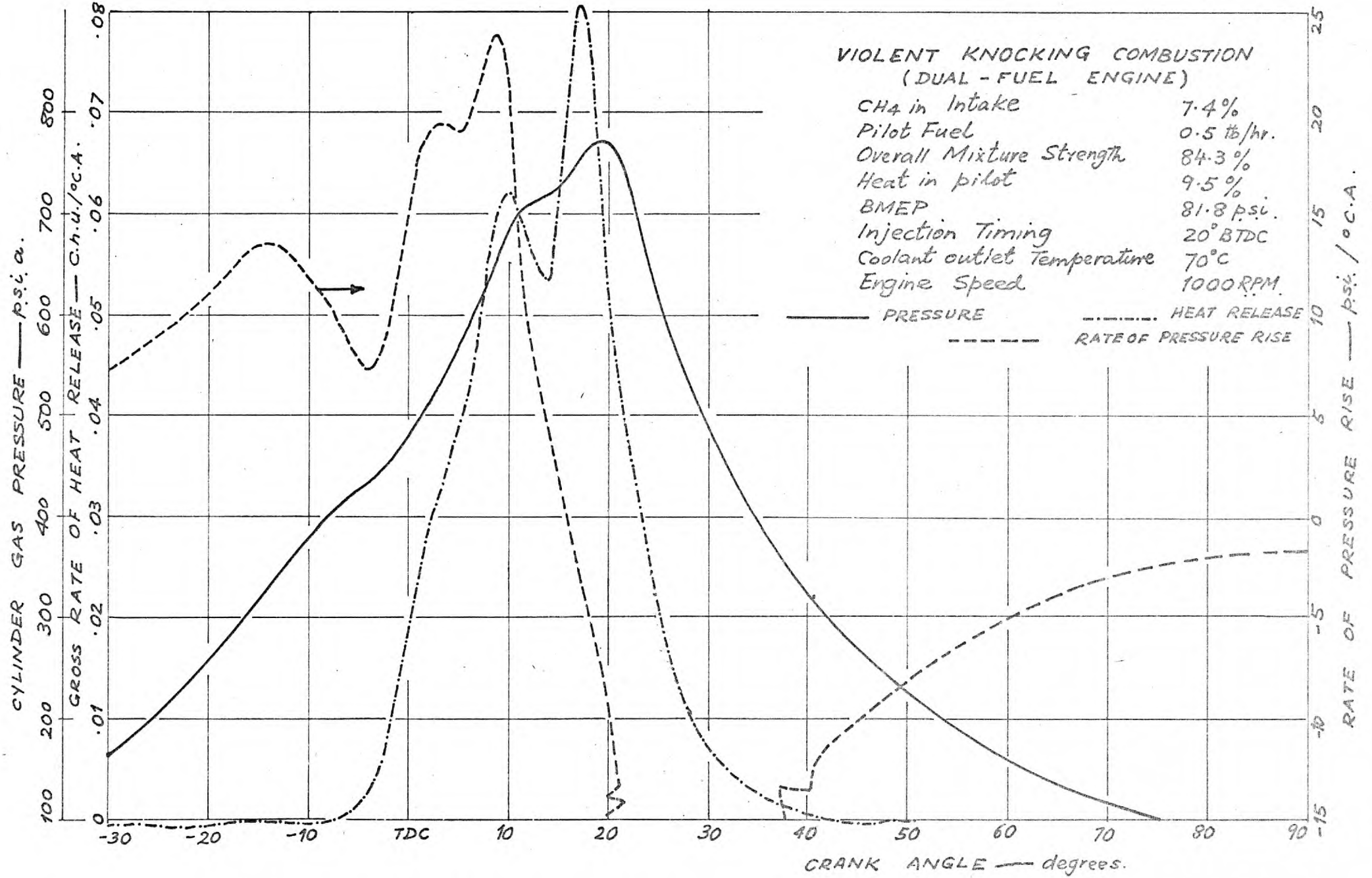


Fig. A2.15: Analysis of heat release variations during a violent knocking dual-fuel engine cycle.

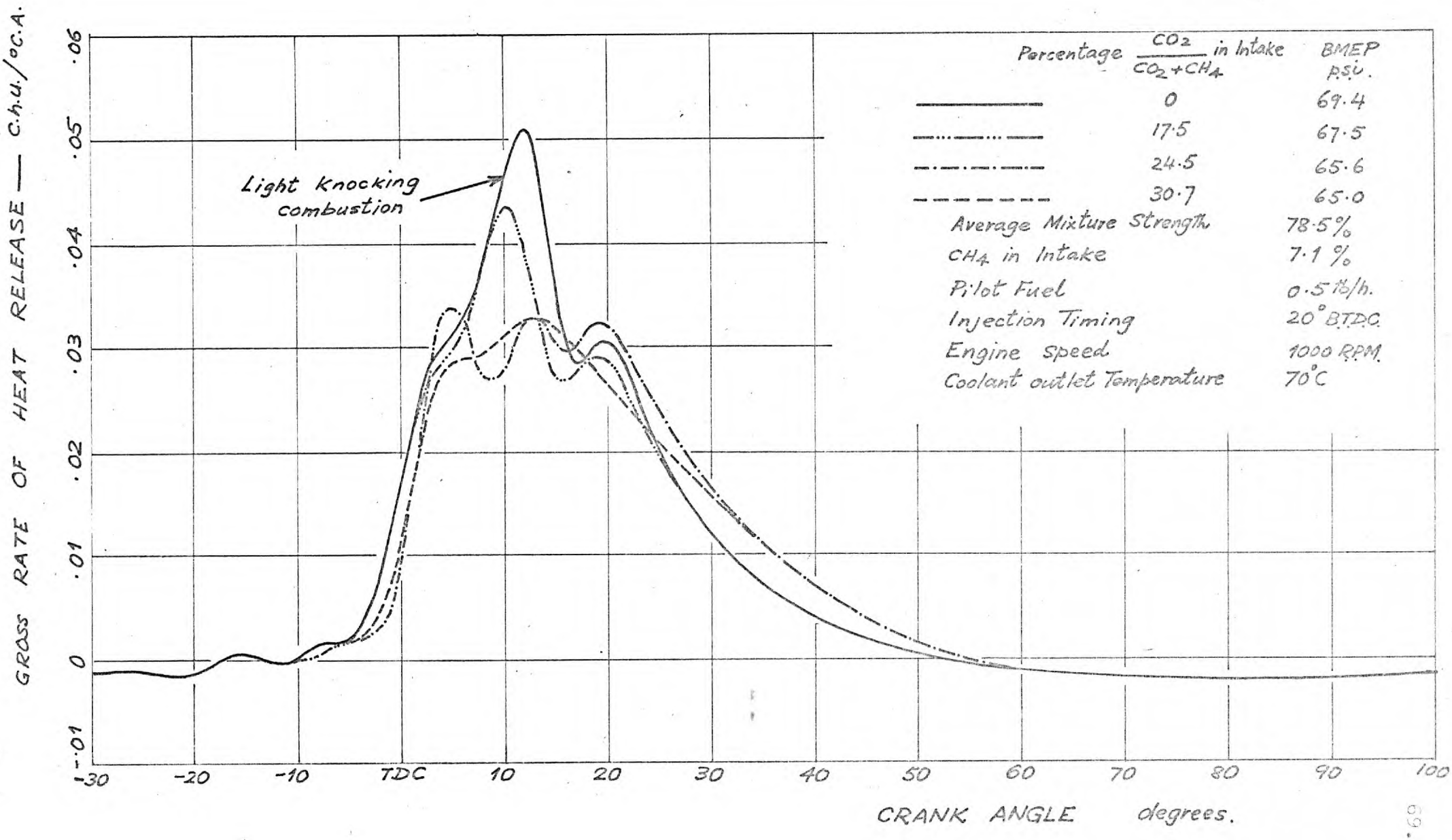


Fig. A2.16: Analysis of heat release variations for a dual-fuel engine: effects of varying CO_2 concentration in intake for a constant average mixture strength and pilot quantity.

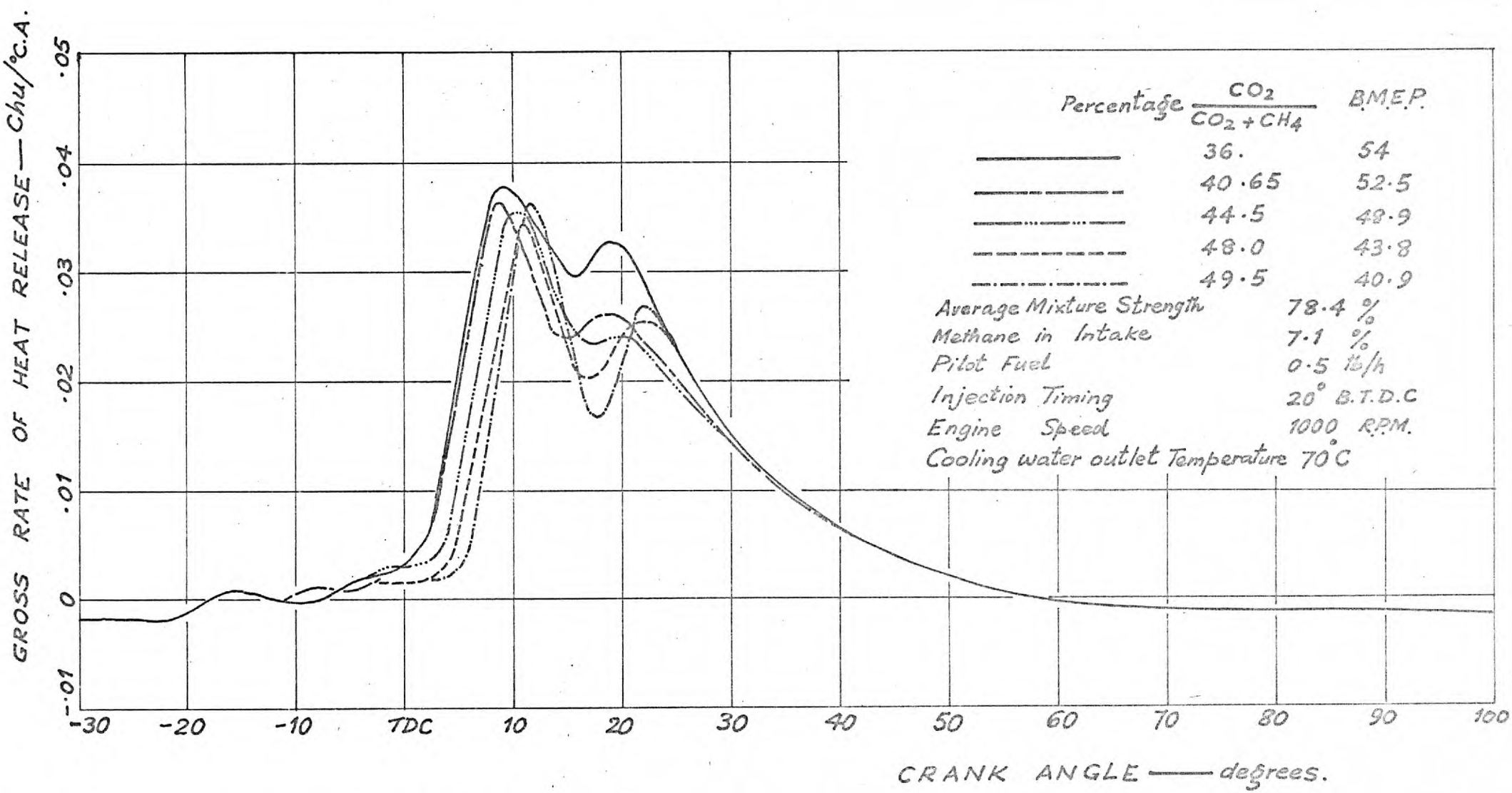


Fig. A2.17 : Analysis of heat release variations for a dual-fuel engine : effect of varying CO_2 concentration in intake for a constant average mixture strength and pilot quantity.

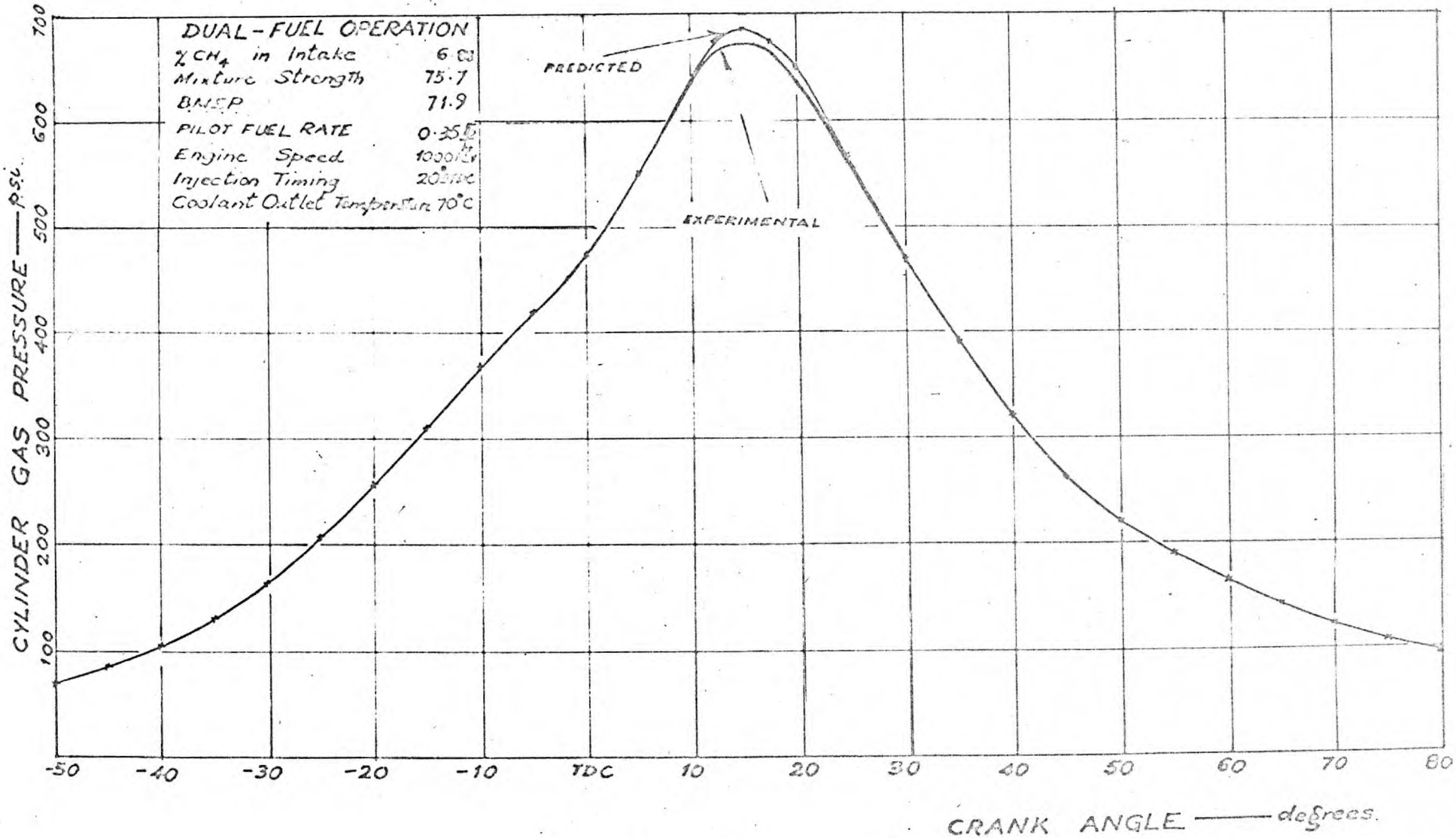


Fig. A2.18: Computed pressure variations from known heat release rates.

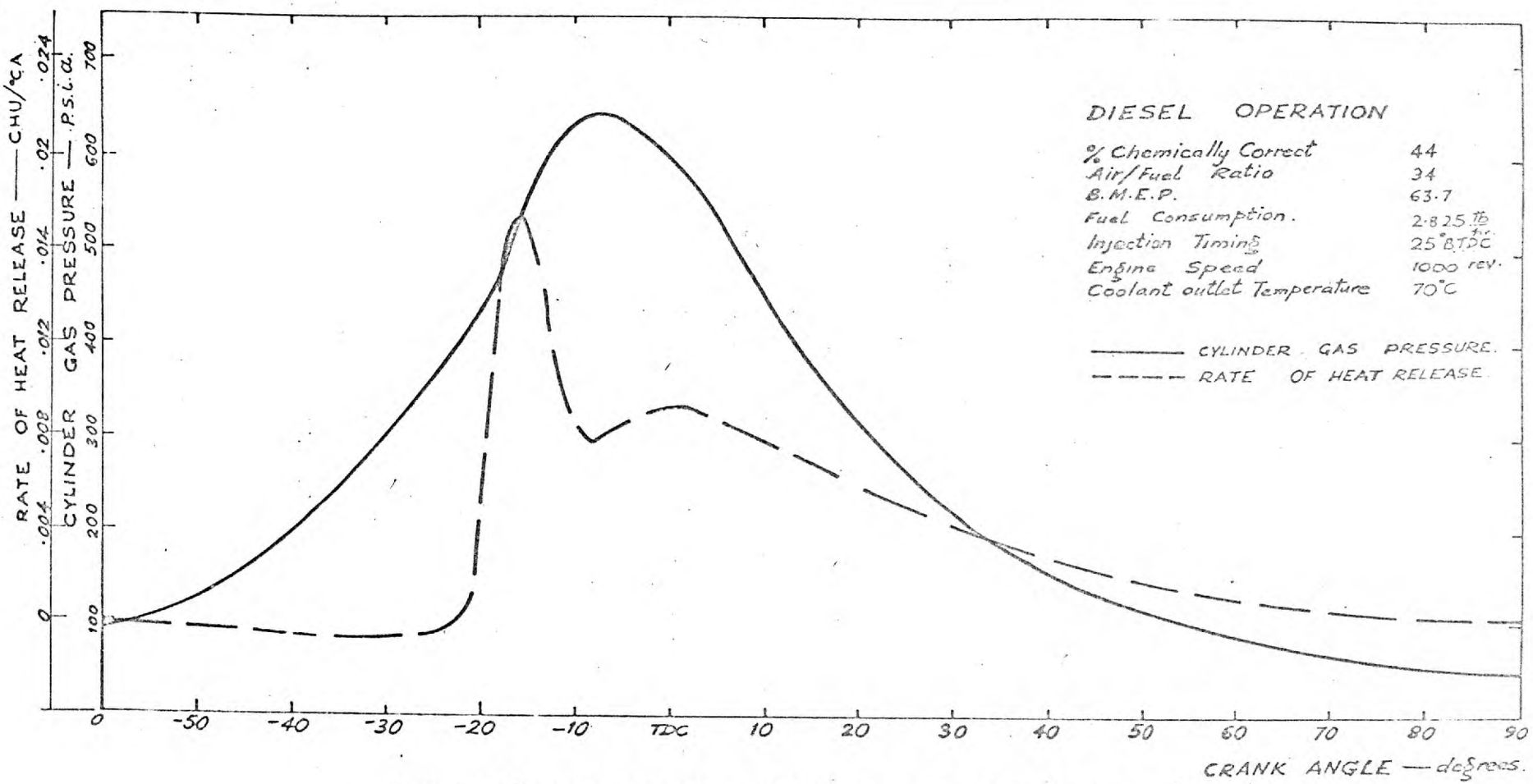


FIG. A2·19: HEAT RELEASE ANALYSIS OF DIESEL "CYCLE".

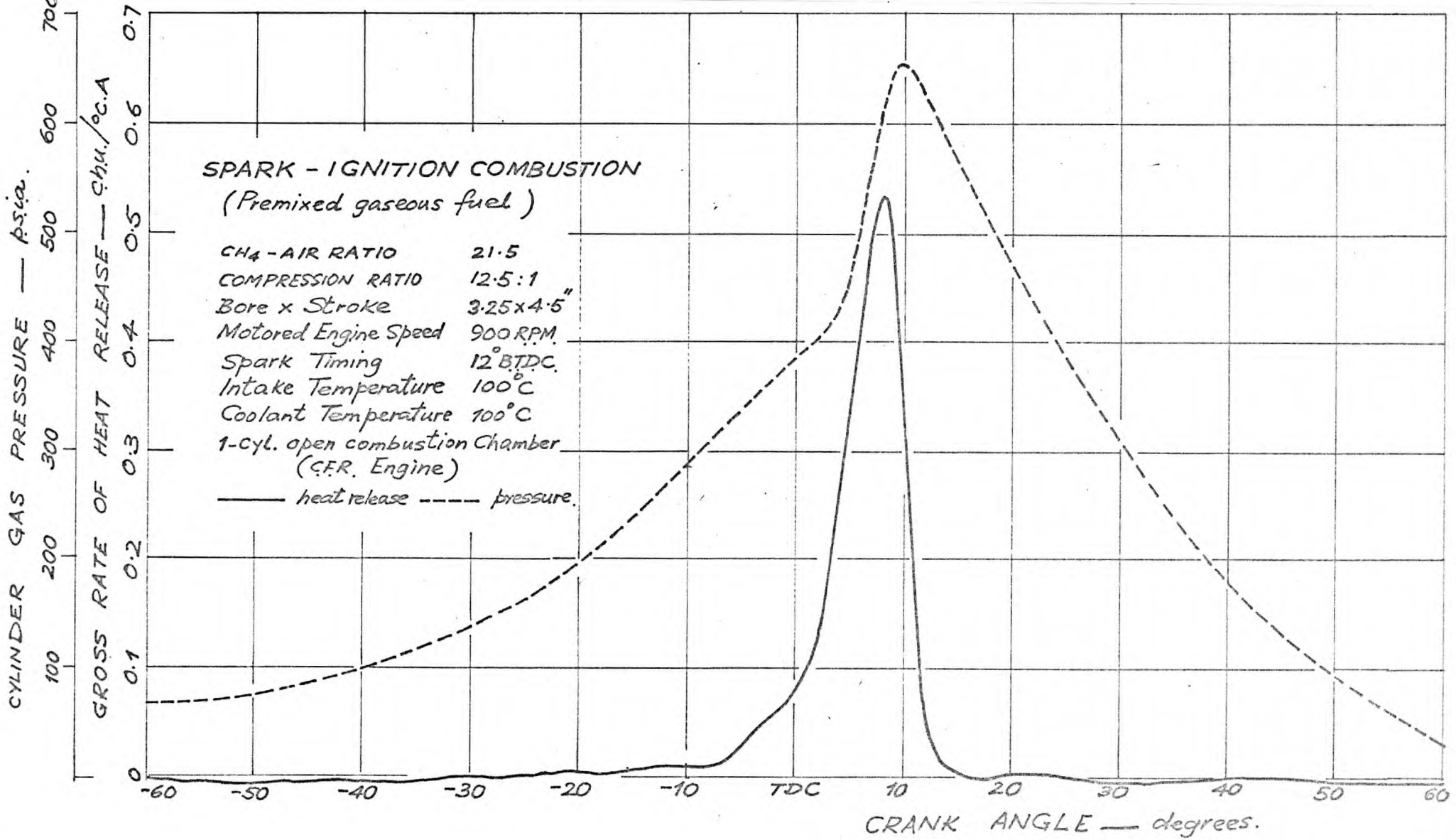


Fig. A2.20: Analysis of heat release variations for a gas engine cycle.

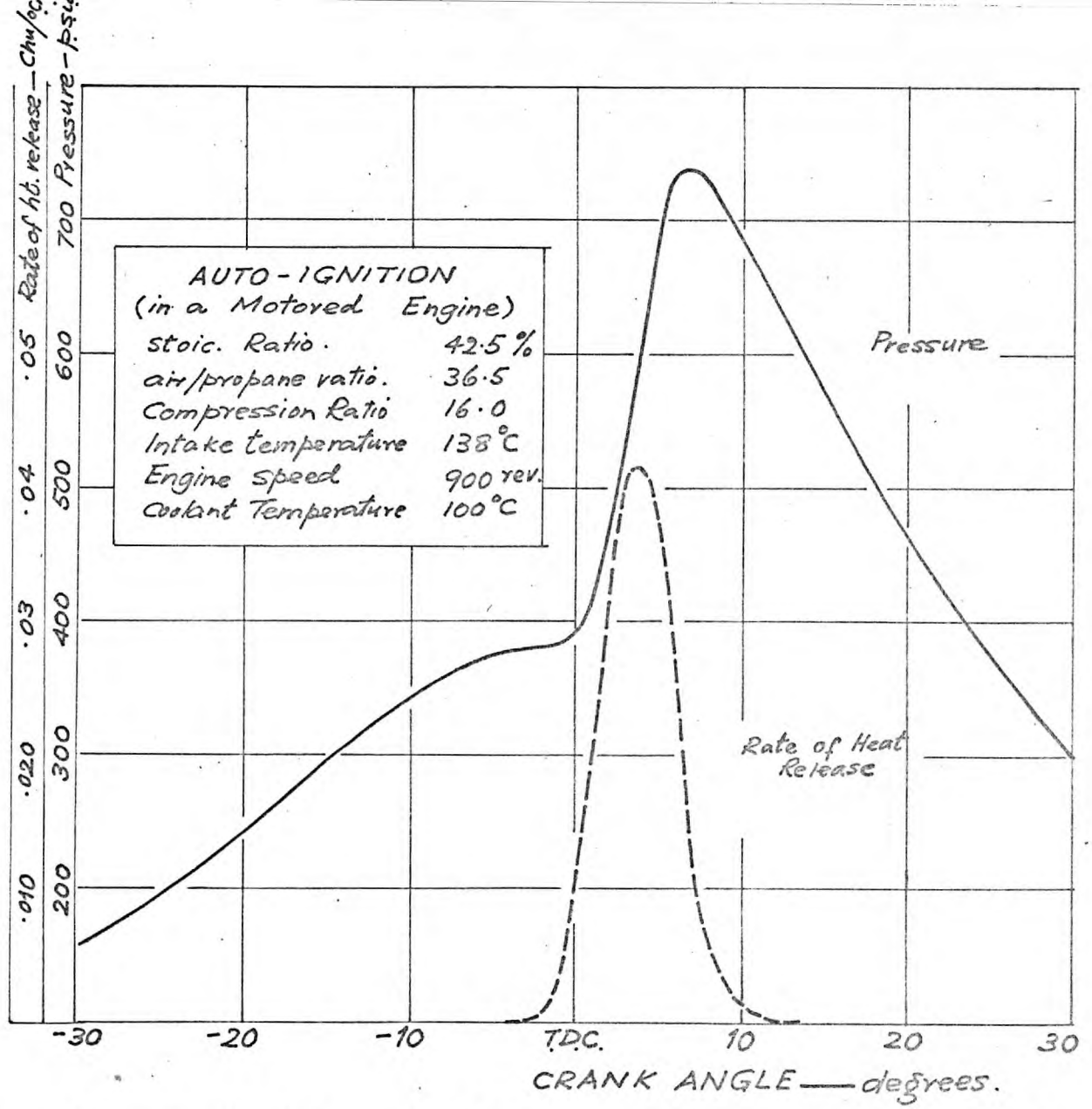


FIG. (A2.21) Analysis of heat release variations for a motored autoigniting engine cycle.
(Premixed Gaseous Fuel)

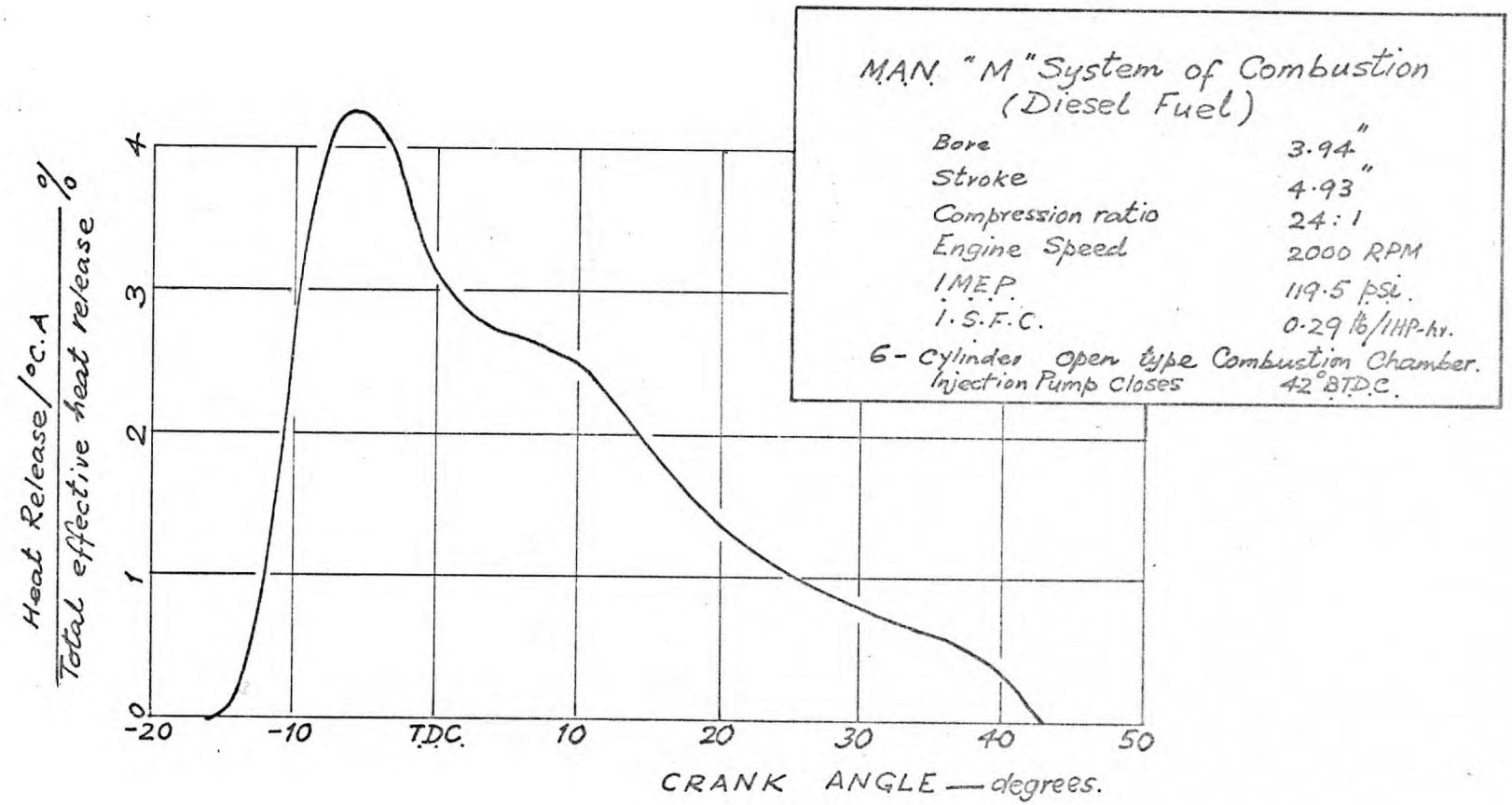


Fig. A2·22 : Analysis of heat release variations for a M.A.N. 'M' System diesel cycle.*

* After Goudie (28) and Kakimoto (34).

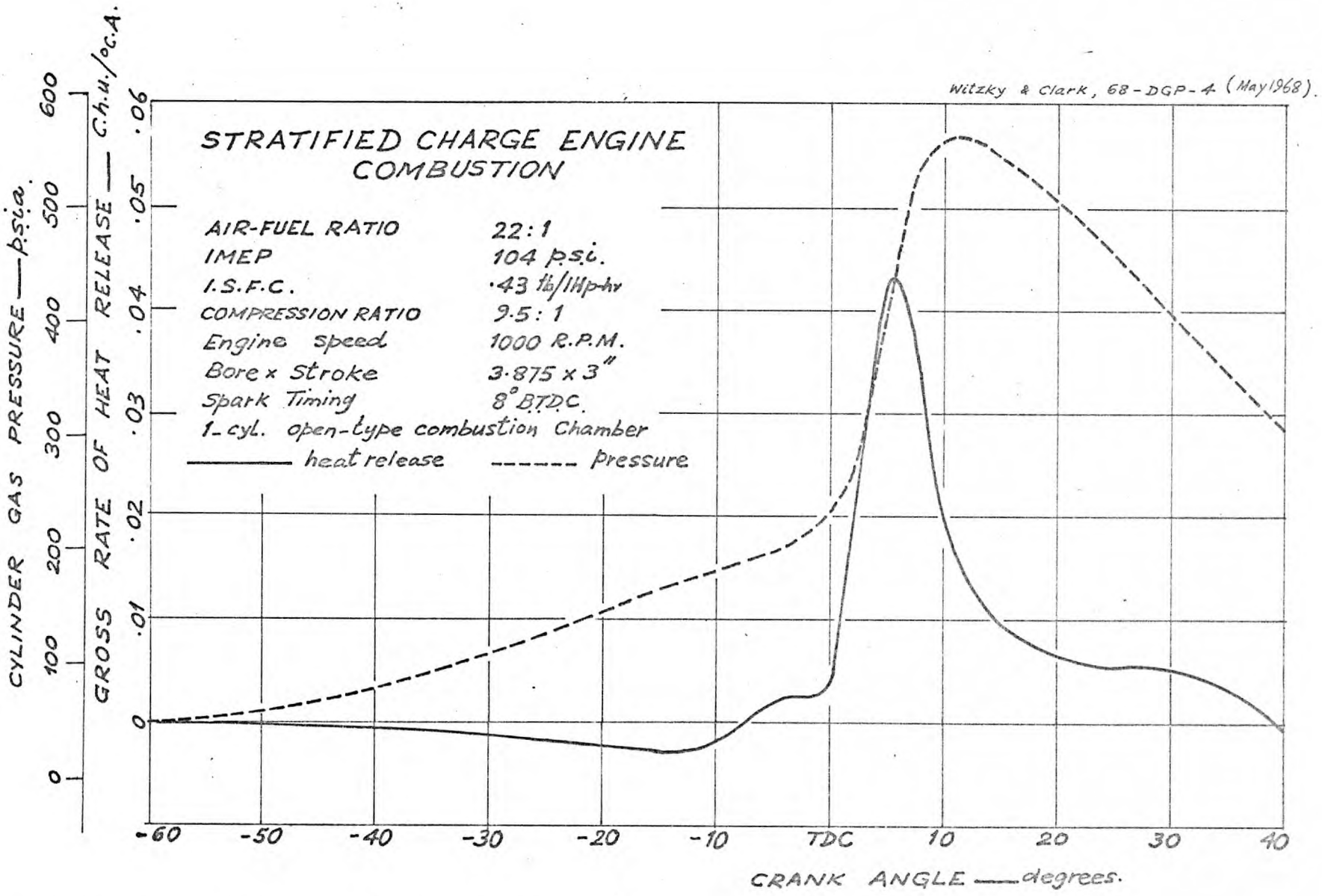


Fig. A2.23: Analysis of heat release variations for a stratified charge spark ignited gasolene engine cycle.

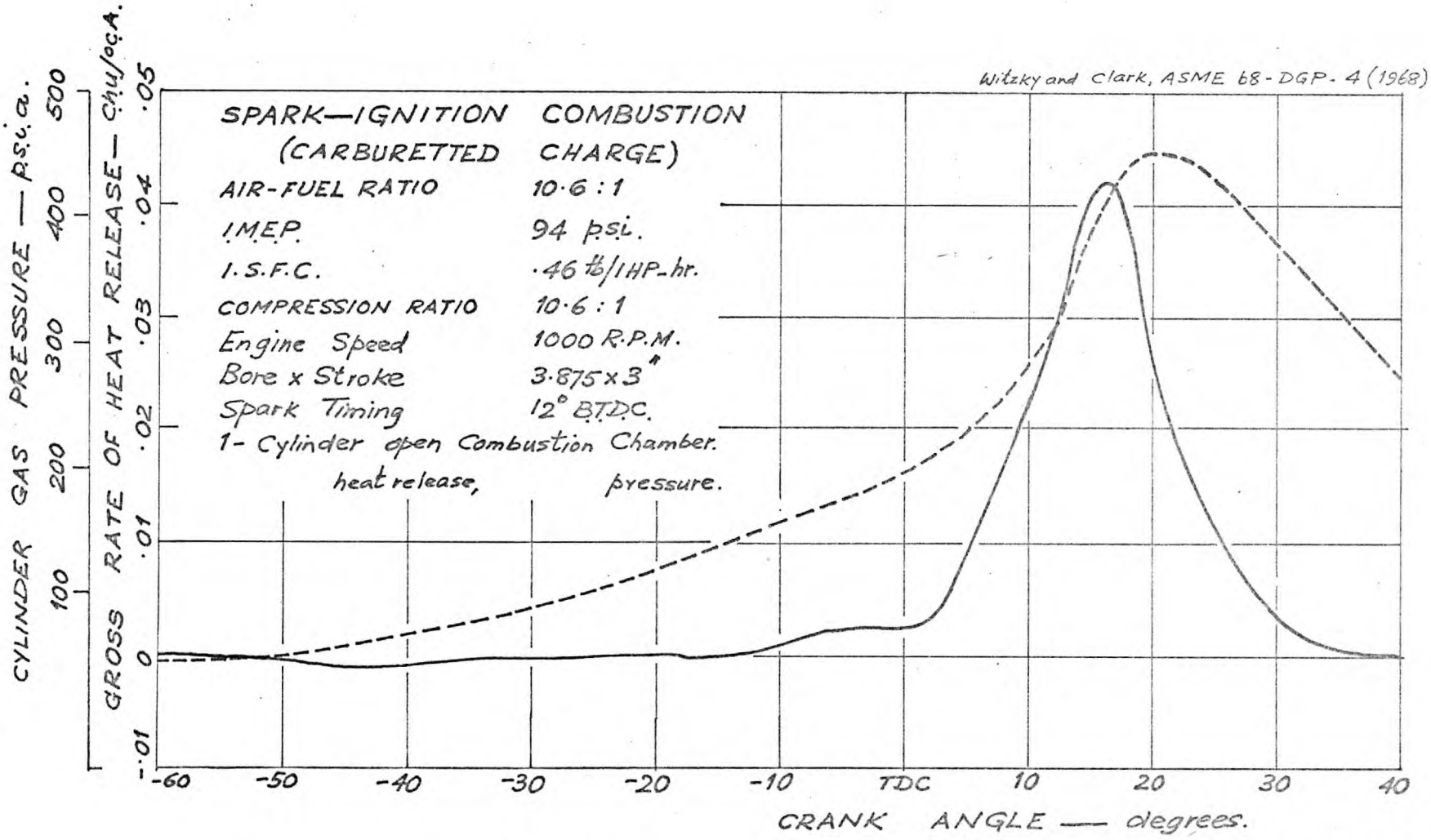


Fig. A2.24: Analysis of heat release variations for a spark ignition carburetted gasolene engine cycle.

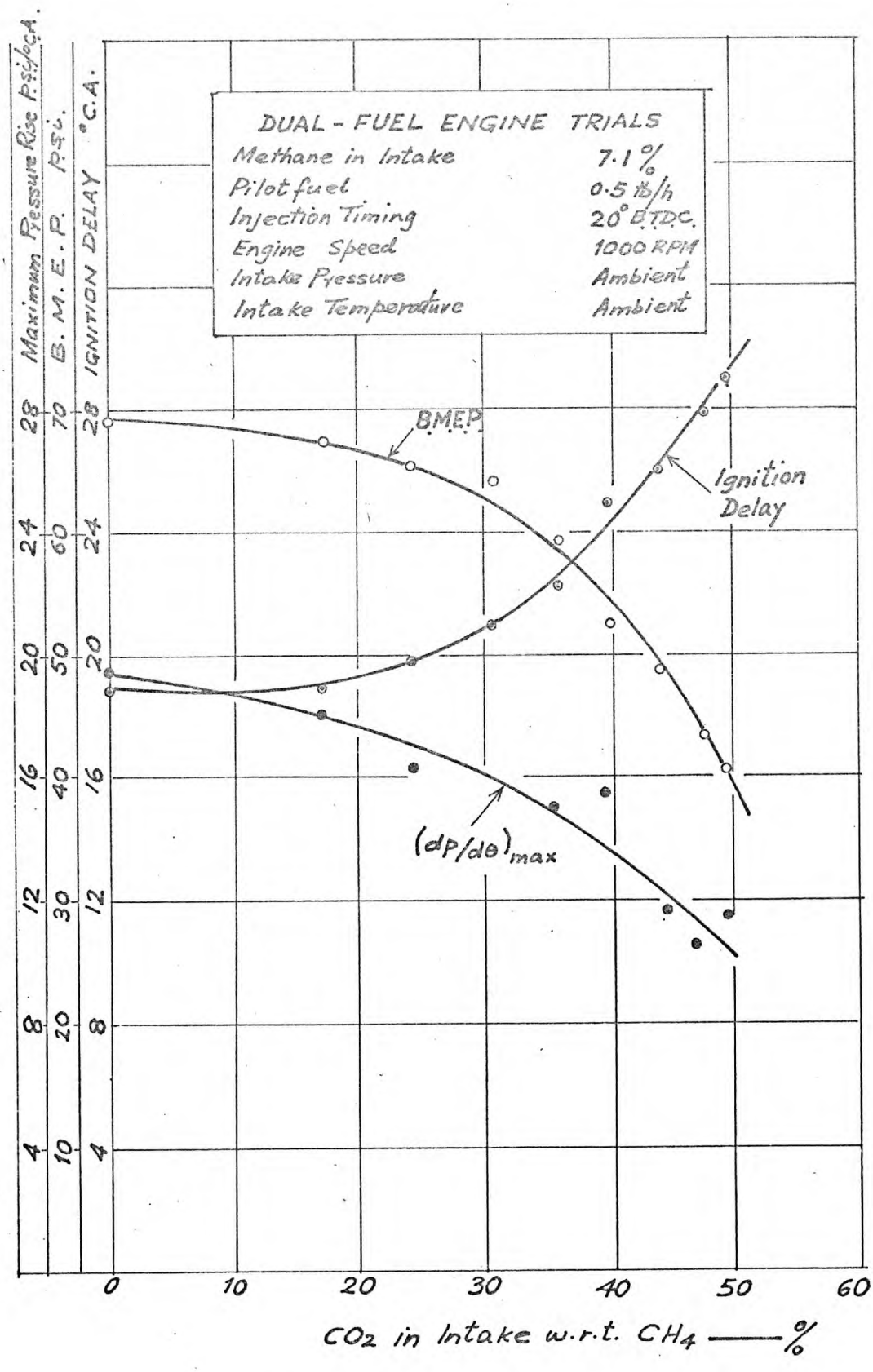


FIG. (A2.25) Effect of CO_2 addition on Engine Performance.

C H A P T E R A3

ERROR ANALYSIS OF COMPUTATIONS OF HEAT RELEASE

A3.0 Introduction

Previous studies of heat release variations in reciprocating engines paid little or no attention to evaluating the accuracy of results affected by various variables. Austen and Lyn (63) attempted to explain the influence of inaccuracy in pressure scaling, phasing of crank angle and the measurement of air flow, while Whitehouse et al. dealt with, in addition to these, base-line errors (104). Krieger and Borman (52) also attempted to show the influence of these variables. They demonstrated that these parameters though affect the magnitude of rates of heat release, but the shape and duration of the diagrams remain unaltered. However, to the knowledge of the present author, there exists no systematic study which considers all possible errors influencing the heat release variations. As a part of the present extensive heat-release analysis in a dual-fuel engine, it has been attempted to fill this gap.

A3.1 Purpose of the Chapter

The main theme of the present work is to characterise rather complex combustion processes in dual-fuel engines through heat-release analyses. The nature of these processes is too complicated to be presented exactly by a single analysis. In an attempt to describe them adequately, investigators usually resort to some experimental evidence, duly interpreted by certain simplifying assumptions. The present analyses of combustion heat release rest on the pressure development records obtained experimentally. Certain simplifying assumptions are used in the computations.

It is the purpose of this chapter to examine systematically all those errors and simplifying assumptions which have bearing on the conclusions to be inferred

from the heat-release analysis of dual-fuel engine combustion processes. The errors which are likely to creep in during the course of observations, data analysis and computations, have been classified and dealt with individually in so far as they affect the construction of heat release diagrams. Basing on a typical heat-release record constructed in the usual way, it is illustrated as to how the various inaccuracies affect the magnitude and shape of the heat-release diagram during the cycle.

The significance of such an error analysis is manifold; for example, it enhances the reliability of results and the conclusions drawn therefrom by indicating the likely pitfalls; it indicates the plausible improvements in the method and procedure adopted and it rationalises the simplifying assumptions used.

A3.2 The Type of Errors Considered

Any experimental investigation supplemented by computational techniques for its interpretation embodies accidental as well as systematic errors. The accidental errors are usually due to the observer and are often revealed by repeated observations while the systematic errors may arise either from the observer or from the limitations imposed by the inaccuracy of the instruments used (93). Moreover, the simplifying assumptions adopted in the interpretation of data may also entail some incorrectness or incompleteness in representing the processes adequately and we shall include them in systematic errors. Chart (A3.1) summarises all types of errors which shall be dealt with in detail in the following section. It is to be noted that various errors of different sources occurring in the observation or presentation of the same parameter have been accumulated to establish their cumulative influence on the results, although they may not necessarily be of the same direction.

A3.3 Presentation of Error Analysis

We shall now examine all plausible considerations to which the construction of rate of gross heat release diagram is sensitive. The issues of fundamental importance to the concept of heat release will be dealt with at length, so that both merits and demerits of such an analysis be revealed in the perspective of its limitations and refinements in the treatment.

Fig. (A3.1) presents a typical variation of computed gross rates of heat release during the cycle. The assumptions used and all the computational techniques developed have been discussed in Chapter (A2). For the sake of comparison of the differences brought about by various errors, we shall regard the values of gross rate of heat release to be 'standard'. Any deviation in this value of the rate of heat release has been termed as percentage error and is defined as follows:

$$\epsilon = \frac{\dot{q}_g - \dot{q}_g^*}{\dot{q}_g^*} \times 100$$

where, ϵ = percentage error caused by the source considered

$\dot{q}$ = computed value of 'erroneous' rate of heat release

$\dot{q}^*$ = computed value of standard rate of heat release

A3.3-1 Methodical Errors

A3.3-1a Method of derivation of rate of heat release equation

It is shown in Appendices IV and V that the differential and finite-difference forms of the equation of rate of heat release are:

$$\dot{q} = \frac{1}{J(\gamma-1)} \left(\gamma P \frac{dV}{d\theta} + V \frac{dP}{d\theta}\right) \qquad (1)$$

$$\Delta q = \left[1 - (\gamma-1) \frac{\Delta V}{V_1 + \Delta V}\right]\left[\frac{\gamma p_1 \Delta V + V_1 \Delta p}{\gamma - 1}\right] \qquad (2)$$

In our usual computations, the differential form of the equation is used for the fact that the steps taken

are of 1° crank angle rotation rendering the fraction

$$[(\gamma-1)(\frac{\Delta V}{V_1 + \Delta V})]$$

negligibly small. This view is further confirmed in Fig. (A3.2) which plots the differences of the computed values of heat release during the cycle by both methods. A maximum difference of 2%, and as small as - 0.68%, occurs in the maximum rate of heat release, which is insignificant. However, a large difference may arise if the time interval for each step is increased.

A3.3-1b Calculation of gas temperature

The process of combustion with the consequent release of energy manifests itself in the change of internal energy and change in the system boundaries, if permitted, which in turn determine the amount of external work done and the heat transferred to or from the system. It is essential to know the temperature of the gas to describe adequately its thermodynamic behaviour. The gas temperature cannot be measured directly in an engine, as the combustion processes are very fast, unsteady and heterogeneous. The temperatures in the combustion chamber vary spatially according to the mode of ignition and subsequent flame propagation processes. In view of the formidable difficulties in the direct measurement of temperature, investigators invariably resort to the measurement of pressure variation whereby the mass-averaged gas temperature can be calculated. The usual concept of mean gas temperature is unrealistic as the combustion processes in a fired engine do entail temperature gradients across the flame front. In addition to non-uniformity of temperature within the charge in its burnt and unburnt mass the development of boundary layer alongside the walls of combustion space introduces another inequality of temperature distribution. It can, however, be argued that the processes prior to or after combustion follow the mean temperature level, as during these processes there is no adverse temperature gradient, otherwise imposed by combustion.

Unlike diesel and spark-ignition engines, dual-fuel engines do not present the extreme picture of non-

uniformity in charge temperature. This can be visualised from the fact that the initiating source of pilot fuel having undergone inordinate delay, in comparison with diesel combustion , gets the opportunity to vapourise, while the subsequent processes of combustion are duly shared by the premixed gaseous fuels. Hence, the reservation of the concept of uniform temperature distribution is not so grave in the dual-fuel combustion and the calculated mean temperature before, during or after combustion can be taken to represent the driving temperature for the heat transfer to or from the system. The present analysis makes use of the mass-averaged gas temperature obtained from the ideal gas relationship.

A3.3-1c Rate of heat transfer calculation

The knowledge of heat transfer to or from the working system is essential if gross rates of heat release are to be obtained. Also the knowledge of heat transfer helps in the design of cooling systems, the assessment of thermal stresses and the drawing of heat balance to ascertain cycle efficiency. The heat transfer coefficients can also, in general, be valuable in ascribing the heat transfer processes within the charge; for example, formation of fuel vapour from liquid and propagation of combustion.

Taken overall, the problem of calculating instantaneous rates of heat transfer has been approached in two ways: firstly, in the internal combustion engine cylinders, the rates of heat transfer from the working fluid are assumed to be governed by the well-established convective laws as in the case of pipe flow, while the radiative component of heat transfer is superimposed; and, secondly, the approach rests on the analytical considerations of the energy and momentum balance in the control volume of the working system resulting in complex expressions whose solution can only be obtained with certain gross assumptions.

The well-known formulations developed by Nusselt (78) and Eichelberg (19) followed the first

approach. They based their formulations on experimentally obtained temperatures probed at various stations of the combustion space. Recent efforts by Overbye et al. (80), Sitkie(88), Annand (5) to preserve the dimensional consistency in prescribing the heat transfer coefficient with due recognition of convective and radiative components, have resulted in establishing generalised correlations. Some efforts by the present investigator to obtain the required coefficients 'a' and 'b' in the basic convective heat flow dimensionless relationship, $Nu = a(\overline{Re})^b$, indicated that extensive data of motored engine with extremely sensitive pressure pick-ups are needed to arrive at some tangible results. It was, therefore, resolved that the well-known formulations of Eichelberg and Annand be used with due recognition of their limitations.

The constants given by Annand in the following relationship,

$$\dot{Q}''_{HT} = a \frac{k}{D} (\overline{Re})^b + c (T^4 - Tw^4)$$

were: $a = 0.26$, $b = 0.75 \pm 0.15$, $c = (1.6 \pm 0.67) \times 10^{-12}$,

where, $\dot{Q}''_{HT}$ = heat transfer coefficient

k = conductivity of gas

D = engine bore

$\overline{Re}$ = Reynolds number based on mean piston velocity and engine bore

T = temperature.

Obviously the constants as noted above have considerable tolerance and unrealistic figures of heat transfer rates may be arrived at if a tentative comparison with some other formula is not made. Eichelberg's formula has been used for this purpose.

Fig. (A3.3) presents the sensitivity of rate of heat-release calculation to the formula of heat transfer employed. It can be seen that for the order of the mean coefficients adopted in Annand's correlation, viz $a = 0.26$, $b = 0.75$, $c = 1.6$, Eichelberg's formula renders the gross rate of heat release underestimated by 10% in the region of significant energy release. It is felt relevant to present comparative details of Annand's and Eichelberg's

formulae. Figs. (A3.4 - A3.6) serve this purpose. In Fig. (A3.4) comparison is made of the cumulative effect of the heat transfer as computed by both correlations. A superimposed record of computed cumulative heat release explains the relative inadequacy of Eichelberg's formula as it accounts for 11.5% of the cumulative heat release, while Annand's correlation up to 17% for the range of crank rotation shown, which undoubtedly is the region when the combustion processes can be taken to have been completed. Fig. (A3.5) shows the variations of rates of heat transfer as computed during the cycle by both the formulae. The temperature and pressure variations during the cycle have also been displayed as both the formulae in general and that of Eichelberg in particular, largely depend on them. It is apparent that the rates of heat release as computed by Annand's formula are quite sensitive to the exponent 'b', while 'c' is not likely to alter the overall heat transfer rates as the radiative component is even at its peak only 1/5th of the total heat transfer. This is best explained by Fig. (A3.6).

A3.3-1d Assessment of progress of reactions

The composition and properties of the working system is required to ascribe the thermodynamic and transport properties such as molecular wt, specific heat, viscosity and conductivity, during the cycle. The composition of the charge prior to and at the end of combustion can readily be computed from the knowledge of approximate fuel composition, aspirated amount of charge with due allowance for the residuals. However, the estimation of real composition during the combustion phase is impossible, as there is no known reaction mechanism which could present reaction scheme of the hydrocarbons commonly used in engine combustion. This is mainly because the reactions do not take place in a single step and under engine operating conditions they are too complicated to be presented because of unsteady combustion under high temperature and pressure being influenced by the dissociation, heat transfer, residuals and mixing of the fuel with the air.

A gross assumption is to regard a step change from the reactants to products at the point when ignition takes place. The products so formed may be regarded as an outcome of complete combustion as dictated by stoichiometry. Obviously, this assumption over-simplifies the complex processes and leads to over-estimation of products (i.e. the extent of reaction) at the initial stages of combustion. In the present analysis a further step is taken to repeat the grossly calculated rates of heat release by ascribing a realistic rate of conversion law to the reactants to convert into products following the pattern of cumulative heat release. The complete combustion products so obtained are then modified taking into account dissociation. The effect of dissociation shall be discussed in the following section. The fraction 'f' at any instant after the combustion has started is defined as:

$$f_\theta = \int_{\theta_i}^{\theta} \dot{q} d\theta \Big/ \int_{\theta_i}^{\theta_n} \dot{q} d\theta \qquad (3)$$

where θ_i = crank angle at the start of combustion

θ_n = crank angle at the end of computation

θ = crank angle at any instant

$\dot{q}$ = gross rate of heat release.

Thus, $f_{\theta_i} = 0$, $f_{\theta_n} = 1$.

In Fig. (A3.7) is shown a typical variation of the fraction, i.e. reactedness during the cycle. It will be noticed that reactedness defined by equation (3) follows the cumulative heat-release pattern as shown in Fig. (A3.4). Fig. (A3.8) shows the relative difference in the computed values of rates of heat release if the modification to the progress of combustion as outlined above, is not adopted. It is interesting to note that while a gross underestimation of rates of heat release occurs at the initial stages of combustion, insignificant errors can be expected in the later stages.

A3.3-1e Variability of thermodynamic properties of the working system

One of the merits of the use of fast computers in engine combustion cycle analysis is that one can improve upon the simplifying assumptions on a more rational basis. Not long ago, the air cycles were attributed to represent the thermodynamic cycle efficiency. In reality, however, the varying composition of the charge and the rising level of temperature greatly influence its properties and to regard them as remaining constant during the whole cycle is far from the truth. In our analysis it is assumed that at all likely partial pressures during the course of the cycle, the thermodynamic properties of the gas are temperature dependent. For the sake of ease in computations, the specific heats of the probable constituents of reactants and products have been defined as polynominals in temperature following the most comprehensive and reliable data made available by the Joint Army-Navy-Air Force (J.A.N.A.F.) of the U.S.A. (31).

The guiding relationships for the calculation of mixture properties from the knowledge of the properties of its constituents may be summarised as quoted by Annand (5) from (48):

$$Cp_j = a + bT + cT^2 + dT^3 + eT^4 + fT^5$$

$$\overline{Cp} = \Sigma\, n_j M_j Cp_j \;/\; \overline{M}$$

$$\overline{M} = \sum_n n_j M_j$$

$$\overline{\mu} = \frac{\sum_n n_j \mu_j \; M_j}{\sum_n n_j \; M_j}$$

$$\mu_j = \mu_{o_j} \; T^{0.645} \quad ,$$

where $\overline{Cp}$, $\overline{M}$ and $\overline{\mu}$ are the mean specific heat, molecular weight and viscosity of the mixture. The subscript j represents a specie, while n is the number of species in the mixutre. It may be pointed out that in engine combustion, air dominates in the reactants, whilst Nitrogen, excess oxygen, if any, carbon dioxide and water vapour are

the important constituents of the products and carbon monoxide and Hydrogen may be present, whose concentration is governed by the extent to which reaction progressed and the consequent temperature level attained.

Fig. (A3.9) shows clearly the difference in the computed values of rate of heat release if the thermodynamic properties of the cylinder contents are taken to remain constant, irrespective of the change in composition and temperature during all the phases of compression, combustion and expansion. Values of $\gamma = 1.35$ and $\overline{Cp} = 0.24$ were used as input data and the subroutine of specific heat was deleted such that the same values remain constant for the whole cycle. These pre-set values represent those of air at initial conditions of the engine cycle.

The error analysis suggests that the computations of heat release are sensitive to the thermodynamic properties of the working system as gross under-estimation of rates of heat release occurs during compression and combustion, while the reverse happens in the latter part of expansion, if they are assumed to remain constant. Fig.A3.9 illustrates well the above observation.

A3.3-1f Accounting for dissociation

It is seldom that the complex and unsteady combustion processes taking place in an engine cylinder attain equilibrium. They can, however, be assumed quasi-steady during a finite interval, which is 1° crank angle - 0.16 m sec., at 1000 r.p.m., such that the concept of driving temperature in the determination of thermo-chemical equilibrium be employed. The assumption of uniform properties throughout the charge precludes that there exist no temperature, pressure and concentration gradients within the charge, which may well offset the consideration of dissociation.

Purely for the sake of illustration as to what extent one can expect the rates of heat release to be modified if dissociation of carbon dioxide and water vapour is taken to be operative at the mean temperature

level, a subroutine has been incorporated in the computer programme. The equilibrium constants have been defined as polynominals in temperature in accordance with J.A.N.A.F. tables, as shown in Appendix IX. It has been found that under the normal operating engine combustion at prevalent maximum temperatures of the order of 1600°K, dissociation does not exercise any significant influence by way of modifying the initial concentrations of 'complete' combustion products.

A3.3-1g Step length

As mentioned in the preceding considerations, the accuracy with which the unsteady combustion processes can be regarded quasi-steady is essentially dependent on the break-down of the time interval infinitesimally. The advent of computers extended unparallel facility to look into the combustion processes with finer details which were almost impossible.

In our heat-release analyses the pressure time history is examined for each degree of crank rotation. Fig. (A3.10) presents the differences in the computed values of gross rates of heat release if the step length for computations is changed to 2° crank angle. It suggests that, although a maximum of - 2% difference may occur in the combustion region, it is pointless to break down the degree into further fractions at the expense of computer time and labour with no remarkable gain.

A3.3-1h Initial and boundary conditions

(i) Reference pressure

In the interpretation of pressure records, the absence of any accurately known reference pressure offers the difficulties in accurate scaling out the pressures over the cycle. During the initial stages of the present heat-release analysis the manifold pressure was regarded as datum. The manifold depression registered during the trials was ascribed to the start of compression while analysing the records. Shown in Fig. (A.11) is the sensitivity of the heat-release rates to the inaccuracy in

ascertaining the correct datum pressure. It will be noticed that the heat-release rates prior to or after the combustion processes are quite sensitive. However, the nature of this type of error is such that it does not alter the cumulative heat release significantly as differences arising in the earlier and later part of the cycle tend to cancel each other.

ii) Cylinder wall temperature

A factual wall temperature of the combustion surface needs be known for the calculation of rates of heat transfer at any instant during the cycle. The combustion surface temperature varies from point to point and from time to time depending on how it comes in contact with the combustion products on one side and with the coolant on the other. It also varies from cycle to cycle and from design to design. To assign any surface temperature distribution is, therefore, impossible without probing at various stations of the cylinder assembly over a vast range of operating conditions so that a representative configuration may be arrived at which is, undoubtedly, beyond the scope of the present work. During the trials, the cooling water outlet temperature was kept constant to ensure that combustion chamber surface temperatures remain comparable under various operating conditions.

Realising the practical difficulties and scanty knowledge available on temperature distribution of the combustion surface, the heat transfer area is subdivided into two: one is the area of the liner exposed by the piston movement and the other is that of piston crown and the cylinder head. Unlike effective cooling afforded by the jacket to the liner and, less effectively, to cylinder head, the piston crown relies on the cooling effected by the lubricant. In order to account for these differences in cooling, it is assumed that the piston crown and cylinder liner remain at 20°C and 10°C respectively, above the cooling water outlet temperature. The differences arising in the computed values of rates of heat release, if the assumption of temperature difference is altered to be 40°C and 20°C, are shown in Fig. (A3.12). It is also

shown that rather insignificant difference may occur even if the entire surface is assumed to remain at the same temperature as that of the outgoing cooling water, i.e. $\Delta T_1 = \Delta T_2 = 0$. It is, therefore, apparent that sub-division of areas of heat transfer and surface temperatures ascribed to them do not influence the heat-release diagram significantly. The knowledge of actual temperature differences across the surface is, however, desirable for accurate analysis.

A3.3-2 Instrumental Errors

A3.3-2a Pressure measuring instruments

The reliance on pressure as the basic parameter for heat-release analysis warrants the necessity of its accurate measurement as prevalant inside the combustion chamber. The accuracy with which the pressure signal is transduced from the combustion chamber depends on two factors: one is the imminent delay in equalising of pressure throughout the charge following the release of combustion energy and piston movement, while the other is the delay of the equalised pressure pulse so generated to reach the diaphragm of the transducer situated at one end of the combustion space. The pressure pulse in a working system travels at sonic velocity, and is proportional to the square root of the temperature at that instant. The small combustion volumes around T.D.C. and the elevated temperatures render the aforementioned delays smallest and hence insignificant.

The rigorous search by Watson (103) and Milkins (68) for accurate pressure measuring pick-ups concluded the use of catenary diaphragm piezoelectric type transducers. The following merits can be cited in favour of its adoption:

(i) accurate frequency response and wide-ranged linearity;

(ii) high input impedence rendering the charge leakage slow and small;

(iii) the calibration can readily be carried out statically; and

(iv) considerable improvements in the design of these transducers has been made towards accuracy; for example, the diaphragms can be effectively shielded agains the undesirable temperature effects caused by the contact with combustion products at high temperatures, the diaphragms are compensated for transverse vibrations such that the mechanical vibrations ensuing as a result of steep rise of pressuring during combustion can be eliminated and the recent development of adapter pick-ups made it possible to create a reliable dynamic reference pressure, while recording the actual pressure during the cycle.

In addition to the inherent inability of the transducer to reproduce the pressure accurately, despite the above-mentioned striking improvement, errors arise while displaying, recording, interpreting and processing the pressure-time data which we shall now discuss.

The drift introduced to the pressure signal by the pre-amplifiers before it is displayed on the oscilloscope can safely be ignored, being of the order of -0.005%.

The errors introduced by the oscilloscope are as follows:

(i) un-parallelism of the graticule and the trace;

(ii) distortion of the signal at the ends of the screen; and

(iii) crude focussing thereby rendering the signal ill-defined.

The errors introduced by recording and reading equipment may be noted as follows:

(i) optical distortion arising from the inadequacy of 'f' no. of the camera, which is defined as the ratio of focal length to aperture; and

(ii) unavoidable enlargment of the trace for scaling out the pressure variation with consequent lack of well-defined traces and the limiting accuracy of the digitaliser operated manually.

In view of the above inaccuracies, a maximum of $\pm$ 2% error in pressure measurement can be ascertained, which precludes sufficient latitude to account for any other minute errors not discussed here. Fig. (A3.13) presents the effect of erroneous pressure measurement on the construction of heat release diagram. It can be seen that the negative error in pressure measurement, i.e. its under-estimation reflects relatively more adversely as compared to its over-estimation. It is apparent from this figure that a + 2% error in pressure entails a + 2.5% error in the gross rate of heat release in the combustion zone, while the error of the same order, but of opposite sign, brings about a - 3.5% error in the same region.

A3.3-2b Recording of crank rotation

In addition to the knowledge of cylinder gas pressure, the movement of the piston should also be accurately known, so that the work transfer to or out of the system may be established from the changing boundaries. Unlike rapid compression machines, the piston movement in reciprocating engines can accurately be related to the rotation of the crank shaft or the flywheel which is rigidly mounted on the shaft. The method and instruments used for registering crank rotation are described in the relevant section dealing with apparatus. We shall discuss here only the probable errors arising in recording crank rotation. They are as follows:

1. The error in referencing the T.D.C.: despite special markings on the flywheel for T.D.C., a shift may occur during the process of enlargement which renders the traces crudely defined.
2. The subdivision of large intervals of 5^{o} crank angle into each degree interval: the acceleration and deceleration of the piston movement around T.D.C. makes the time interval inequal on a linear scale. The subdivision of time interval of 5^{o} into 5 equal intervals ignores this effect. Accurate location of 5 and 10^{o} markings tends to cancel this inequality effectively. Hence, this inaccuracy is insignificant.

In order to demonstrate the extent of error introduced in reckoning the T.D.C. position from the experimentally obtained pressure-crank angle diagram, a deliberate shift of $\pm 2^{o}$ was introduced. In conformation with the observation of Whitehouse et al. (104) it can be seen from Fig. (A3.14) that an error of the order of $\pm$ 15% in the peak value of gross rate of heat release may arise, while the cumulative heat release affected is of the order of 10%. These large errors arising from the erroneous reference to T.D.C. may well be due to erroneous volume, $dv/d\theta$, and specific heat ratio caused by the shift. In view of the seriousness of this type of error for the investigations on the motored engine, the timing signals were superimposed on the pressure signal with the aid of Cathode Ray Tube (C.R.T.) external circuit. Additionally, an extra channel was utilised for displaying the crank rotation and a qualitative check of the occurrence of zero rate of pressure rise was applied later in computations.

A3.3-2c Air and fuel flow measurement

The following inaccuracies can be cited which have direct bearing on the air and fuel flow measurements:

(i) The unsteady head across the viscous flow air meter because of the pulsating nature of the flow in reciprocating engines. The observational error is, therefore, likely to occur while noting the head across the flow meter.

(ii) The assumption that the air flow registered at the inlet manifold and the liquid fuel noted through the burette represents the cylinder contents, ignores the mass trapped in the cylinder ports and any leakages occurring due to blow-by during compression.

(iii) The inaccuracy caused by any incidental error during the calibration of viscous flow meter and the choked nozzle meter.

(iv) The pilot liquid fuel escaped atomisation due to overflow remains unregistered.

(v) The deviation from the calibration curve due to partial blockage with the passage of time.

The comparative insensitivity of the choked nozzle gaseous fuel flow meters to the pulsating flow downstream enables accurate measurement of gaseous fuel as compared to air flow measurement. A liberal inaccuracy of $\pm$ 2% in air and $\pm$ 1% in fuel flow measurement was introduced to find out the consequent differences in the computed values of gross rates of heat release and is presented in Fig. (A3.15). It is apparent that the over-estimation of the charge is more detrimental as it reduces the mass-averaged temperature and this, in turn, effects specific heat ratio.

A3.3-2d Speed measurement

Two types of error may arise in speed measurement: namely, instrumental type if the revolution-counter used registers the speed incorrectly, or operational if the engine is not operated at a constant speed during the trial. The speed recorded by the big dial-type speedometer was checked by a standard rev.-meter, while the precise Ward-Leonard speed control made it possible to run the engine at constant speed by varying the field resistance of the motor or generator, as the case may be. Even so, any inaccuracy creeping in during observation may bring about the same effect in the time-averaged cylinder contents as discussed in the preceding section. In other words, the inaccurate speed measurement will increase or decrease the computed value of cylinder contents per stroke, whose effect will be of the same nature as that under- or over-estimation of air and fuel flow measurement.

A3.3-3 Computational Errors

Smoothing of data was found to be necessary because of various intermediately lying procedures of data processing which do tend to introduce scatter.

Numerical smoothing with the aid of the computer is preferred over hand-smoothing for its ease of application with iteration, if need be, and digital accuracy maintained by the computer. Similarly, the computations of rate of pressure rise were found to be best carried out by

numerical techniques rather than linear interpolation or graphical determination of the tangent.

A3.3-3a Data smoothing

The nature of unavoidable accidental errors is such that the pressure data processed into computable form do not remain free from scatter. A simple numerical procedure based on the use of fourth differences has been adopted in the present analysis, as discussed in Appendix VII. Fig. (A3.16) shows the percentage differences in the rate of gross heat release expected if smoothing is not effected. It serves to explain that the heat-release analyses of pre-combustion and the latter part of the combustion processes are likely to yield intangible results if smoothing of the scatter is avoided. It is interesting to note that the rates of heat release in the region, when significant combustion energy is released, remain unaffected.

A3.3-3b Computation of rate of pressure rise

The rates of pressure change ($dp/d\theta$) are derived by least-square curve fitting, as shown in Appendix X. In order to project the differences, the values of rates of change of pressure have been calculated by interpolation as below:

$$\left(\frac{dp}{d\theta}\right)_n = \frac{p_{n+h} - p_{n-h}}{2h}$$

where $\frac{dp}{d\theta}$ = rate of pressure change

h = step length

n = crank angle at which $\left(\frac{dp}{d\theta}\right)$ is required.

Fig. (A3.17) presents the differences between the computed values of heat release basing on these two different methods for calculating $\frac{dp}{d\theta}$. It is apparent that the heat release rates do not differ significantly. However, the least-square curve fitting procedure is preferred as it weighs the derived values of $\left(\frac{dp}{d\theta}\right)$ with its neighbouring points.

A3.3-3c Smoothing of rate of pressure rise

Fig. (A3.18) displays the difference in the computed values of rate of heat release if, in addition to smoothing pressure, the rates of pressure are also smoothed. Relatively insignificant differences in the values of heat release do not justify the smoothing of $(\frac{dp}{d\theta})$ in addition to pressure at the expense of computer time.

A3.3-4 Observational Errors

The errors which are accidental to an experimental observation do, in general, arise from the inherent inconsistencies of the instruments used and the human element involved in observation, recording and processing of data. In the preceding sections we have made due provision in the limits to include the observational errors so that a cumulative effect of each source of error could be established.

The analysis of a cycle made to represent a particular operating condition presumes all the working cycles to be repetitive with no cyclic dispersion. In practice, however, we come across cyclic dispersion which necessitates the recording of a large number of cycles which could be analysed to obtain a mean cycle to be analysed to present the mean rates of heat release. Such an elaborate proposition is not practicable without the aid of computerised data-logging. In the present investigation, 'combed' pressure records were obtained to visualise the cyclic dispersion and to facilitate the realistic selection of a representative cycle. It may be noted that the moderate nature of cyclic dispersion in dual-fuel engines, which lies in between diesel engines and spark-ignition engines, makes it possible without much difficulty to bracket a representative mean cycle. Notwithstanding, erroneous selection of a non-representative cycle may have occurred during the trials under lean operating conditions when cyclic disperison in dual-fuel engines gets pronounced.

The point of ignition is reckoned either by superimposing a motoring diagram on the combustion cycle which makes the point of departure of the combustion cycle

from the motoring diagram. Fortunately, the delayed combustion of pilot fuel under dual-fuel engine combustion renders the point of ignition easily ascertainable. In the later part of our investigations, the rate of pressure rise diagram was also recorded, which indicates clearly the sudden rise of pressure even due to the pre-ignition activity.

A3.3-5 Reliance on Design Parameters

The computation of cylinder volume and rates of change of volume is a simple trigonometric proposition which requires the length of the connecting rod, crank-throw, bore, stroke and the compression ratio. This information is usually supplied by the manufacturer. However, by the passage of time, the clearances in the piston-liner, connecting rod-crank shaft assemblies grow thereby altering the parameters. We shall now try to trace the effects of various possible design inconsistencies which may influence the construction of heat-release diagram.

A3.3-5a Compression ratio

The compression ratio may be altered by the formation of deposits and change in clerances. A deliberate change of $\pm$ 2% in compression ratio is presented in Fig. (A3.19). It is evident that the heat-release diagram is sensitive to the accuracy of the compression ratio. It, therefore, warrants the necessity of checking the compression of the engine in use.

A3.3-5b Connecting rod-crank throw ratio

The connecting rod to crank throw ratio is likely to alter in the following ways because of the change in effective length of the connecting rod:

(i) The eccentricity caused by the increase in clearances and the bending of the connecting rod during the course of cyclic loading.

(ii) The increased clearances in the big and small ends.

A change of $\pm$ 2% in the connecting rod to crank throw ratio was introduced. Fig. (A3.20) illustrates the sensitivity of the heat release to such a change. It is obvious that the error so introduced is insignificant and self-compensating as it changes sign around T.D.C.

A3.3-5c Angular twist

The torque impressed by the reciprocating piston motion on the crank shaft gives rise to angular twist which advances the T.D.C. during compression, while the retard is introduced in the expansion stroke. This, in effect, changes the usually accepted crank to piston movement. Taking the crank shaft to be of poor quality a twist of $1/4^{\circ}$ has been introduced to illustrate this effect. Fig. (A3.21) shows that the heat release diagram is sensitive to such an error.

A3.4 Discussion

In the derivation of rate of heat release it is shown that:

$$dQ = fn\ (p, V, dp, dV, \gamma) \quad ,$$

wherefrom the measurement of pressure (p) and volume (V) comes out immediately to be of fundamental importance. The derivative dp and dV depend, in turn, on how p and V are obtained. In our analyses of errors we have introduced systematically all the probable maximum errors which can be conceived of in the measurement of these parameters.

Table (A3.1) summarises the effects of various accidental, systematic, methodical errors considered. In order of adversity of all the errors considered, the following important sources of error will be noticed; the criterion for the seriousness to which the construction of the rate of heat release is affected is taken to be the extent its maximum and cumulative values are affected:

(i) assumption of constant thermodynamic properties,

(ii) erroneous reference to T.D.C.

(iii) assumption of step change in reactants to products,

(iv) if the heat transfer rates are computed from Eichelberg's formula,

(v) erroneous datum pressure,

(vi) erroneous pressure measurement.

It is significant to note that all the errors considered do not bring about any radical change in the shape of the heat-release diagram, suggesting at least that the conclusions drawn are valid qualitatively. However, for accurate analysis of heat-release diagram, errors (ii), (v), and (vi) need to be eliminated in the experimental procedure. Additional care is also required to consider and eliminate the other errors discussed so far. Errors arising due to manual component can effectively be eliminated by employing a multi-channel data acquisition system which could digitalise and store in memory the fast changing pressure during the cycle. In addition to this the cyclic dispersion can be looked into more detail by analysing few consecutive pressure records and arriving at an average pressure diagram as being representative of the operating conditions under study.

Reliance on pressure alone as a basic parameter for the computations of heat release seems as yet to be necessary ~~decisive~~ important unless drastic improvements in temperature measurements be made. Nevertheless, further improvements in the pressure transducer ought to be effected, particularly in their sensitivity to higher temperatures and in the methods of their use to justify it with increased faith.

The calculation of rates of heat transfer is another issue of uncertainty which ought to be explored. In spite of rational formulation for heat transfer coefficient by Annand in separating out the convective and radiative components with dimensional consistency, it leaves large room in assigning the factual values to the coefficients which could accurately suit the design of any engine under trial. Elaborate efforts in detailing the constants of the form as given by Annand are needed, which require accurate pressure measurement and the instantaneous velocity distribution in the combustion chamber. It is

realised, therefore, that tenuous data even so obtained on the engine under study may fall short of the requirements of prescribing the coefficients accurately (68).

As conclusively shown by the present error analysis, the instrumentation for pressure measurements was improved by selecting the piezo-electric pick-ups of comtemporary design. Assumptions (i) and (iii) were replaced by suitable temperature dependent thermodynamic data and by using a realistic definition of reactedness as against the gross assumption of step change from reactants to products. Reliable detailed information on the mechanism and progress of combustion is highly desirable in order to rationalise this assumption.

The last column of Table (A3.1) needs particular mention as it brings out the overall result of the inaccuracies over the cycle. In general, it will be noticed that the difference in the maximum rate of heat release is also reflected in the cumulative heat release and has the same order. This is why the pronounced cumulative effect of the errors due to erroneous datum pressure and the inadequacy of Eichelberg's formula for heat transfer are noticeable.

A3.5 Conclusions

Taken overall, it can be concluded that the present analysis of accidental and systematic errors has warded off the doubts about the suitability of computations of heat-release analysis with the aid of fast computers. It is shown that any error, however significant it may be, does not alter the shape of the heat-release diagram; thus suggesting the utility of heat-release analyses in providing some insight into the controlling processes unquestionable.

The error analysis proved successful in suggesting possible improvements in various sources of error. It underlined the shortcomings of various assumptions of a fundamental nature in the determination of rates of heat release.

It pointed out the practical necessity of adopting a multi-channel data acquisition system which could eliminate all the intermediate procedures of data processing from the engine bed to the computer.

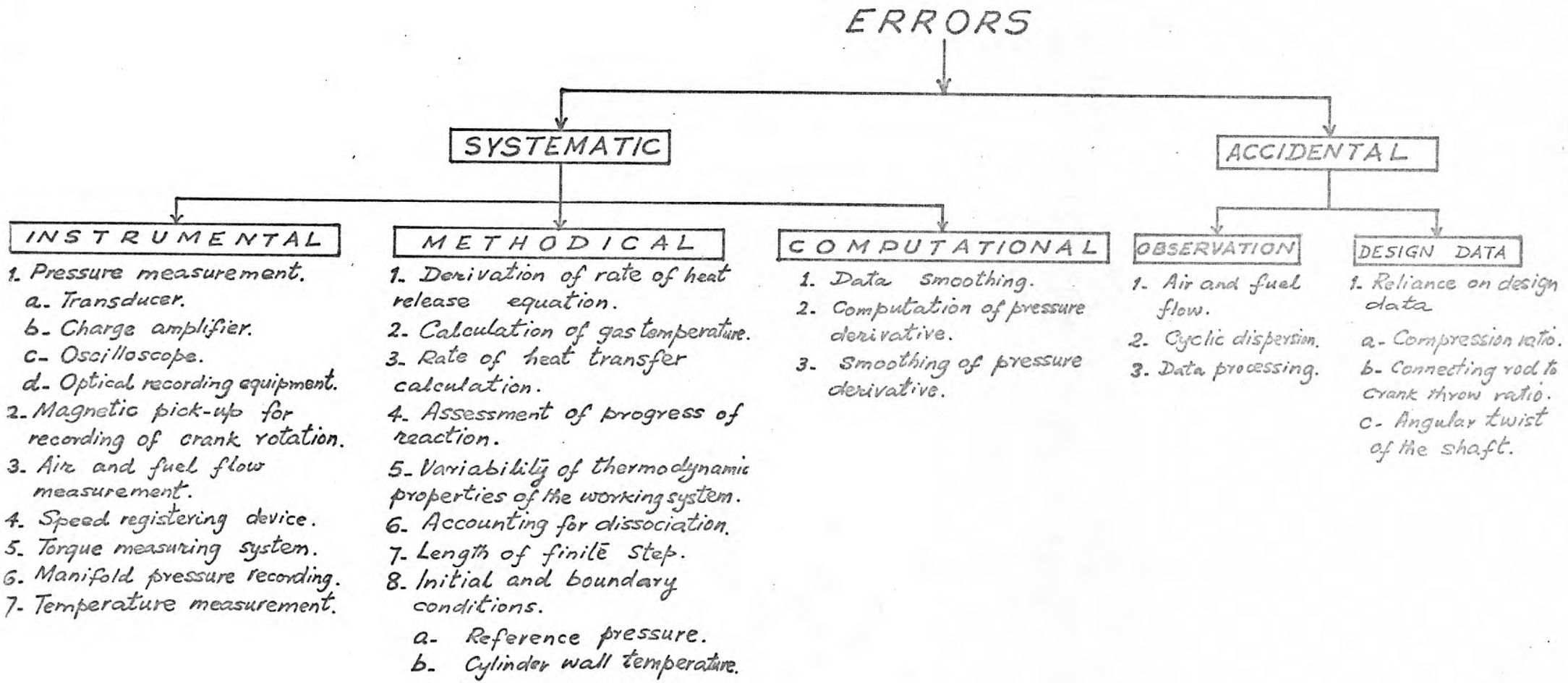


CHART (A3.1) SOURCES OF ERRORS

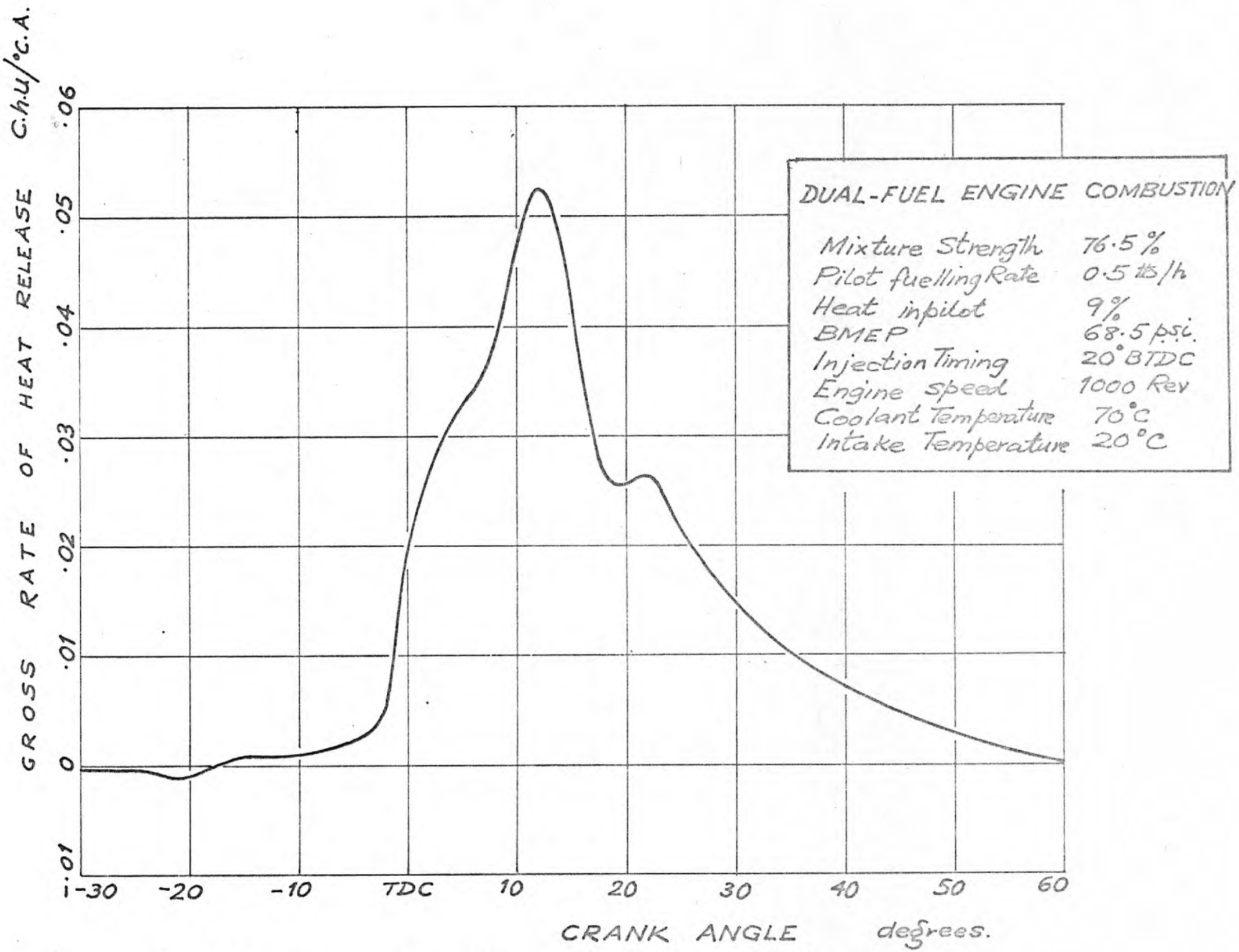


Figure (A3.1) Variation of rate of gross heat release

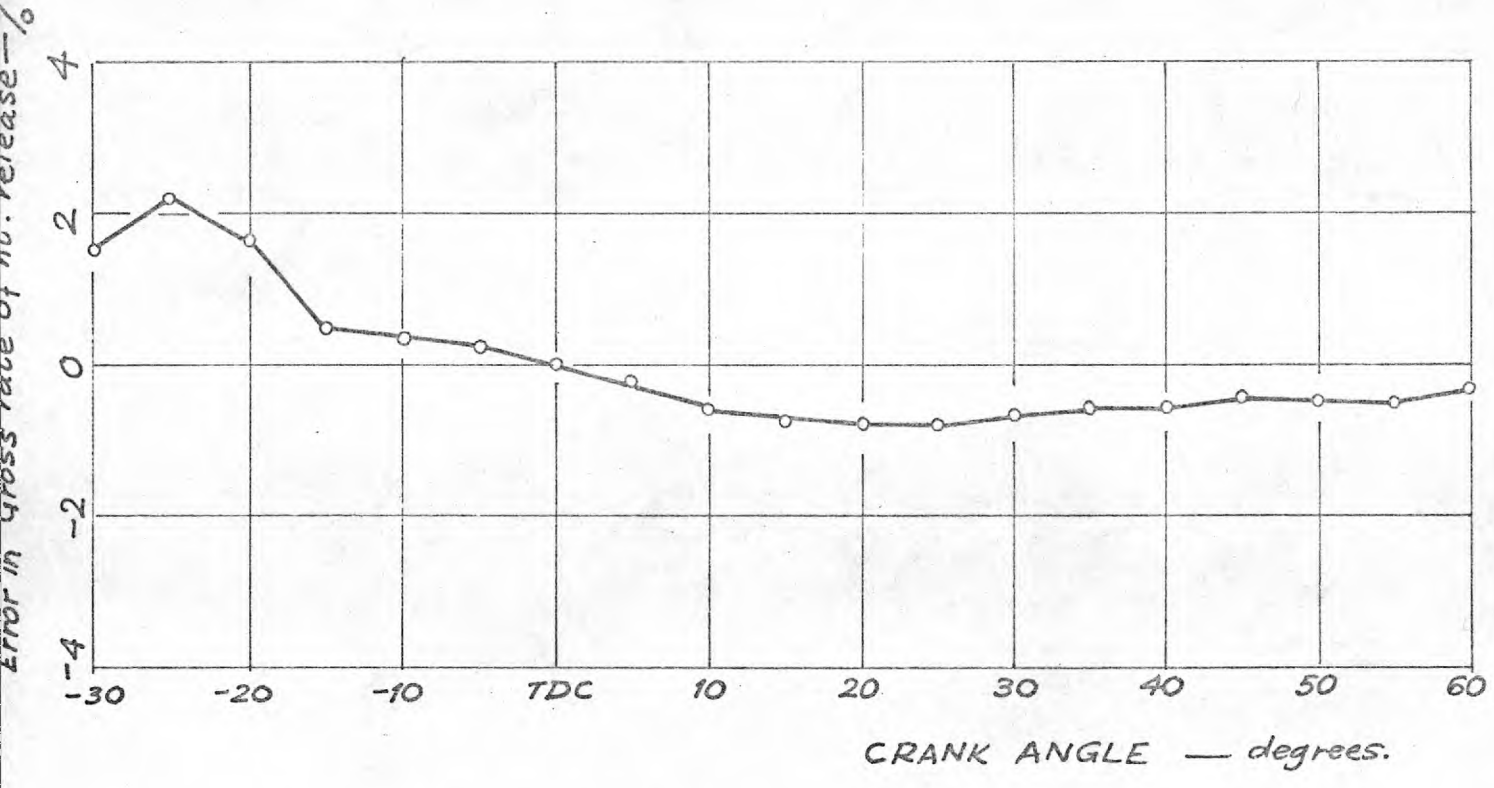


FIG. (A3.2) Accuracy of the method of derivation of the rate of heat release equation

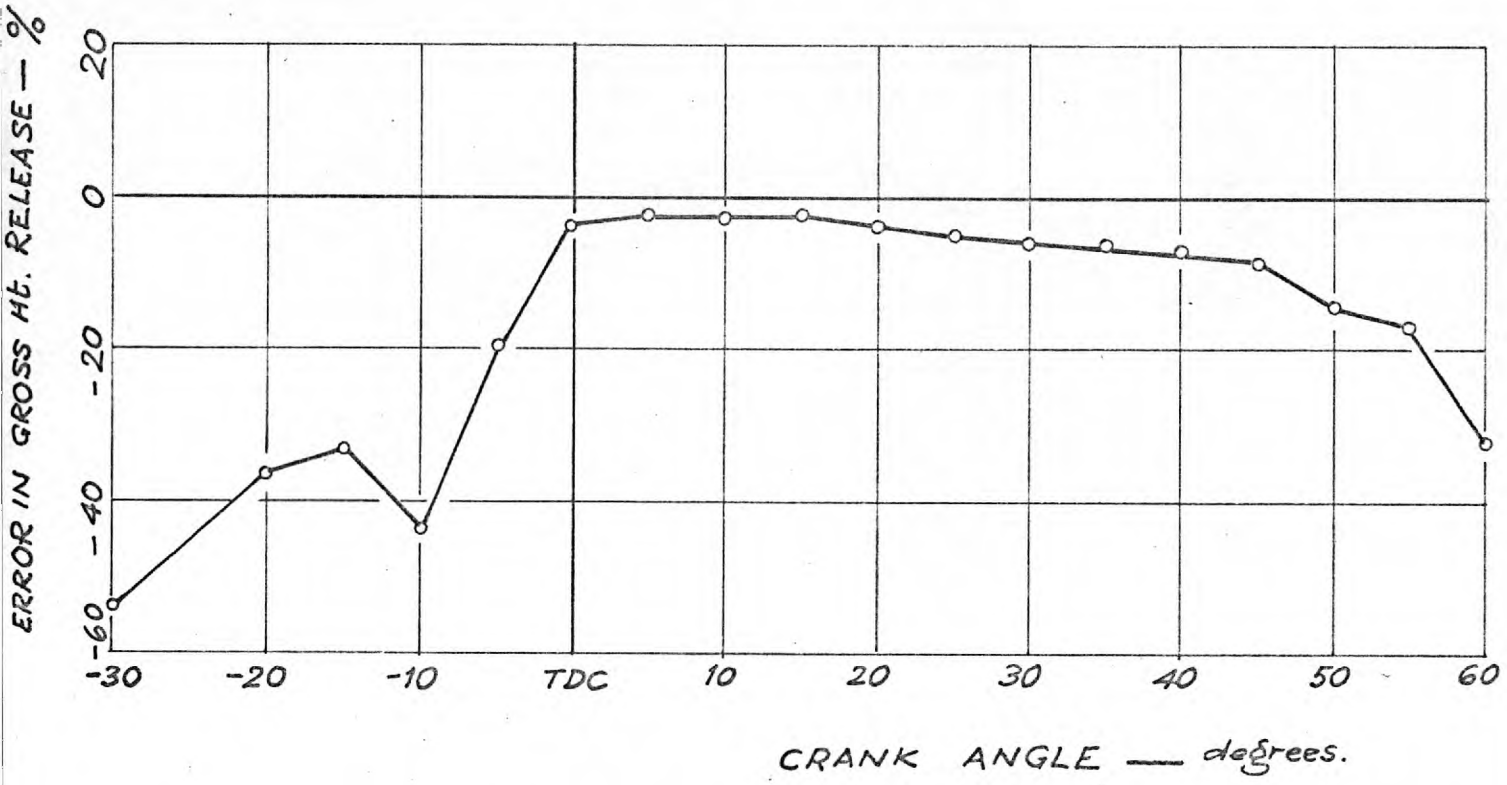


FIG (A3.3) Effect of the use of Eichelberg's formula for heat transfer calculations

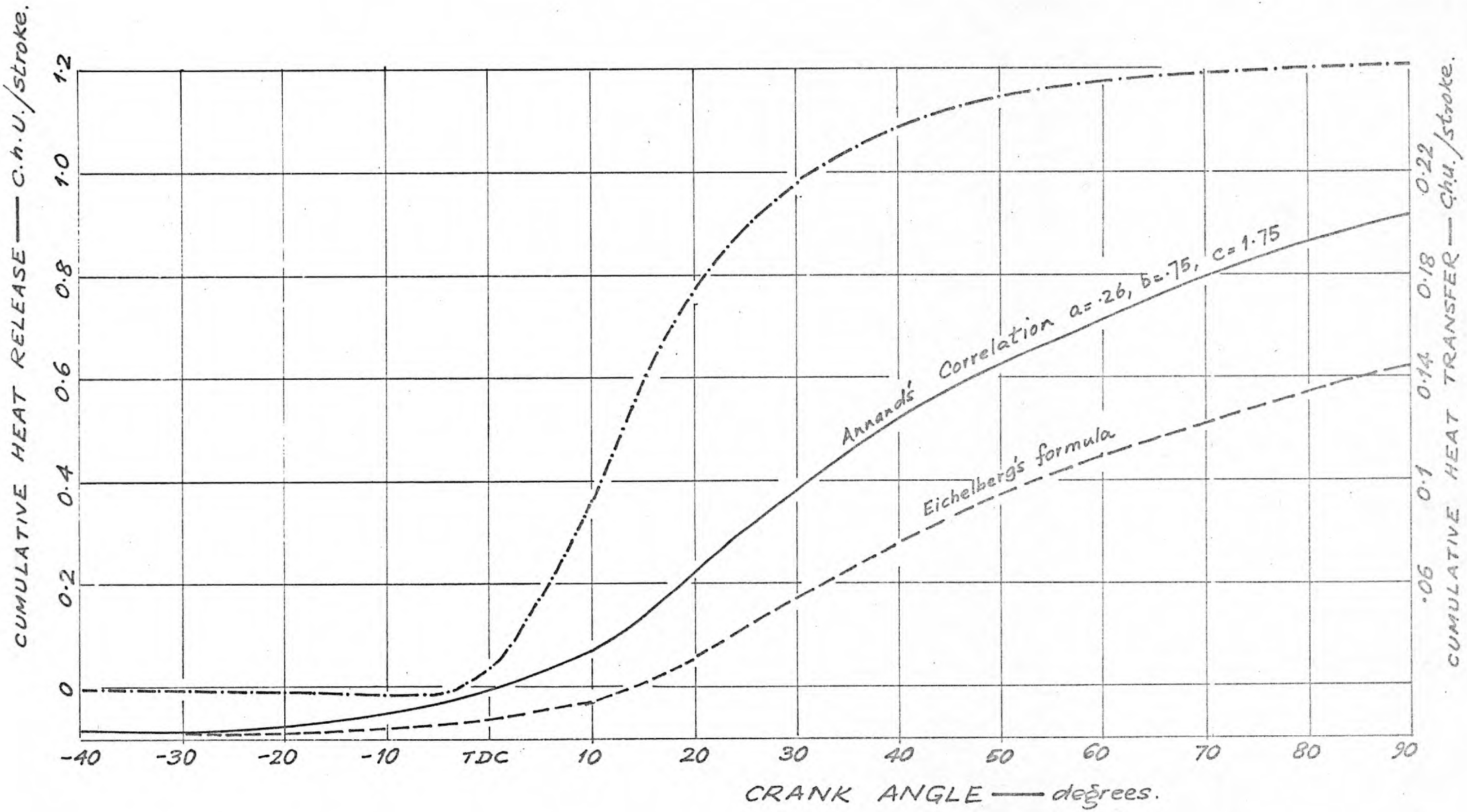


Fig. (A3.4) Comparison of Annand's Correlation with Eichelberg's formula

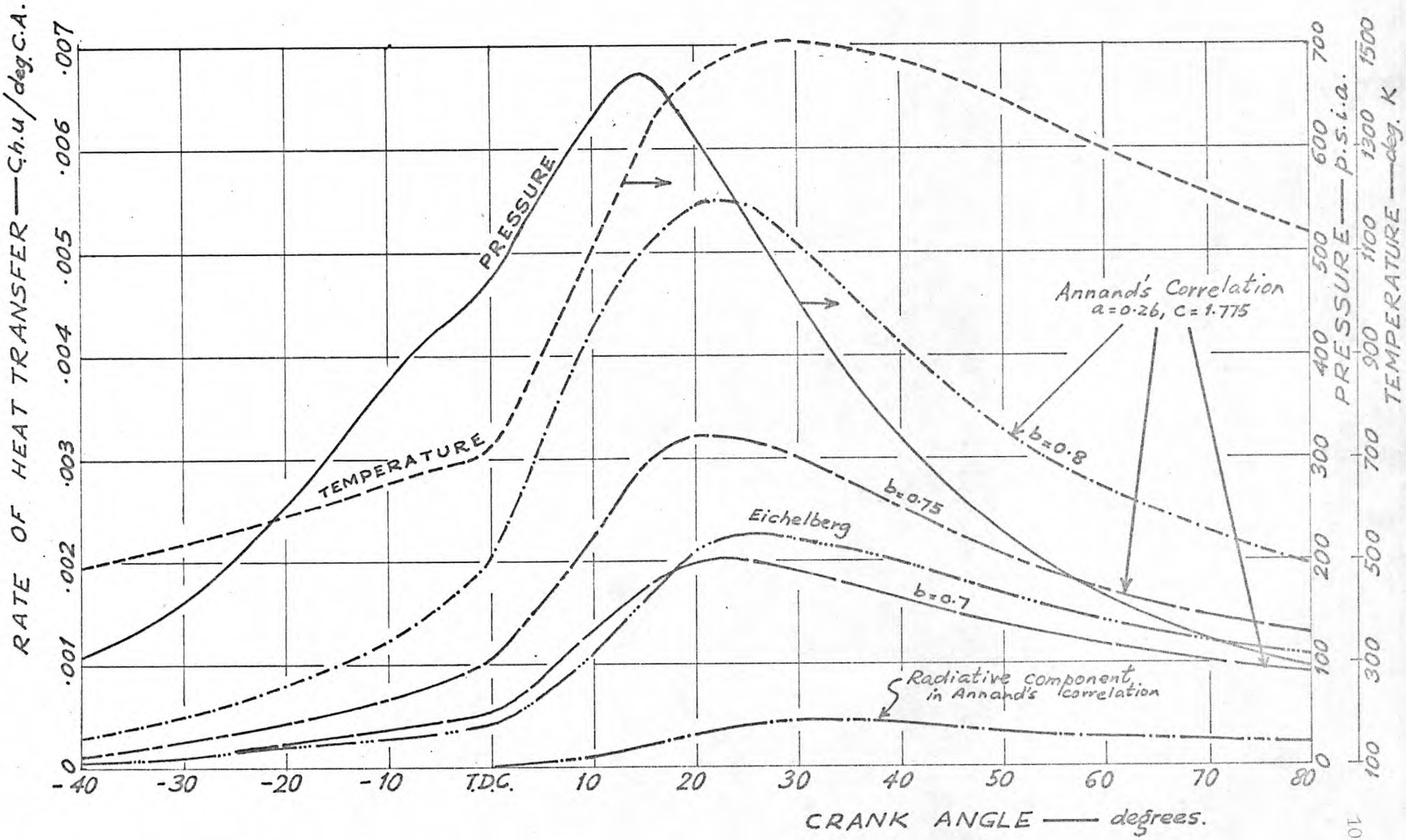


Fig. (A3.5) Analysis of rate of heat transfer variations — The effect of varying constant 'b' in Annand's correlation

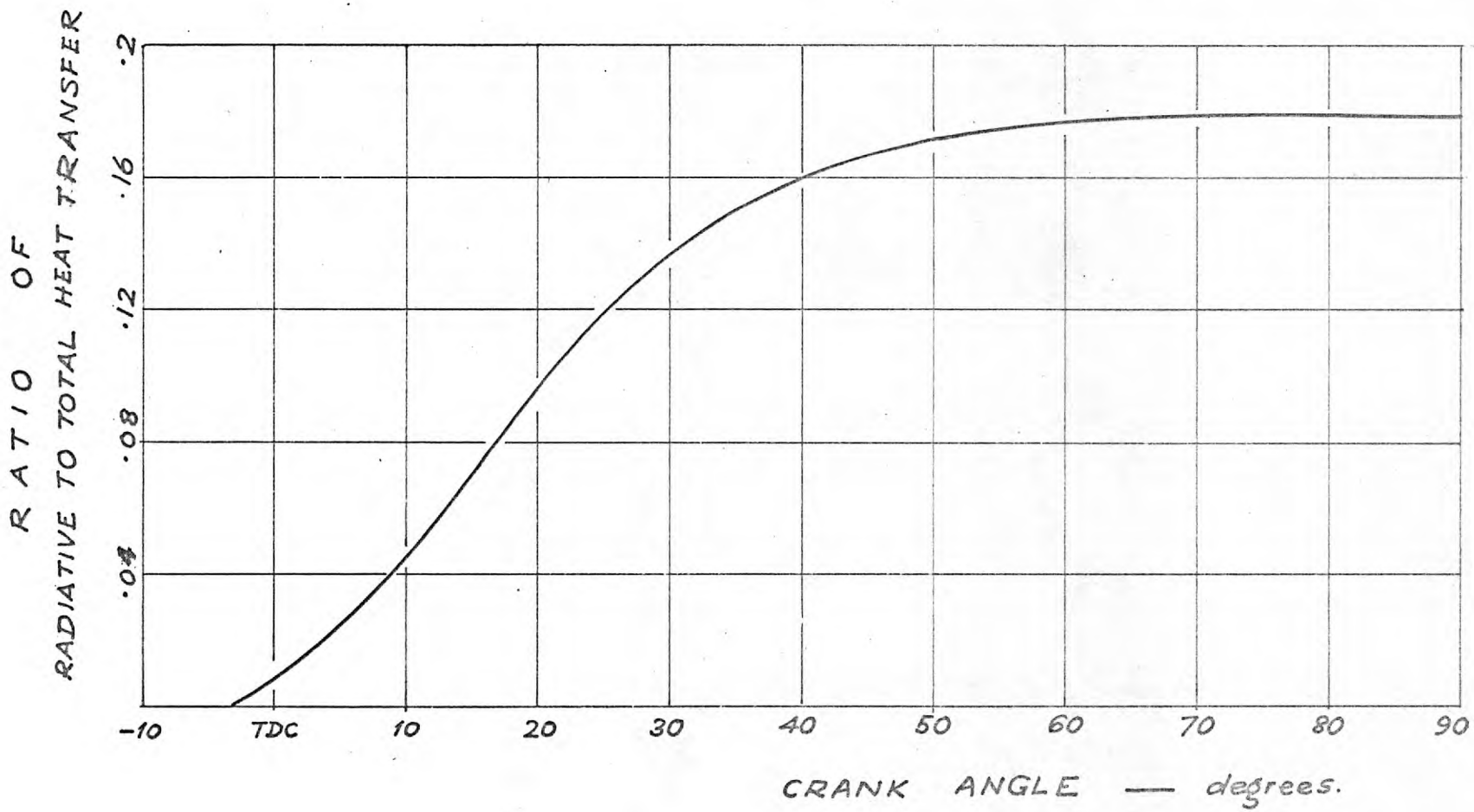


Fig. (A3.6) Analysis of radiative heat transfer computed by Annand's Correlation

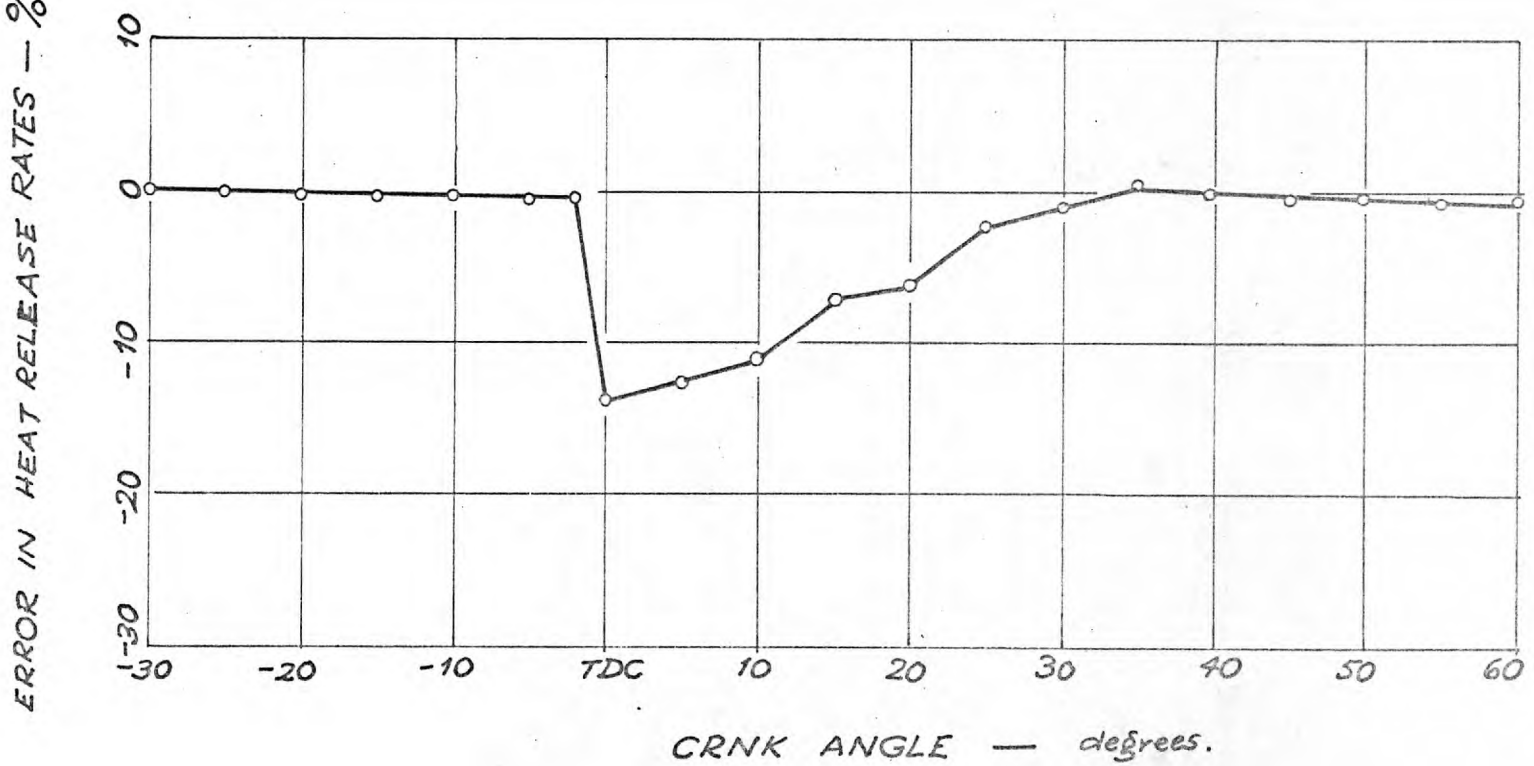


Fig. (A3.7) Effect of the assumption of step-change from reactants to products at ignition

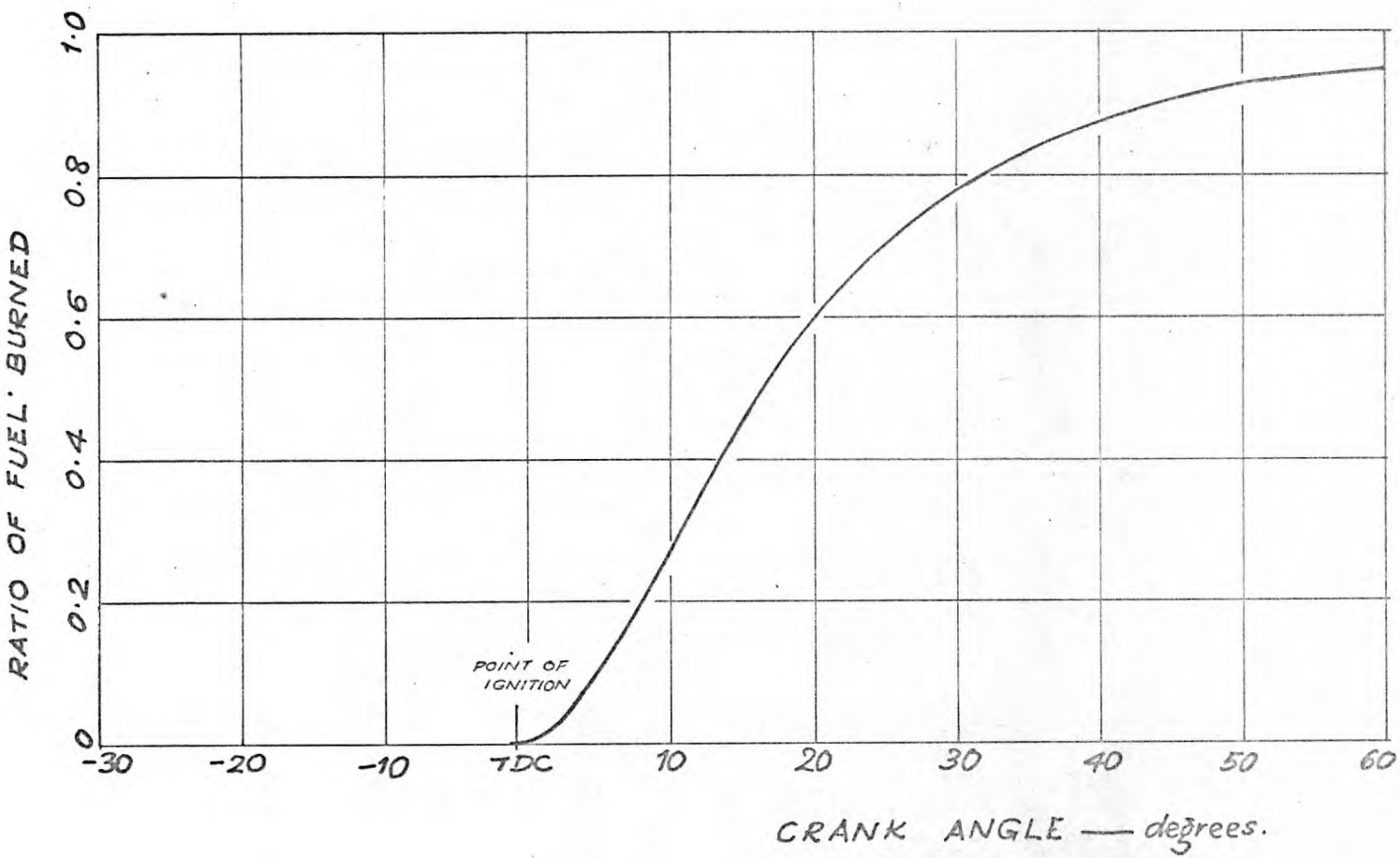


Fig. (A3·8) Variation of computed reactedness of the fuel during the cycle.

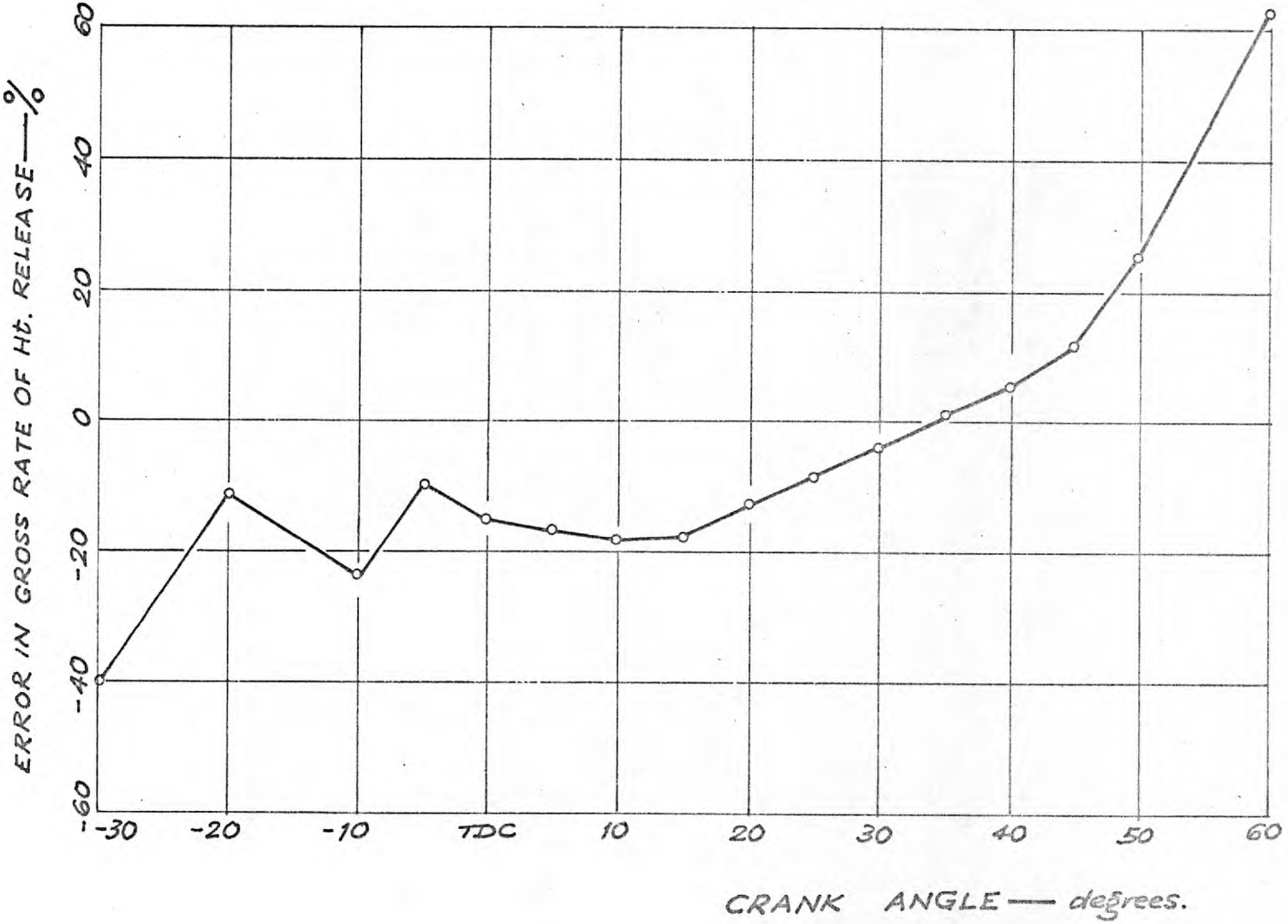


Fig. (A3.9) Effect of the assumption of constant thermodynamic properties of the charge during the cycle.

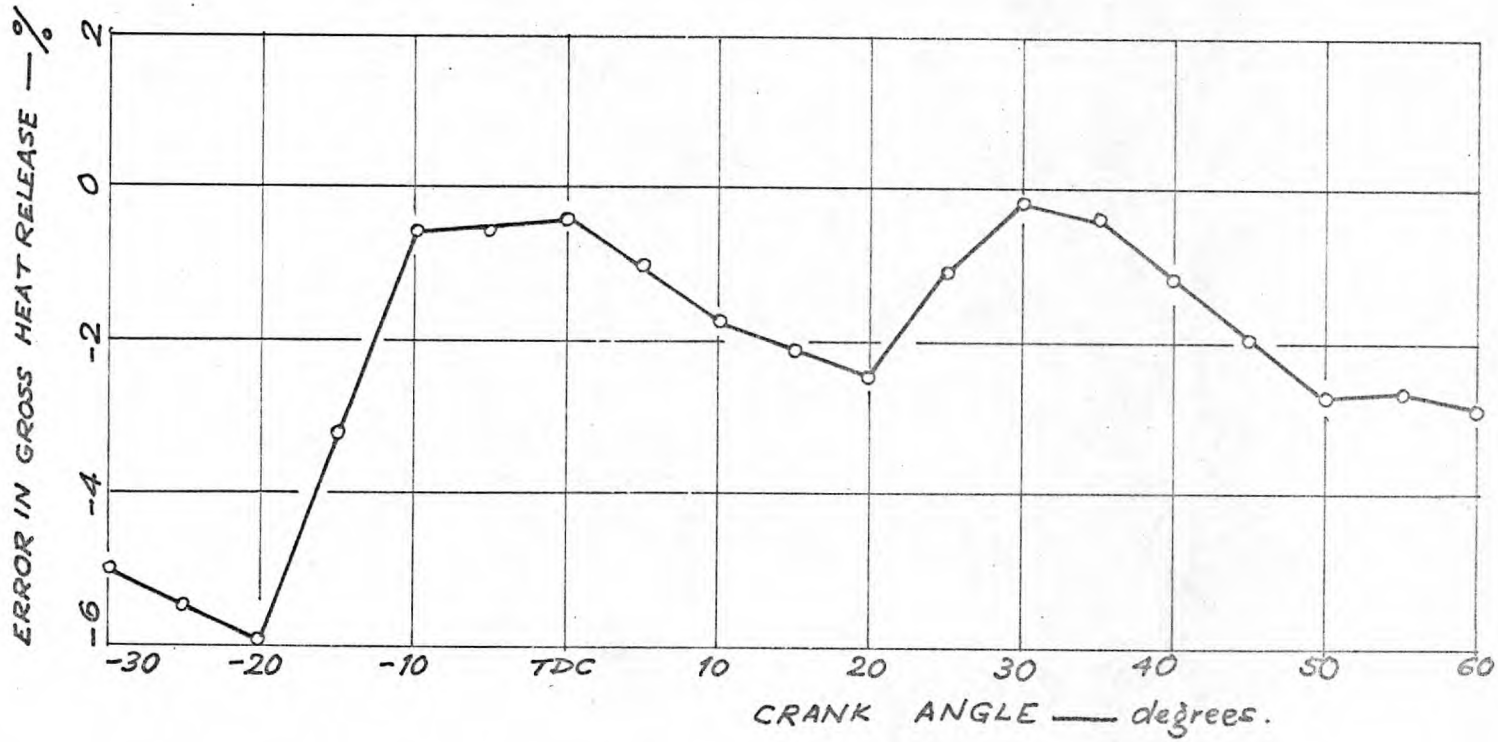


Fig. (A3.10) Error in the computations of heat release rates — effect of increase in step length from 1°C.A. to 2°C.A.

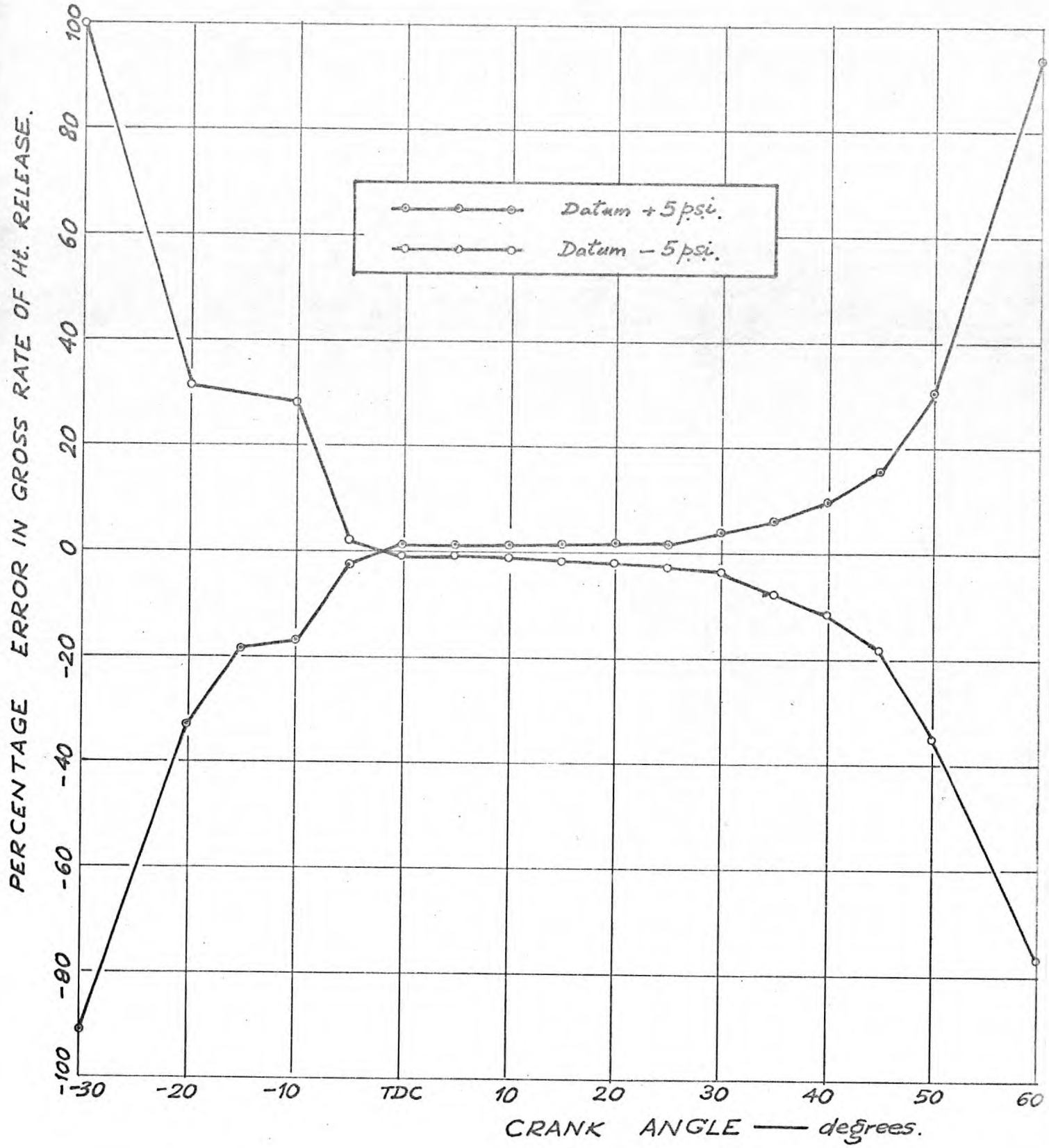


Fig. (A3.11) Effect of the erroneous datum pressure

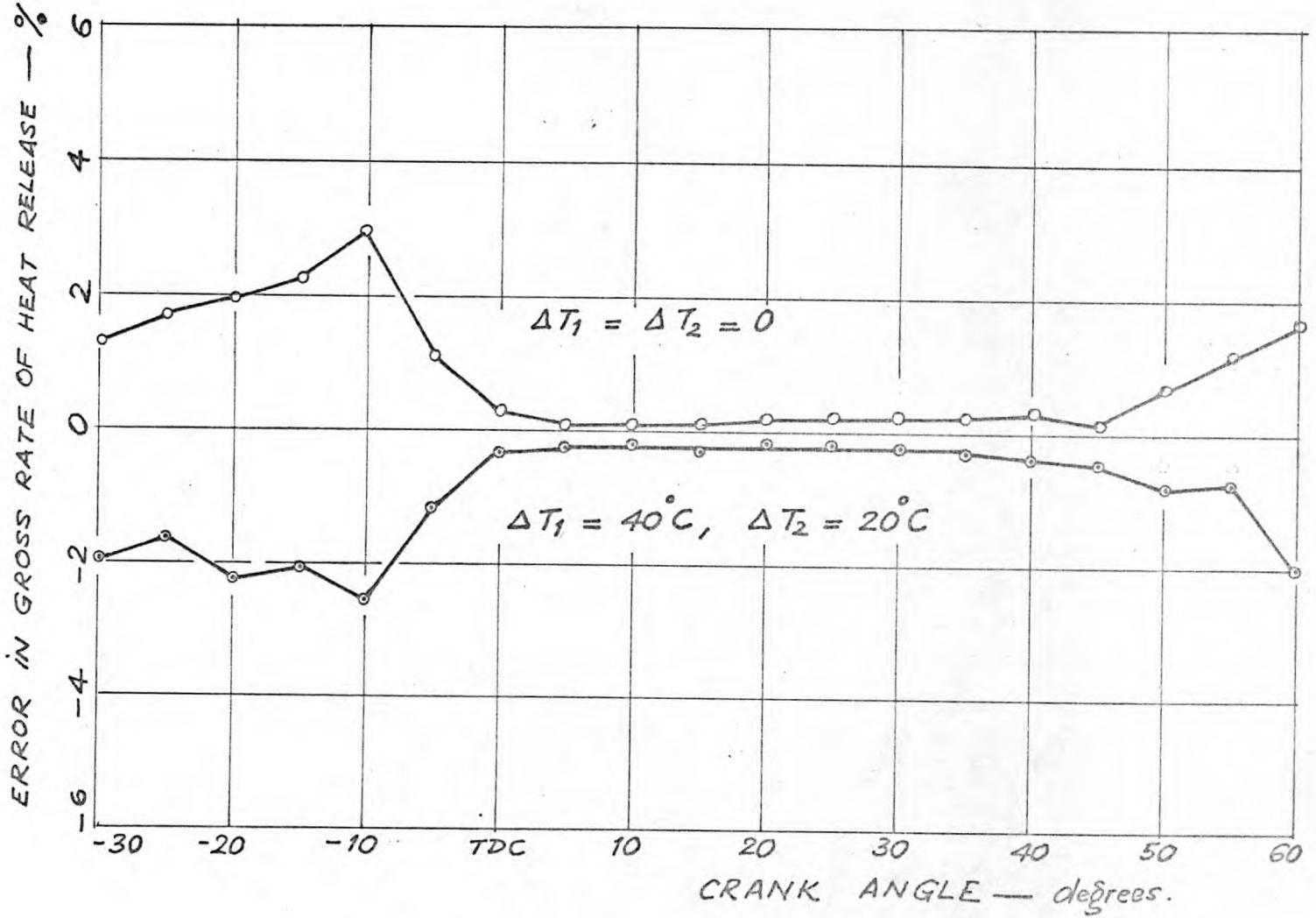


Fig. (A3·12) Effect of change in the combustion chamber wall Temperature on rate of heat release

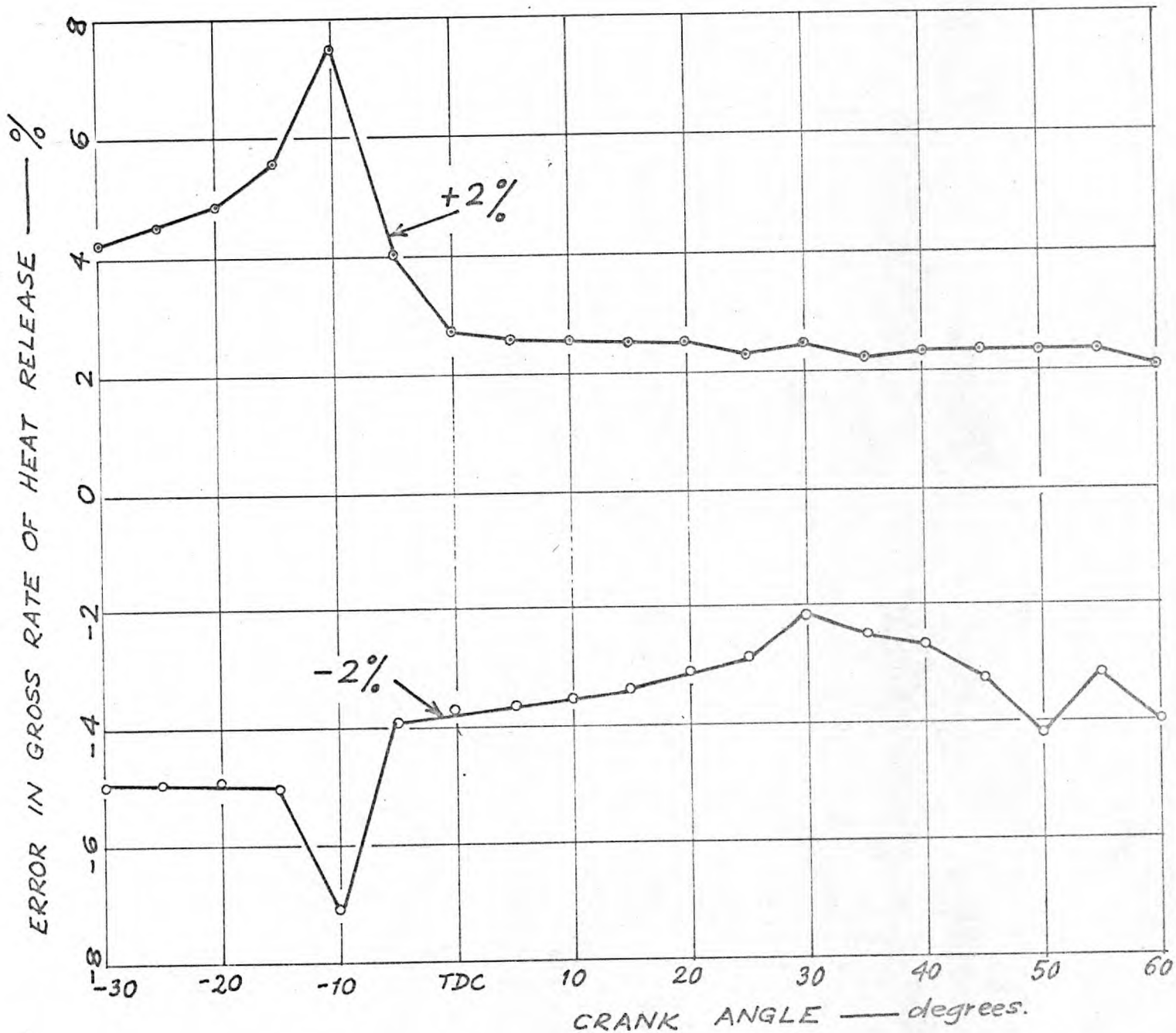


Fig. (A3.13) Effect of error in pressure measurements on gross rates of heat release.

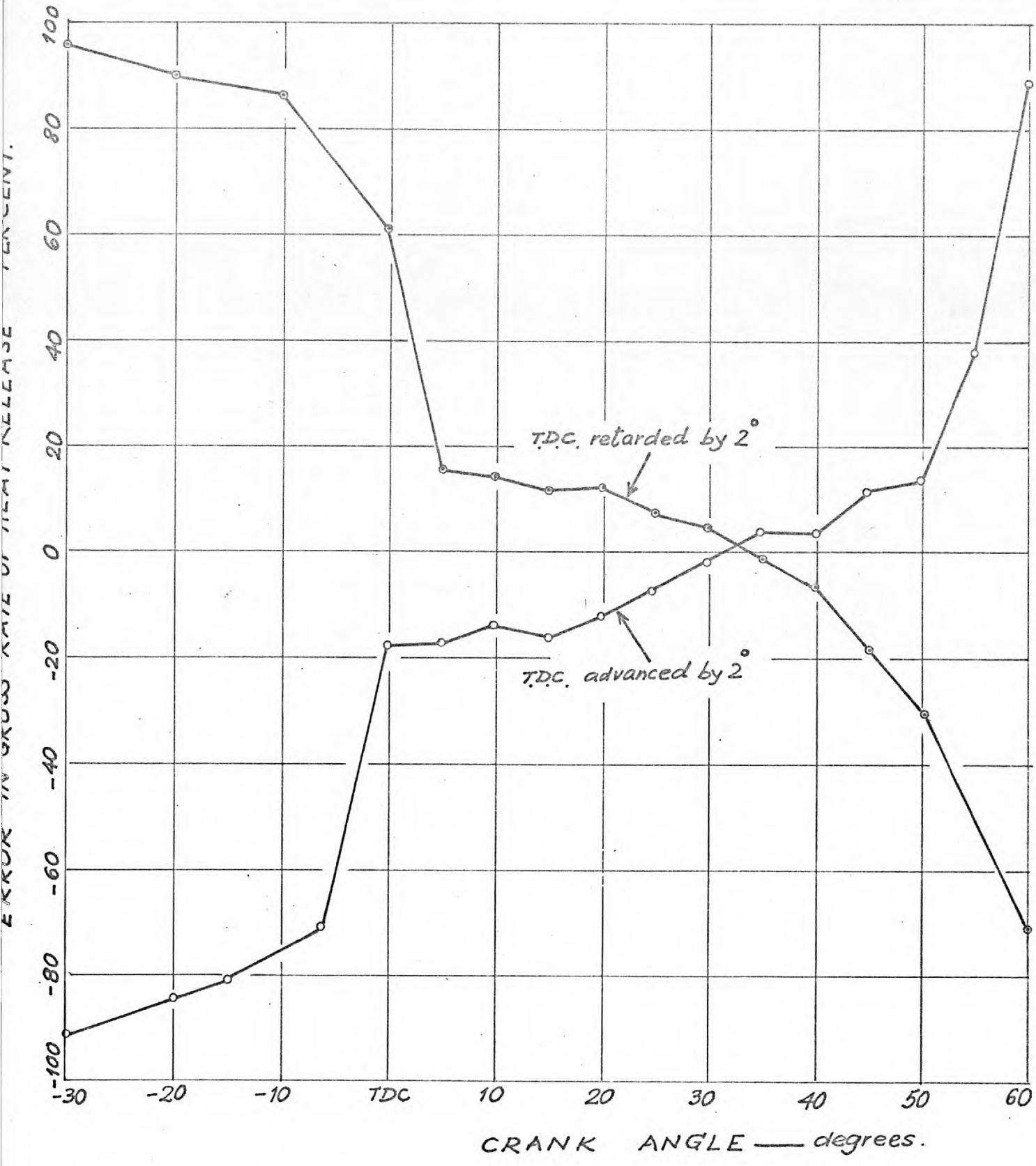


Fig. (A3.14) Effect of erroneous reference in T.D.C. position

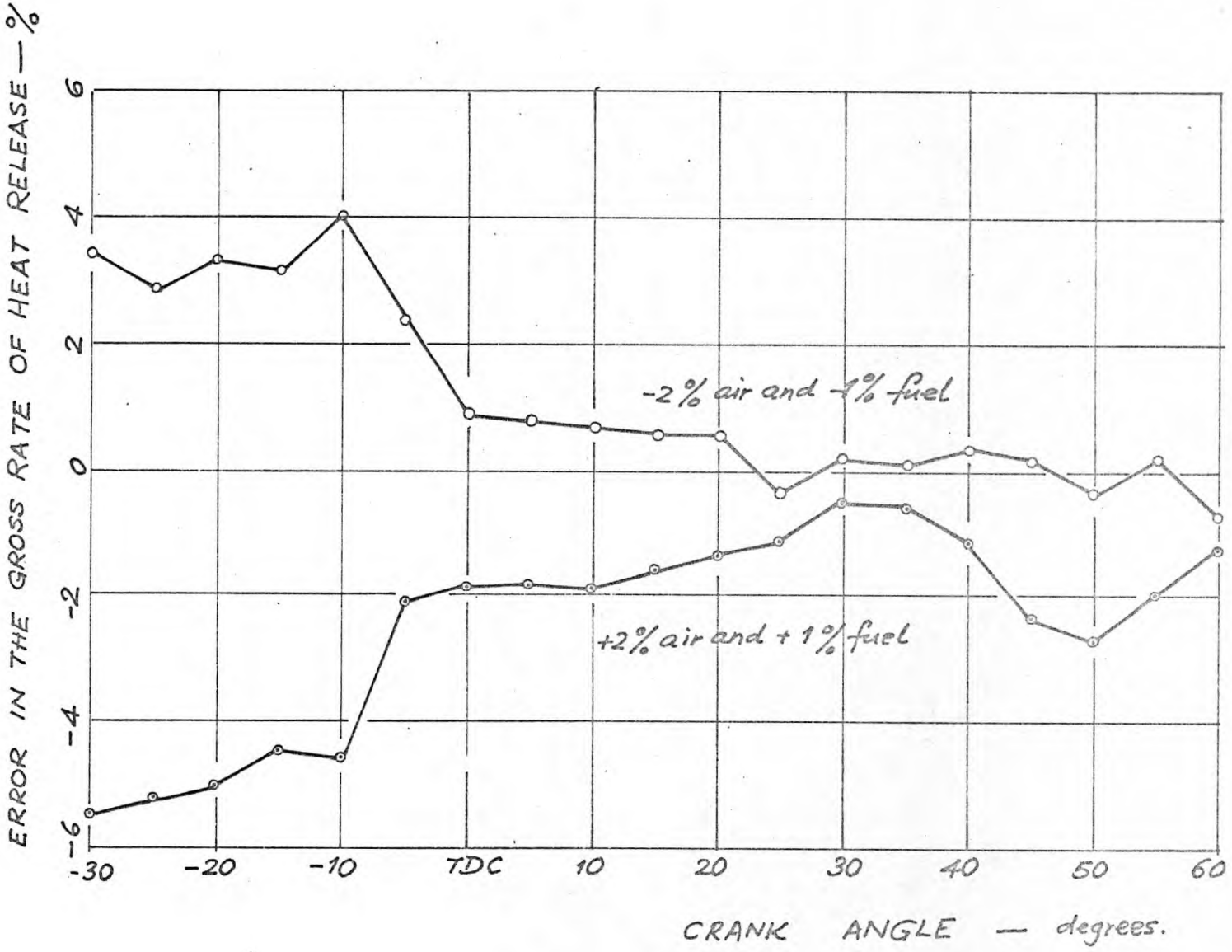


Fig. (A3.15) Effect of inaccuracy in air and fuel flow measurements

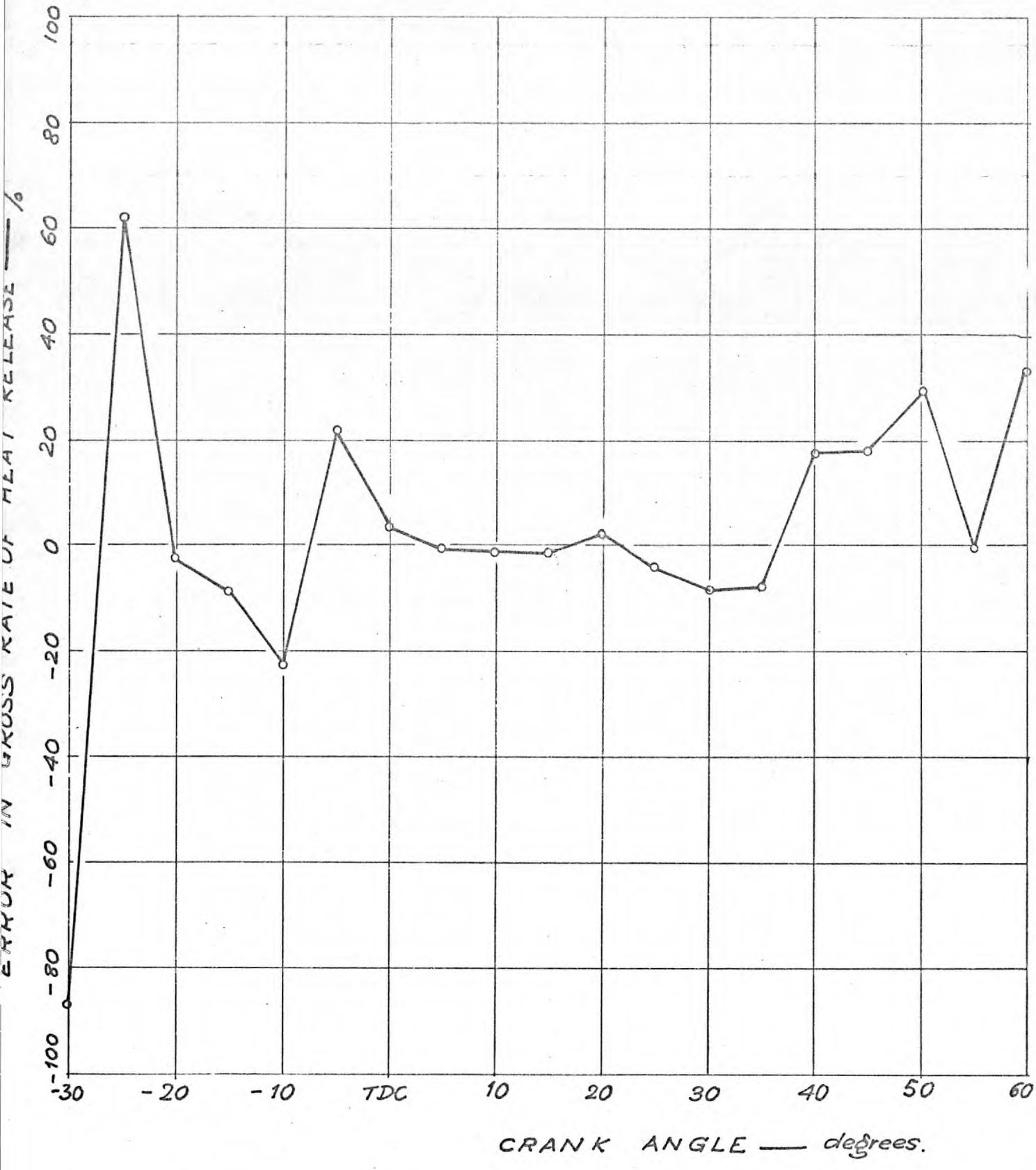


Fig. (A3·16) Effect of data scatter — computations of rates of gross heat release without smoothing data scatter.

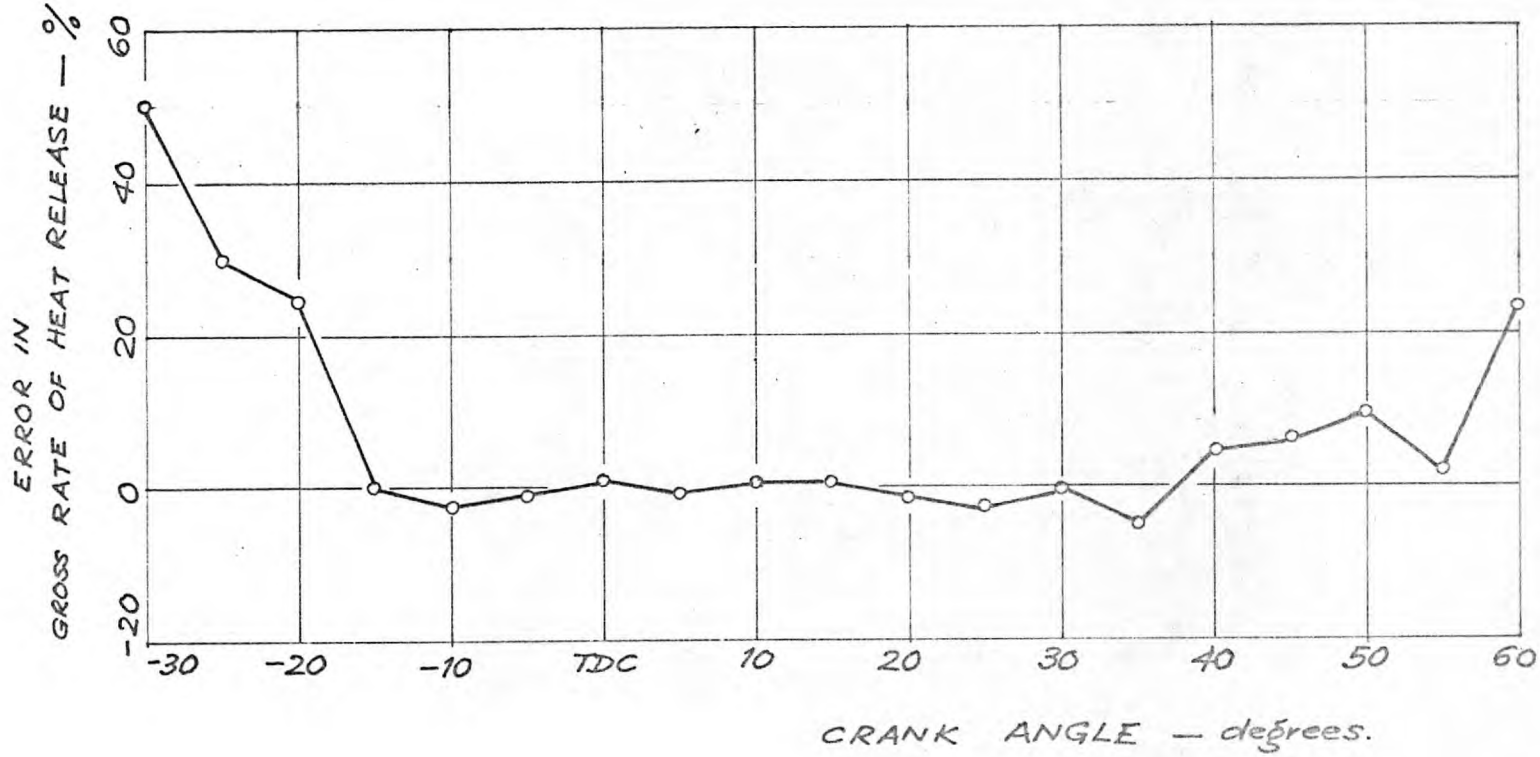


Fig. (A3.17) Accuracy in the method of pressure rate calculations — error if simple interpolation is adopted.

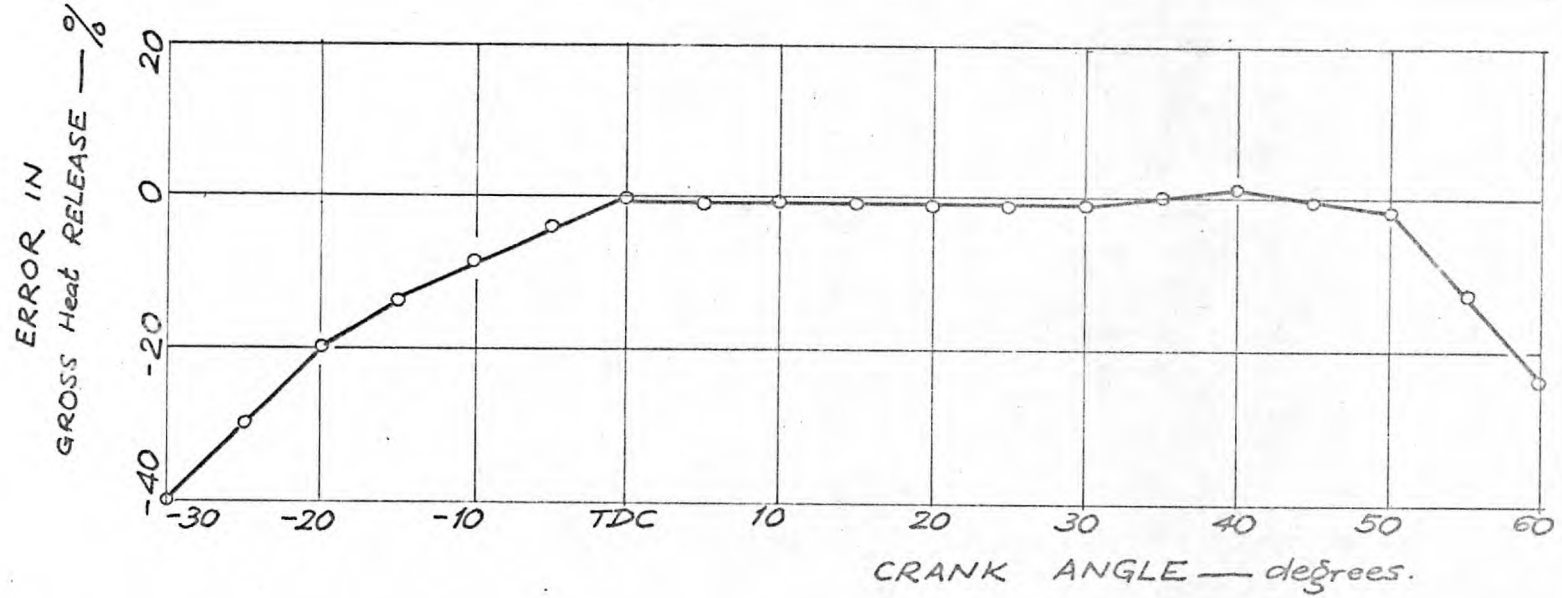


Fig. (A3.18) Effect of smoothing of rates of pressure rise

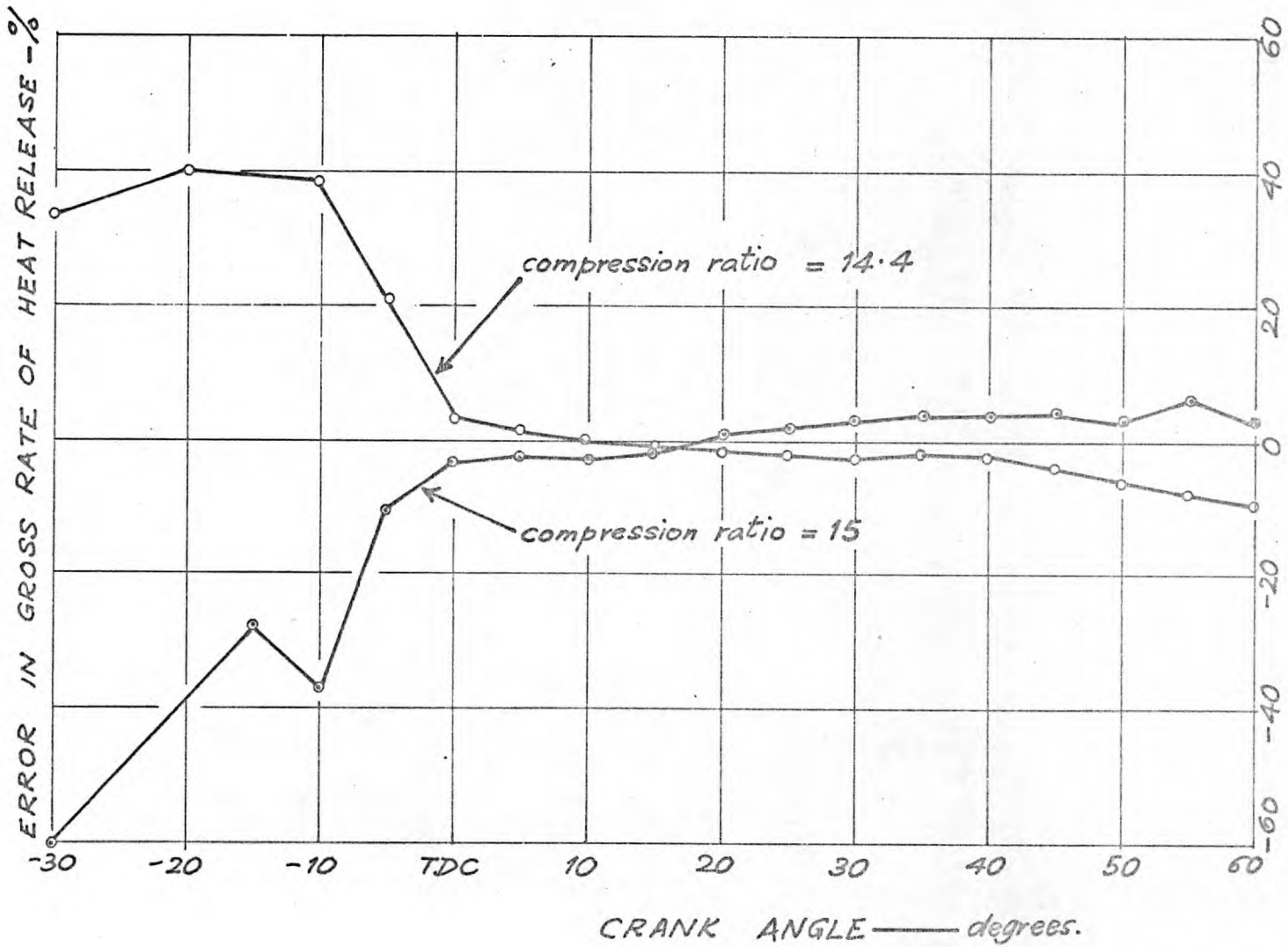


Fig. (A3.19) Effect of erroneous compression ratio

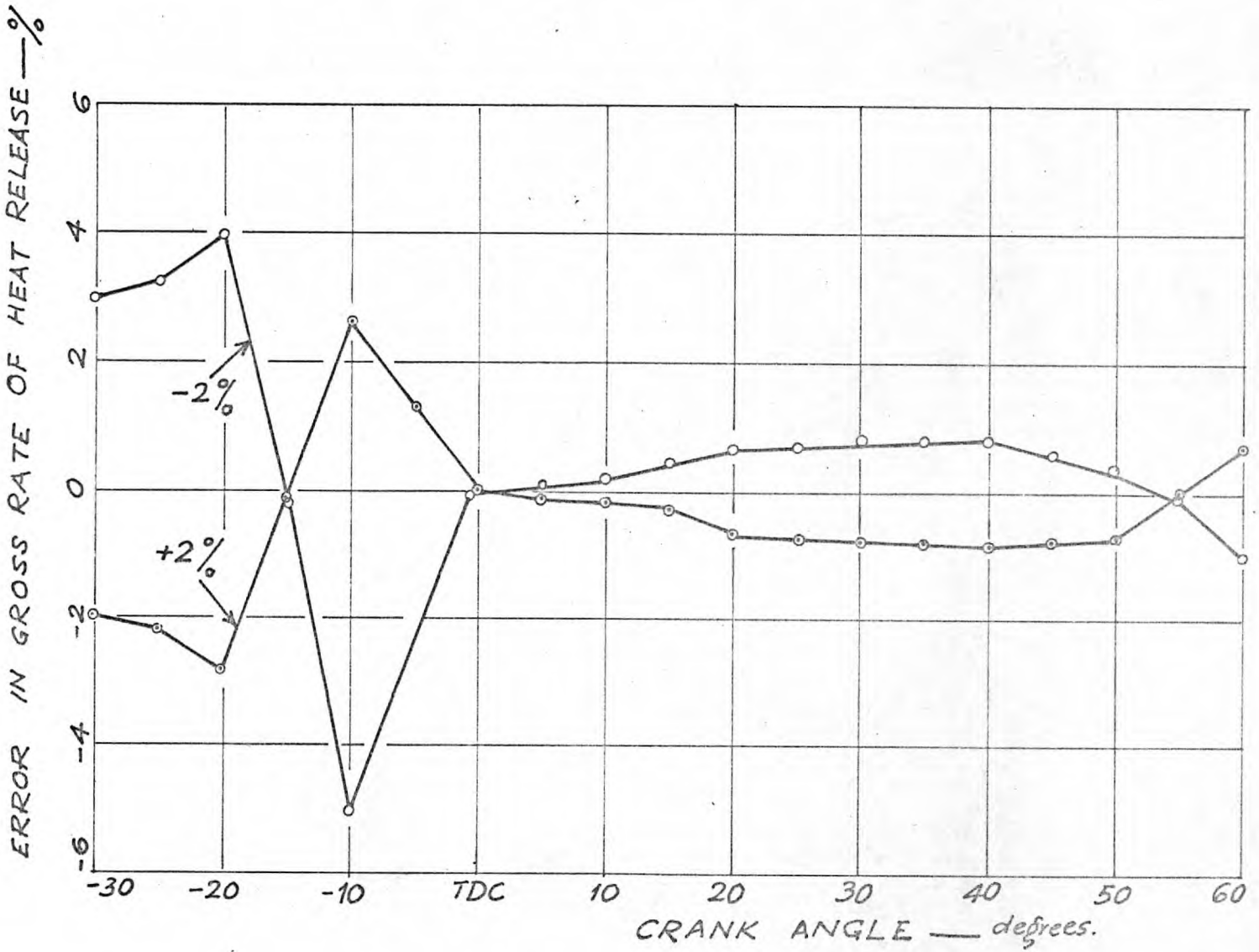


Fig. (A3.20) Effect due to erroneous measurement of connecting rod to crank throw ratio.

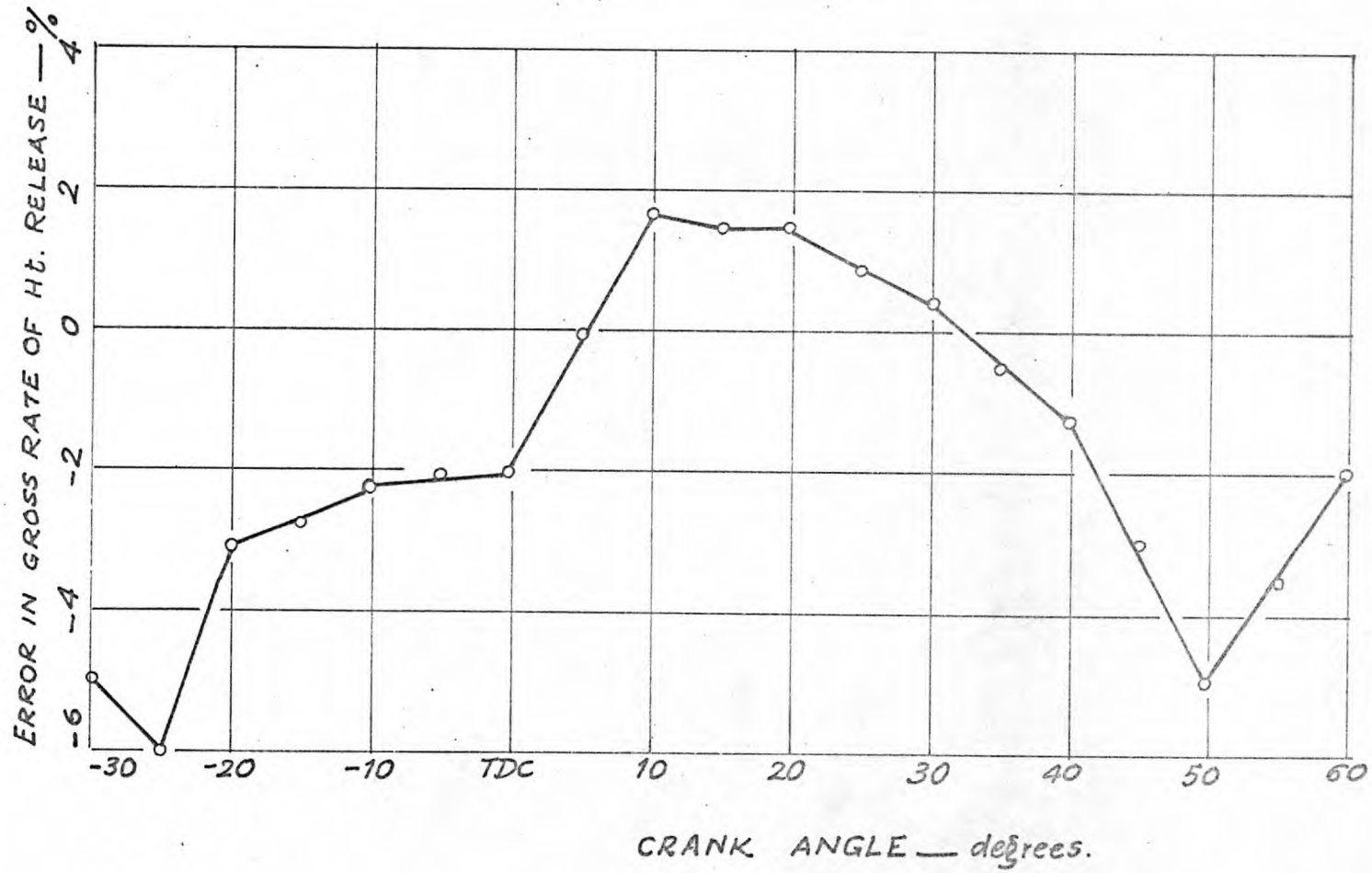


Fig. (A3.21) Effect of angular twist in the shaft.

S. No.	ERROR INTRODUCED		Maximum Error in $\dot{q}^*$			Error in $\dot{q}^*_{max}$	% error in Cumulative heat Release.
	Nature of the error	Magnitude	Magnitude %	Angle of occurance °C.A.	$\dot{q}^*/\dot{q}^*_{max}$ at that angle %		
1	If finite difference form of heat release equation is used.	—	2·1	-24°	-0.7	-0.68	-0.658
2	If Eichelberg's formula for heat transfer is used.	—	-53·5	-30°	-0.29	-2.29	-5.25
3	Step change in reactants to products.	—	-15.	-15	22.9	-10.	-7.08
4	If thermodynamic properties assumed to remain constant.	—	60.	60.	1.79	-19.0	-10.92
5	If step-length is doubled.	2°C.A.	-6.	-20.	-1.9	-2.58	-1.47
6	Erroneous datum pressure.	+5 p.s.i.	-90	-30	-0.29	1.01	4.6
		-5 p.s.i.	100.	30	-0.29	-0.87	-4.93
7	combustion chamber wall temperature.	$\Delta T_1 = 40°C$ $\Delta T_2 = 20°C$	-3.	-10	1.153	-0.11	-0.329
		$\Delta T_1 = \Delta T_2 = 0$	3	-10	1.153	0.11	0.329
8	Erroneous reference in T.D.C.	2° advanced	100.	-30.	-0.29	-14.9	-10.7
		2° retarded	100.	-30.	-0.29	13.69	9.05
9	Erroneous air and fuel flow measurement.	+2% air +1% fuel.	-5.7	-10.	1.153	-1.72	-1.645
		-2% air -1% fuel	-5.7	-10.	1.153	0.68	.658

* denotes usually computed values as shown in Fig. (A3.1)

TABLE (A3.1) SUMMARY OF ERRORS CONSIDERED.

continued on p.125

S. No.	ERROR INTRODUCED		Maximum error in $\dot{q}^*$			Error in $\dot{q}^*_{max}$	% error in Cumulative heat release.
	Nature of the error.	Magnitude	Magnitude %	Angle of occurance °C.A.	$\dot{q}^*/\dot{q}^*_{max}$ at that angle		
10	Erroneous pressure measurement.	+2%	7·5	-10	1·153	2·53	2·47
		-2%	-7·0	-10	1·153	-3·57	3·45
11	If pressure data is not smoothed.	—	60	-25	-0·125	-0·24	-0·165
12	If $\left(\frac{dp}{d\theta}\right)$ is determined by linear interpolation.	—	50	-30	-0·29	1·78	-0·247
13	If $\left(\frac{dp}{d\theta}\right)$ is also smoothed.	—	40	-30	-0·29	-0·96	0·0
14	change in compression ratio.	+2%	-60	-30	-0·2	1·52	0·986
		-2%	40	-20	-1·9	1·04	0·165
15	change in con. rod to crank-throw ratio	+2%	2·6	-10	1·153	-0·29	-0·247
		-2%	4·0	-20	-1·9	0·3	0·247
16	Torsional twist.	-0·25°	-6·0	-25	0.	1·62	0·329

TABLE (A3.1) SUMMARY OF ERRORS CONSIDERED

C H A P T E R A4

DISCUSSION OF RESULTS AND CONCLUSIONS

A4.1 Introduction

A preliminary examination of effective rates of combustion heat release in a dual-fuel engine has been reported in a paper to the Institution of Mechanical Engineers (42), wherein only a limited number of key heat release records were appended on account of space limitations. Since then, the computer programme has been generalised, Annand's correlation for rate of heat transfer has been introduced and a finite reaction rate subroutine has been incorporated. The reader may well like to be shown the virtues of such improvements which have been exhaustively discussed in the preceding chapter. It has been demonstrated there that, in spite of certain limitations, tangible conclusions can effectively be drawn from this analysis towards developing better understanding of the underlying combustion processes.

A4.2 Discussion of Results

The small negative gross heat release rates that can be observed prior to ignition on all the records can be the direct consequence of the inadequacy of Annand's correlation to account for heat transfer. It was found that this situation was more aggravated with the use of Eichelberg's formula. Therefore, the relative contribution to the apparent heat release of the processes of pilot fuel evaporation and the preignition processes cannot adequately be established. Such uncertainties are not unexpected in an overall analysis of this nature as reported by Austen and Lyn (63). It may well also be that the small pilot quantity employed in dual-fuel operation rendered these processes insignificant on the heat release pattern. This is well illustrated in Fig. (A2.19) of diesel cycle analysis where a significant 'negative' heat release is noticeable.

In contrast to 'pure' diesel combustion, the pilot fuel in a dual-fuel engine normally undergoes more delayed ignition. This is believed to be mainly due to the influence of the gaseous fuel present in the charge. A protracted delay should enable the pilot injection to be completed with substantial evaporation and mixing of the pilot vapour with the gaseous fuel charge, before ignition begins. Once ignition commences, therefore, some of the gaseous fuel present in the vicinity of the multiple ignition sources will inevitably be involved. It will make a substantial contribution to the initial part of the heat release if the charge is rich enough to be beyond the effective lower flammability limit of the mixture.

An examination of various heat release records, of which Figs. (A2.4 - A2.7) represent a typical cross-section, suggests that dual-fuel combustion generally undergoes two distinct phases. The first phase is associated mainly with the consumption of the pilot charge and some associated gaseous fuel,whilst the second phase is almost entirely dependent on the concentration and the quality of the gaseous fuel employed.

It can be seen, for example, from Fig. (A2.4) that for a given pilot fuelling rate, the initial rate of heat release remains almost the same as the gaseous fuel concentration is increased. This similarity of the initial rates of heat release tends to keep close together the cumulative heat-release diagrams around T.D.C point and marked changes become apparent only over the latter part of the cycle, as is evident from Fig. (A2.8). As the main fuelling rate was increased further, there occurred a proportionate increase in the heat release during the first phase indicating that a larger proportion of the charge was involved. When the pilot fuel is increased, however, for a constant addition of gaseous fuel, the initial rates of heat release show a marked difference accordingly.

It is interesting to note from Fig. (A2.14) that under lean mixtures of gaseous fuel the heat release during the first phase corresponds to the heat value of the

pilot fuel itself, confirming that the first phase is associated primarily with pilot fuel combustion. It can also be seen from the same figure that, even under rather lean mixture conditions, the first phase shows the tendency to project over the second as the pilot is increased. If the premixed gaseous fuel mixture is rich enough, the increased pilot fuelling rate will incorporate in the combustion a substantial amount of the gaseous charge which would eventually give rise to a considerable increase in the rate of heat release and may lead to knock. This is fully explained by Fig. (A2.10).

The ignition characteristics of the pilot fuel are pronouncedly affected by the gaseous charge under small pilot fuelling rates. This is evident in Fig. (A2.4) where a reduction of the gaseous fuel in the charge shows substantial delay in the initial release of heat. The ignition delay was observed to diminish slightly with richer gaseous fuel concentrations. This could be due to higher exhaust and combustion chamber wall temperatures which offer the pilot hotter environment thereby influencing the pre-ignition reactions of the pilot fuel leading to earlier combustion.

Under the conditions of light audible knock, the initial rates of combustion remain the same except that the first stage of combustion gets prolonged and persists over a much longer period than the knock-free combustion. The rates of burning are excessively high and project well over the second phase. This is indirectly indicative of the autoignition nature of knock (43) and the simultaneous rapid burning of the pilot together with a very substantial fraction of the gaseous charge. Under violent knocking the same conditions prevail but with larger magnitudes. Fig. (A2.15) presents the heat release analysis of a violent knocking engine cycle. It is apparent from this figure that the release of energy is exceedingly high and both stages exist in close proximity, unlike that under normal working conditions.

The second phase of dual-fuel engine combustion with normal knock-free operation is indicative of much

slower burning. With lean mixture strengths and with relatively small pilot it separates out from the first phase indicating unfavourable conditions for the rapid consumption of the gaseous fuel, thus contributing only marginally to the heat released. Under such conditions, a substantial percentage of the fuel has been found to appear in the exhaust (10, 72). Fig. (A2.8) illustrates well the significant reduction in the cumulative heat release associated with the reduction of methane concentration in the intake.

In the present analysis, four pilot fuelling rates, viz 0.35, 0.5, 0.75 and 1.0 lb/h, have been covered. They covered a vast range of 8 - 50% of the total heat input. Although higher pilot rates of more than 10% are not adopted in practice for economy, it was thought worthwhile to study the influence of increased pilot rates to throw some light on combustion processes as a transition from diesel to dual-fuel operation entails 'pilot' variation from 100% to about 10% of the total heat input. Increased pilot fuelling rates with a constant methane concentration bring about higher peak pressures, see Figs. (A2.9 and A2.12), higher pressure-rates Fig. (A2.13), slight reduction in ignition delay Fig. (A2.10) and improvement in thermal efficiency. Whereas higher pressure and its rates are the direct consequence of combustion heat release, the reduction ofignition delay can be inferred due to higher cycle temperatures influencing the pre-combustion reactions. A close examination of Fig. (A2.10) reveals that the increased pilot fuelling rates are responsible for higher rates of combustion heat release in the first stage although the combustion processes tend to slow down in the second stage, thus terminating earlier. This can be attributed to partaking in combustion of large proportion of gaseous charge entrained into the fringes of the pilot, which increase in accordance with the pilot rate, thereby rendering comparatively lesser quantity of the rest of premixed charge to be enflamed. It lends to explain as to how the onset of knock can be averted with an increase in pilot. It is

apparent from Fig. (A2.11) that, except for very low pilot rate, the cumulative heat release does not differ significantly with the increase in pilot, suggesting that there is no significant gain in thermal efficiency. This is why most dual-fuel installations offer an economic edge in their operation with nominal pilot quantities in comparison with diesel engines operating at comparable load conditions.

The analyses of heat release rates with carbon dioxide addition indicated that, although the initial rates of burning remained substantially the same, the peaks of the heat-release rates of both stages and the cumulative heat release were reduced. The flame seems to be restricted to pass through the charge rendering an increased amount of fuel to escape without being fully consumed. This entails loss of useful output as indicated by Fig. (A2.25).

The knocking intensity was found to reduce with the increased addition of carbon dioxide. For the case presented in Fig.s (A2.16 and A2.17) knock was found to persist until a concentration of 25% carbon dioxide was reached in the fuel. Under these conditions, the two phases of combustion merged toger, thus exhibiting a more progressive burning and producing a heat release rate variation with time in a way not unlike that of spark-ignition engines.

Fig. (A2.18) illustrates the reversed technique of predicting the cylinder pressure development from a known heat release pattern following the computing procedure as described in Fig. (A2.2). It demonstrates the utility of the heat release analysis for predictions of the engine performance at the design stage. Detailed discussions are to follow in Part C of the thesis where the understanding of the combustion processes generated with the present exercise will be synthesised to develop a model with due reference to its limitations.

Figs. (A2.19 - A2.24) serve to compare rates of heat release under various modes of operation. It is apparent that dual-fuel engine combustion lies in between diesel and gas engines, both of which undergo characteristic

three and single-stage combustion, respectively. In dual-fuel engine combustion the absence of the trailing stage commonly referred to in diesel combustion (see Fig. A2.19), is indicative of the fact that if the initial stage is established, the second stage occurs subsequently and faster combustion ensues, which terminates earlier leaving no tail-ender, unlike diesel combustion. Faster combustion in the second stage is mainly due to the pre-mixed gaseous fuel present in the engine cylinder. This is further evidenced from the heat release diagram of a spark-ignition gas engine as shown by Fig. (A2.20), wherein the combustion processes can be seen to undergo completion in a single stage following ignition and are short-lived, lasting about 20° of crank rotation as against 70° and 50° in the case of diesel and dual-fuel combustion, respectively. Figs. (A2.22 and A2.23) present heat release records of compression ignition of diesel oil and spark-ignition of gasoline under the 'M' system. It is interesting to note that the stratification of charge, whether in compression ignition or spark ignition, renders the combustion processes controllable by prolonging the duration of significant combustion heat release period. Table (A4.1) presents a comparative study of rates of heat release under various configurations of reciprocating engine combustion. Three parameters have been selected for comparison, namely: a distinct number of stages of heat release, time in terms of crank angle required to reach the peak from point of ignition, and the duration for which the significant combustion heat is released. The relative differences are obvious in the table.

It has been demonstrated that the approach of heat release analysis, when adopted with the aid of high-speed computer techniques, can offer a useful means for the interpretation of the overall nature of some of the complex combustion phenomena in dual-fuel engines. The evidence so obtained is in general agreement with and supplements the relatively limited experimental evidence available as to the nature of the combustion processes in these devices (43, 74).

A4.3 Conclusions

An examination of various heat-release records suggests that the dual-fuel combustion generally appears to undergo two distinct phases. The first phase is associated mainly with the consumption of the pilot liquid fuel together with a part of the gaseous fuel, depending on the concentration of the latter in the main charge. The second phase which tends to be much slower, is dependent mainly on the concentration and quality of the gaseous fuel employed. The heat-release analyses of lean mixture operation indicate, in conformity with other experimental evidence, that comparatively inefficient combustion under such conditions is due mainly to the inability of the gaseous charge to supplement effectively the heat release of the first phase. The use of larger pilots has been found to offset this inefficiency.

Under light audible knock the two phases of combustion merge together and produce excessive rates of heat release which persist over a much longer period than that under knock-free operation. This is indirectly indicative of the autoignition nature of knock and the simultaneous burning of the pilot together with a substantial fraction of the gaseous charge.

The presence of carbon dioxide in methane as a contaminant, although favourable for knock-free operation, brings about a loss in efficiency by reducing heat-release rates.

A comparison between the rates of heat release of various modes of operation is revealing and supplements the understanding of the combustion processes in dual-fuel engines.

S. NO:	SOURCE OF IGNITION	MODE OF OPERATION	NO. of STAGES	Duration between point of ignition and peak of ht. release rate °C.A.	Duration of Combustion °C.A.	Reference Fig. No.
1	compression-ignition	Dual-fuel	2	8° C.A.	50° C.A	A2.3
2	"	Diesel	3	5° C.A.	70° C.A	A2.19
3	"	MAN 'M' System	1	7° C.A	80° C.A	A2.22
4	"	Motored Engine	1	5° C.A	14° C.A.	A2.21
5	Spark-ignition	Gaseous fuel	1	15° C.A.	25° C.A.	A2.20
6	"	Stratified gasolene	1	14° CA	45° CA	A2.23
7	"	Carburetted gasolene	1	12° CA	40° CA	A2.24

Table(A4.1) Comparison between rates of heat release of different modes of Reciprocating Engine Combustion.

C H A P T E R BO

INTRODUCTION

BO.1 Motivation

In dual-fuel engines where the premixed gaseous fuel-air charge is ignited by a small quantity of pilot liquid fuel, knock is now generally believed to be due to the autoignition of the end-charge in a way similar to that in spark ignition engines (22, 43). Recent studies of spark knock by Haskell and Bame (29) and Affleck and Fish (1) have confirmed earlier evidence as to the similarity of pressure development, emission spectra and the nature of products of combustion of a homogeneous charge under spontaneous ignition conditions and the flammation of end-charge under knocking in a spark ignition engine. Although the problem of knock in dual-fuel engines may have been overcome tentatively by derating engines (30), it yet remains a necessity to develop a rational understanding of the underlying combustion processes involved and means for predicting reliably engine behaviour under varied operating conditions.

Most autoignition studies have in the past involved heavier hydrocarbons similar to those utilised in gasolene engines. Relatively little attention has been paid to the understanding of the behaviour of common gaseous fuels and how it is affected by the presence of some heavier hydrocarbons as is the case with some natural gaseous fuels and the important case of the dual-fuel engine. The compression ignition of the pilot fuel charge in these engines is normally responsible for the flammation of the premixed gaseous fuel charge and under knocking conditions the uncontrollable autoignition of the bulk of charge, constituting mixtures with varied concentrations of the gaseous fuel and the pilot fuel vapour.

The analysis of heat release variations in a dual-fuel engine has already been shown to be indicative of combustion processes as a whole under various conditions of

operation studied. A detailed study of the dual-fuel combustion phenomena responsible for the limiting performance of these engines, however, warrants the necessity of a simpler environment wherein combustion reactions due to compression-ignition of the fuels and their blends could be observed individually in the absence of any deliberate ignition source and consequent flame development which otherwise introduce complications. The use of a motored engine is the present choice which qualifies the above requirements in addition to being operational under the conditions similar to those of dual-fuel engines, thus rendering the data pertinent to engine operation without the necessity of any extra- or interpolation.

In most practical combustion systems it is seldom that physical processes alone exercise overall control and hence any attempt to present the combustion processes entirely on thermodynamic bases has only limited application. Therefore, in order to provide a rational basis for the prediction of the gross behaviour of a combustion system, kinetic data are needed. Only in a few instances of practical engineering importance does the reaction process proceed in a single step from fuel and oxidant to combustion products. The conversion from reactants into the products proceeds usually through a number of intermediate steps. The present knowledge of chemical kinetics does not permit us to present a reliable detailed kinetic scheme for the reaction of common fuels and a resort to overall-chemical kinetics is inevitable at this stage, excepting a few cases such as hydrogen-oxygen mixtures.

Most of the established methods for deriving kinetic data experimentally, such as optical studies of flames, shock-tubes, steady-flow reactors, and well-stirred reactors, deal with the combustion processes in situations far removed from that prevailing in actual devices such as the internal combustion engine. Moreover, the available kinetic data in the literature exhibit considerable quantitative variation thus rendering their application full of uncertainty.

The present part describes the use of a motored engine for the determination of relatively reliable kinetic data as a function of temperature for a range of fuel-air mixtures involving common fuels.

B0.2 Literature Survey

In an attempt to establish the nature of reaction mechanisms that lead to autoignition of various hydrocarbon fuels and their blends, investigators have resorted to the use of various types of apparatus such as constant volume bombs, reaction tubes, compression machines of various designs, motored and spark-ignited engines. Early classical bomb experiments, notably those of Townend and collaborators (94, 95), demonstrated the multistage ignition behaviour of different hydrocarbons and the existence of cool flame peninsula over a limited temperature and pressure range. A more recent study over a wide range of temperature and pressure in a static vessel by Yantovski (106 - 109) presented macro-kinetic ignition parameters, such as pressure rise (Δp), the two ignition lags τ_1 and τ_2, flame intensity and the overall activation energy E relating to the two-stage ignition of n-heptane, iso-octane and their mixtures. Such bomb experiments deal generally with relatively slow reactions at low temperatures and pressures far removed from those prevalent during operating engine conditions; thus necessitating the extrapolation to correspond to 'end-gas' conditions of a knocking engine. In addition to this, the surface effects entailing the necessity of larger physical scale, absence of high concentrations of absorbing species to facilitate spectroscopic studies and confinement to systems with low reaction system, introduce limitations to low pressure ignition studies in the bombs.

Another method for studying autoignition is to use a rapid compression machine which, in comparison to static bomb or tube experiments, enabled the prompt control of pressure and temperature over a wider range and offered the facility of direct visualisation of combustion processes

and withdrawal of samples for accurate analysis. Moreover, the uncertain roles of residuals, the mode of mixture formation and heat transfer can be controlled more closely. The rapid compression machines presently employed have undergone three phases of development (3), which span over more than half a century, resulting in more sophisticated designs to cope with the rapidity of compression. Ng (77), Jost (32), Voinov et al. (98), and more recently Affleck and Thomas (3) and Watson (103) have developed compression machines belonging to the third generation.

Valuable qualitative information with regard to the autoignition reaction mechanisms has resulted with recent efforts (2, 33, 99, 100). Watson's approach of detailing the reactions proceeding with rapidly compressed $H_2 - O_2$ mixtures added a new dimension in the use of rapid compresssion machines (103). However, despite certain virtues, as mentioned earlier, there are some limitations in the use of rapid compression machines. The pressure readings during these stages are invariably suspect since the pressure transducer would respond to thermal exposure in addition to any pressure changes taking place over what can be effectively an appreciable period. This renders the thermodynamic analysis on the basis of pressure measurements problematic (68). And for very fast reacting mixtures the compression stage cannot be made rapid enough to ensure negligible reactivity of the charge during compression. Furthermore, the emission spectra obtained with a single cycle carry inadequate information such that multiple exposure becomes necessary if some tangible results are desired. The data obtained from these experiments remain, therefore, largely qualitative and confined to early stages of combustion. Thus the use of rapid compression machines has the limitations of being complicated in construction and the rate of production of data is relatively slow.

Motored and fired engines have been extensively employed in the past to study the autoignition reactions with reference to knock in spark-ignition gasolene engines. Most of these studies, which were undertaken to observe the

pressure-temperature-time history of end-gas prior to and at the autoignition, based on sensing pressure, calculating or measuring the temperature in the end-gas region and the chemical or chromotographic analysis of the samples. Whilst the pressure and temperature measurement served to ascribe the limiting conditions for the onset of auto-ignition - hence knock - the sample analyses proved useful in postulating the mechanism of intermediates in these reactions. Some of the important previous attempts in the studies of end-gas autoignition have been summarised in Table (B0.1). It presents all the important experimental techniques adopted on five types of apparatus discussed in this section. Fired engine studies are faced with the formidable task of defining the ever-changing volume of the end-charge as it is continually affected by the propagating flame and the piston travel. Moreover, large heat transfer between the reacting and the unburned zone introduces uncertainties in calculating accurately the end-gas temperature. The temperatures in such cases were therefore indirectly observed by the measurement of the transit time of high frequency sound pulse projected through the end gas (60).

In contrast, the motored engine technique makes use of the engine under normal operating conditions and offers the facility of reliable and reproducible quantitative data related to both stages of combustion and, in particular, the controlling effect of the first stage over the subsequent stages of combustion. The end-gas temperature is calculable without difficulty as the charge remains homogeneous with no temperature and pressure gradients, otherwise impressed by the propagating flames in fired engines.

In an attempt to study end-gas reactions so as to develop information on the chemical factors causing knock, Pastell (82) used a motored engine running on a binary mixture of n-Heptane and iso-octane which happen to be on the two extremities of the knock scale. He utilised a photomultiplier for recording cool flames while pressure was recorded with a piezoelectric transducer. The

significant part of this study has been in providing a quantitative basis to the extent of reactions preceding combustion.

The thermodynamic analysis of precombustion reactions by Walcutt and Rifkin (102) extended Pastell's work. In their analysis the polytropic coefficient was assumed constant and heat losses were neglected. Large step length was adopted, perhaps due to lack of computing procedures those days. In our error analysis it has already been shown that large step length may affect results. Despite these limitations, they could demonstrate that a significant fraction of fuel aspirated (as much as 27%) gets burnt in precombustion reactions. They were unable to correlate the extent of precombustion reactions with the effectiveness of a hydrocarbon to knock resistance.

Downs and Wheeler (16) surveyed exhaustively the development of knock research up to that date. They considerably refined the technique of sampled analysis of the end-gas mixture during the course of knocking combustion. The chemical analysis of the samples indicated that organic peroxides are the most important intermediates which condition the end gas to explode. They concluded that with most of the higher paraffinic and napthenic fuels, the preflame combustion mechanism is two-stage low temperature type. They cited cool flames being formed prior to the autoignition of the end-charge, which was later studied by them with more detail (17). Later, the elaborate spectroscopic studies of Moore and Simonson (75) confirmed the existence of blue glow which exhibits the band of formaldehyde. It was shown that the preheated autoignition of methane is akin to knocking combustion in an engine, which is due to end-gas being sensitised by pre-reactions. Whereas most of the evidence gathered clearly supported the autoignition phenomena of the end-charge as responsible for the onset of knock in engines, Downs et al. (16) were uncertain to rule out the possibility of flammation of the end-charge with exceedingly high rates such that knock could be looked upon as the flammation of the entire charge swept by the flame front. Recent work, e.g. (29),

on a spark-ignition engine has ruled out the later concept as they (15) could, by displaying the knocking combustion events with a fast sweep of 50 cm/m sec, duly triggered by the approach of flame front, show that it is the end-charge which autoignites rather than the flame sweeping the whole charge.

Introduction of partly reacted fuel in the intake of a normally operating engine then followed to simulate the externally produced effects for the onset of knock. Walcutt et al. (101), for example, used two C.F.R. engines in tandem for this purpose. The fuel and air charge was inducted through the motored engine whose compression ratio was varied to control the degree of pre-reaction of the whole charge which was led into a spark-fired engine. Their analysis was based on the criterion of knock limited compression ratio. In another set-up, as a part of the same study, they pre-reacted a fraction of the fuel in a heated tube and introduced it in a normal operating engine to observe the influence of the pre-reacted mixture to produce knock. They found that in both cases the knock-limited compression ratio is quite sensitive to the presence of pre-reacted products in the intake. On the same lines, Moore and Roy (73) studied comparatively the knock resistance of methane and propane fuels in a spark-ignition engine by introducing a fraction of the intake charge pre-reacted through a heated tube. It was found that there is distinct dissimilarity of knock resistance mechanism in methane and propane combustion. Whereas methane exhibits steady reduction in the knock-limited C.R., propane gives strong evidence for the production of pro-knock substance of slow oxidation markedly in the range of 80°C to 400°C compression temperature. They revealed the striking similarity of the effect of slow oxidation reaction on knock limit for a number of fuels with propane. It was, perhaps, the first systematic study of autoignition of gaseous fuels with particular reference to gas and dual-fuel engines.

Klat's work (51) was primarily concerned with the combustion mechanisms in dual-fuel engines. He

obtained extensive data on the knock-limited performance of a dual-fuel engine utilising various gaseous fuels and their mixtures. The significant conclusions reached by him were: the necessity of devising a knock-rating method to correspond to the knocking behaviour of gaseous fuels; the existence of inverse relationship between knock-limited B.M.E.P. and intake temperature and a detailed experimental determination of knocking regions of various fuels in a dual-fuel engine.

The present part of this study had the following aim: to focus attention on the chemical factors in dual-fuel combustion phenomena with particular reference to knock in dual-fuel engines; to analyse , through heat release computations, the autoignition characteristics of common gaseous fuels such as methane and propane and that of a heavier hydrocarbon similar to diesel oil (in our case n-heptane) when they are autoignited individually and together in a motored engine, and to provide a rational basis towards formulating an approach for describing these processes as adequately as possible with the help of understanding generated so far.

B0.3 Present Contribution

Following the results of error analysis, improvements in the experimental and computational techniques have been effected for the accurate determination of the rate of heat release due to autoignition reactions. Dual-fuel combustion phenomena are examined through the analysis of combustion heat release in a motored engine running on a gaseous fuel (methane or propane) blended with n-heptane. It is shown that the heat release analyses of autoignition reactions of individual hydrocarbons and their blends explain substantially the resulting behaviour of these mixtures thereby casting light on the underlying combustion processes in dual-fuel engines. It lends to establish the chemical nature of precombustion reactions which lead to autoignition in a motored engine; thus explaining that knock in dual-fuel engines could well be due to the auto-

ignition of the end-charge conditioned by precombustion reactions. Relative differences in the autoignition of methane and propane when blended with n-heptane are examined in detail to demonstrate the comparison of both the gaseous fuels to knock-resistance.

An experimental and computational approach is established, which derives gross chemical kinetic data of the combustion of common gaseous fuels, using a motored engine. Gross chemical kinetic data, as pertinent to engine operating conditions, are provided for the auto-ignition of n-heptane, propane, methane and their blends. A comparison is made with these data and the ones available in the literature. The implications and importance of these data arefully discussed in relation to dual-fuel engines.

B0.4 Outline of Part B

Basically, part B follows the same format as Part A. It presents the experimental studies conducted on C.F.R. Engine. It contains three chapters. Chapter B1 describes the experimental apparatus and procedure.

Chapter B2 presents the computing procedure and results. Discussion of results and conclusions follow in chapter B3.

Table (80.1). Summary of reported measurements in autoignition studies with various apparatus.

S. No.	Investigated Parameter			APPARATUS				
				Static – Vessel or Bomb.	Shock Tubes	Rapid Compression Machine	Fired Engine	Motored Engine
1	PRESSURE			106, 107, 108, 109	91	98-100, 1-3, 23, 33, 57, 85	29, 76	57, 61, 66, 75, 81, 82, 102
2	End-gas Temperature	Sound Velocity Method						
		Absorption Spectra					12, 84	75
		Infra red Radiation Pyrometer					96	96
		Gas Law			91	85	76	61, 82, 102
3	Combustion heat – release Analysis							61, 82, 102
4	ANALYSIS	Via Sample	Chemical				16	75, 81, 101
			Chromato-graphic			1, 2, 3, 23		
			Polaro-graphic				66	66
		Spectrographic				1, 2, 3, 23		
5	Cool Flame Detection	Photomultiplier			91	33, 98, 99, 100	29	16, 57, 66, 81
		High Speed Photography				92	11, 29, 70	11
		Schlieren Photography			91		11, 65	11
6	Time Measurement					1, 2, 3, 57, 85, 98, 99, 100	29	57, 61, 82, 102
7	Overall Chemical Kinetics	Ignition Delay		106, 107, 108, 109	91	1, 2, 3, 23, 57, 85, 98-100	29	57
		Activation Energy		106, 107, 108, 109		98, 99, 100		75
		Order of Reaction		106, 107, 108, 109		98, 99, 100		
8	Reaction Scheme			106, 107, 108, 109		98, 99, 100 2, 23	16	66
9	Special Techniques	Ionized Gap					29	
		Introduction of prereacted fuel in intake					76, 101	101

* References appear in Appendix XII.

C H A P T E R B1

APPARATUS AND EXPERIMENTAL PROCEDURE (MOTORED-ENGINE TRIALS)

B1.1 Apparatus

B1.1-1 The Engine

A cooperative Fuel Research (C.F.R.) variable compression-ratio engine was used for this part of the present investigation. The ASTM Manual (6) describes fully its construction and operation, together with the calibration of compression ratio. Some salient features are, however, presented here.

The C.F.R. engine conformed to the following particulars:

Bore	3.25"
Stroke	4.0"
No. of Strokes	4
Compression-ratio	Variable from 4:1 onwards
Motoring Speeds	600 and 900 R.P.M.
Combustion Chamber	Open type
Con. rod - Crank throw ratio	4.44:1
Inlet Valve	Shrouded
Valve Overlap	5^{o}C.A.

The engine was modified so that gaseous fuels could be introduced and metered accurately using choked nozzle meters. Fig. (B1.1) shows a schematic layout of the apparatus used while Plates (B1.1 - B1.2) present two general views of the engine assembly. Air and fuel flow circuits and electronic measuring circuits are presented in the layout. The engine was driven at constant speeds by a reluctance-type synchronous motor through belts. The electrical machine was capable of starting the engine, absorbing the power developed by it and maintaining the speed either at 900 R.P.M. or 600 R.P.M.

B1.1-2 Air and fuel flow measuring system

The air flow rate was measured by a viscous flow air meter connected to an inclined manometer. The meter was cleaned and calibrated periodically to avoid partial blockage. The calibration was carried out in the manner as described previously in subsection (A1.1-2). Fig. (B1.2) shows the calibration curve obtained while the correction factor, which was applied for viscosity changes with change in ambient temperature, appears in the same figure.

Methane, propane and carbon dioxide flows were metered with choked nozzles whose theory appears in Appendix II. The nozzles were calibrated against a soap bubble displacement meter. For effective flow control and in order to cover a wide range of mixture strength, a parallel circuit, as shown in Fig. (B1.1), was used for introudcing gaseous fuels in the intake manifold through a venturi. Figs. (B1.3 - B1.5) show the calibration curves of choked nozzle meters. n-Heptane was introduced through a carburettor. Its flow was recorded by a standard burette of 10 and 25 cc. Precise adjustment in heptane flow could be effected by adjusting the position of the auxiliary fuel tank (see No. 6 on Fig. B1.1). The Nomogramme shown in Fig. (B1.6) was found to be of great help for quick reference to obtain a desired volumetric flow. A typical analysis of the fuels used appears in Appendix III.

B1.1-3 Electronic measuring instruments

The cylinder gas pressure, pressure-rate, crank rotation and the scavenging pressure, which were sensed by pick-ups, were displayed on a C.R.O. Their relative position in general layout is presented in Fig. (B1.1). Permanent photographic records were obtained on a film.

B1.1-3a Cylinder gas pressure measurement

Two Kistler piezo-electric pick-ups were used to record cylinder pressure during scavenging and combustion. As indicated by the error analysis, it was decided to provide a dynamic datum pressure for pressure development

records. A chopper adapter type 741A was used with a 701A quartz pressure transducer. Plate (B1.3) shows the blown-up view of the assembly. This arrangement greatly improved the pressure measurements by offering an independent dynamic pressure signal for each pressure cycle recorded. A reference pressure of 50" water gauge was used as chopper reference pressure. It was found to be necessary for operating the adapter at some precisely known gauge pressure. A constant outflow of small quantity of leaking gas ensured proper functioning of the adapter. The transducer 701A was calibrated by mounting into adapter 720 specially supplied for this purpose. A Budenberg dead weight tester was employed while the hydraulic oil was kept at a constant temperature of 100°C to simulate the cylinder jacket conditions. The calibration appears in Fig. (B1.7). The adapter pick-up was water cooled internally and was housed in the 14 mm Ø tapped hole meant for the spark plug. It conformed to the following data as supplied by the manufacturers:

Maximum measuring range	0 - 250 atü
Resolution	.0004 atü
Maximum Pressure	400 atü
Sensitivity	80 pC/atü
Resonant Frequency	65 KC/s
Rise Time	6μ sec
Linearity Error	± 0.5%
Insulation Resistance	$10^{14}\Omega$
Capacity	9pF
Acceleration Sensitivity	.0001 atü /gm
Temperature Coefficient	0.01% per deg C
Working Temperature Range	-150 to 240°C
Admissible Shock and Vibration	15000 g

The cylinder gas pressure during autoignition reactions was recorded by a special Kistler piezo-electric pressure transducer type 7051. A silicon-asbestos laminate was used as a shield for the elimination of

inaccuracies caused by the sensitivity of the diaphragm to hot combustion products. This experimental unit has recently been developed by Kistler and is compensated for transverse vibrations. It proved to be of particular importance when dealing with autoignition and the consequent structural vibrations, which otherwise impose inaccuracies on the transducer. The linearity of this transducer was found to be exceptionally good over a wide range after both static and dynamic calibrations in situ (68, 103). Fig. (B1.8) presents the static calibration obtained with Budenberg dead weight tester, while keeping the hydraulic oil temperature at 100°C and maintaining the cooling air supply to the transducer. The transducer was flush mounted in the place where the knock-meter pick-up is housed.

The following particulars pertain to the range of operation and permissible accuracy of the transducer:

Maximum measuring range	0 - 250 atü
Resolution	0.001 atü
Maximum Pressure	300 atü
Sensitivity	40 pC/atü
Resonant Frequency	100 KC/s
Rise Time	4μ sec
Maximum linearity error	± 1%
Hysteresis	± 1%
Insulation Resistance	$0.5 \times 10^4 \Omega$
Capacity	15pF
Acceleration Sensitivity	.0001 atü /g
Temperature Coefficient	-.02% per deg C
Working Temperature Range	-190 to 300°C
Cooling Air Pressure	4 - 8 atü
Air Flow	6.5 litres/min - atü

(1 atü = 14.22 p.s.i., 1 litre = .0353 cft.)

Filtered shop air was supplied for transducer cooling at 80 p.s.i.g. The silicon-asbestos laminate was replaced after every 50 trial running hours and calibration was carried out after every renewal.

B1.1-3b Recording of crank rotation

An electromagnetic pick-up was used to record the crank shaft movement in terms of 5^{o} crank intervals. Its principal features of construction and operation have already been described in section (A1.2-3c). In addition to displaying the crank rotation markings straight on the oscilloscope through an independent channel, they were superimposed externally on to C.R.T. cathode after due amplification via an operational amplifier shown as No. 23 in Fig. (B1.1). Owing to the construction of the oscilloscope screen and the way in which the trace is projected, it is imminent that a trace spanning whole of the screen suffers some distortion. This was visualised, for example, by displaying a sqaure wave which did not remain consistant with reference to graticule suggesting that there is lack of orthogonality. The superimposition of time markings improved the pressure readings even under extreme cases of large pressure traces. Plate (B1.4) shows the installation of electromagnetic pick-up.

B1.1-3c The Cathode Ray Oscilloscope (see plate B1.5)

A dual-beam Tektronix Cathode Ray Oscilloscope type 533 was used for displaying pressure and crank-timing records. The facility of adopting four independent signals for display was found to be an added advantage over type 502A used in dual-fuel engine trials. All the four beams were utilised in displaying cylinder pressure, scavenging datum pressure, rate of pressure rise and the crank-timing scale. Triggering voltage was developed by mounting a permanent magnet at the end of the ignition breaker assembly (see plate B1.6). Triggering could effectively be altered to the required region of interest in the combustion cycle by adjusting the position of the rotating magnet. All these traces, together with "combed" type pressure signals, as was necessary in some cases, were recorded by a general purpose Polaroid camera, using an f1.9 lens. The film used was Polaroid positive transparency type 46L. The fast process time of two minutes for the transparency used was found to be helpful in checking the results immediately

and in the event of any discrepancy, the filming was repeated for the same trial conditions.

B1.2 Experimental Procedure

The following test conditions were adopted for the present investigation:

Engine motoring speed	900 $\pm$ 9 R.P.M.
Intake pressure	ambient
Intake temperature	ambient or heated, if needed
Coolant temperature	100^{o}C
Compression ratio	10:1 or above to give rise to incipient autoignition
Mixture strength	lean to stoichio-metric
Carbon dioxide concentration	varied to the extent to give incipient autoignition with richer mixtures of propane- and heptane mixtures.

The engine was warmed to the desired level of hotness by motored operation at high compression ratio on air alone. This was thought to be necessary to avoid undue deposit formation during cold starting.

The present analysis required pressure development records of incipient autoignition such that representative cycles under these conditions could be compared. Cyclic dispersion was checked for every cycle recorded and in the event of difficulty in visual judgement, a combed record of forty cycles or so was obtained by multiple exposure of the film. It was found that an improvement in cyclic dispersion could be effected with increase in compression ratio. In general, cyclic dispersion under incipient autoignition was found to be less than spark-ignition combustion in the same engine with the same mixture strength of gaseous fuels. This was indirectly indicative of the fact that the flame propagation in spark ignition causes higher cyclic dispersion since the initiating and subsequent ignition processes are physically dependent on mixture formation in and around spark gap. Plate (B1. 7) illustrates the cyclic dispersion between

autoignition and spark ignition for methane and propane as fuels. Methane was found to be better in this respect as the cyclic dispersion was significantly low as compared to propane. We shall discuss in detail this aspect of comparative study between these two fuels in chapter B3. Difficulty was experienced when dealing with blends of methane- and propane-heptane. It was found, in general, that, although the cyclic dispersion was reduced with increased quantity of heptane, the autoignition of small quantities of heptane occurred with increased cyclic dispersion. However, under such conditions, higher compression ratio around 15 or more were resorted to in order to attain stable conditions.

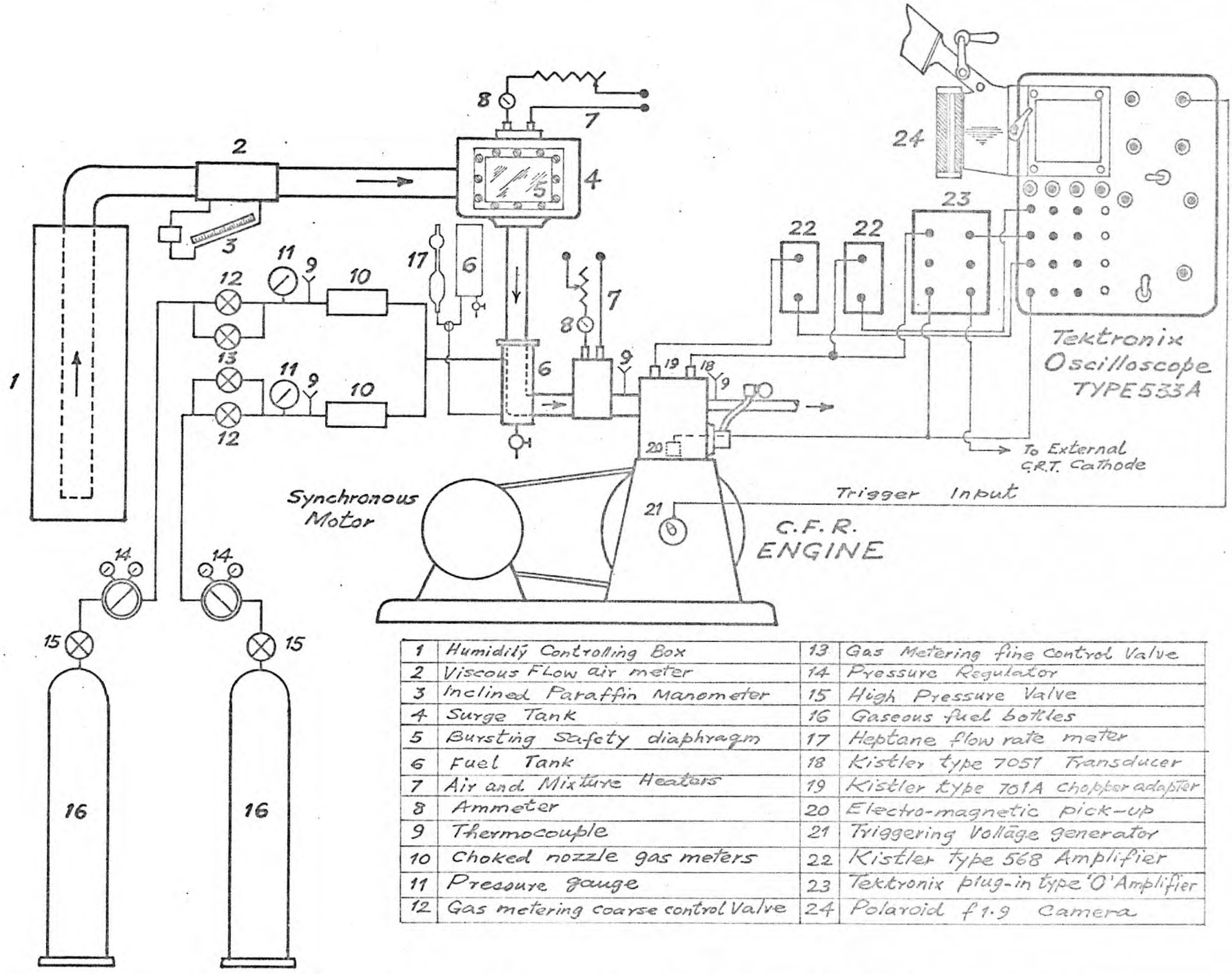
The onset of autoignition was determined through pressure-rate records constantly displayed on the screen. An operational Tektronix 'O' Amplifier was employed for this purpose, through which was passed the main charge developed by the pick-up in parallel to displaying the pressure trace straight on to the oscilloscope. In addition to display the consistence or otherwise of the autoignition reactions from cycle to cycle, the pressure-rate records offered qualitative check as to the point of ignition and its variance, if any, due to the cyclic dispersion. It was noticed invariably in all the trial conditions observed that the cyclic dispersion manifested in the second stage combustion thus indicating noticeable variations in the peak pressure rather than the point of ignition. The point of ignition was initially reckoned through the examination of pressure-rate curve during data processing and was later readjusted by heat release analysis to the crank angle where $dq^2/d\theta^2$ is greater than zero. Violent autoignition was avoided as, in addition to being easily discernible by virtue of its audibility with severe note of kinking sound, it entailed undesirable mechanical and thermal loading of the engine structure. Moreover, the oscillations in the pressure records render it difficult to analyse without the aid of hand smoothing in addition to iterative numerical smoothing which incurs large deviations from the actual pressure. Also under these conditions

the point of ignition advances to the extent that it cannot be regarded to have taken place at or around T.D.C.

Blending was done by introducing independently the gaseous fuels and n-Heptane through their individual routes, as shown in Fig. (B1.1). In dealing with the mixtures of propane- and methane-heptane it was found necessary to start with heptane as a base fuel and increase the gaseous fuel concentration gradually until the limit of either border-line violent autoignition or sporadic combustion is reached. The procedure of increasing compression ratio followed the course of examining of autoignition cycles as to whether they are satisfactorily reproducible with permissible cyclic dispersion.

Plate (B1.8) presents a set of typical records obtained following the above procedure.

A universal quarter-plate enlarger with a good quality lens was used for projecting the pressure trace on enlarged scale. Enlargement by 6 to 7 times of the trace could be obtained without the sacrifice of sharpness of the image on the base board. A film reader was constructed in the laboratories for digitalising the pressure scale. It consisted essentially of a base board on two sides of which were mounted two long screws having a pitch of 20th threads per inch. The screws were coupled by a toothed belt and an idler pulley (see plate B1.9). A hair-line cursor was mounted on the screws, which could be driven by a handle. A reversible indexing counter was attached to the other screw. One pitch length of the lead-screw showed ten divisions on the counter. Thus a division corresponded to 1/10th of the screw pitch, i.e. 1/200 = .005" of the cursor movement in Y-direction, whilst the X coordinates were ascribed by the crank rotation markings superimposed on the pressure diagram.



1	Humidity Controlling Box	13	Gas Metering fine Control Valve
2	Viscous Flow air meter	14	Pressure Regulator
3	Inclined Paraffin Manometer	15	High Pressure Valve
4	Surge Tank	16	Gaseous fuel bottles
5	Bursting Safety diaphragm	17	Heptane flow rate meter
6	Fuel Tank	18	Kistler type 7051 Transducer
7	Air and Mixture Heaters	19	Kistler type 701A chopper adapter
8	Ammeter	20	Electro-magnetic pick-up
9	Thermocouple	21	Triggering Voltage generator
10	Choked nozzle gas meters	22	Kistler Type 568 Amplifier
11	Pressure gauge	23	Tektronix plug-in type 'O' Amplifier
12	Gas metering coarse control Valve	24	Polaroid f1.9 Camera

FIG. B1.1. A Schematic Layout of the Apparatus used.

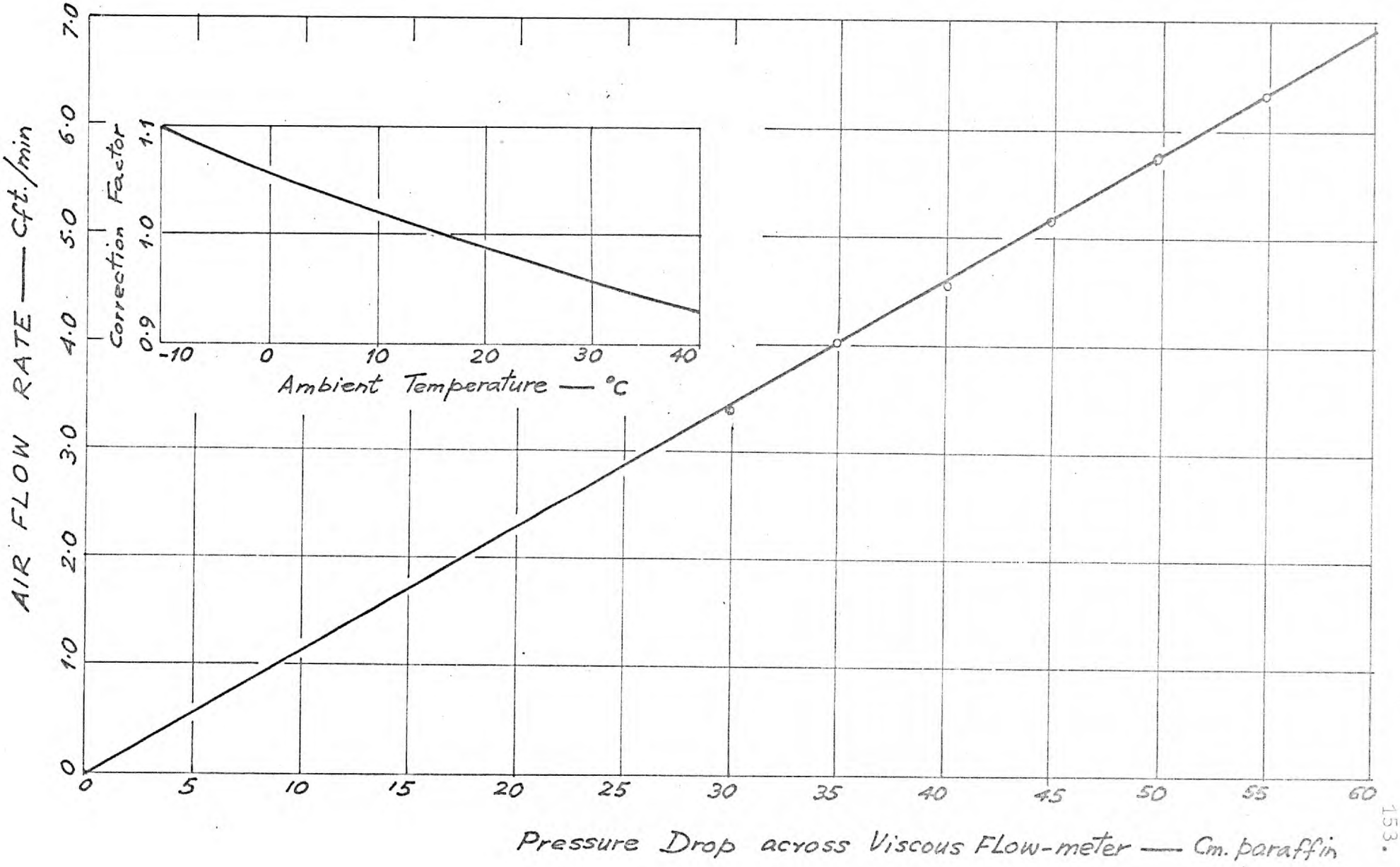


FIG.(B1.2) Caliberation of Viscous Flow Air Meter.

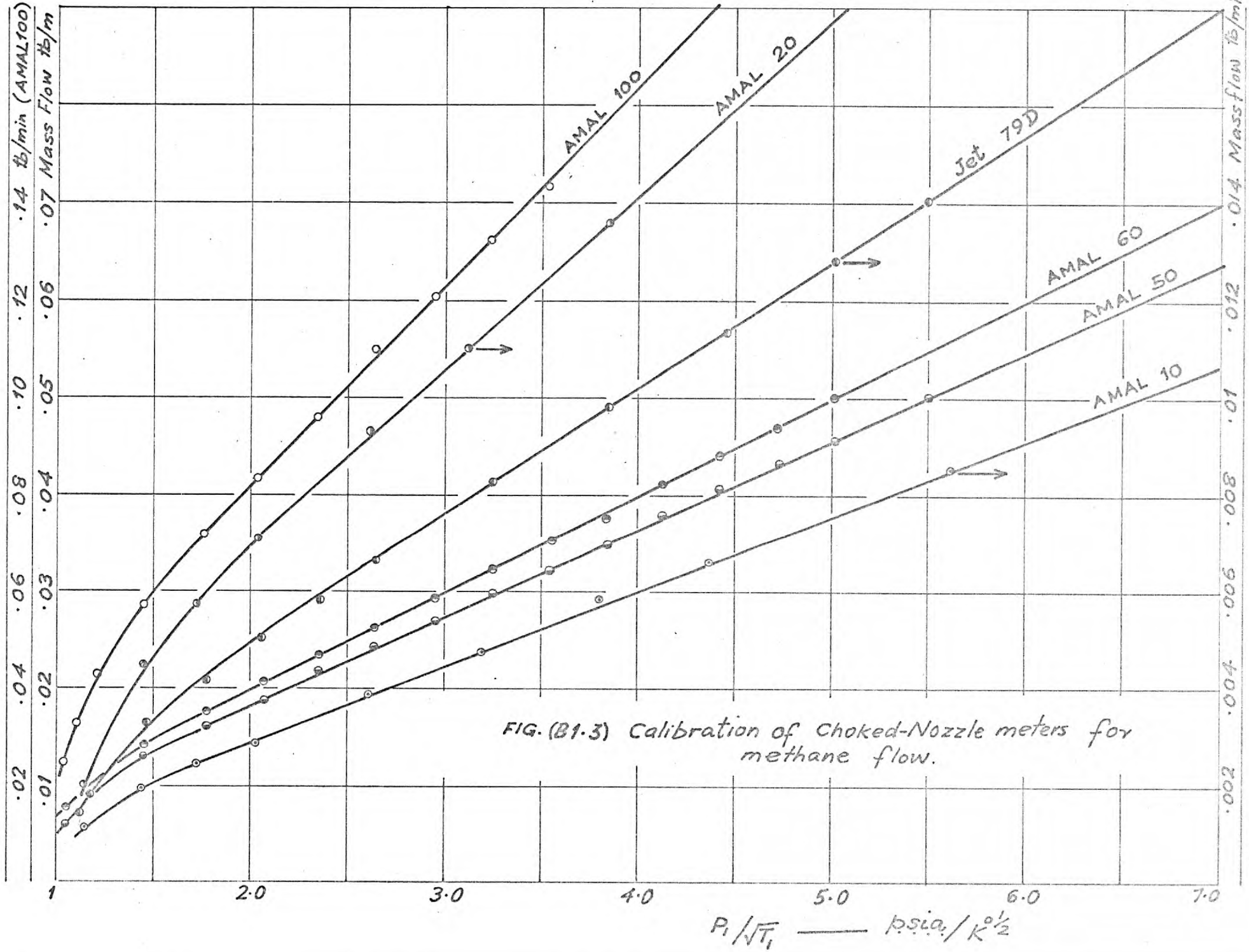


FIG. (B1·3) Calibration of Choked-Nozzle meters for methane flow.

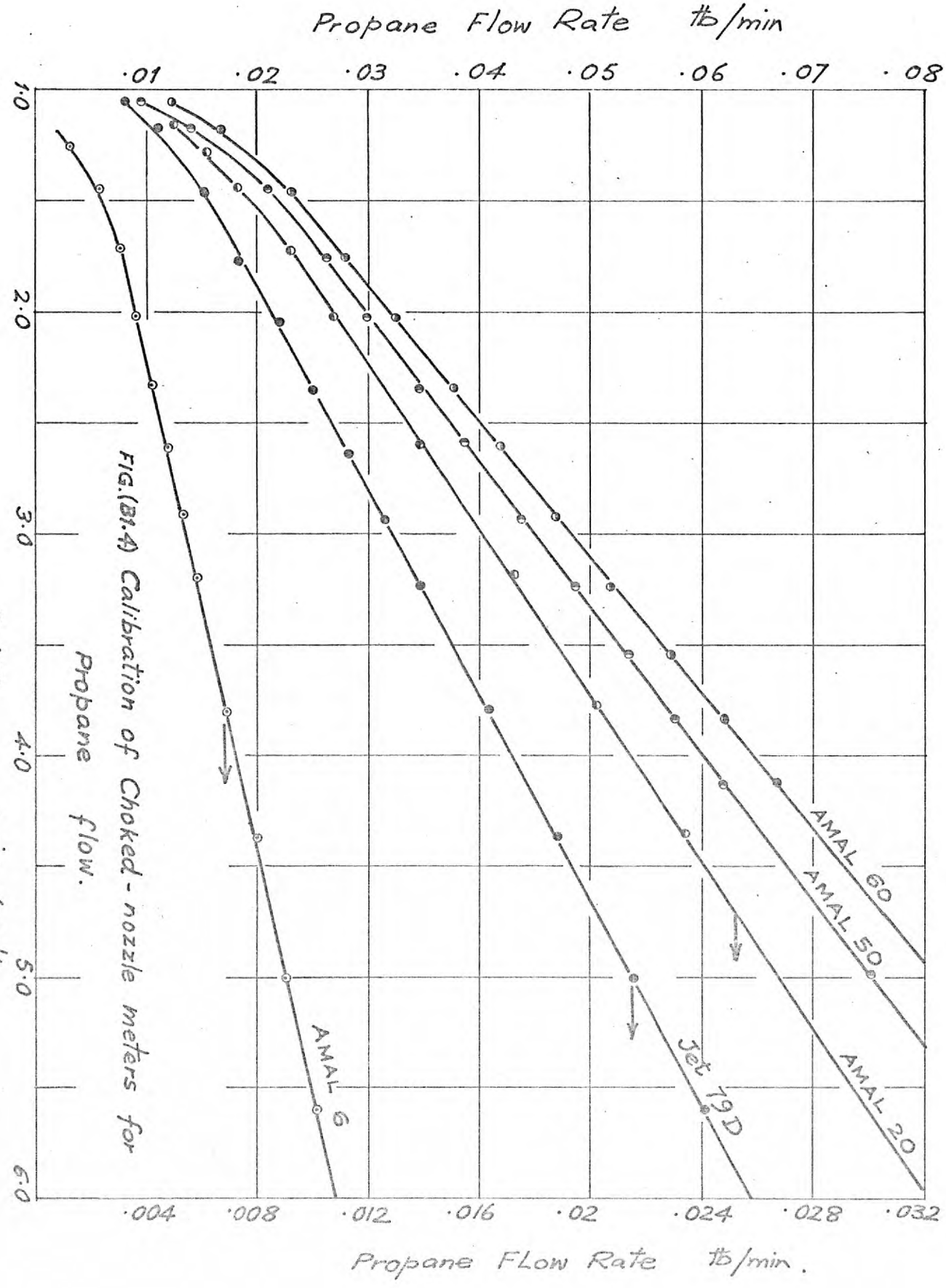


FIG.(B1.4) Calibration of Choked-nozzle meters for Propane flow.

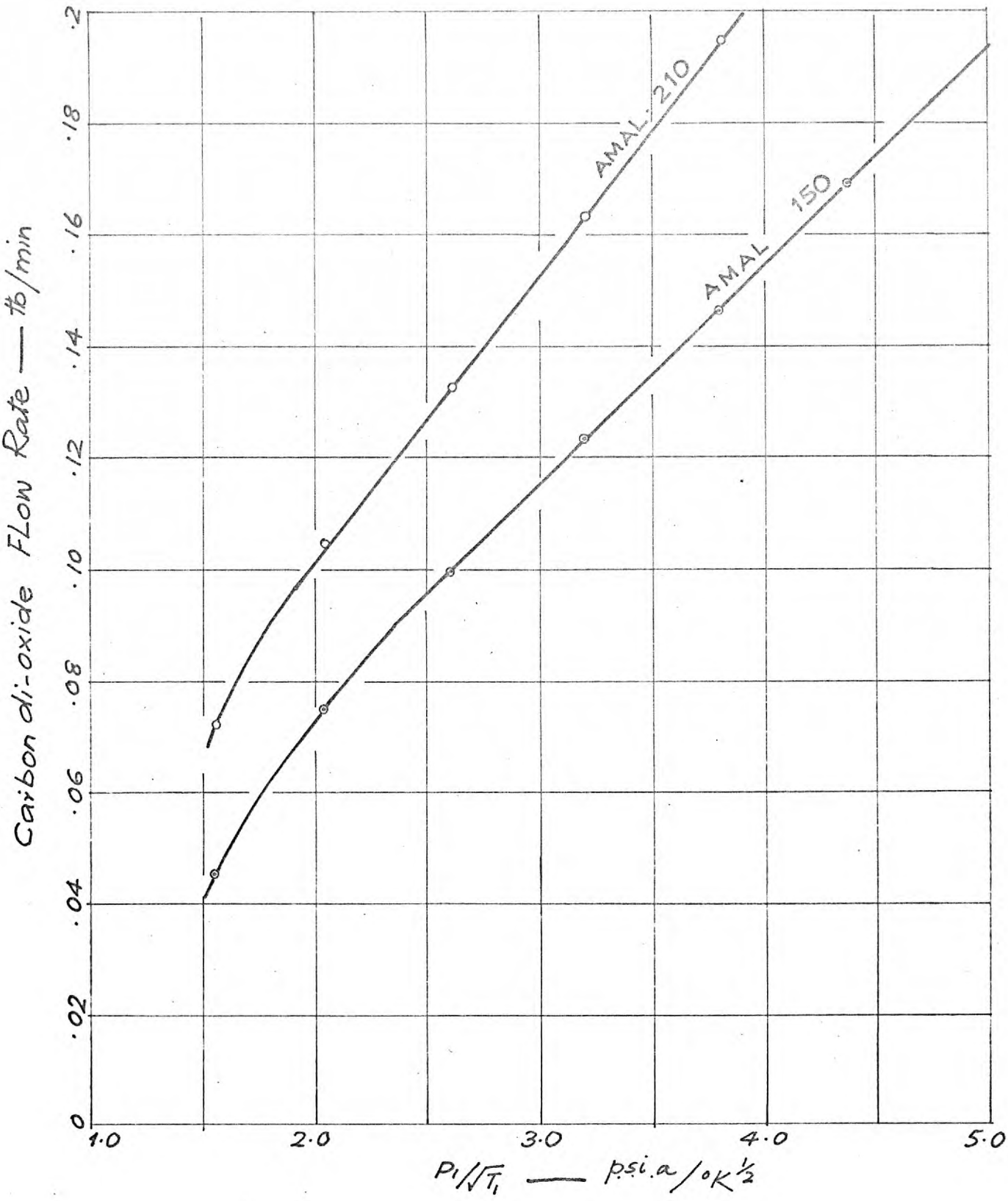


FIG. (B1.5) Calibration of Choked-nozzle Meters for Carbon di-oxide Flow.

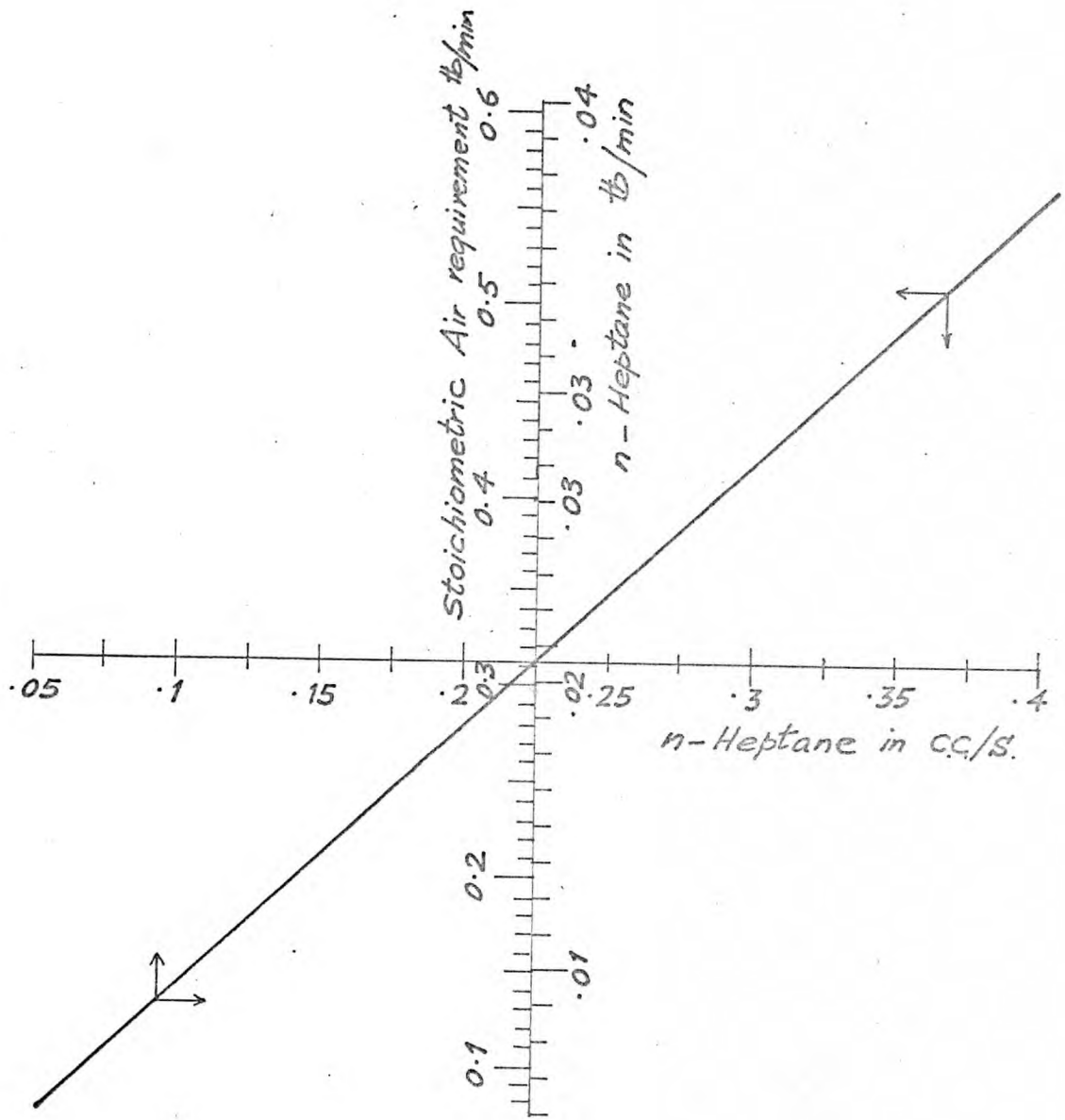


FIG. (B1·6) Nomogram for n-Heptane flow metering.

Preamplification 100 mV/pCb

Oscilloscope setting 0·2 V/cm

Testing Oil Temperature 100°C

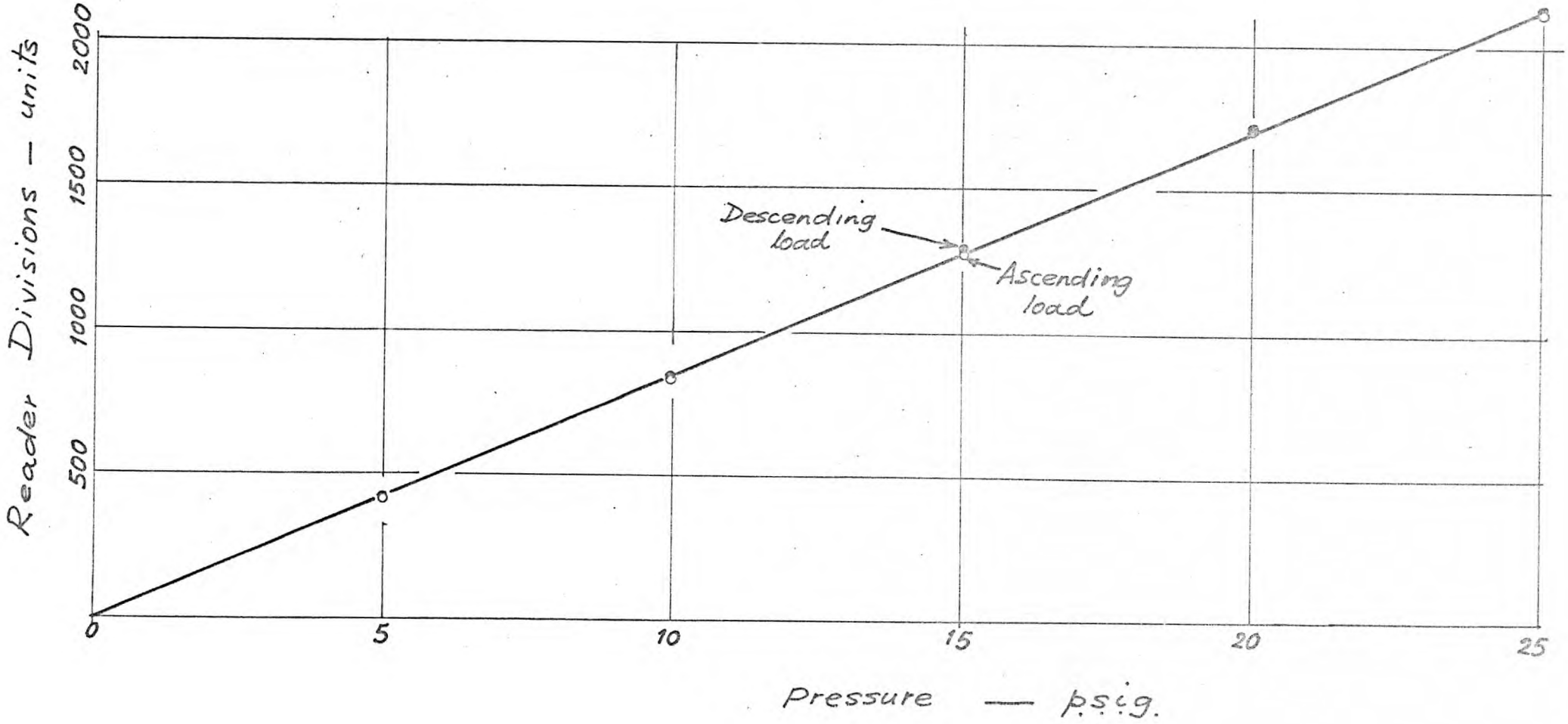


Fig. (B1.7) Calibration of Chopper Adapter Pick-up Kistler Type 701 A.

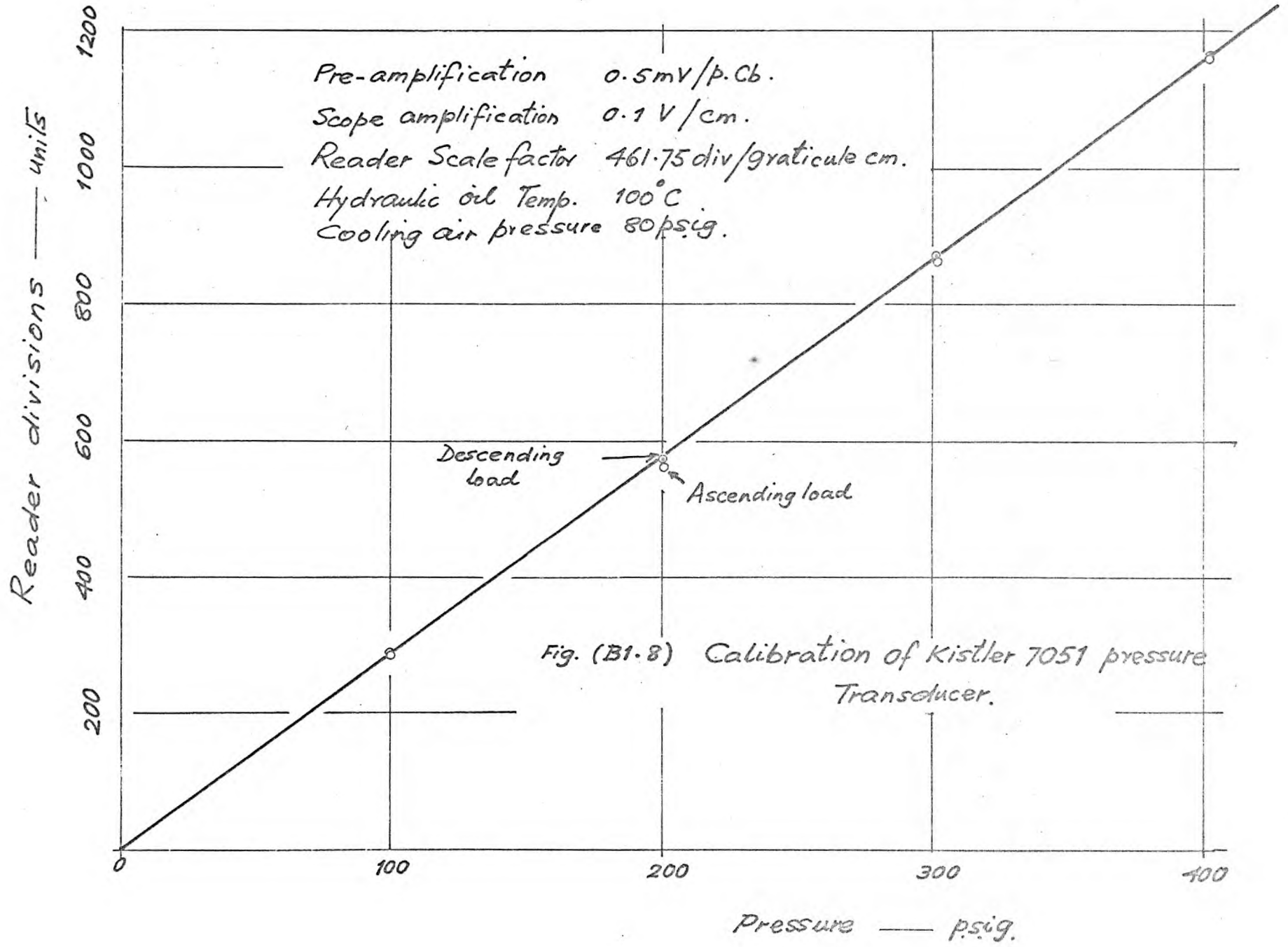


Fig. (B1.8) Calibration of Kistler 7051 pressure Transducer.

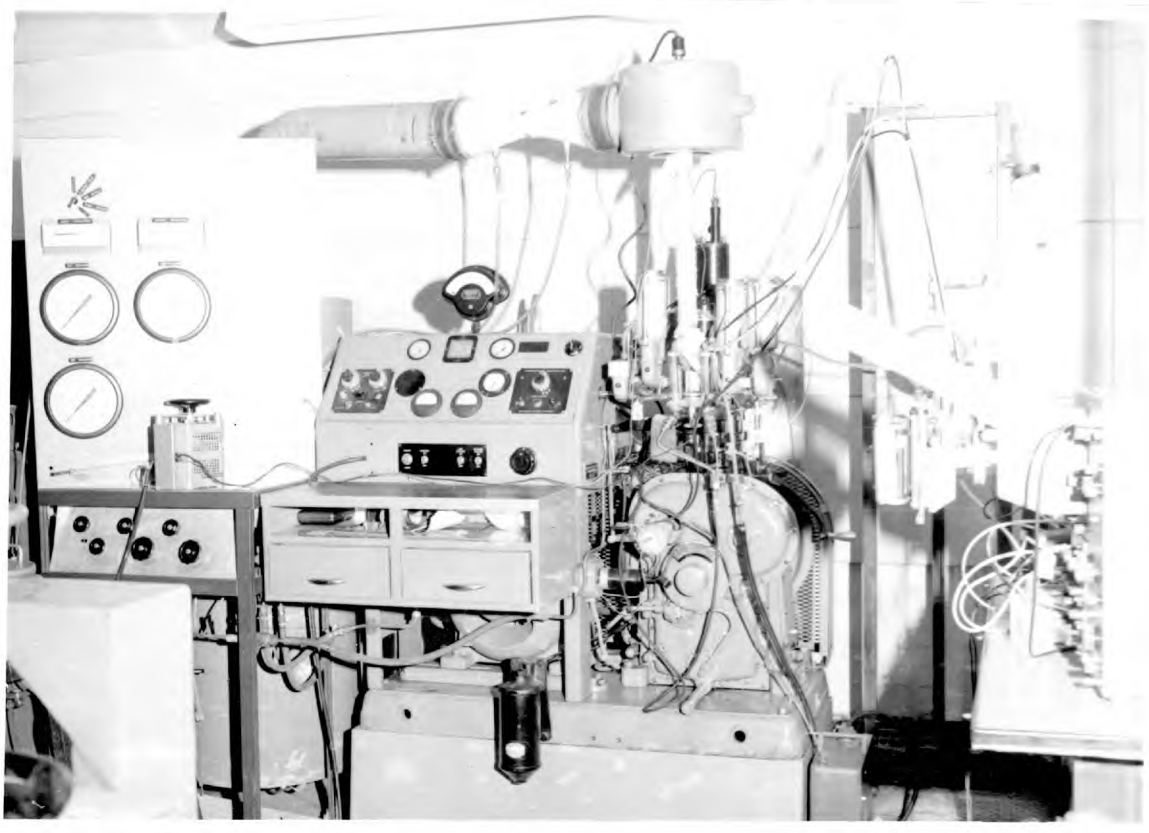


PLATE B1.1: A GENERAL VIEW OF THE COOPERATIVE FUEL RESEARCH ENGINE (C.F.R.) TEST RIG

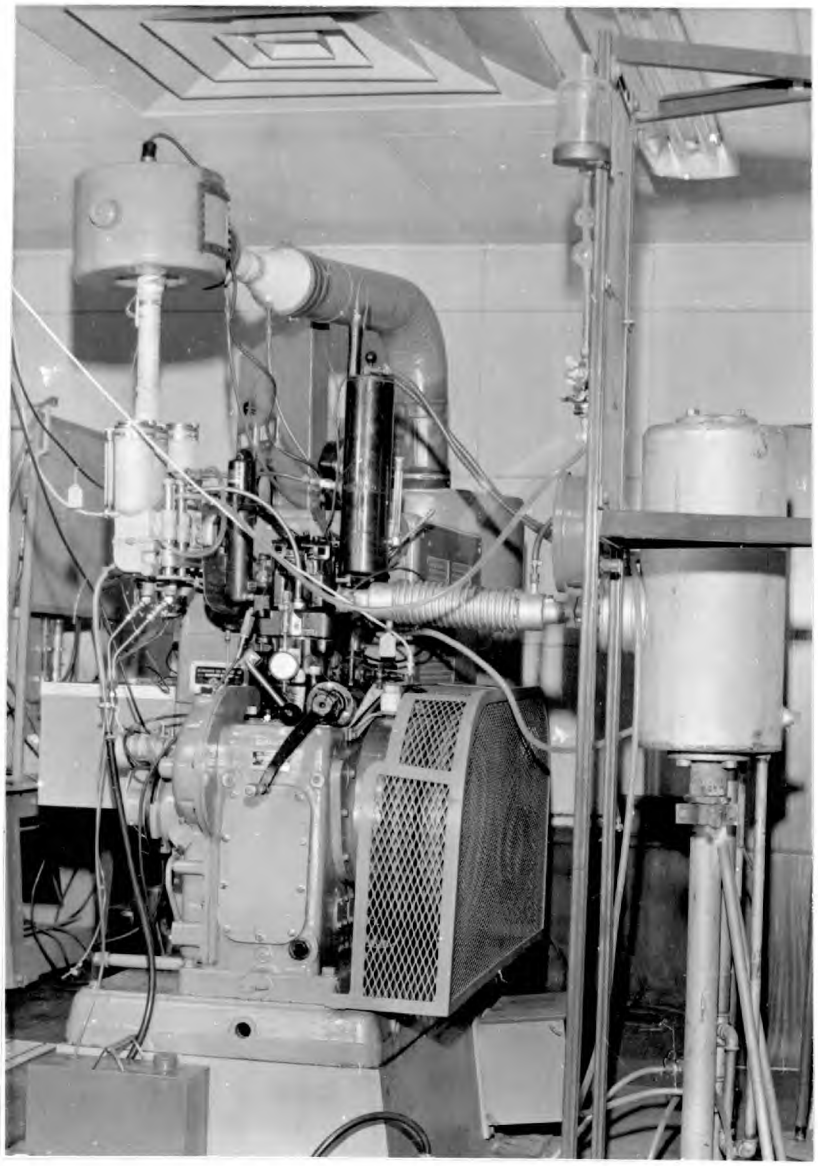


PLATE B1.2: ANOTHER VIEW OF THE C.F.R. ENGINE



1. 14mm Ø socket connection for flush mounting
2. Main adapter
3. Quartz pick-up 701 A
4. Micro-dot connections
5. Cooling water connector for reference pressure
6. Air connector
7. Adapter 720 for the pick-up

PLATE B1.3: A BLOWN-UP VIEW OF KISTLER 741 A CHOPPER ADAPTER ASSEMBLY

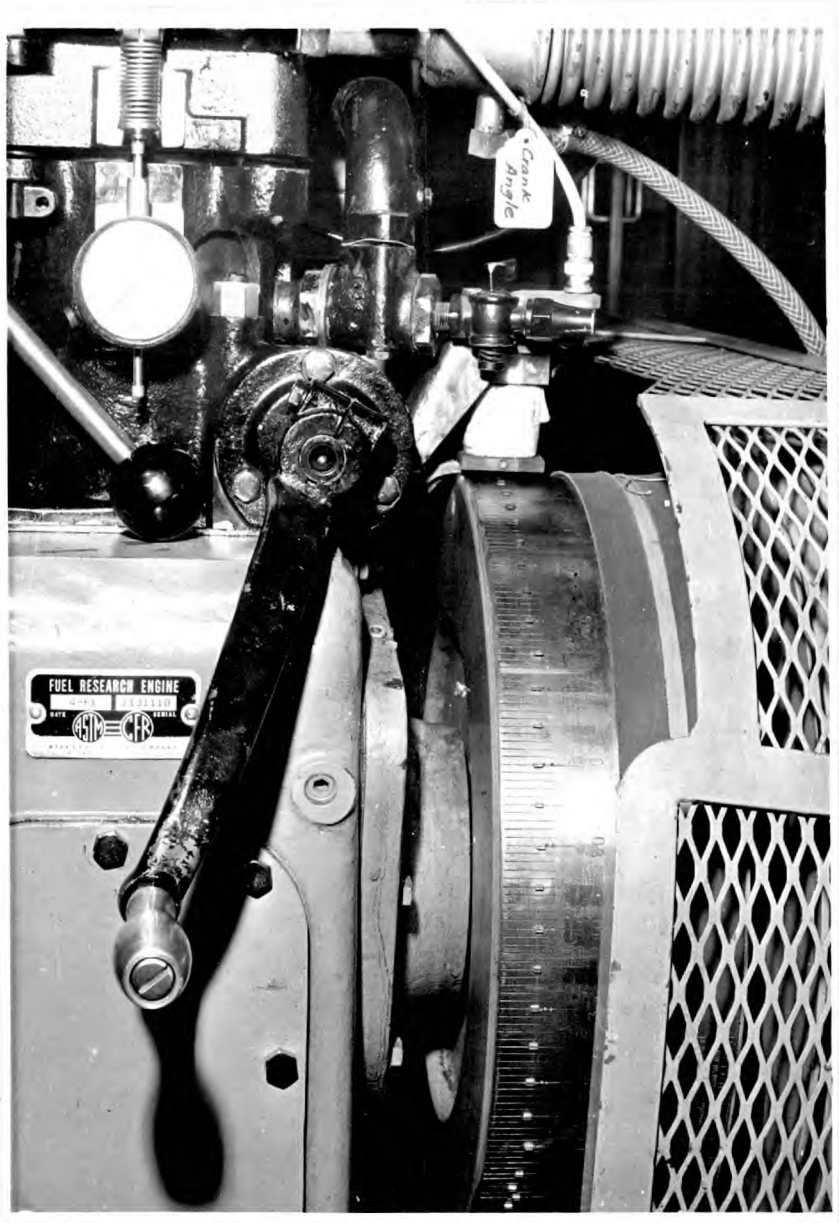


PLATE B1.4: A CLOSE-UP OF ELECTROMAGNETIC PICK-UP FOR CRANK ROTATION

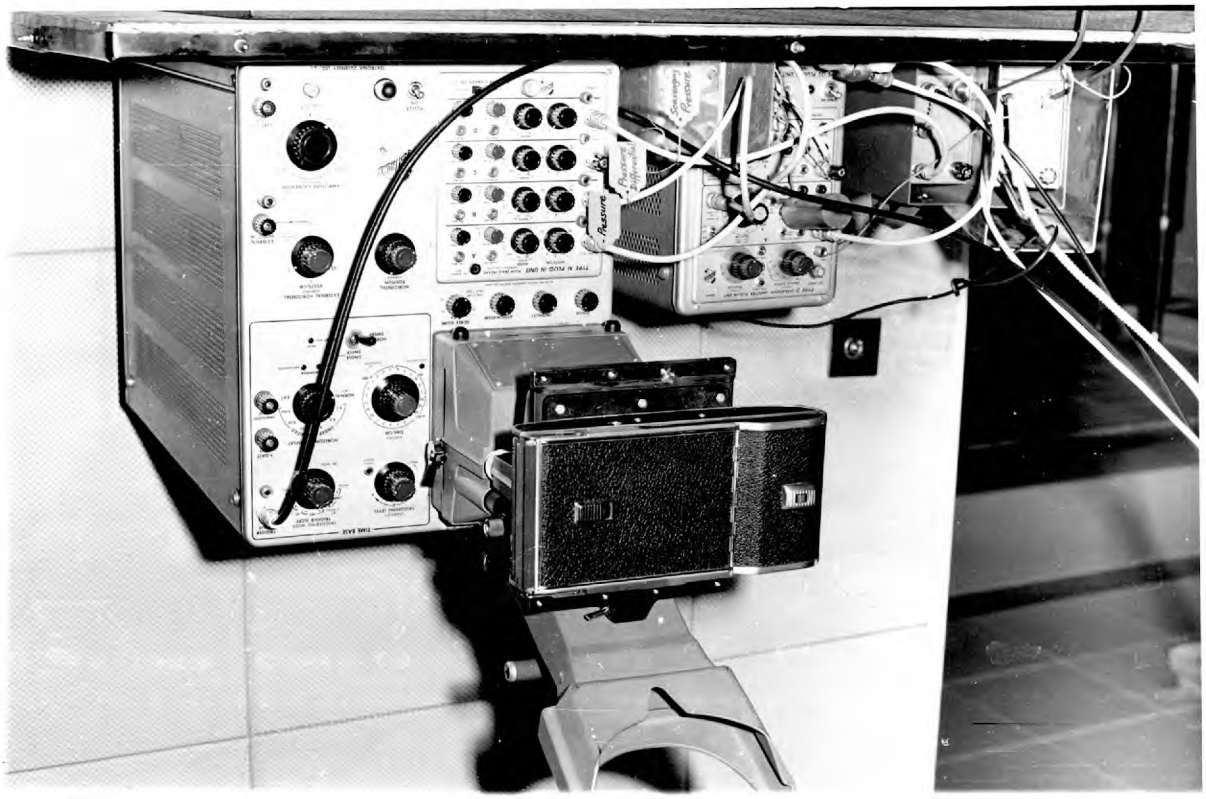


PLATE B1.5: TEKTRONIX 533A CATHODE RAY OSCILLOSCOPE (C.R.O.) AND ALLIED ELECTRONIC EQUIPMENT

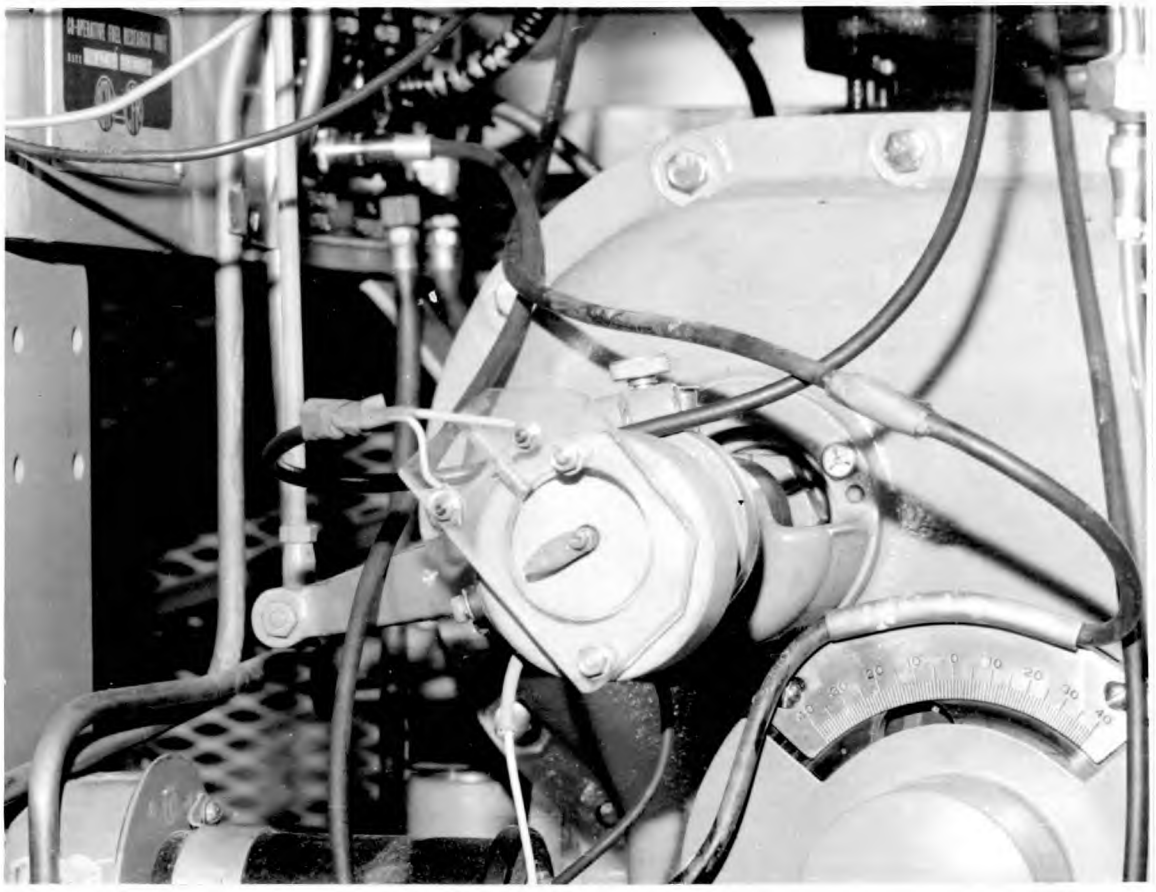


PLATE B1.6: A CLOSE-UP OF CAM SHAFT-MOUNTED TRIGGERING CIRCUIT

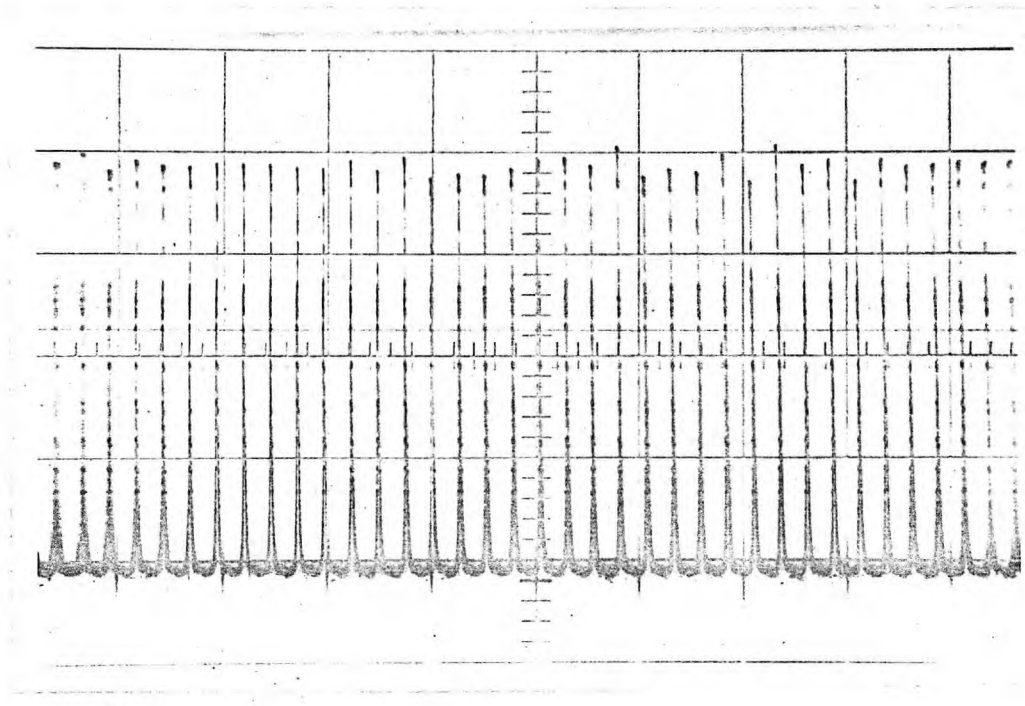


PLATE B1.7a: CYCLIC DISPERSION IN THE AUTOIGNITION OF PROPANE

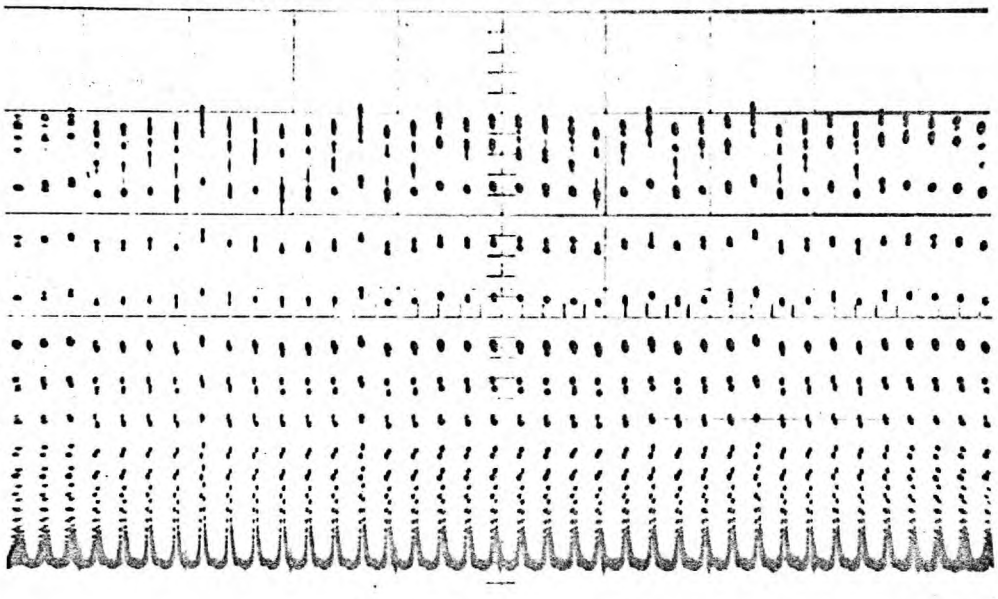


PLATE B1.7b: CYCLIC DISPERSION IN THE AUTOIGNITION OF PROPANE-N-HEPTANE

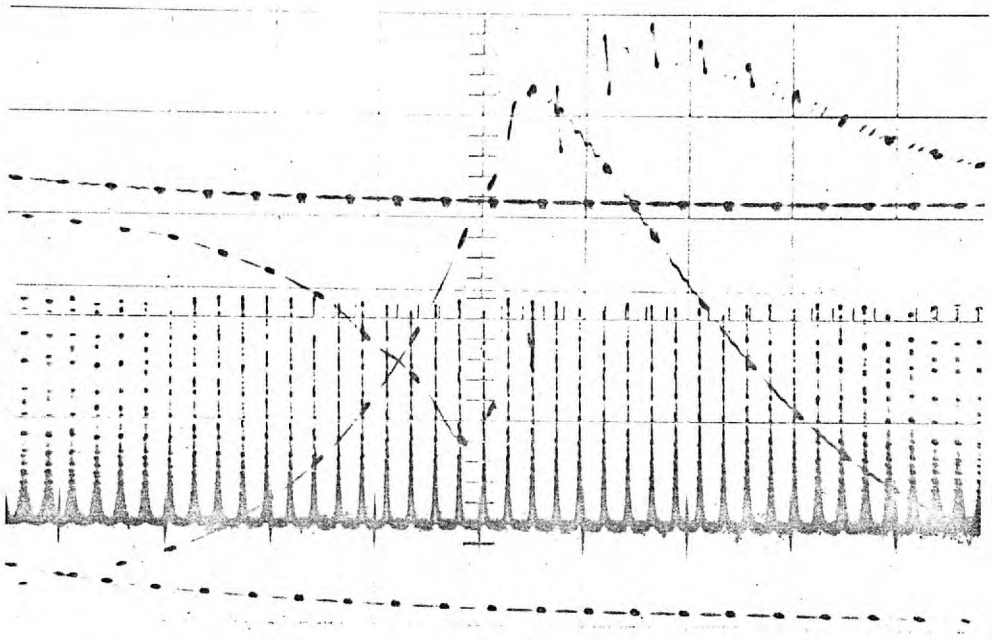


PLATE B1.7c: CYCLIC DISPERSION IN THE SPARK-IGNITION OF METHANE

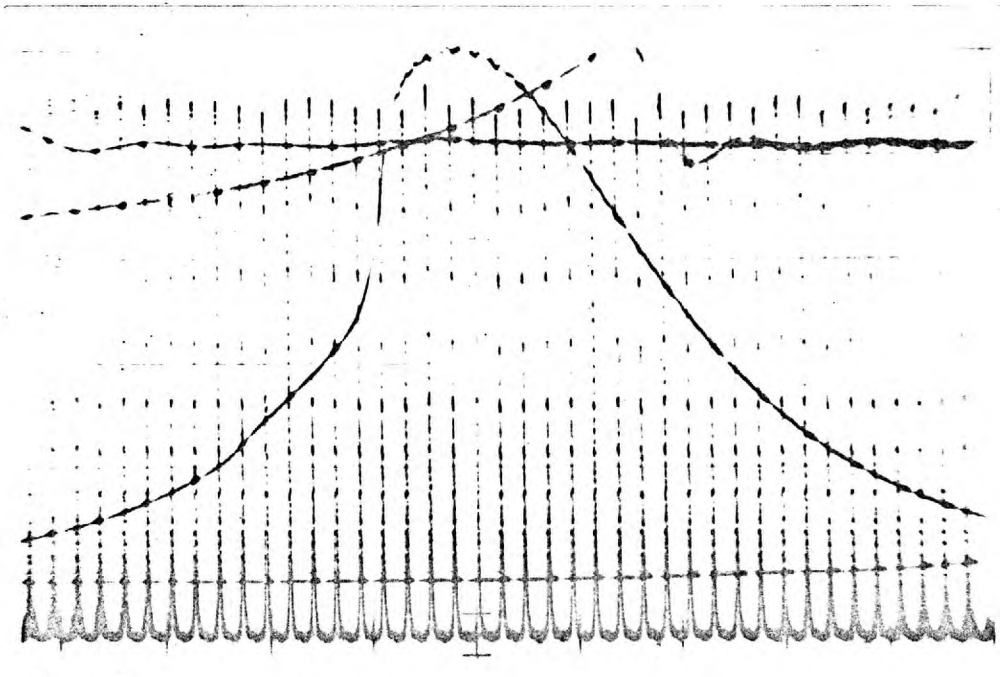
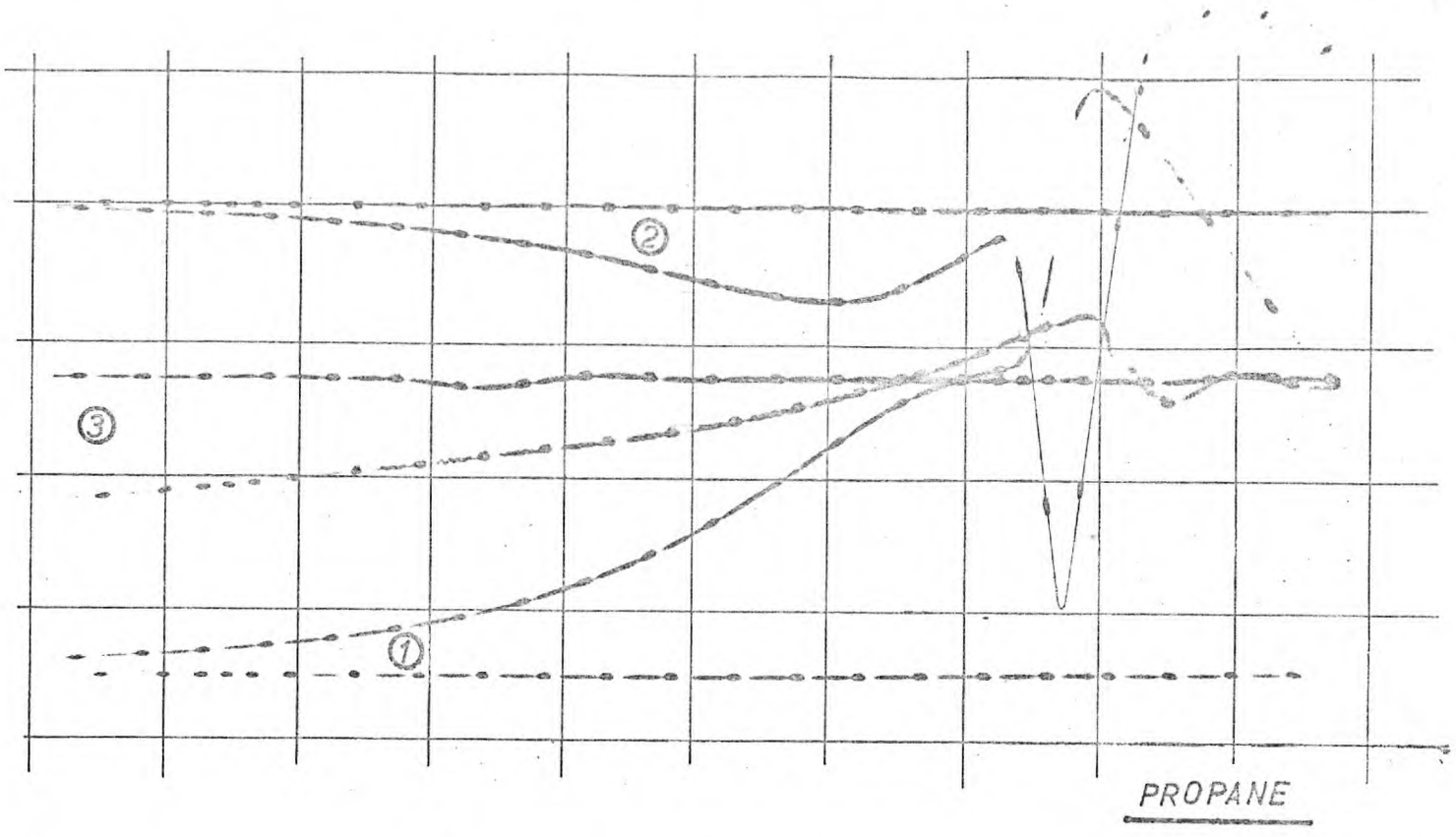
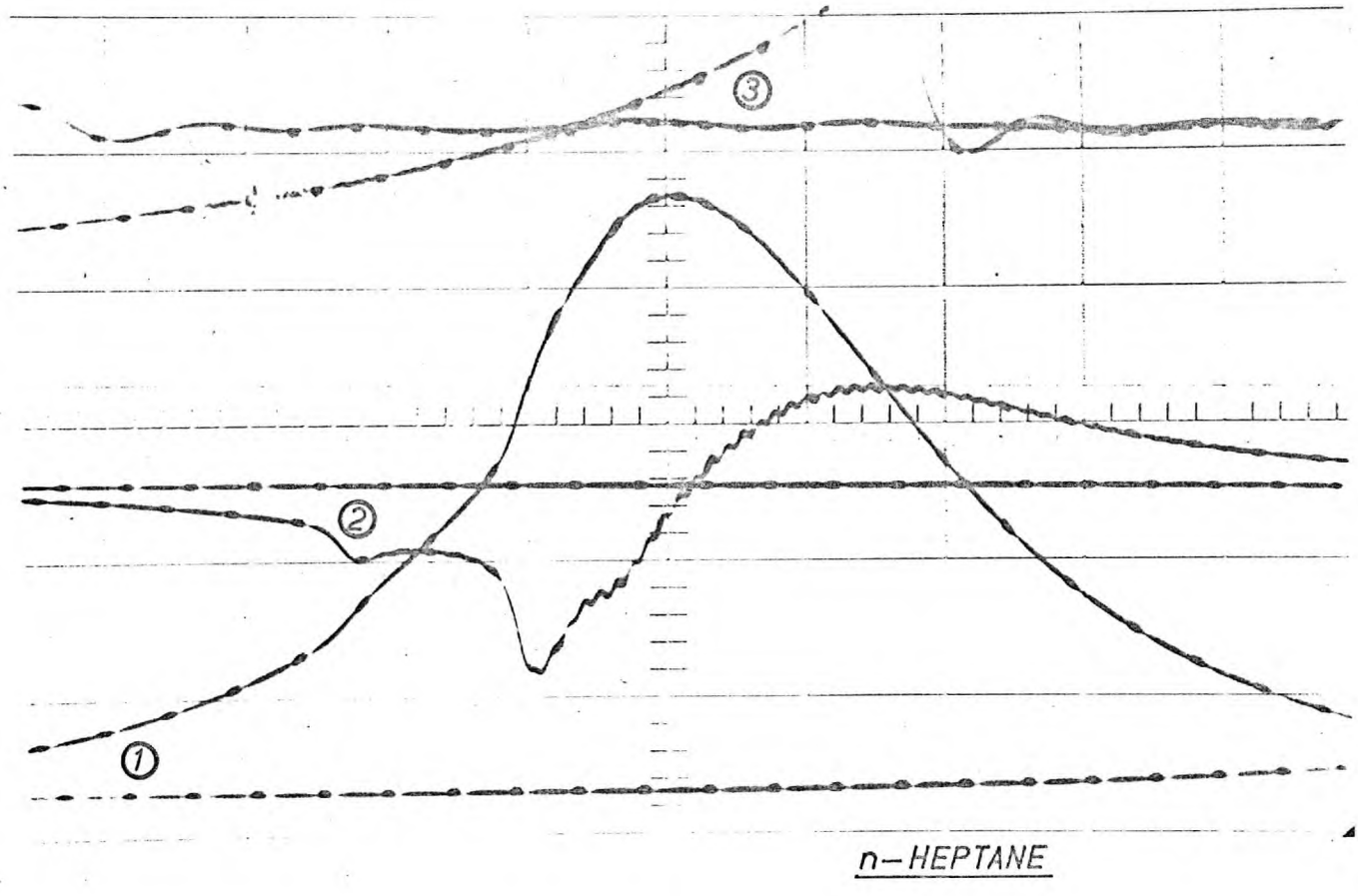


PLATE B1.7d: CYCLIC DISPERSION IN THE AUTOIGNITION OF METHANE-N-HEPTANE





1. Cylinder Pressure 2. Rate of pressure

3. Reference Pressure

Plate B1.8: A set of typical records obtained from motored-engine.

C H A P T E R B2

COMPUTING PROCEDURE AND PRESENTATION OF RESULTS

B2.1 Introduction

The combustion heat release rates during incipient autoignition reactions in a motored engine running on propane, methane, n-Heptane and their blends are computed mainly with the use of generalised computer programme (46) described in chapter A2. However, certain simplifying assumptions need be employed with reference to multistage autoignition reactions. A subroutine is developed which, with the knowledge of initial concentration of oxygen and fuel, the density variation during combustion and the rates of burning, readily computes the overall combustion kinetic data.

Details are provided of the computing procedure adopted for the derivation of overall kinetic data together with the simplifying assumptions. Results follow in the latter part of this chapter, which cover the heat release and macro-kinetic analysis of the autoignition processes.

B2.2 Computing procedure

B2.2-1 Introduction

The kinetic nature of knock has been the subject of many an investigation (16, 32, 89, 98, 106). The studies summarised in table BO.1 and many others had recognised that the first stage preceding the main combustion processes, in addition to being recognisable by the release of combustion energy, exercises kinetic influence on the subsequent stages (23, 89, 98). Evidence gathered by many investigators shows that most of the hydrocarbons undergo one of ~~the~~ three ~~phases~~ processes during ~~autoignition~~ Knock; namely, low-temperature, high-temperature and flame acceleration. Whilst the last process has met with little support, the recent evidence (1, 29) reinforced the earlier commonly held view that either low- or high-temperature

autoignition is responsible for knock. It is now fairly well understood that the high-temperature and low-temperature autoignition are differentiable kinetically; for, Nitrogen oxides, aromatic amines and aldehydes promote the former, while the latter is either inhibited or remains unaffected by the same substances.

Voinov (98-100) and Yantovskii (106-109) determined the kinetic behaviour of the first stage in terms of luminous flux and rise of pressure. Whilst the rise in pressure is measurable quantitatively with the help of accurate pressure pick-ups, the luminosity measurements are purely qualitative and hence can only serve the purpose of a comparative study confined to the same system. Moreover, it has been found that the intensity is, in principle, dependent on the use of colour filters.

Another quantitative basis of establishing the thermal behaviour of the first stage combustion is to analyse the pressure development during this stage. Pastell (82) and Walcutt and Rifkin (102) were among the first to attempt this along these lines. Despite certain limitations, such as oversimplifying assumptions, rather primitive pressure measuring instruments and long step length, they could suggest that: precombustion reactions liberate significant combustion heat release; the increase in Octane Number of the fuels affects directly these reactions, although no apparent correlation could be established, and in the event of the absence of any cool flames and hence precombustion reactions, the knock inhibitors remain ineffective.

In this investigation, a procedure is developed to analyse the autoignition behaviour of common gaseous fuels and to see how it is affected thermo-kinetically by first analysing the rates of heat release and then deriving the chemical kinetic data that could be ascribed to their resultant behaviour.

B2.2-2 The derivation of overall combustion kinetic data from combustion heat release

The underlying assumptions for computations of rates of heat release and heat transfer have been discussed at length in chapter A2. The following comments need, however, to be added with particular reference to the pre-combustion reactions:

(i) The start of the first stage combustion is registered by a sudden rise in the pressure differential $(dp/d\theta)$ displayed on the oscilloscope. It is further confirmed, or otherwise readjusted, by the heat release computations applying to the condition if $d\mathring{q}/d\theta > 0$.

(ii) The above pressure rise is the result of heat liberation together with molar increment in the cylinder contents.

(iii) Purely for the evaluation of the thermo-dynamic and transport properties of the reactants and products at any instant, during the course of both stages, the energy released thus far is due to the complete combustion of proportionate fraction of the fuel aspirated.

(iv) The cylinder contents behave as an ideal gas under all conditions of temperature and pressure.

(v) The heat of combustion of fuel and the thermo-dynamic and transport properties vary, during both stages, according to the mean calculated temperature of the cylinder contents.

(vi) The cylinder contents constitute a homogeneous charge with no temperature and pressure gradients within it.

The above considerations and accounting of heat transfer for each increment of one degree crank rotation are considered to be an improvement on the previous works (82, 102).

The overall reaction rate may be represented adequately for some of the common hydro-carbons by the following form of single step reaction (39).

$$\mathring{m}_f''' = K(m_f)^a \ (m_o)^b \ \rho^{a+b} \ e^{\frac{-E}{RT}} \qquad (1)$$

This simplified rate ($\dot{m}'''_f$) implies that it is a function of the concentrations of fuel (m_f) and oxygen (m_o) and an exponential relationship with respect to temperature (T) which is commonly known as being of the Arrhenius form. The extent of agreement of actual experimental results with this assumption will be expected to apply only over a limited range of operating conditions. The success of overall mechanisms suggests that it is a reaction step that controls the overall conversion rate and at the same time bears some quantitative relationship to the major constituents. Such a controlling step does vary from one fuel to another and depends on the temperature and concentration ranges.

In view of the absence of any deliberate source of ignition and the operation with turbulent homogeneous mixtures, it can be justifiably assumed that throughout the preignition and post-ignition processes there are no temperature and pressure gradients. On this basis, the gross reaction rate ($\dot{m}'''_f$) over any small increment of time Δt can be derived from the gross volumetric heat release values $\dot{q}'''_g$ according to the following relationship:

$$\dot{m}'''_f = \frac{\Delta \dot{q}'''_g}{\Delta H_T} \qquad (2)$$

where H_T is the heating values of the fuel at conditions corresponding to that at the temperature under consideration.

On this basis, the instantaneous relative concentration of the fuel and oxidant will then be given by the following:

$$m_f = m_{f,o} - \int_o^t \frac{\dot{m}'''_f}{\rho} dt \qquad (3)$$

$$m_{ox} = m_{ox,o} - i \int_o^t \frac{\dot{m}'''_f}{\rho} dt \qquad (4)$$

where $m_{f,o}$ and $m_{ox,o}$ are the initial mass concentration of fuel and oxygen, respectively.

Fig. (B2.1) shows the variation of effective rate of gross heat release, pressure-rate, temperature, and heat

transfer rates during autoignition of propane as computed from experimentally obtained pressure development record. Fig. (B2.2) displays the reaction rates ($\dot{m}$), variation of relative mass concentration of fuel and oxygen derived by the procedure outlined above from the gross heat release variation of Fig. (B2.1), while the normalised reaction rates v/s reciprocal of temperature appear in Fig. (B2.3) for the same conditions of autoignition. On the same lines the autoignition of n-heptane and its mixtures with propane and methane have been considered.

B2.3 Presentation of Results

The results are presented in two parts; the first part deals with the heat release analysis of the following:

(i) autoignition of propane-air;
(ii) autoignition of n-heptane-air;
(iii) autoignition of propane-n-heptane-air;
and (iv) autoignition of methane-heptane-air

over the lean autoignitable mixture-strength to Stoichiometric values, while the second part presents the overall chemical kinetic data of the above reactions in the form of normalised reaction rates as a function of temperature.

B2.3-1 Results of the computed rates of heat release due to autoignition

B2.3-1a Propane-air mixtures

Incipient autoignition of propane in a motored engine was obtained covering the following operating conditions:

Mixture strength	27 - 44%
Intake temperatures	106°, 121°, $149^{\circ}C$
Compression ratio	15 - 17.5

Whilst the engine operating conditions were kept constant as described in the experimental procedure.

A typical variation of computed gross rates of heat release, temperature, pressure rate and cumulative heat release appears in Fig.(B2.1).

B2.3-1b n-Heptane-air mixtures

Plate (B1.8) shows some typical records obtained from motored engine tests. The rate of pressure rise indicates clearly two stages of n-Heptane autoignition. The variation of computed parameters such as mean cylinder gas temperature (T), effective rates of combustion heat release ($\dot{q}$), rate of pressure rise ($dp/d\theta$), cumulative heat release (Q), together with experimentally obtained cylinder gas pressure (P) are displayed in Fig. (B2.4). They cover a range of 30°BTDC - 30°ATDC, beyond which it was invariably found that no significant combustion energy is released. In Figs. (B2 - B2.a) is shown the relative significance of the two stages under incipient autoignition, while the mixture strength is increased. Table (B2.1) presents the other parameters , such as temperature and pressure rise and cumulative heat release during the first stage.

In order to study the autoignition of richer mixtures under high compression ratios, it was necessary to make use of some diluent. Carbon dioxide was adopted as diluent: for, its molecular weight is the same as propane; it serves as an effective diluent; it is found in many natural gas sources; and its influence on the knocking performance of a dual-fuel engine has already been investigated (42). Fig. (B2.6), together with Table (B2.2), brings about the influence of carbon dioxide as diluent. Fig. (B2.7) depicts the effect of compression ratio on the extent of the first stage combustion.

B2.3-1c Propane-heptane-air mixtures

Figs. (B2.8 - B2.10) display a typical cross-section of records for the detailed analysis of the effect of propane addition to a fixed quantity of n-heptane. Fig. (B2.11) summarises the computed ignition temperature v/s mixture strength studied for the wide range of propane heptane blends in air.

B2.3-1d Methane-heptane-air mixtures

Figs. (B2.12 - B2.15) present a wide range of mixture strength of the blends studied. The lean mixtures were autoignited without the use of carbon dioxide as diluent. Superimposed on these diagrams are the re-plots of the first stage combustion with a magnified scale of heat release so as to bring out the relative differences. Fig. (B2.16) displays the autoignition temperature versus mixture strength of all types of blends used. Methane autoignition temperatures have been computed from the Klat's plots of compression ratio versus mixture strength (51).

B2.3-2 Results of the computed overall combustion kinetics of autoignition

Fig. (B2.2) presents the kinetic parameters which determine the overall combustion kinetics of the auto-ignition of propane, while Fig. (B2.3) is the plot of normalised reaction rate versus the inverse of temperature, the slope of which, when multiplied by the universal gas constant, gives the overall activation energy. Shown in Fig. (B2.17) are the sumperimposed plots of normalised reaction rates versus inverse of temperatures for the auto-ignition of propane in air under various operating motored-engine conditions as mentioned in the diagram.

On the same lines, the computed kinetic para-meters of the autoignition of n-Heptane are presented in Fig. (B2.18), while in Fig. (B2.19) is shown the normalised reaction rate as a function of temperature. The activation energy values so obtained are affixed on the respective stages of the well-known multistage autoignition of n-Heptane. Superimposed plots of such reaction rates for a narrow range of mixture strength are shown in Fig. (B2.20). Richer mixture strengths of 55% and 100% of chemically correct value are covered by Figs. (B2.21) and(B2.22), respectively.

Figs. (B2.23 - B2.29) present normalised reaction rates versus temperature of the autoignition of propane-n-heptane over a wide range of mixture strength. As the

compression ratio and the concentration of diluents were variables, it is difficult to superimpose all the plots. We shall discuss them individually in the following chapter.

The kinetic parameters of the autoignition of methane-Heptane are depicted in Figs. (B2.30 - B2.35). Table (B2.3) summarises the comparative details of n-heptane, propane-heptane and methane-heptane autoignition. The pressure and temperature rise, the maximum and cumulative heat release and the duration of the first stage of combustion, together with the activation energy, as derived from the normalised reaction rate plots.

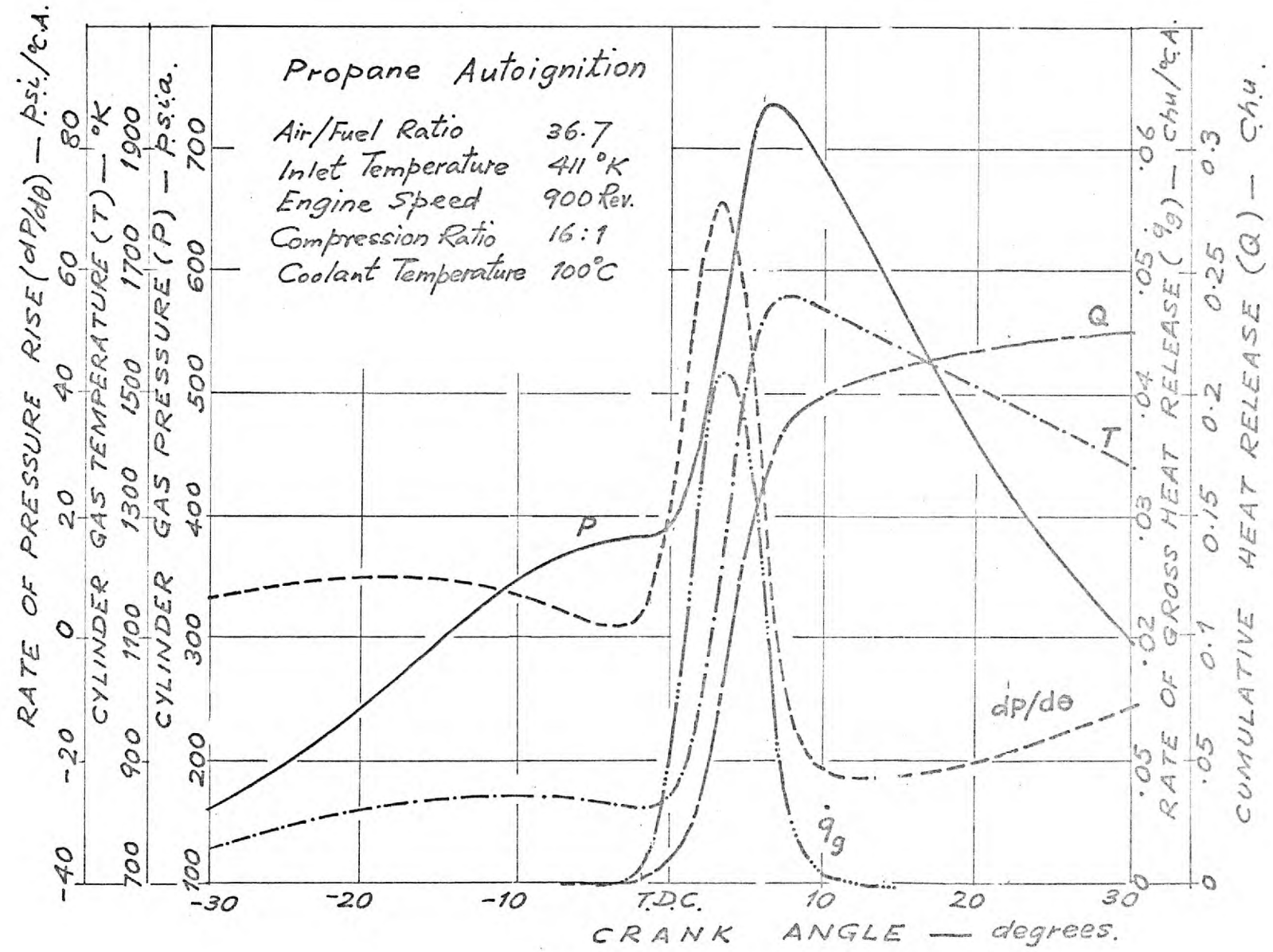


Fig. B2.1 : Variation of computed parameters during autoignition of propane – air mixtures.

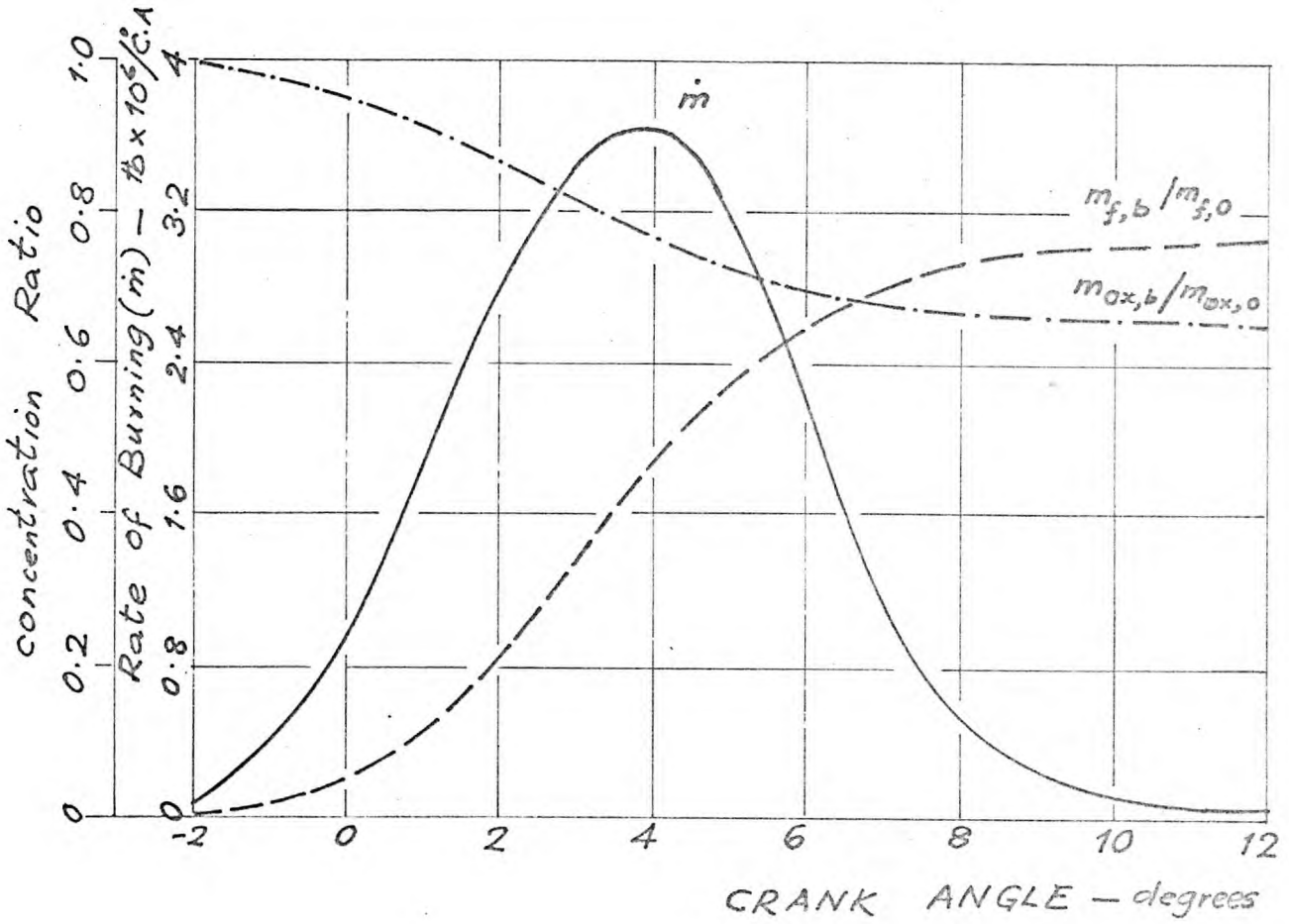


Fig. B2.2 : Variation of reaction rate and relative mass concentrations of fuel and oxygen.

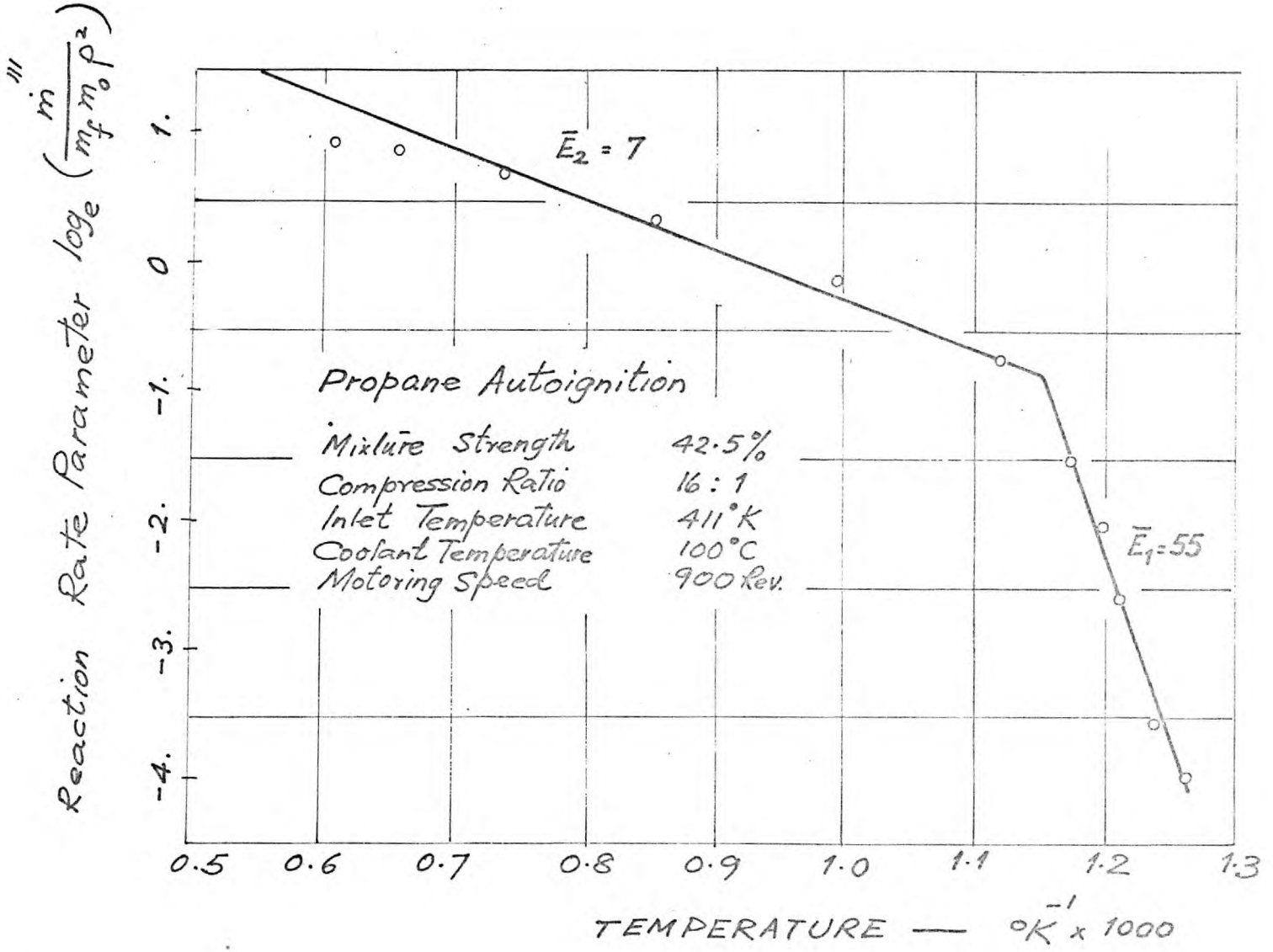


Fig. B2.3: A plot of normalized reaction rate versus inverse of absolute temperature.

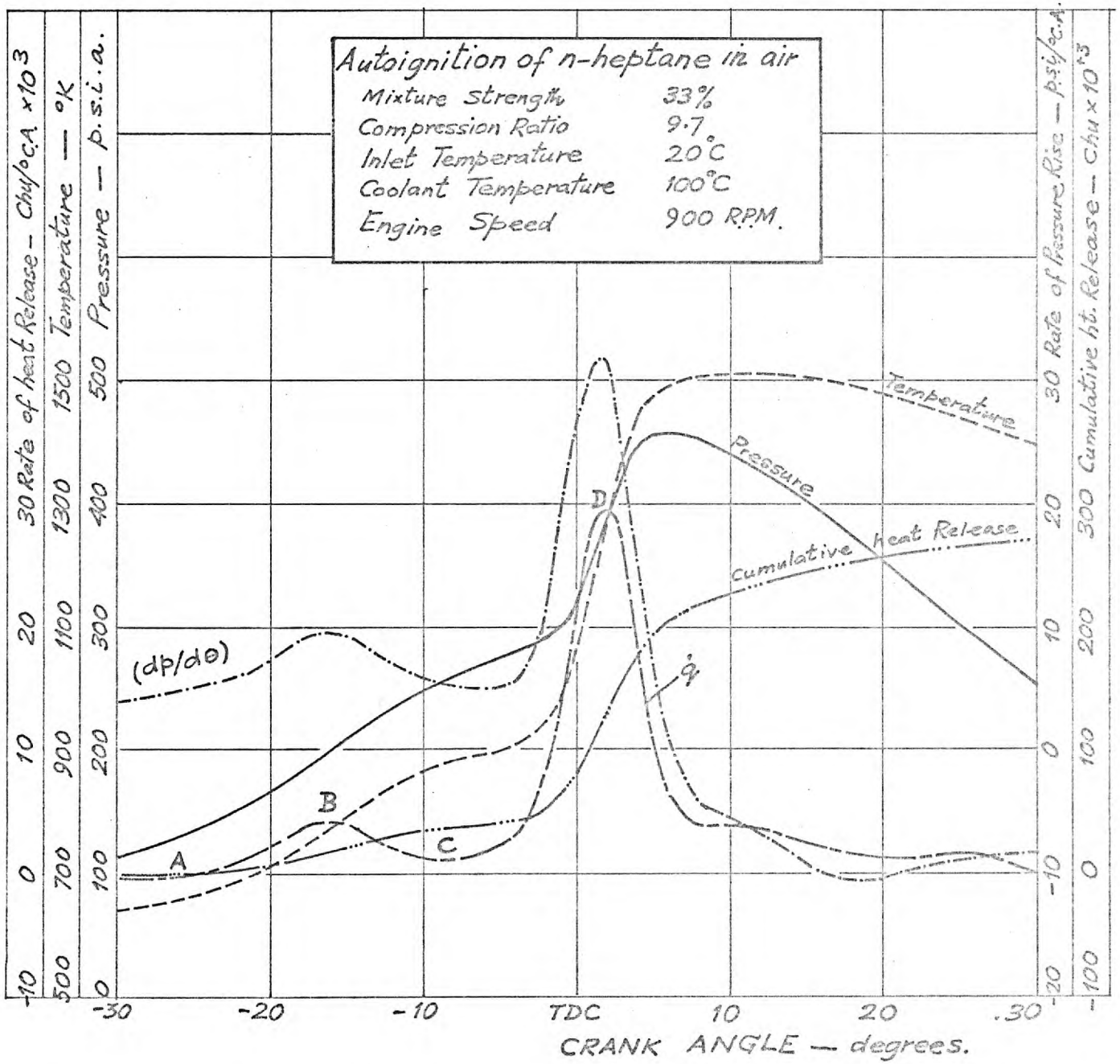
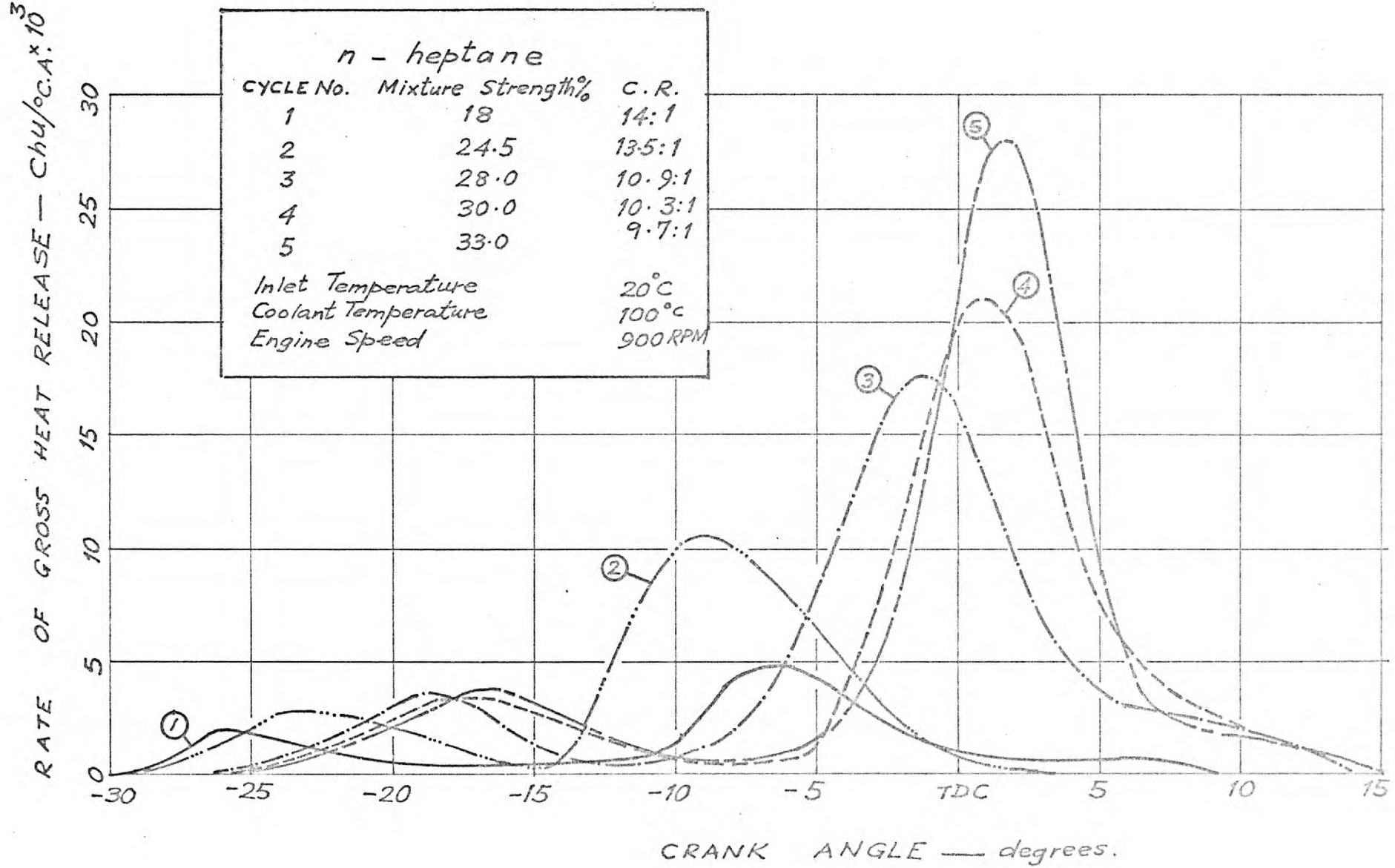


Fig. B2·4 : Variation of computed parameters during autoignition of n-heptane.

Fig. B2.5: Analysis of heat release variation – effect of increase in mixture strength of n-heptane.



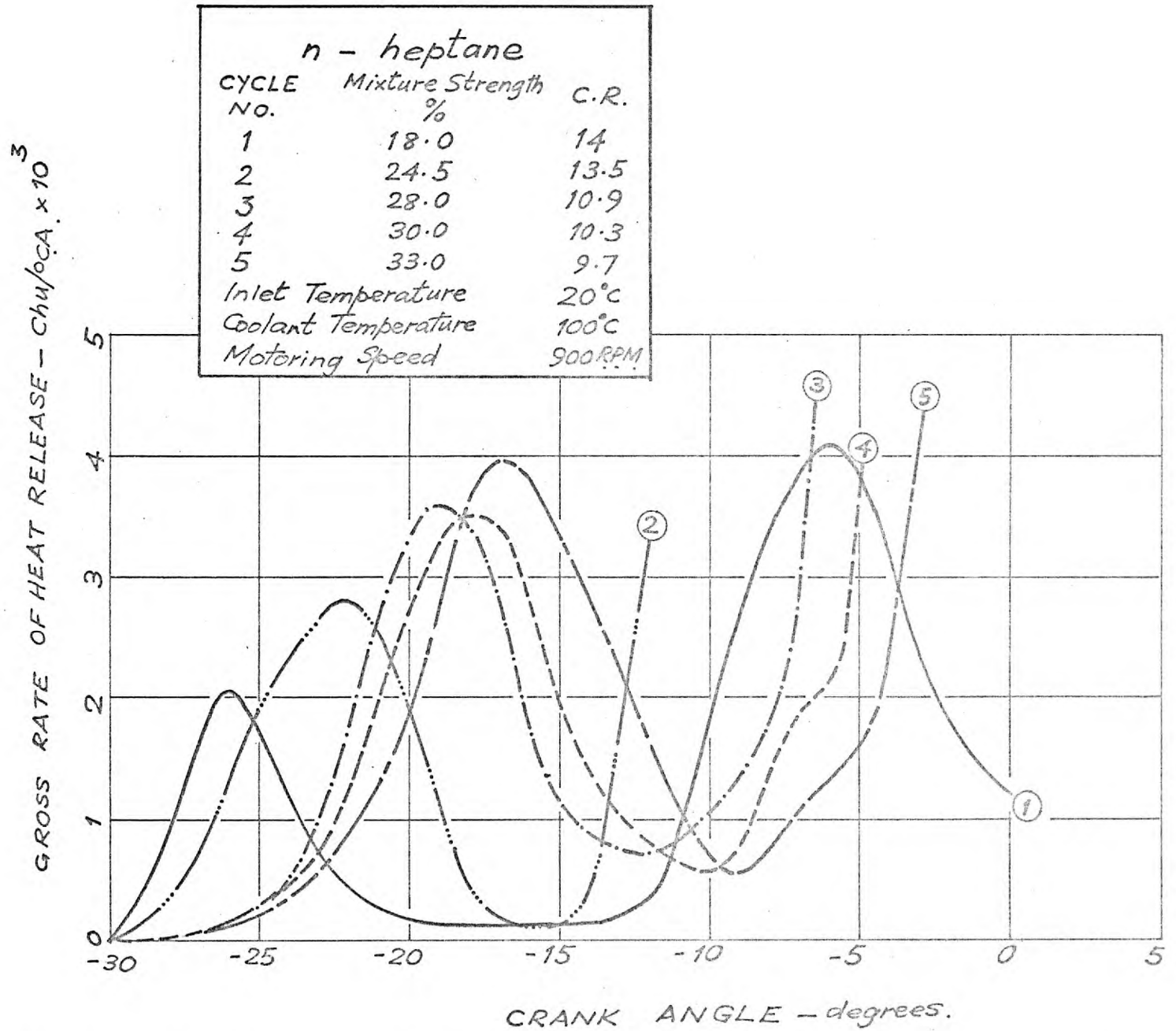
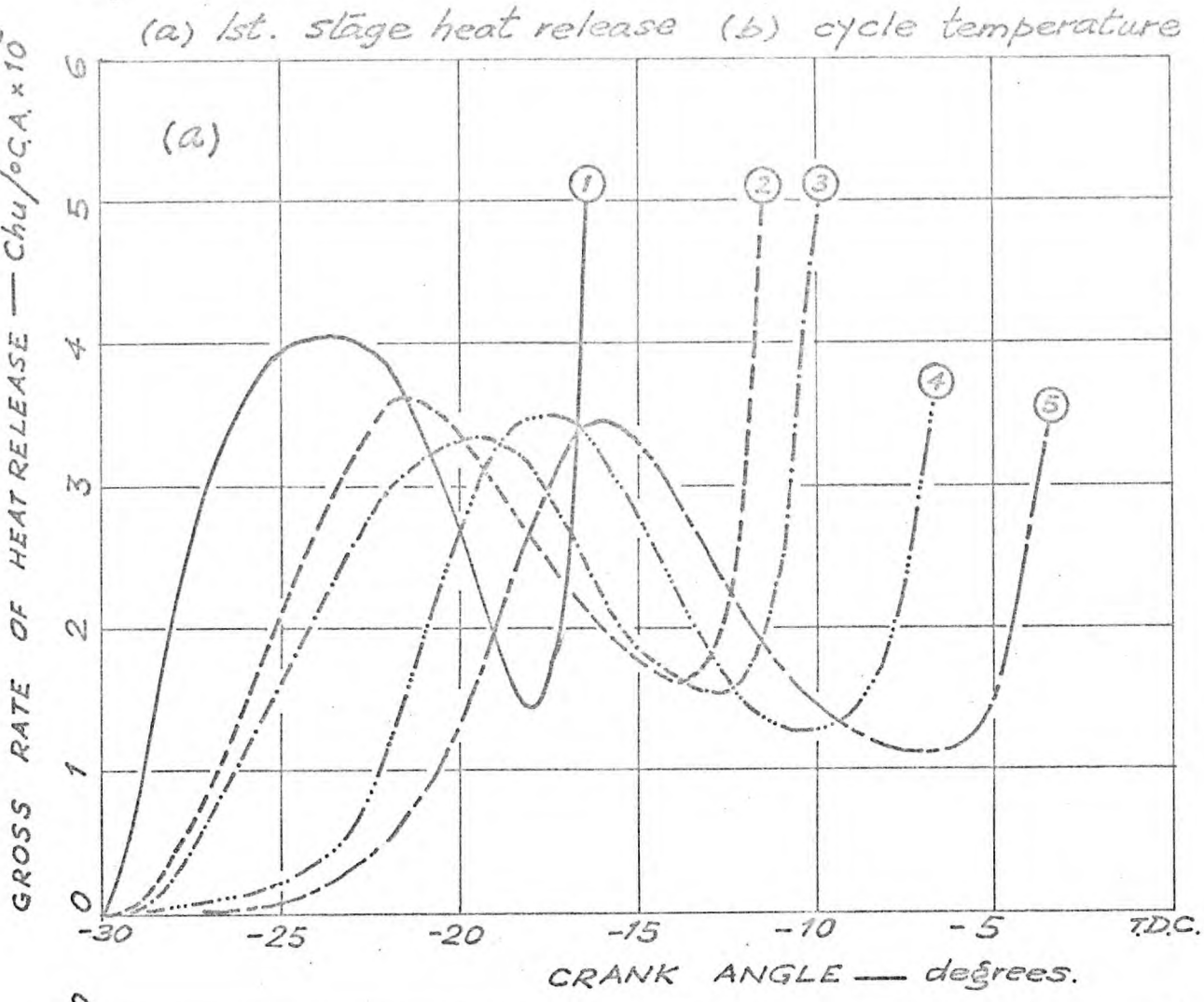
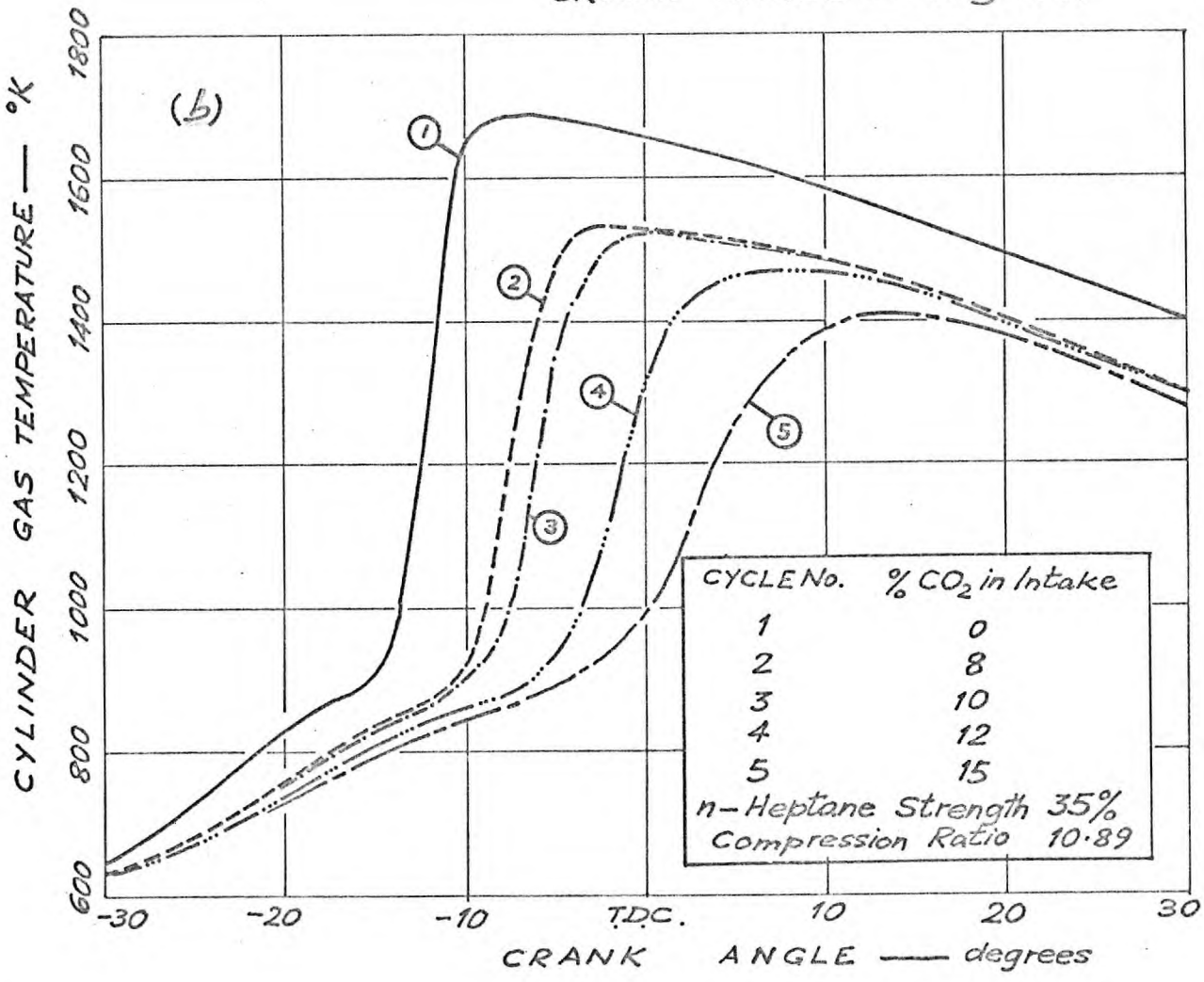
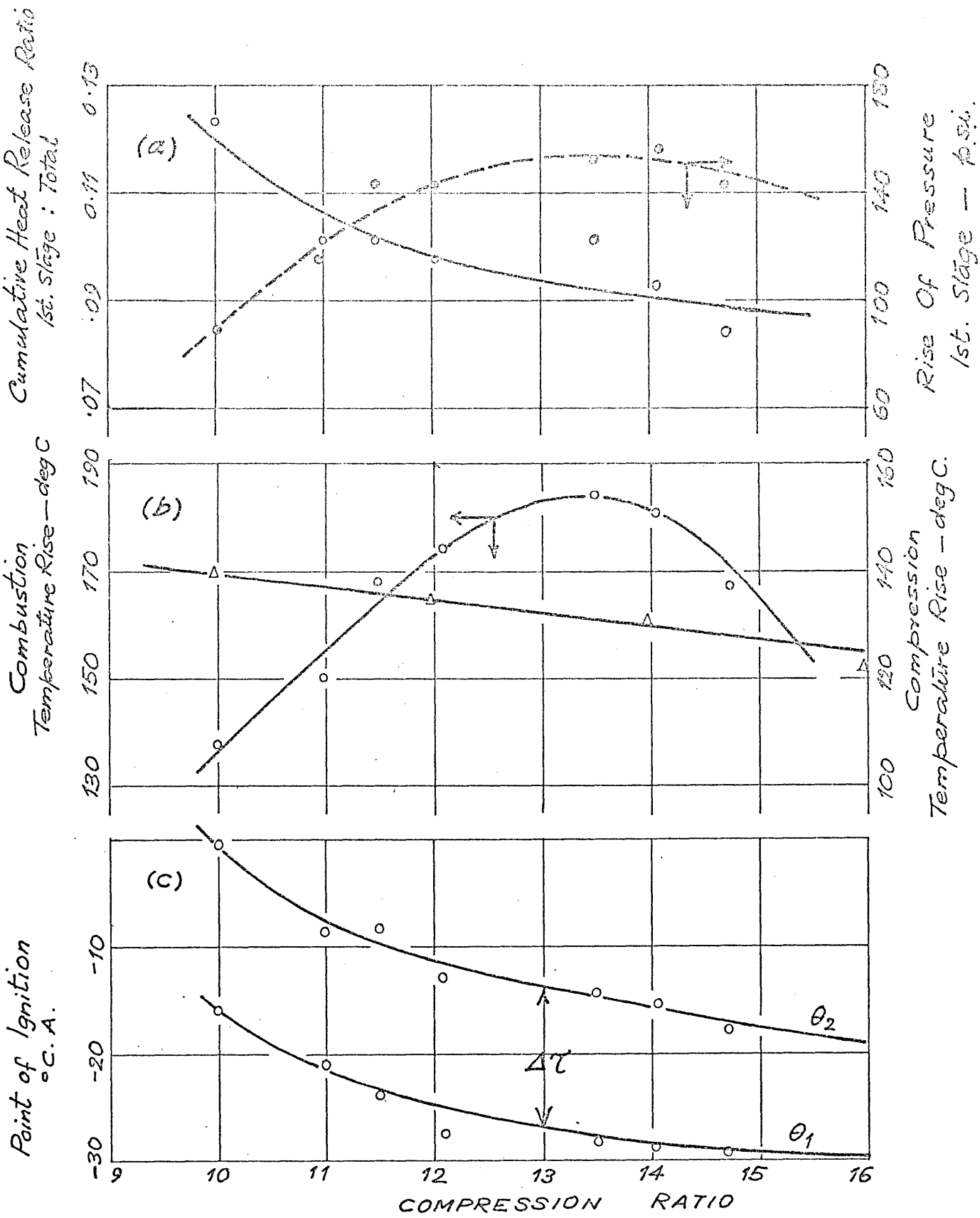


Fig. B2·5a: Analysis of heat release variation – effect of mixture strength on the first stage of n-heptane autoignition.

Fig. 6: Effect of CO_2 addition in n-heptane autoignition
(a) 1st. stage heat release (b) cycle temperature







n-Heptane, Mixture Strength 24%, Inlet Tmperature 20°C
Coolant Temperature 100°C, Engine Speed 900 R.P.M.

Fig. B2.7: Effect of varying compression ratio on the first stage — (a) pressure rise and cumulative heat release (b) compression versus combustion temperature rise and (c) ignition timings of first and second stage.

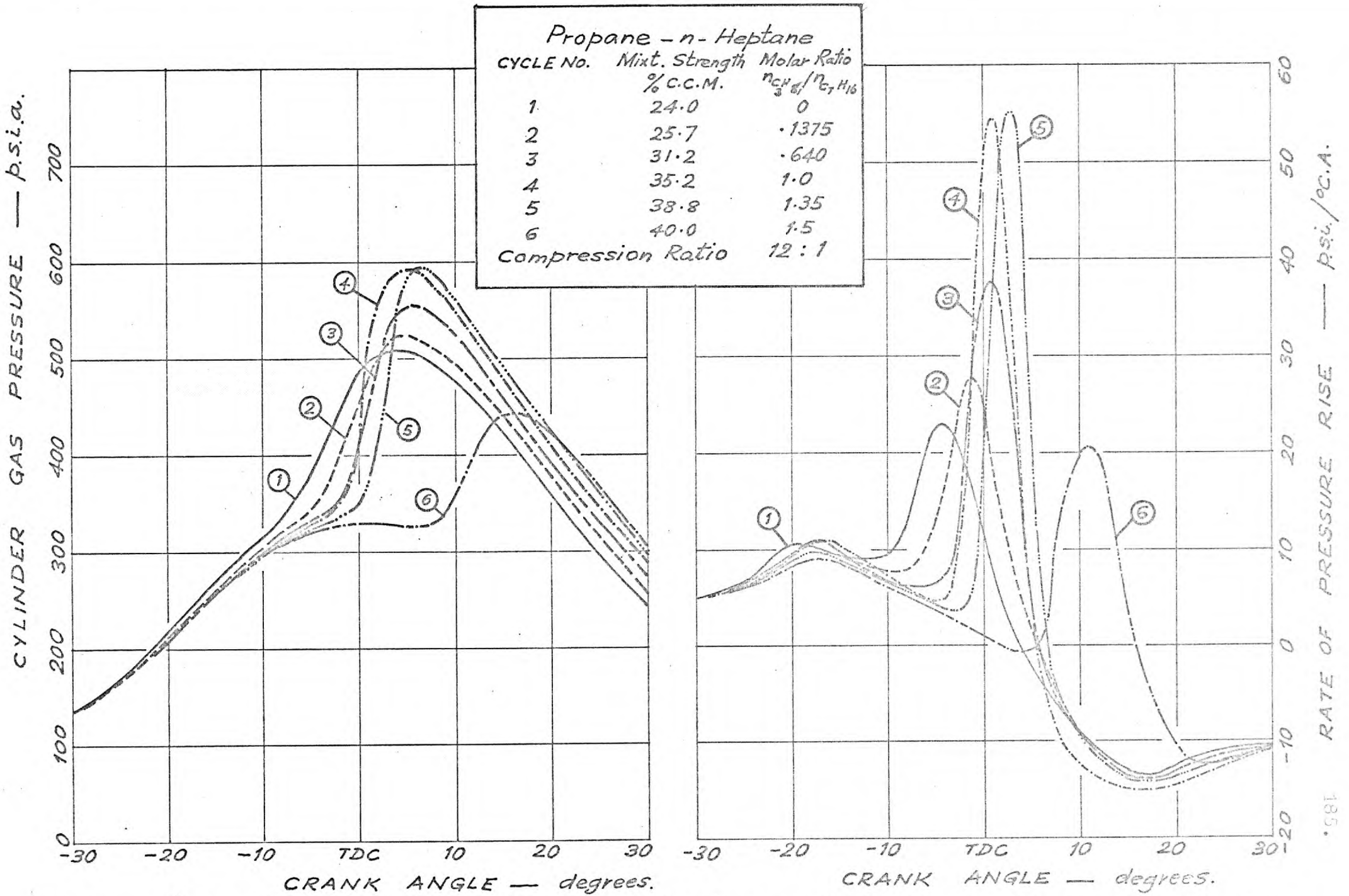


Fig.(B2·8) Effect of propane addition during heptane autoignition – (a) pressure (b) pressure rate variation during cycle.

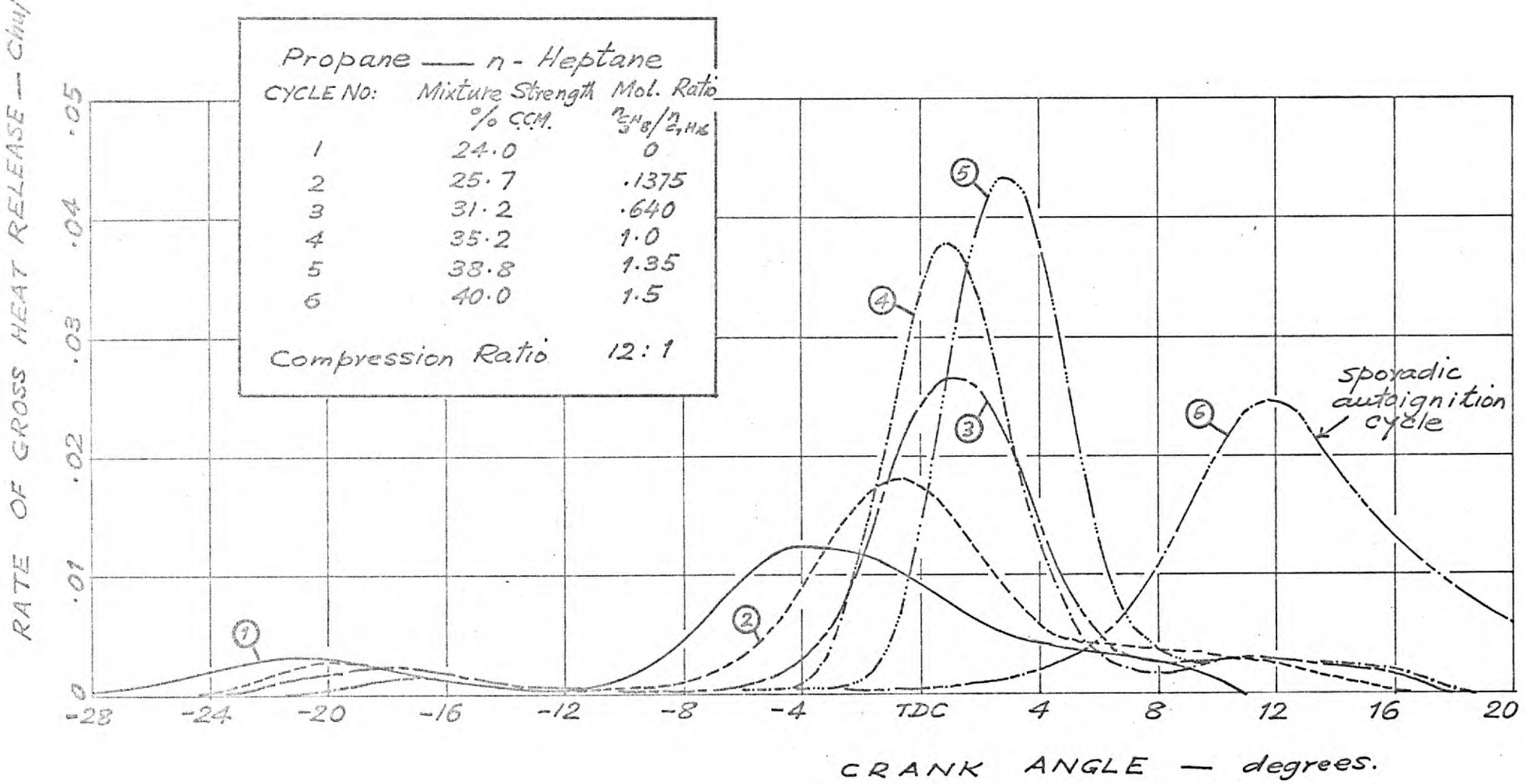


Fig. B2.9: Analysis of heat release variations – effect of propane addition in propane–n-heptane-air mixture.

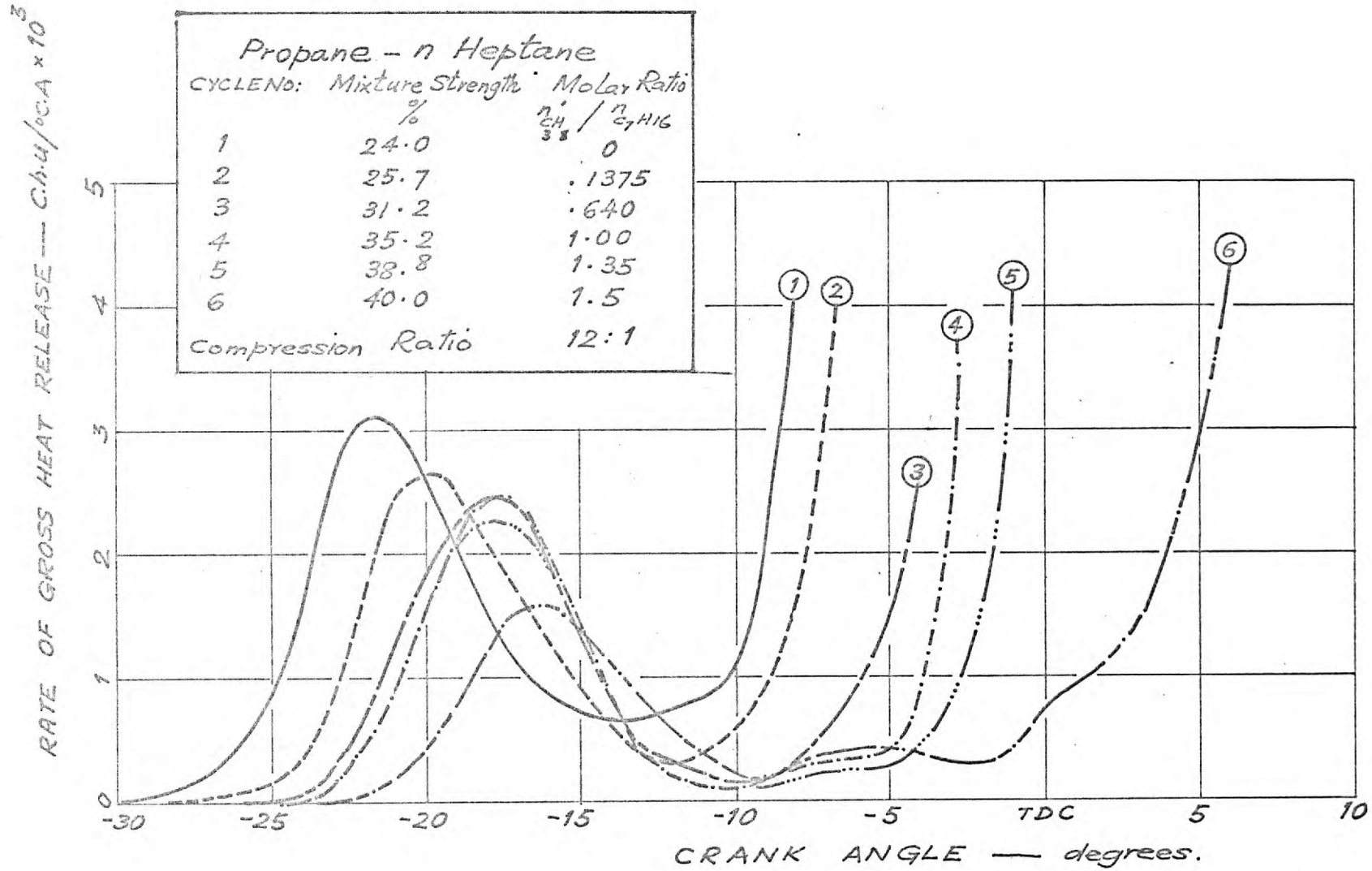


Fig. B2.9a: Analysis of heat release variations during first stage – effect of increase in propane concentration in the blend.

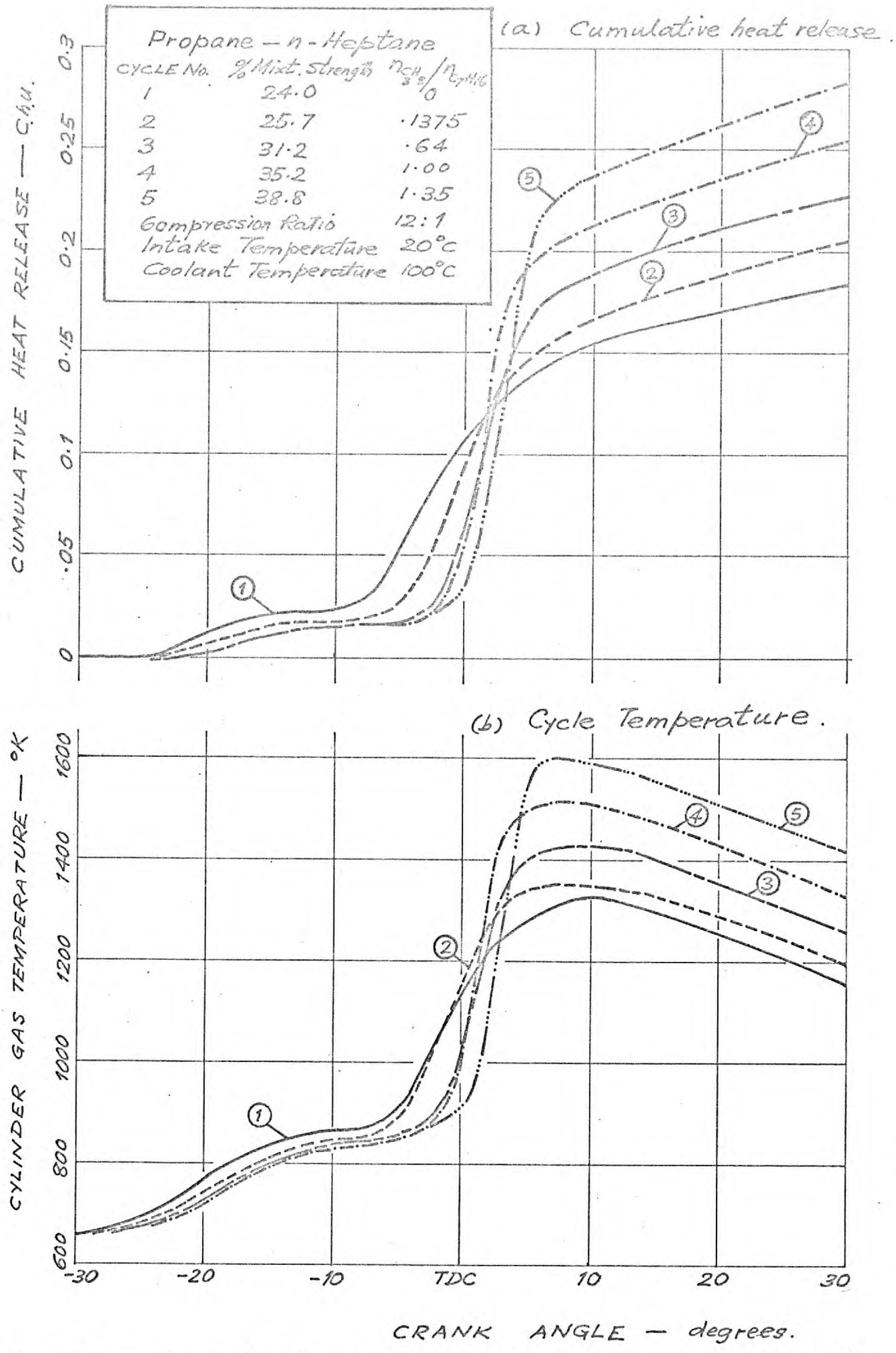


Fig. B2.10: Analysis of cumulative heat release and cycle temperature variation – effect of propane increase in the charge.

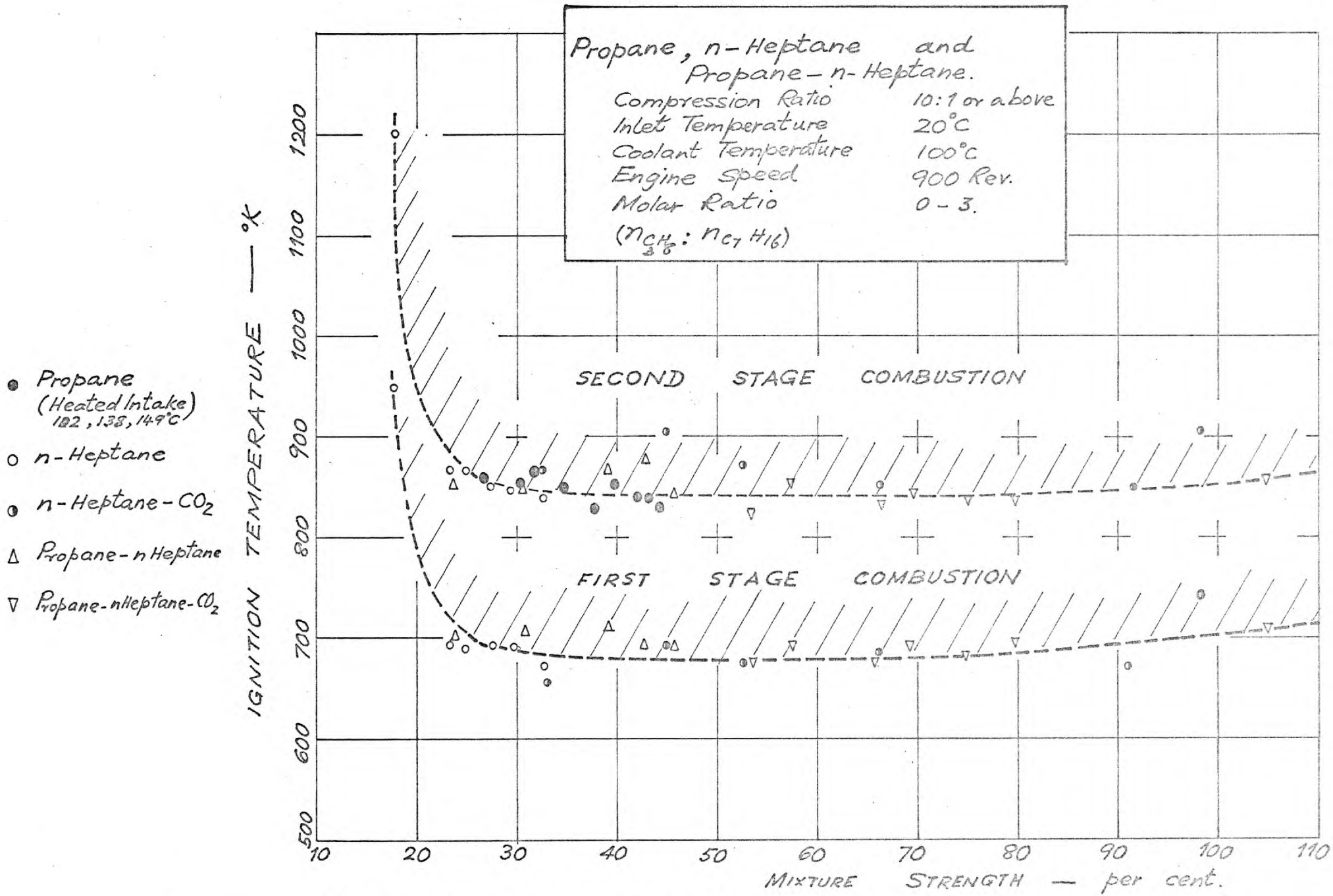


Fig. B2.11: Autoignition temperature boundaries of n-heptane, n-heptane – propane, propane mixtures in air.

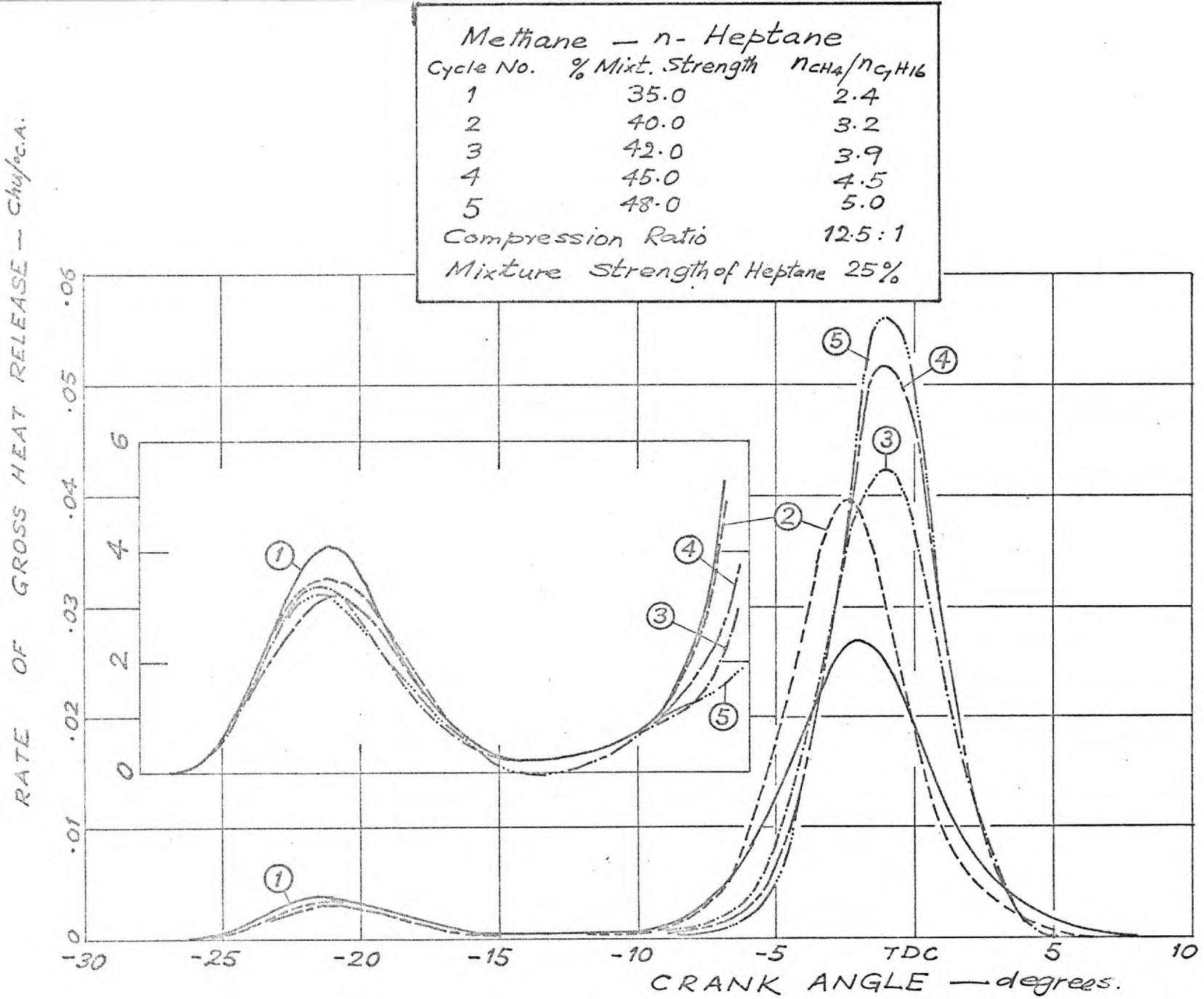
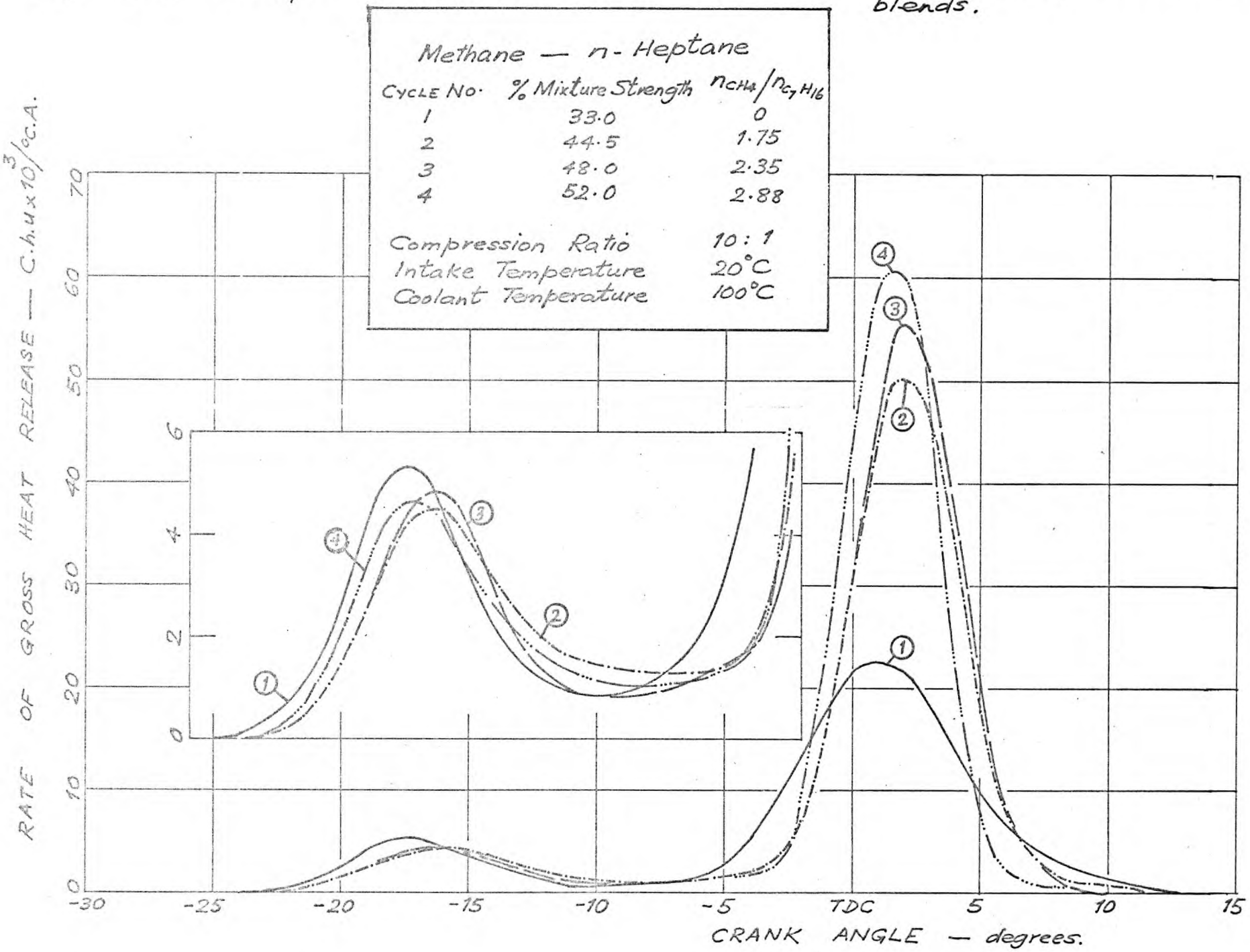


Fig. B2.12: Analysis of heat release variations due to autoignition of methane–n-heptane blends — effect of increase in methane concentration

Fig. B2.13: Analysis of heat release variations due to autoignition of methane-n-heptane blends.



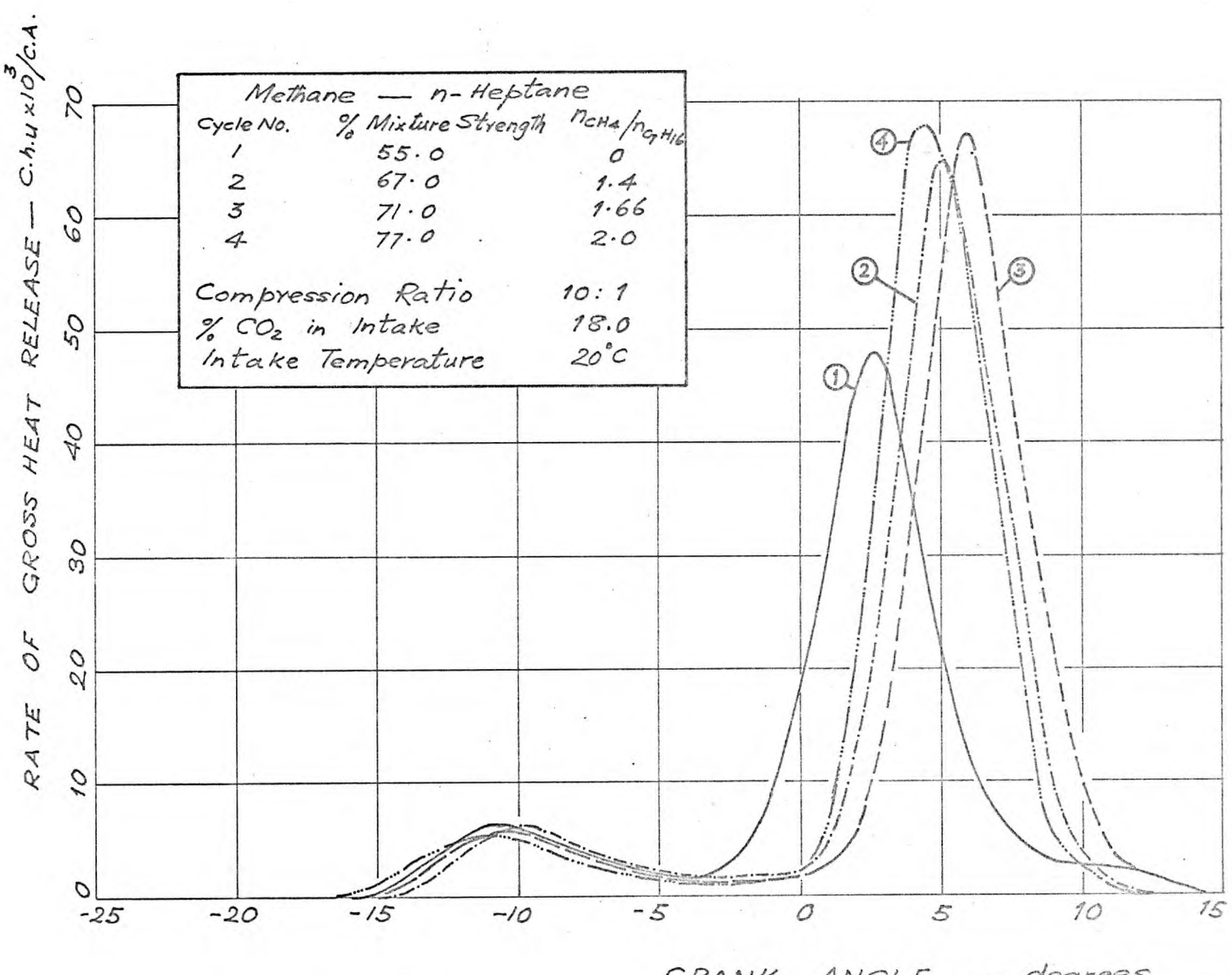


Fig. B2.14: Analysis of heat release variations due to autoignition of methane – n-heptane blends in air; CO_2 used as diluent.

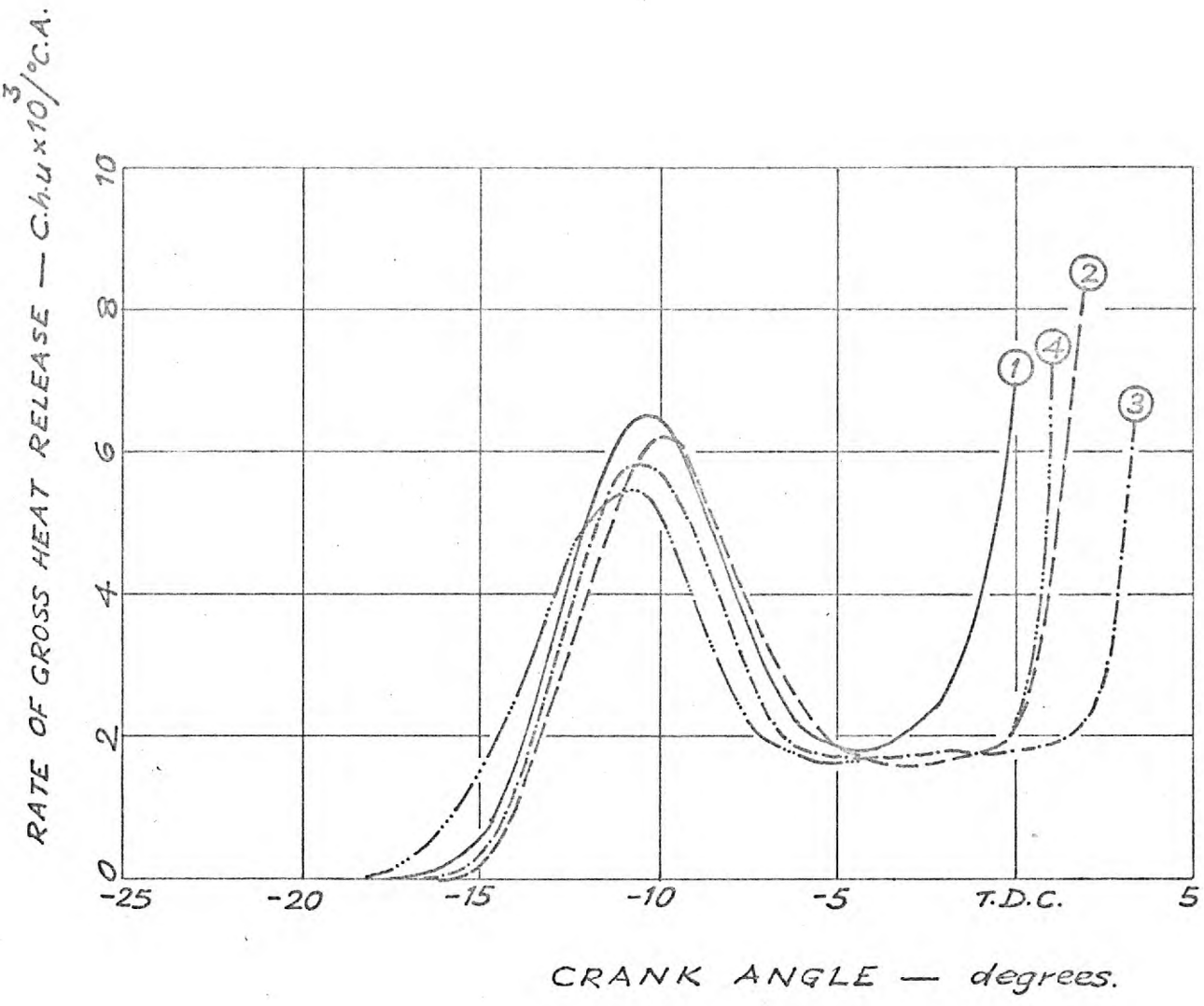


Fig. B2.15.: A magnified replot of the first stage shown in Fig. B2.14.

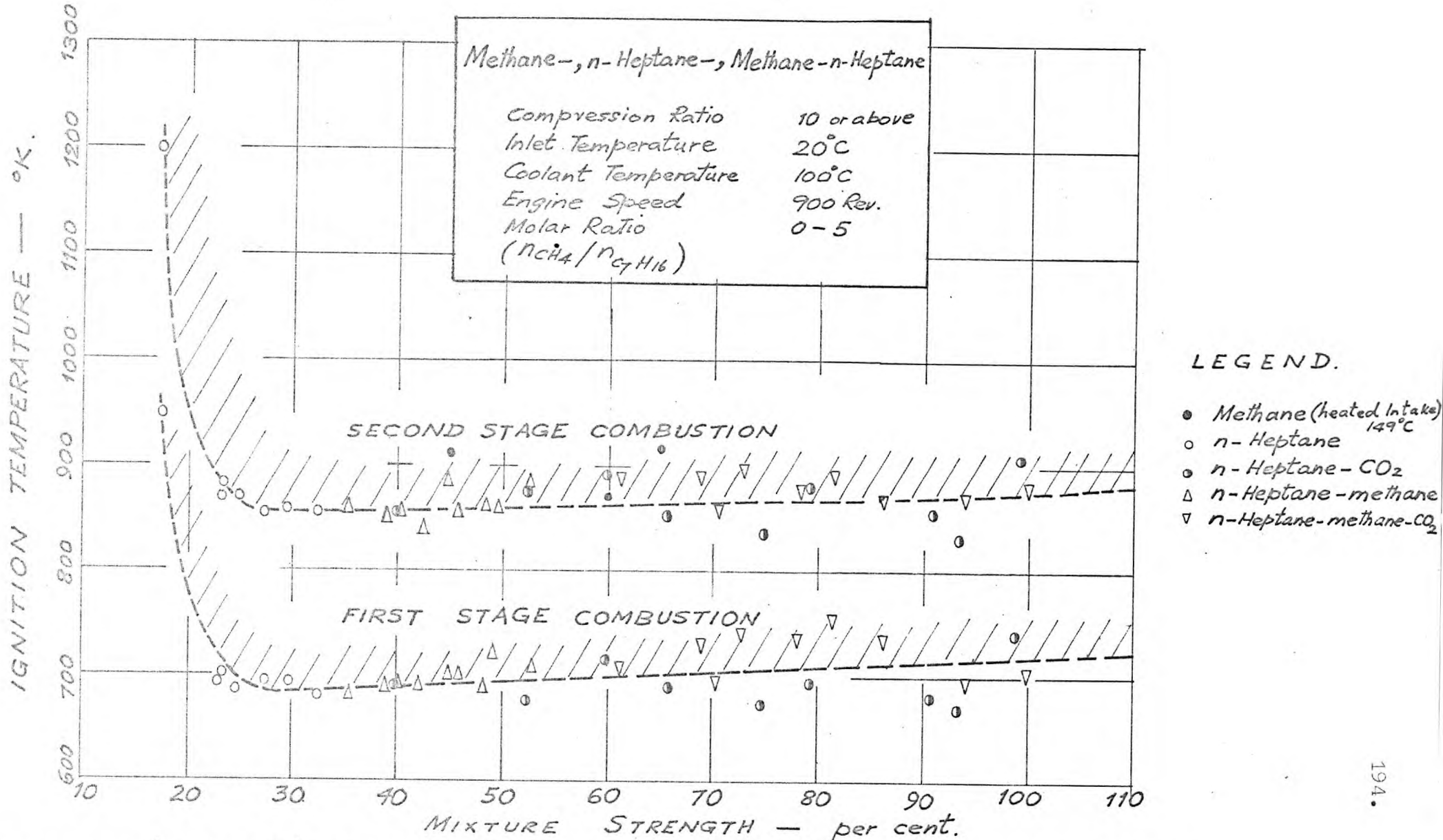


Fig. B2.16: Autoignition temperature boundaries of heptane–, methane and their blends in air.

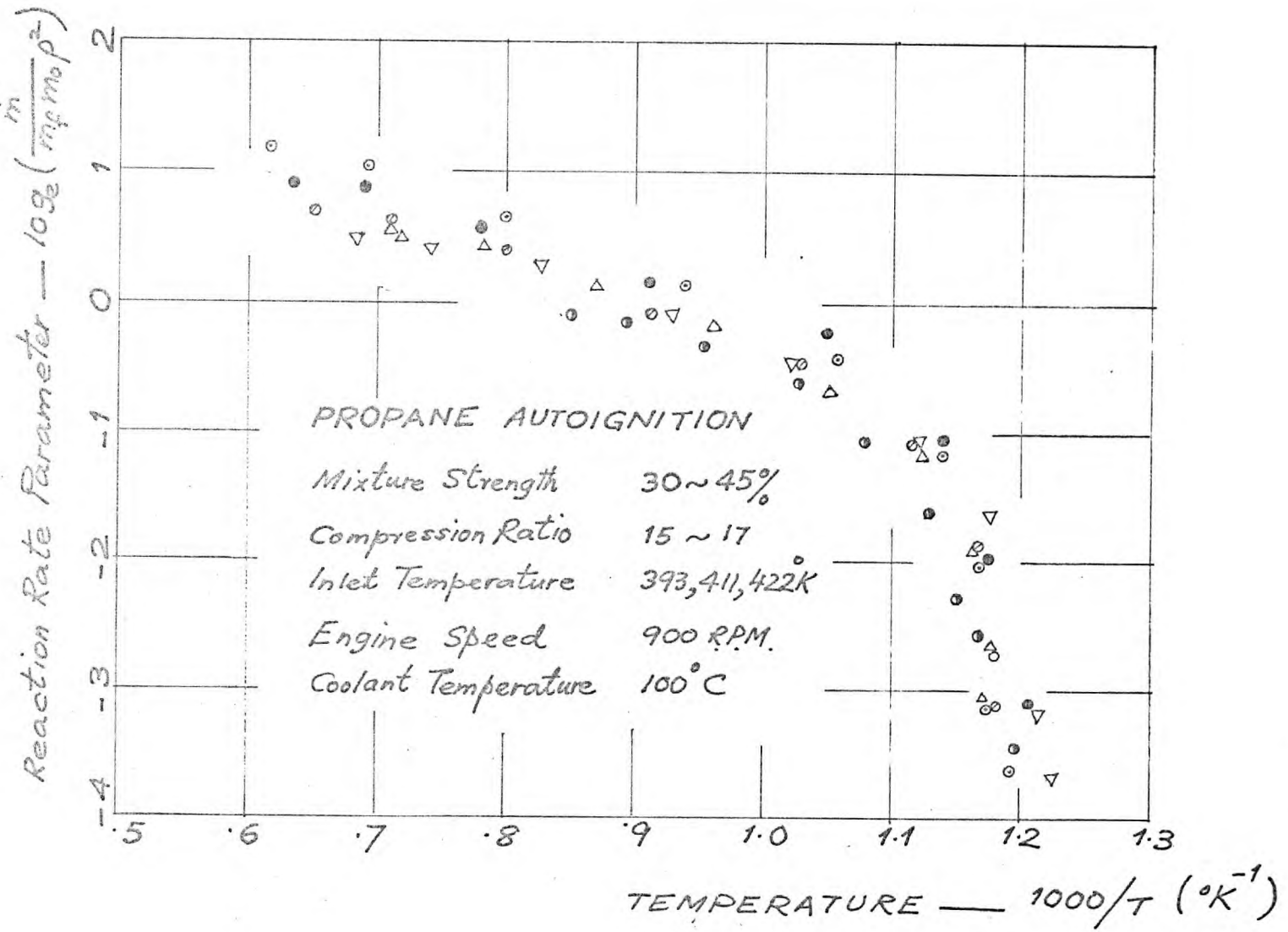


Fig. B2.17: Superimposed plots of normalized reaction rates and inverse of temperature of propane autoignition.

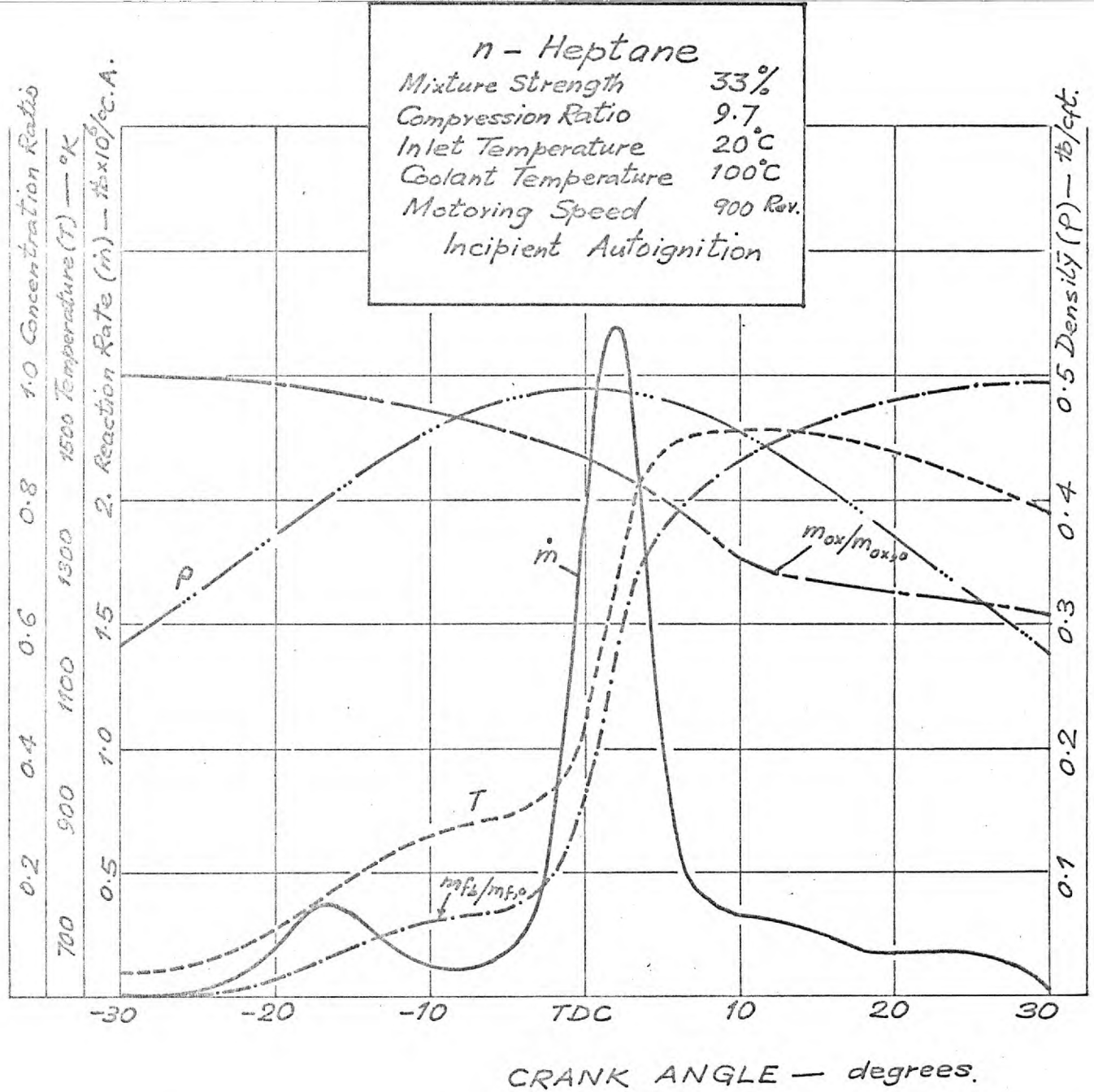


Fig. B2. 18: Variation of computed macro-kinetic parameters of n - heptane autoignition.

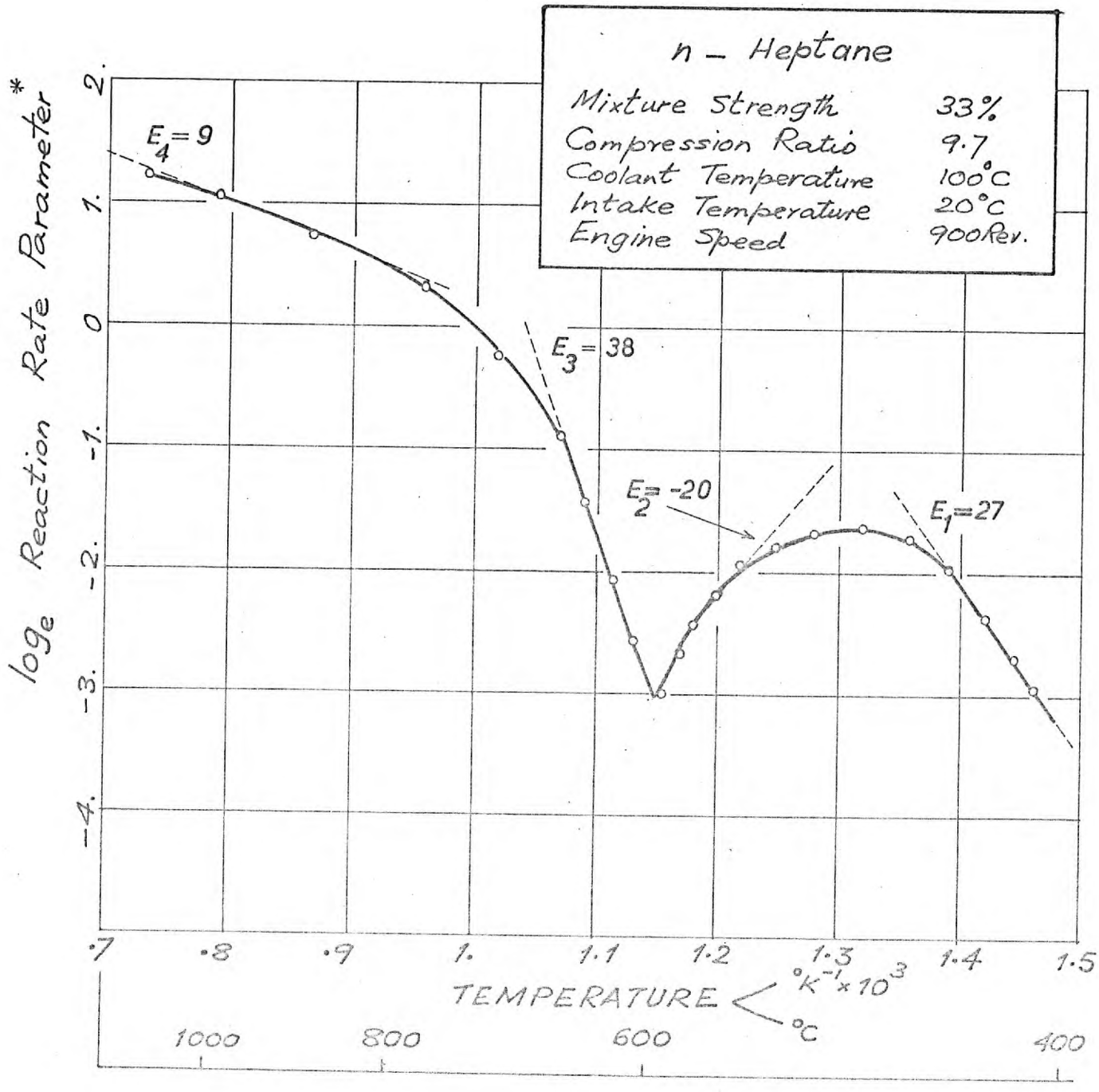


Fig. B2.19: A plot of reaction rate parameter versus inverse of absolute temperature.

* $\log_e \left[\frac{\dot{m}'''}{m_r \, m_o \, \rho^2} \right]$

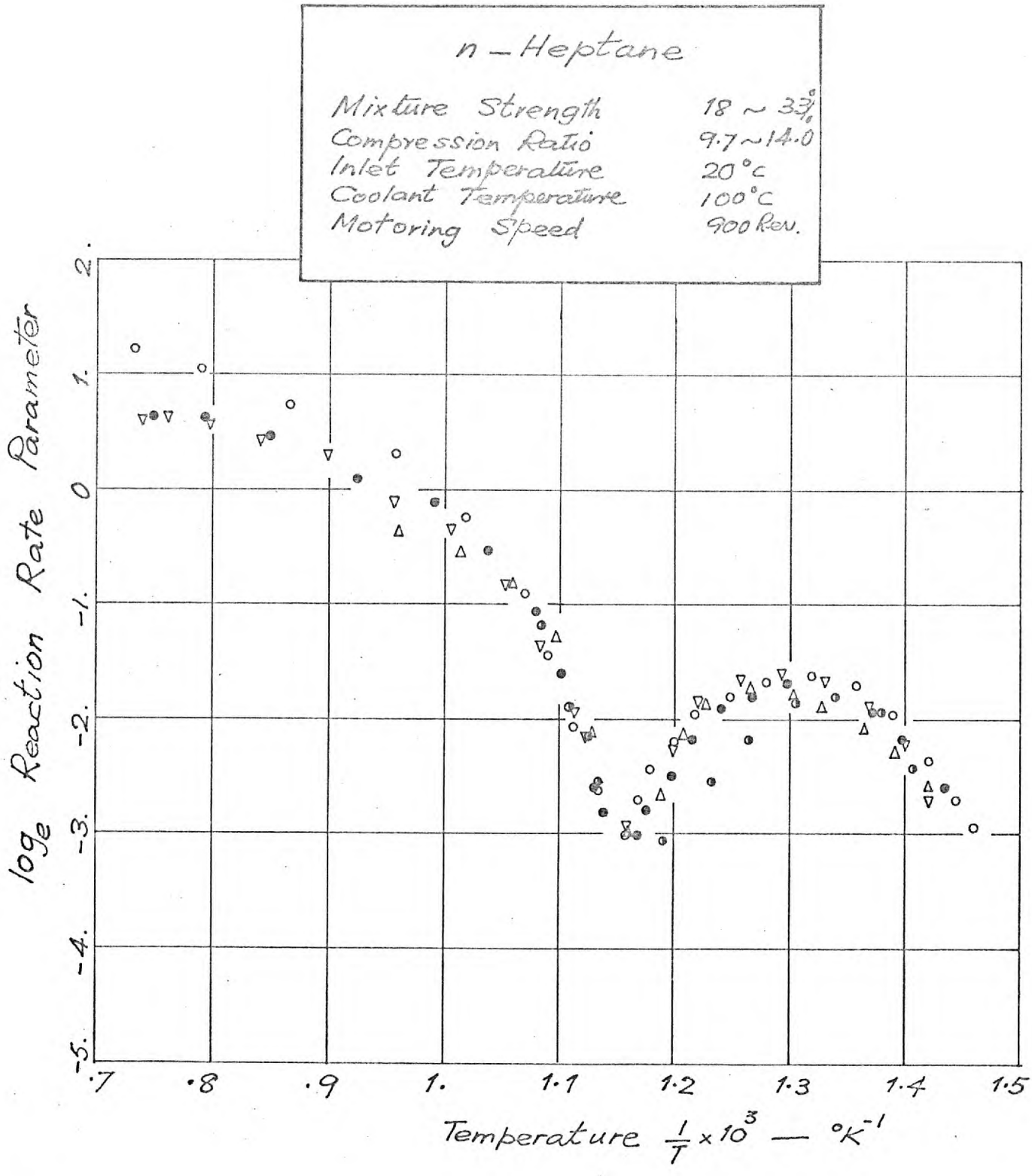


Fig. B2.20: Superimposed plots of normalized reaction rate parameter versus inverse of temperature

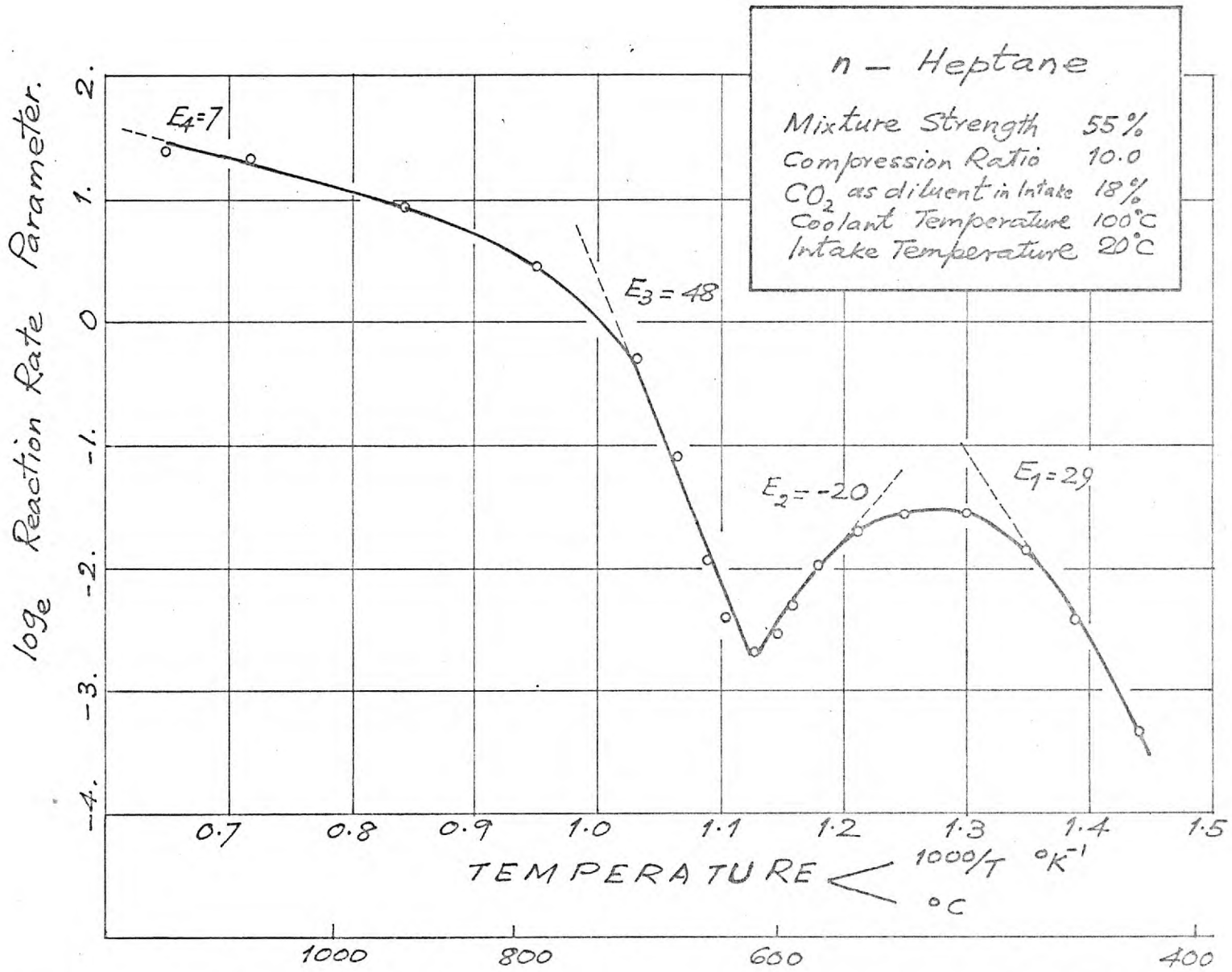


Fig. B2.21: A plot of reaction rate parameter versus $1/T$ of n-heptane autoignition

Fig. B2.22: A plot of normalized reaction rate versus inverse of temperature of n-heptane - CO_2 - air autoignition.

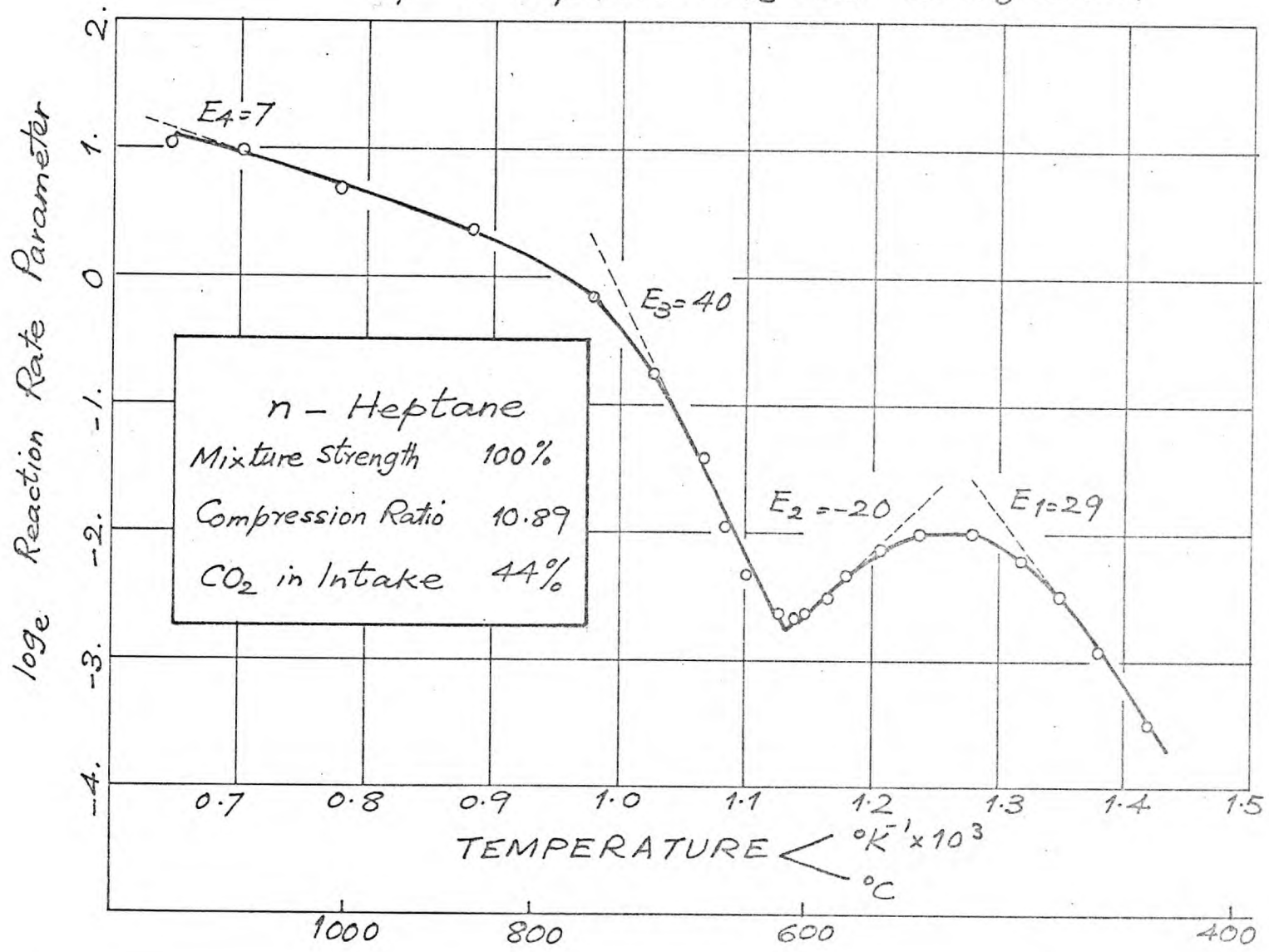


Fig. B2.23a: A normalized reaction rate plot against inverse of temperature of n-heptane autoignition.

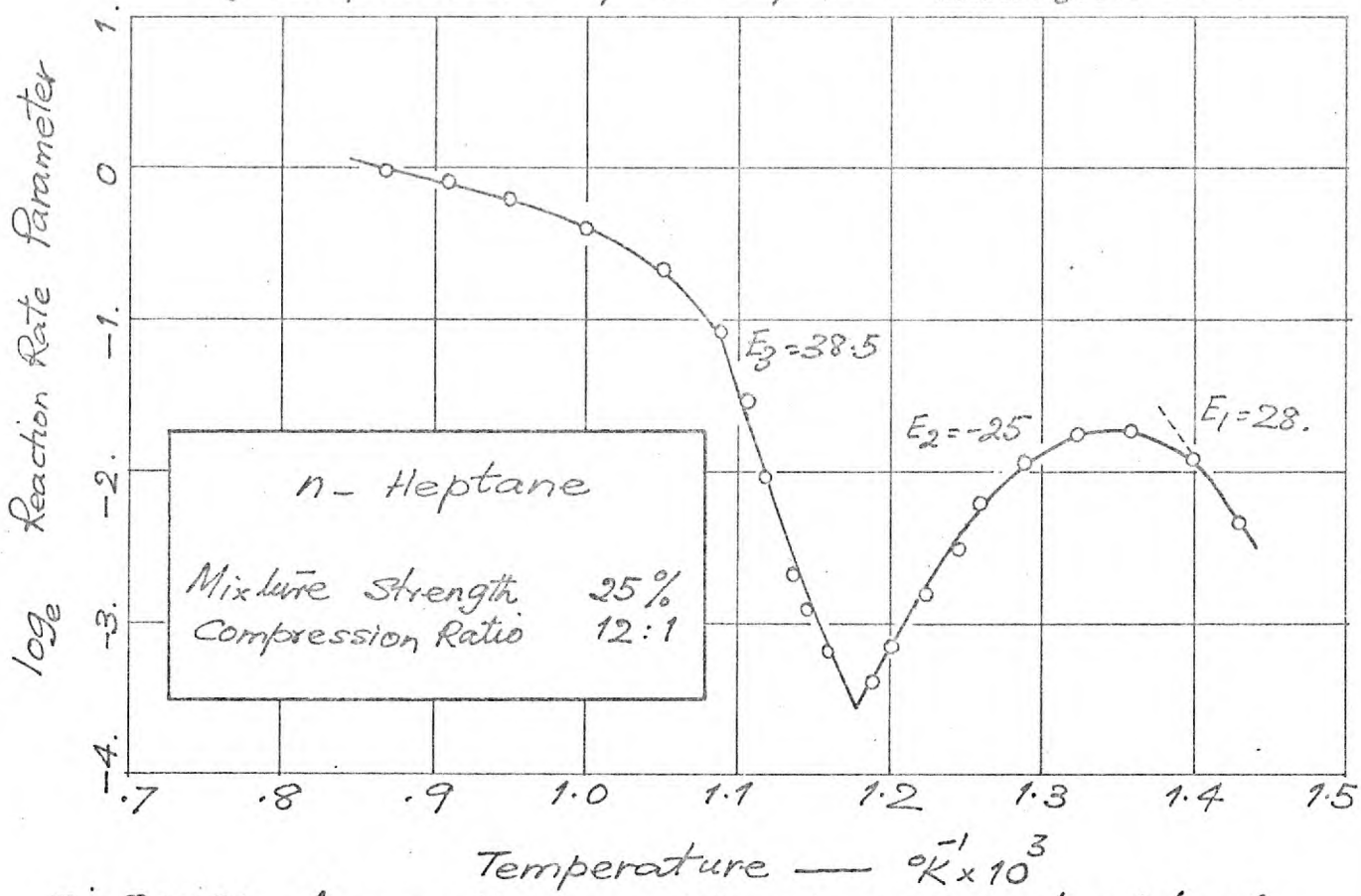
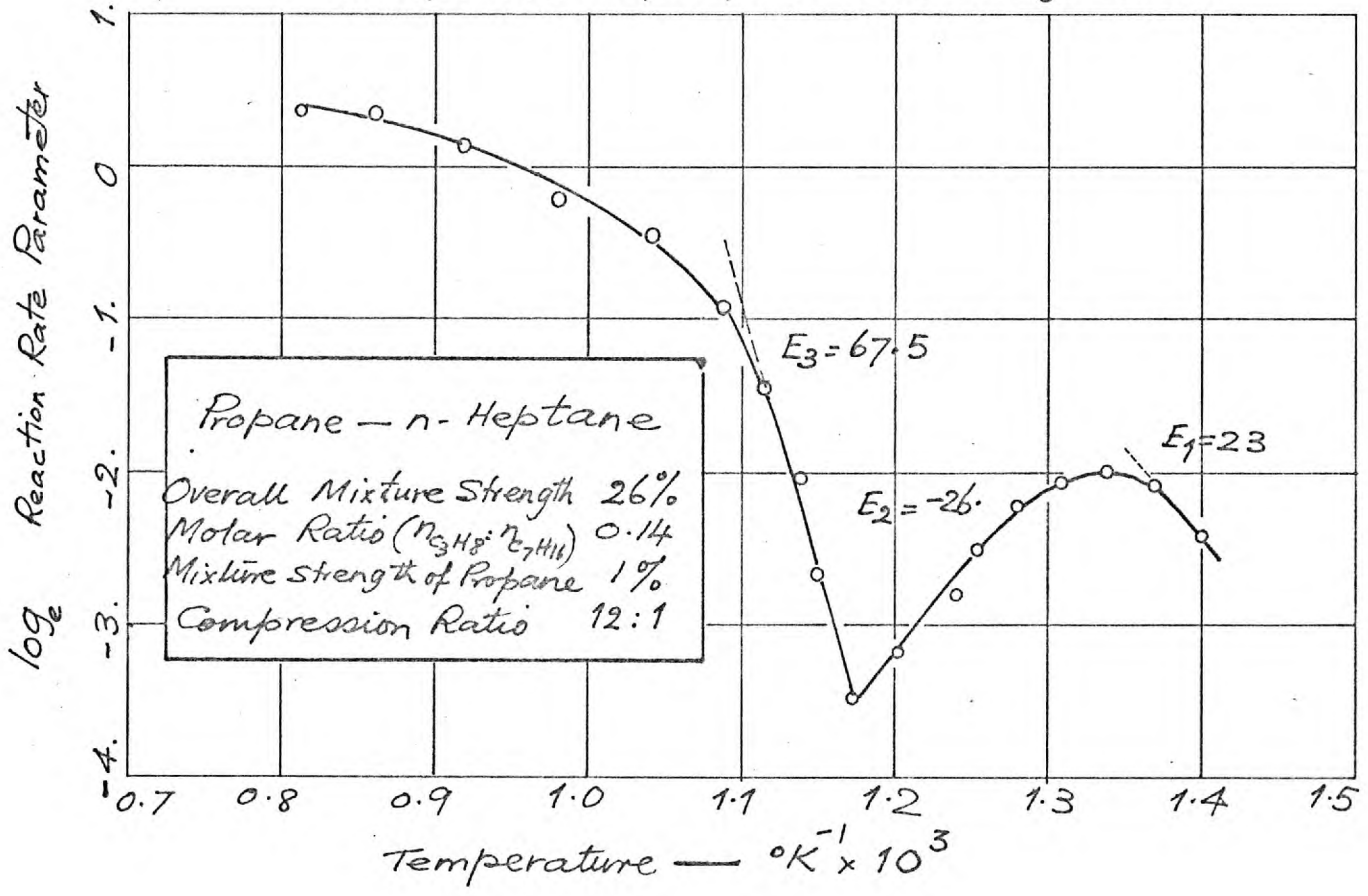


Fig. B2.23b: A normalized reaction rate versus $\frac{1}{T}$ plot of n-heptane — propane-air autoignition.



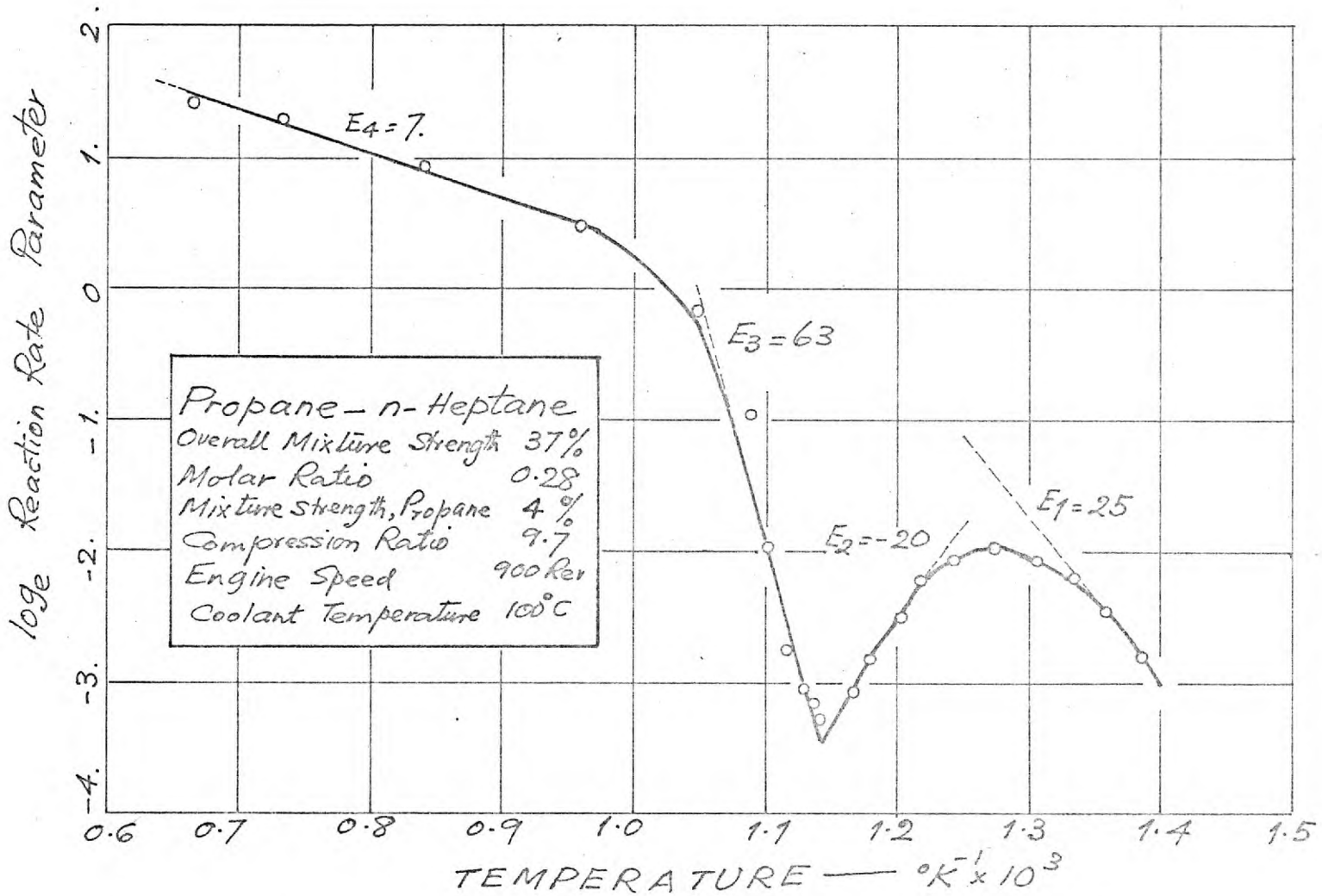


Fig. B2.24: A reaction rate versus 1/T plot of n-heptane – propane autoignition in air

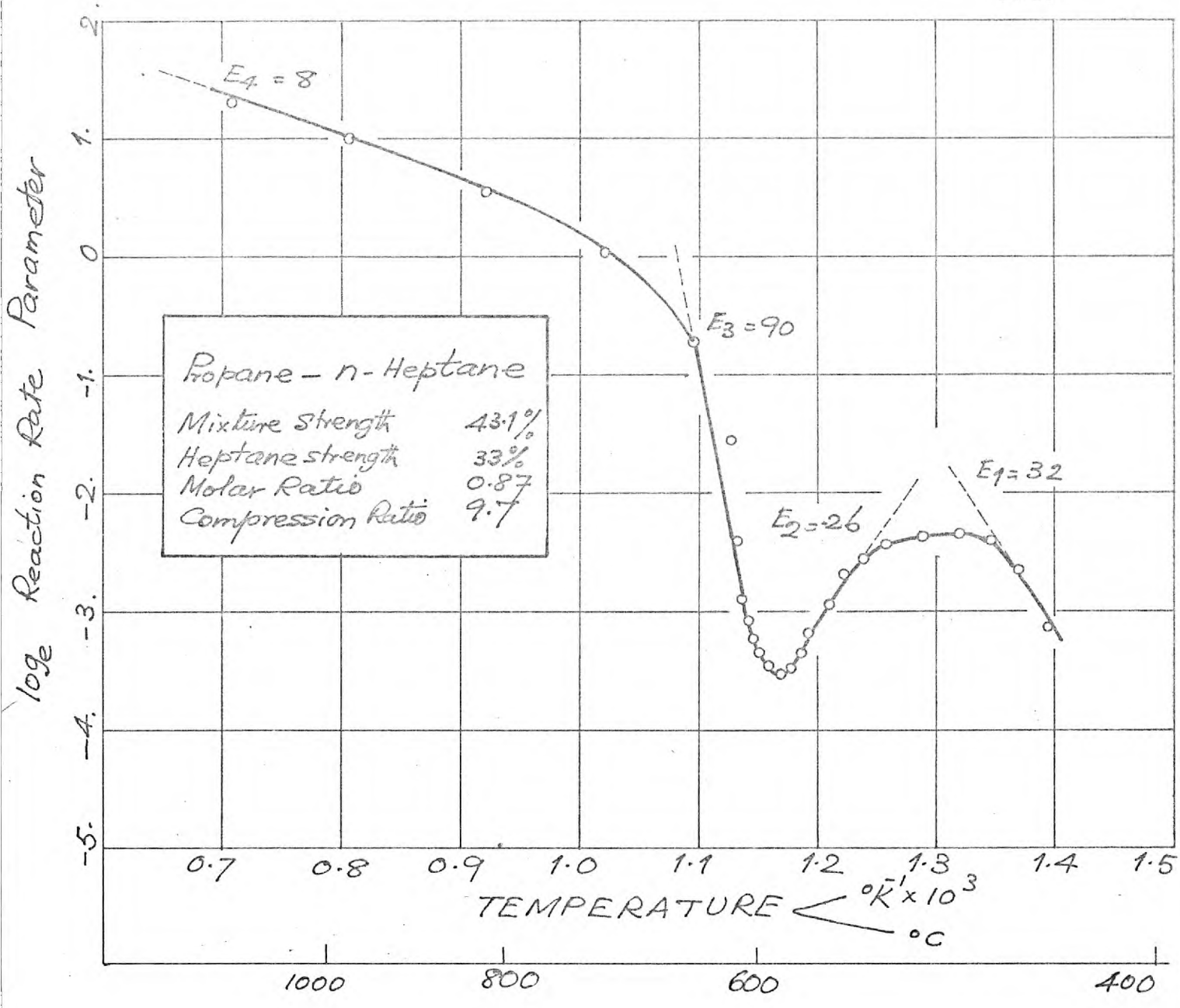


Fig. B2.25: Reaction rate versus $1/T$ plot of propane–n-heptane autoignition in air.

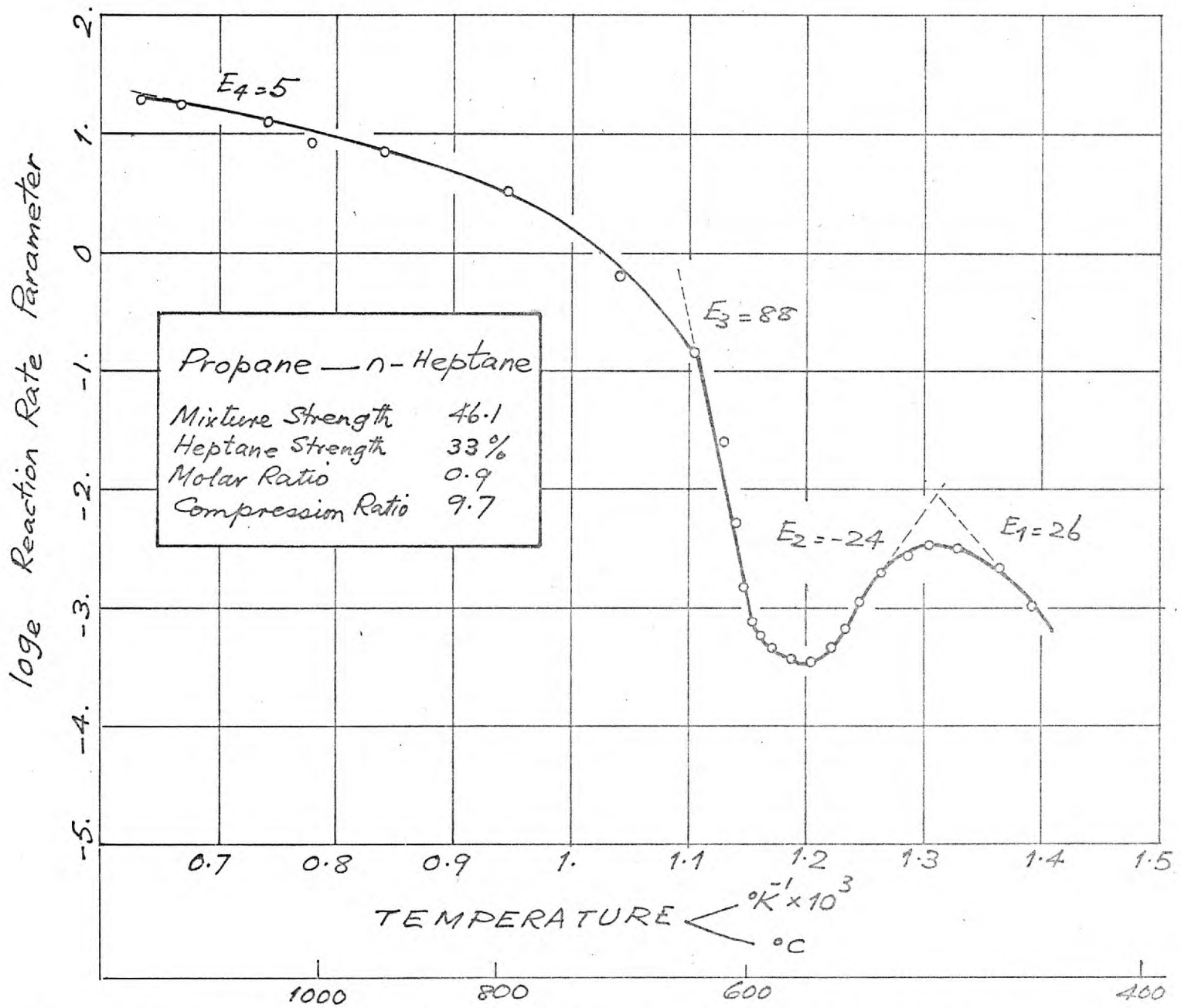


Fig. B2.26: A reaction rate versus inverse of temperature plot of propane-n-heptane autoignition in air

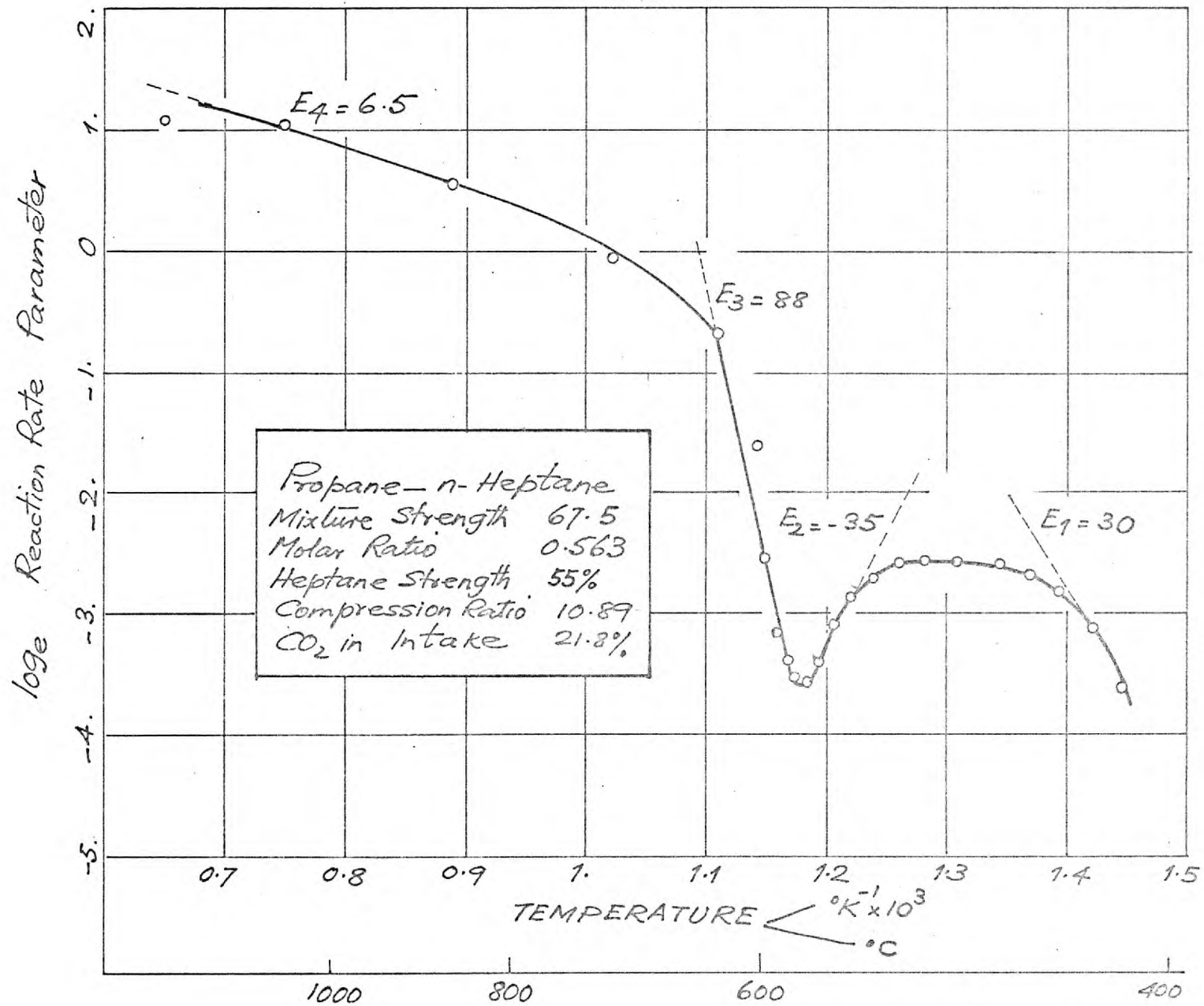


Fig. B2.27: A reaction rate versus inverse of temperature plot of n-heptane – propane – air mixture; CO_2 used as diluent.

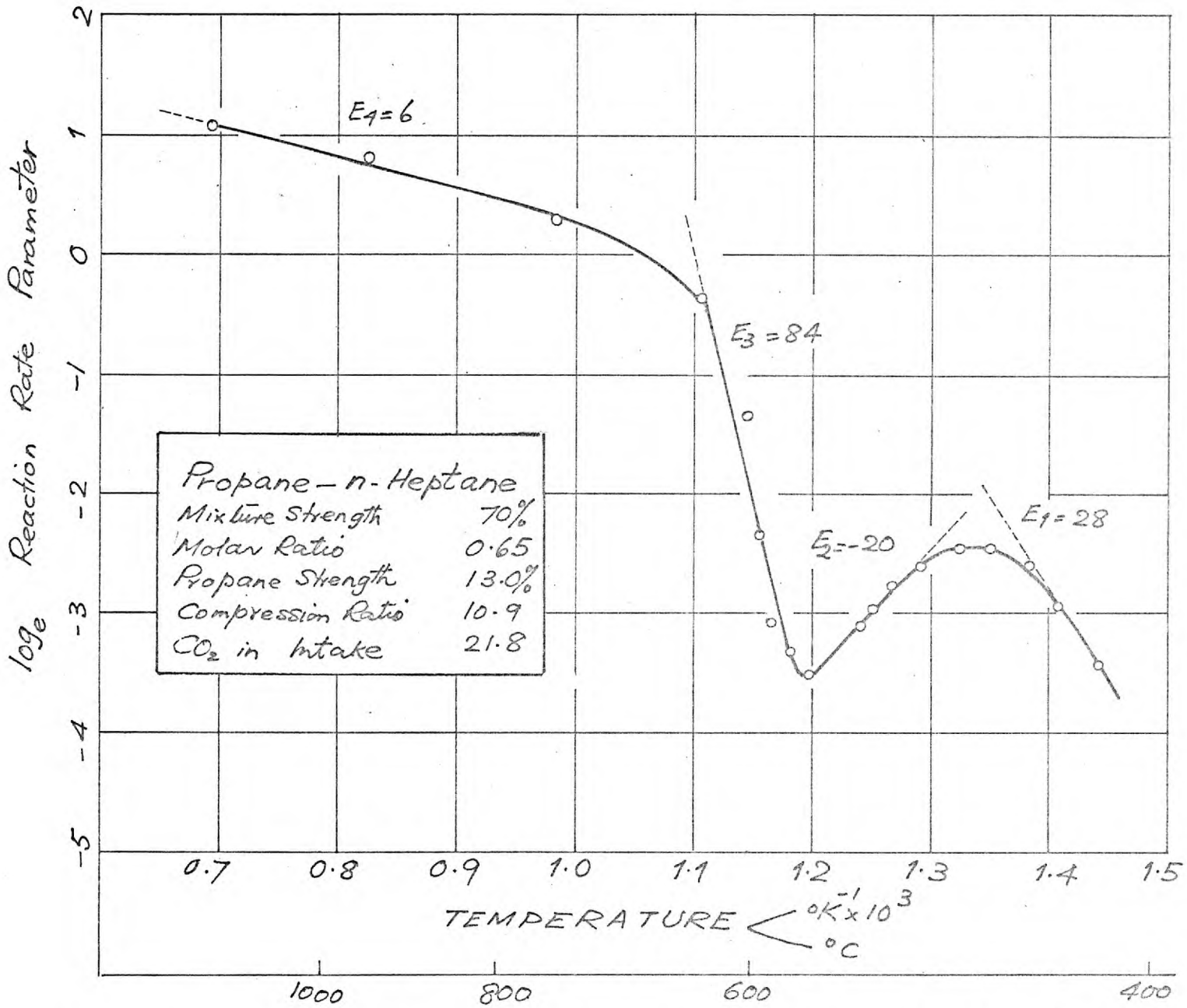
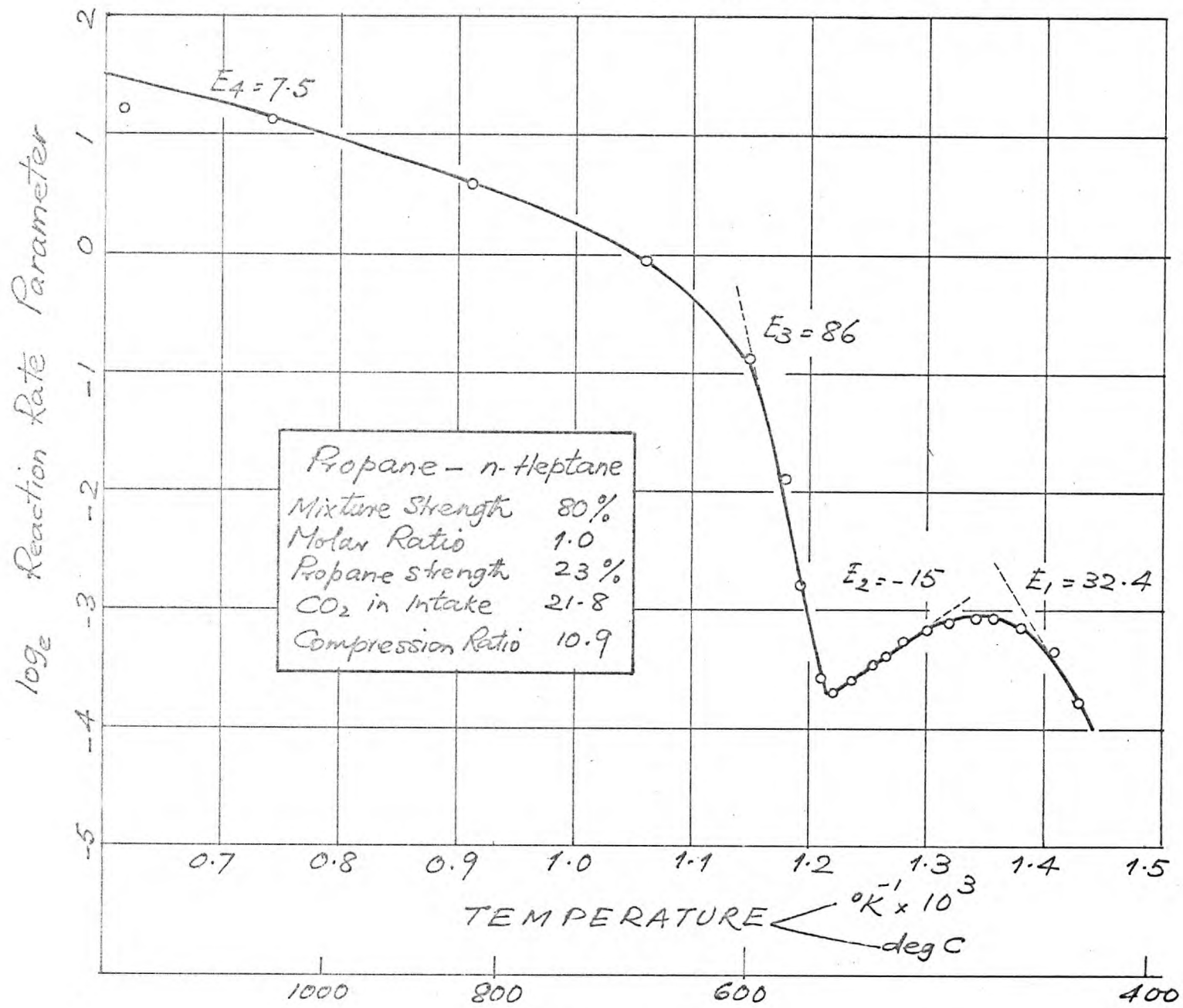


Fig. B2.28: A reaction rate versus temperature reciprocal plot of n-heptane – propane – air mixtures; CO_2 used as a diluent.

Fig. B2.29 : A reaction rate versus inverse of temperature plot of propane – n-heptane mixture; CO_2 used as a diluent.



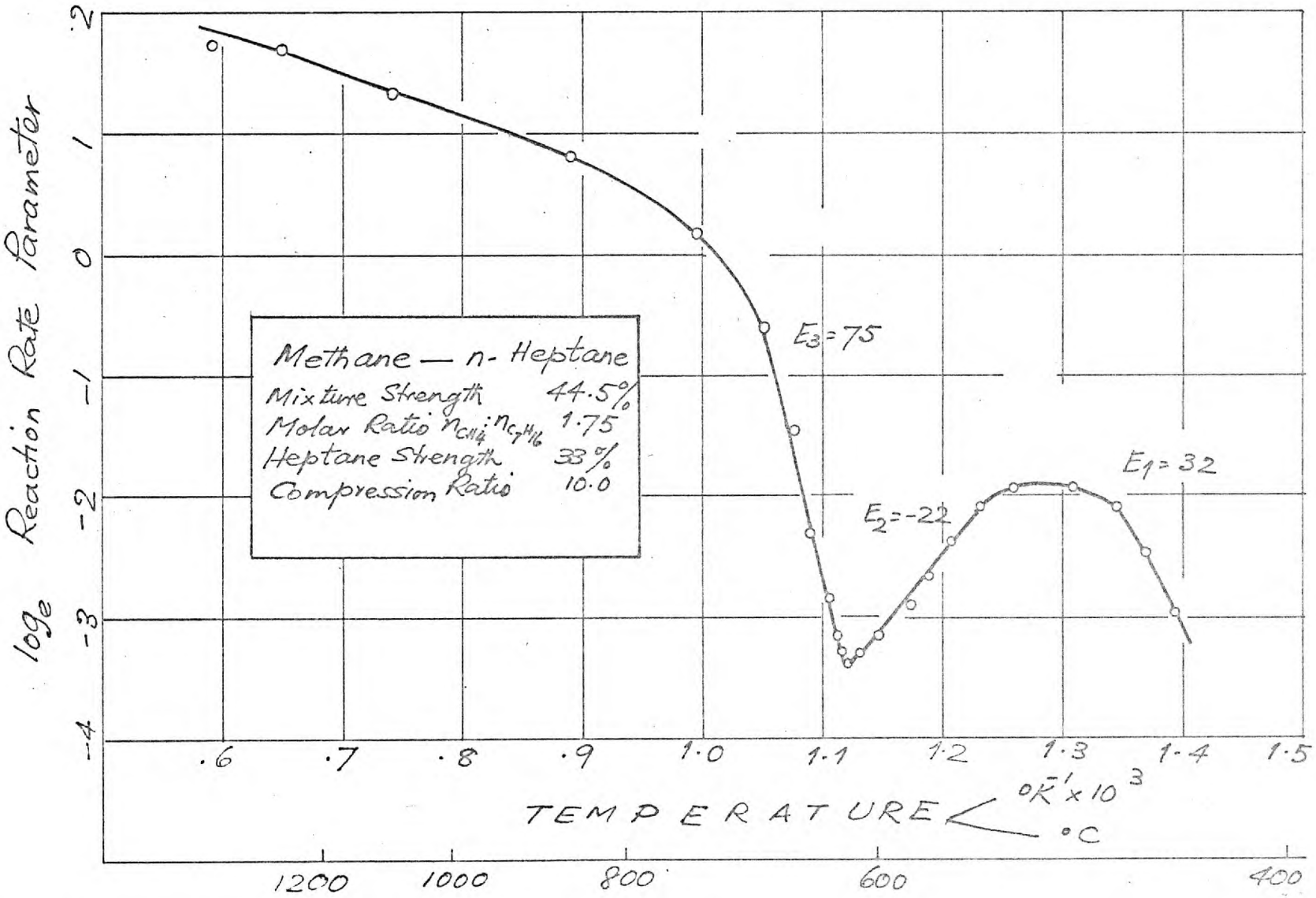


Fig. B2.30: A plot of reaction rate versus inverse of temperature of methane - n-heptane autoignition in air

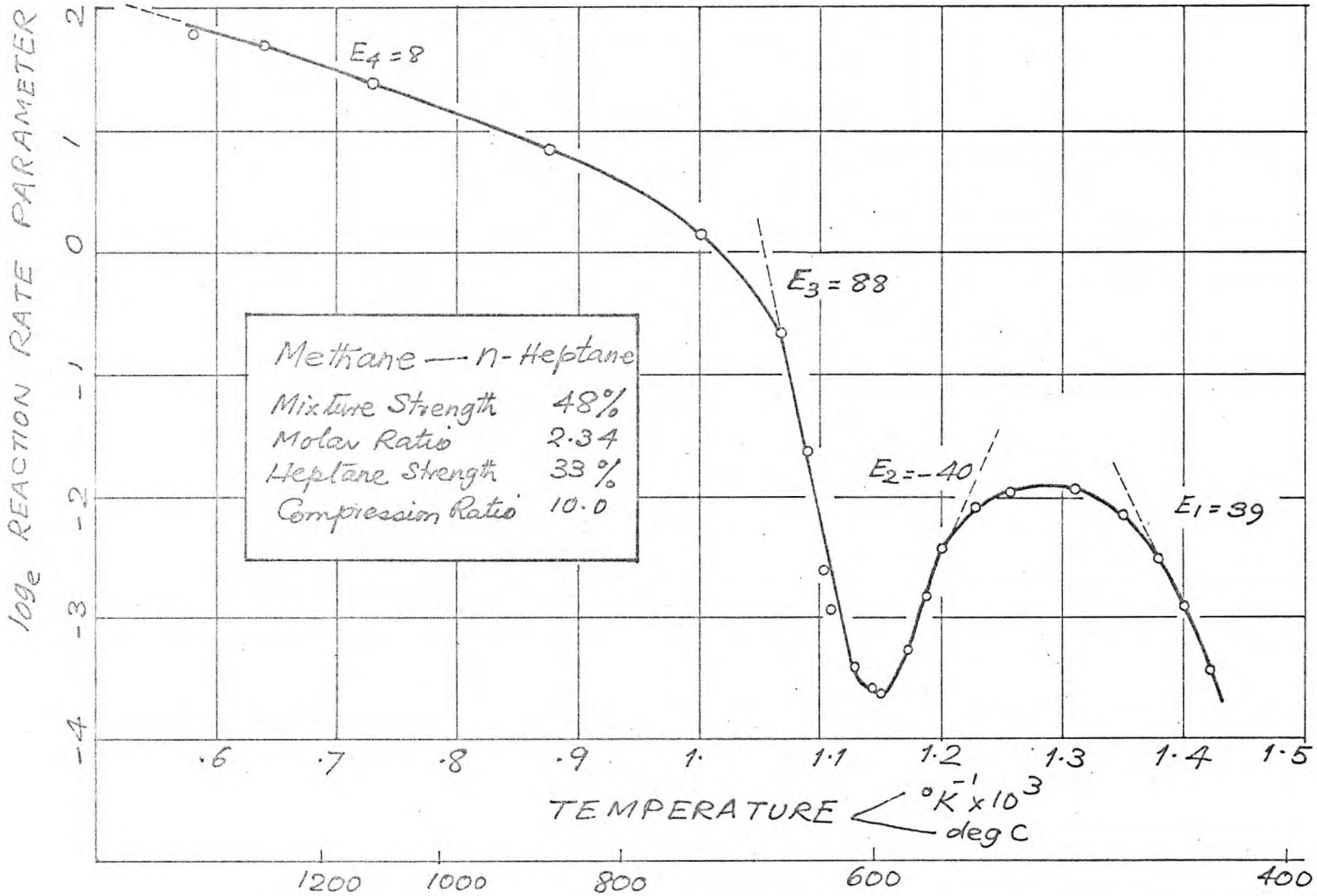


Fig. B2.31: A plot of normalized reaction rate versus inverse of temperature of methane - n-heptane autoignition in air.

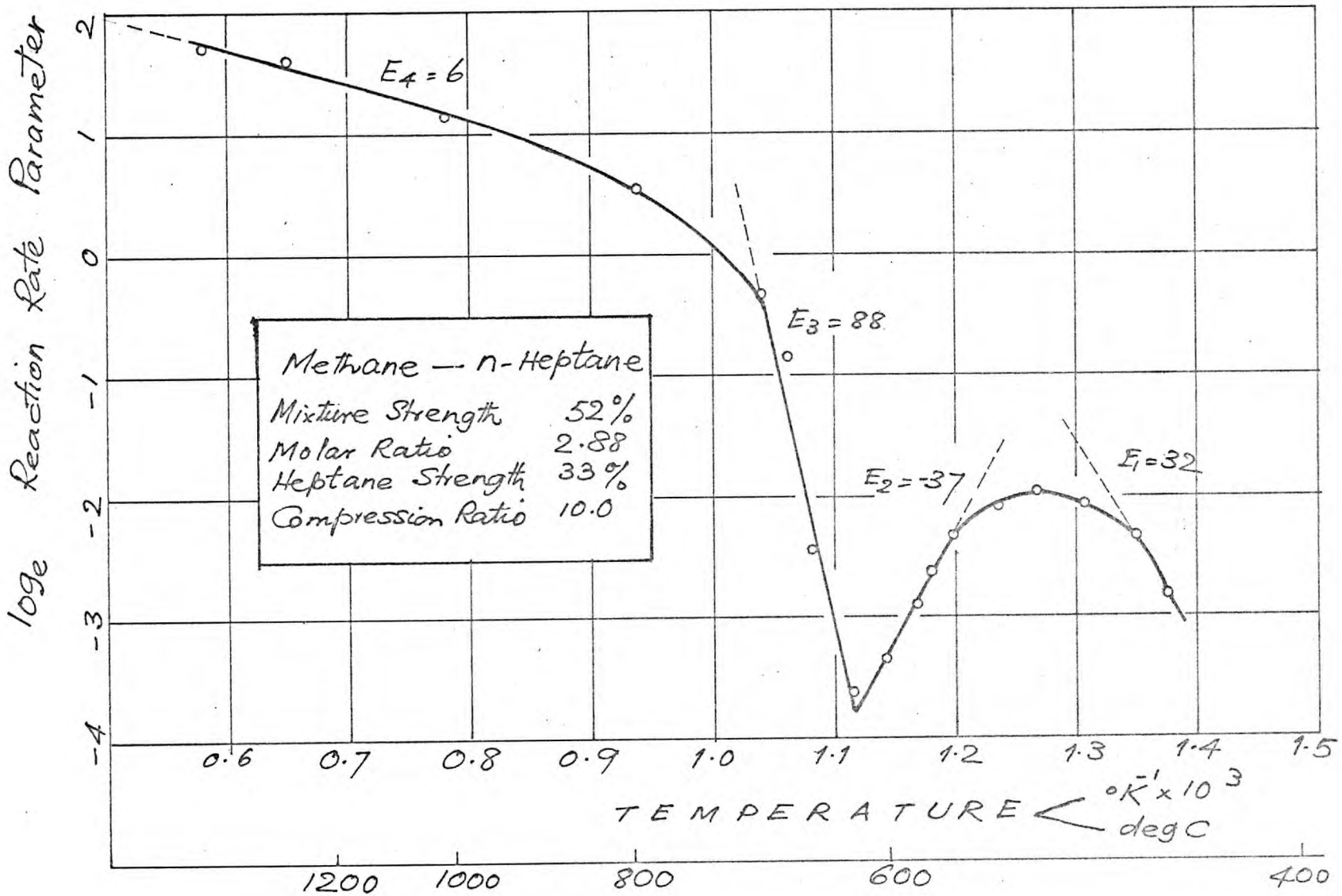


Fig. B2.32: A normalized reaction rate versus inverse of temperature plot of methane–n-heptane motored autoignition in air.

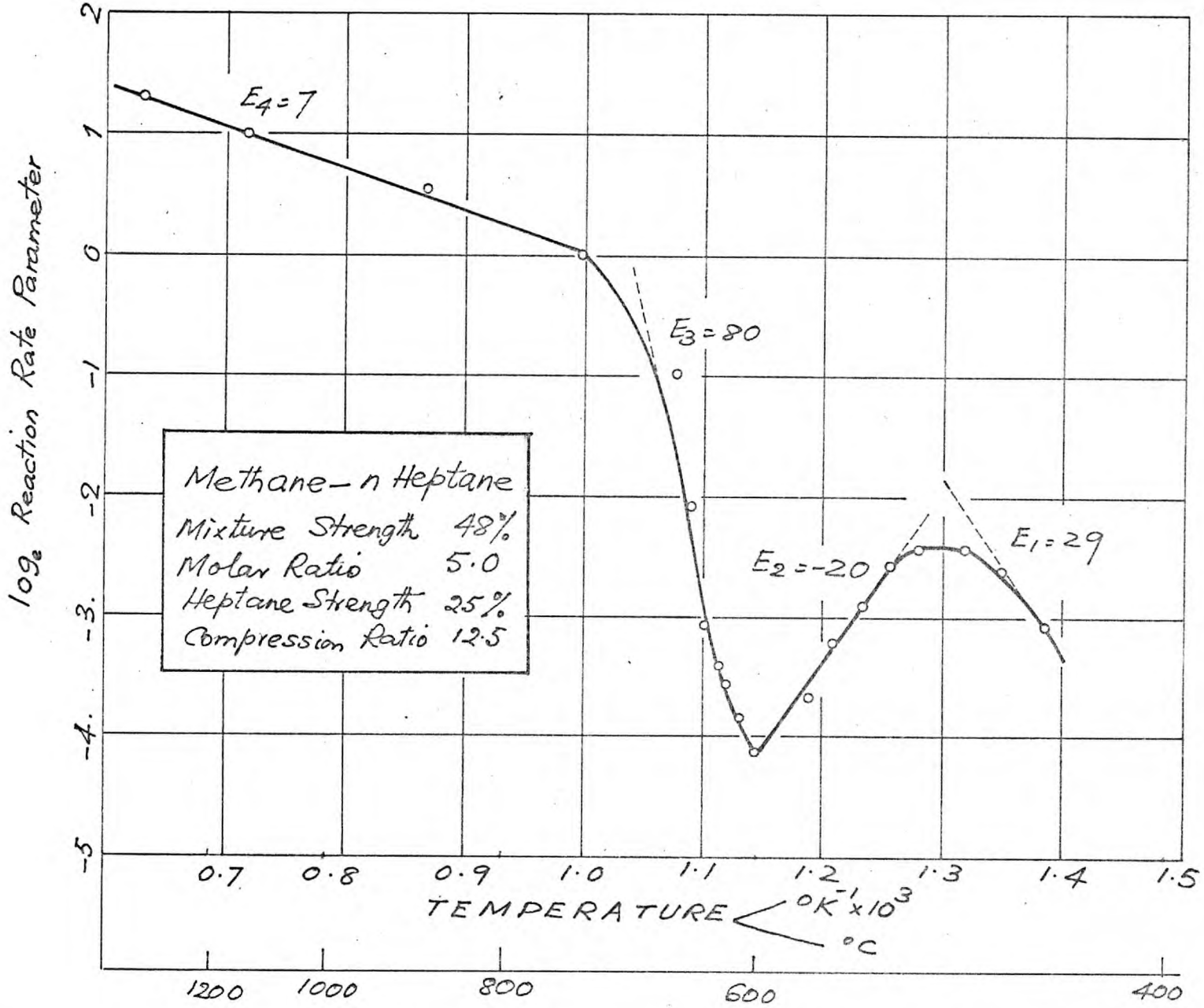


Fig. B2.33: A normalized reaction rate versus $\frac{1}{T}$ plot of methane – n-heptane autoignition.

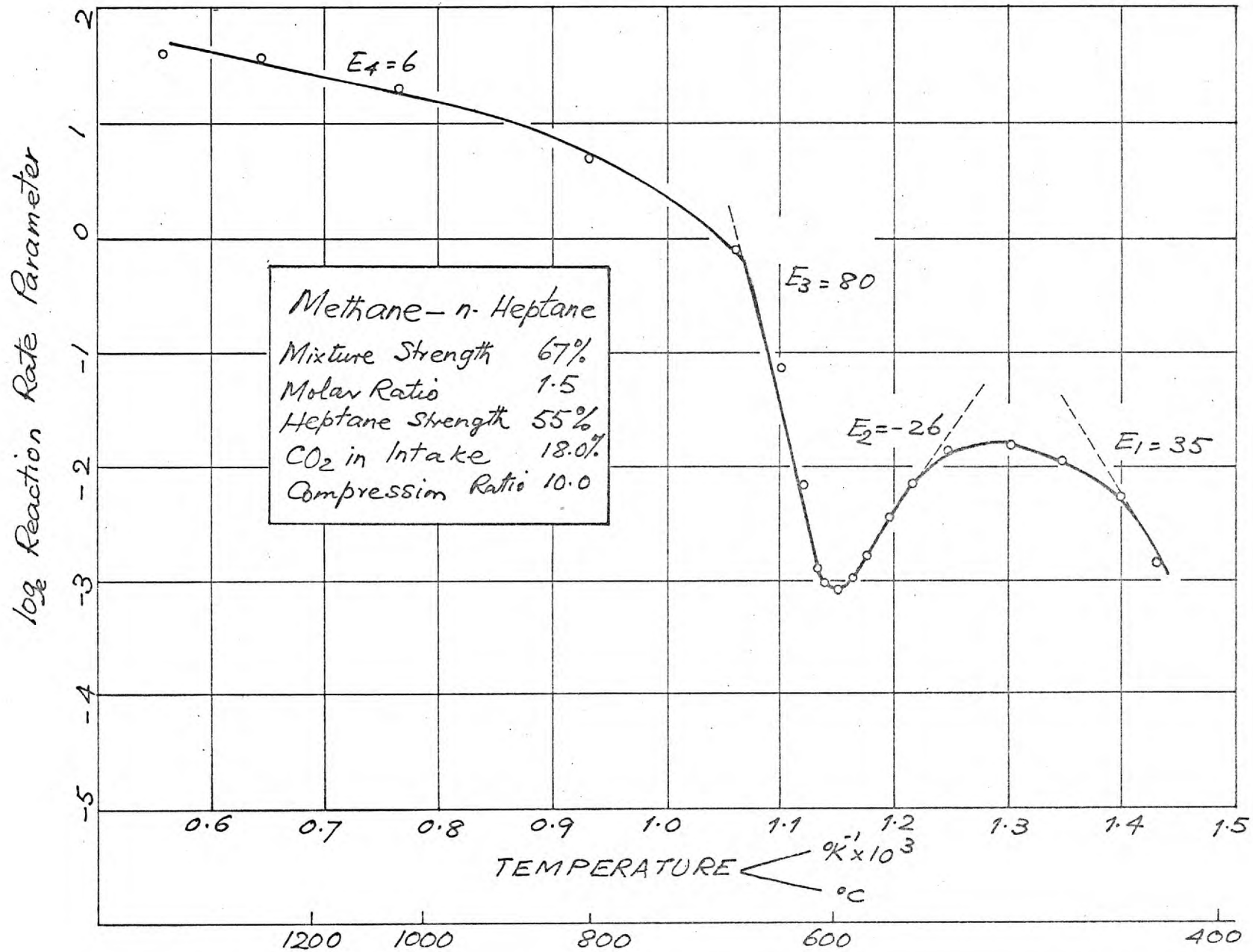


Fig. B2.34: A plot of reaction rate parameter versus reciprocal of temperature of autoignition of methane-n-heptane mixture.

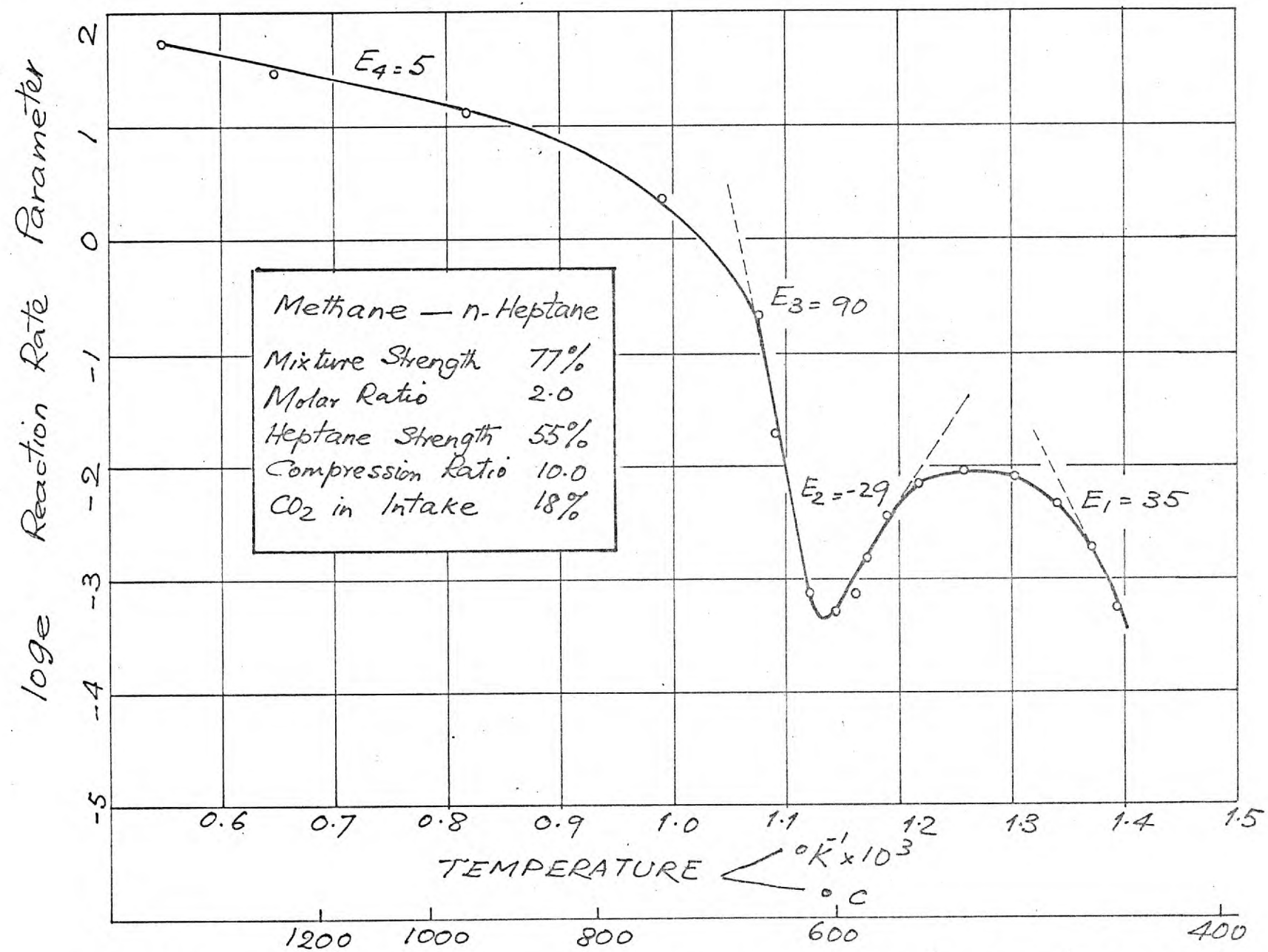
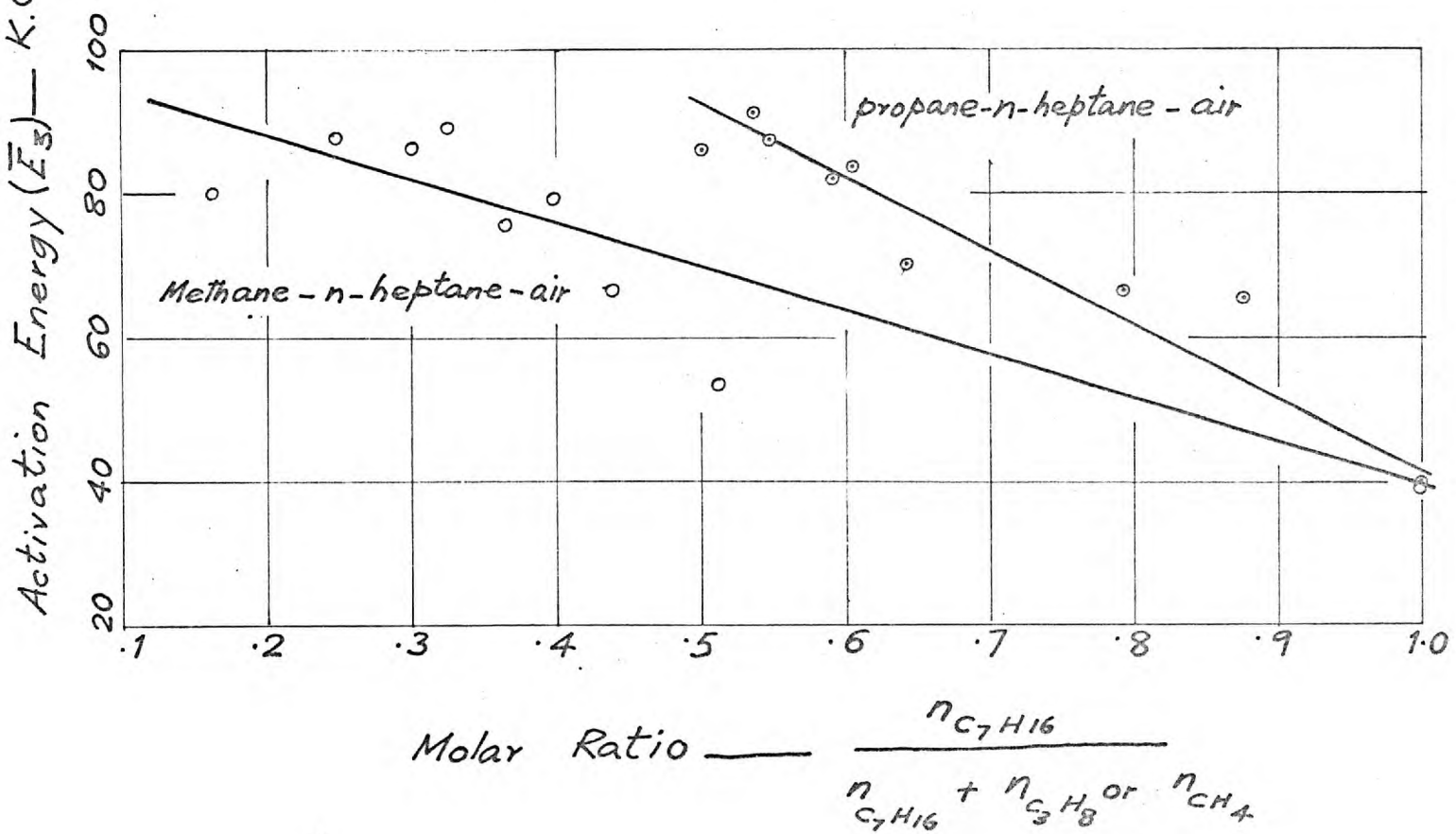


Fig. B2.35: A normalized reaction rate versus inverse of temperature plot of methane–n-heptane autoignition; CO_2 used as a diluent.

Fig. B2.36 : Variation of $\bar{E}_3$ i.e. Activation energy of the second stage due to change in propane and methane to n-heptane ratios in the mixtures.



Engine Speed = 900 R.P.M., Intake Temperature = 20°C, C.R. = 10:1 or above, Incipient autoignition, Mixture strength from lean to violent autoignition.

Table B2.1: Summary of macro-kinetic parameters of n-heptane autoignition

S. No.	Stoic. Ratio %	Compression Ratio	FIRST STAGE COMBUSTION			E_1	E_2	E_3
			ΔT degC	ΔP p.s.i.	Q Chu	KCal/mol		
1	18	14:1	165	182	.011			
2	24.5	12:1	176	138	.023			
3	27.9	10.9:1	156	111	.027	27	-20	38
4	30	10.3:1	179	113	.030	See figures No. B2.9 B2.20		
5	33	9.7:1	196	112	.035			

Table B2.2: Effect of Carbondioxide addition on kinetic parameters of heptane autoignition

S. No.	Stoic. Ratio %	CO_2 in Intake* %	FIRST STAGE COMBUSTION				E_1	E_2	E_3
			ΔT deg C	ΔP p.s.i.	Q Chu	Duration °C.A.	KCal/mol		
1	35	0	209	108	.033	11	25	-20	52
2	36	8	202	124	.031	13	26.8	-20	50
3	37	10	217	130	.032	14	28	-20	46
4	38.5	12.5	223	146	.032	14	28	-20	44
5	40	15	206	137	.032	15	28	-20	41

Compression Ratio = 10.89

* on mass basis

FUEL	Stoic. Ratio %	CO_2 in Intake %	Propane or Methane to n-heptane Molar Ratio	Comp. Ratio	FIRST STAGE COMBUSTION					$\theta_D - \theta_B$	OVERALL ACTIVATION ENERGY K Cal/mol.		
					PRESSURE RISE	TEMP. RISE	$\dot{q}_{max}$	Cumulative ht. Release	DURATION				
					Δp – p.s.i.	ΔT – deg C	C.h.u/°C.A.	Q – Chu	$\Delta\theta$ – °C.A.	°C.A.	E_1	E_2	E_3
n-heptane	25	–	0	12·1	138	176	·0036	·0235	10	18	27	-20	38
* Blend-I	40	–	1·5	12·1	88	100	·0015	·0100	11	28	23	-26	67
** Blend-II	40	–	3·2	12·5	122	164	·0035	·0220	12	23	33	-20	60
n-heptane	33	–	0	10	112	196	·0043	·036	14	17	27	-20	38
Blend I	44	–	0·69	9·7	113	178	·0035	·0276	18	21	32	-26	80
Blend II	44	–	1·75	10	110	187	·004	·036	15	18	32	-22	75
n-heptane	55	18	0	10	95	184	·00635	·045	10	14	29	-20	48
Blend I	80	21·8	1·0	10·9	92	141	·00225	·029	19	21	30	-20	70
Blend II	80	18	2·34	10	109	203	·0055	·044	15	16	30	-26	90
n-heptane	93	43·5	0	14·5	127	172	·00598	·030	9	11	30	-15	46
Blend I	115	40·0	0·41	12·1	75	132	·0035	·027	13	15	30	-10	47
Blend II	115	43·5	1·35	14·5	100	139	·0051	·026	12	13	30	-20	53

* Blend I is propane–n-heptane–air mixtures.

** Blend II is methane–n-heptane–air mixtures.

Table B2·3: A summary of macrokinetic parameters of the autoignition of n-heptane–, n-heptane–propane–, n-heptane–methane–air mixtures.

C H A P T E R B3

DISCUSSION AND CONCLUSIONS

In accordance with the presentation of results appearing in the preceding chapter, we shall first examine the combustion heat release of the autoignition reactions of individual fuels and their mixtures. The analysis of overall combustion kinetics of these mixtures will then follow.

B3.1 Discussion on Heat Release Variation due to Autoignition

B3.1-1 Propane as a fuel

Propane is a major constituent in Liquified Petroleum Gases (L.P.G.) which are a by-product from the distillation unit of oil refineries. L.P.G. have been in extensive use in the U.S.A. as fuel for farm tractors and agricultural machinery, mobile plants, buses, taxis, and even private cars. In Europe it could not gain a place up till now, since a network of refuelling stations would have to be set up to market it in competition with motor spirit. The recent conversion of public municipal transport in Vienna from ordinary diesel to dual-fuel principle operatable on L.P.G. appears to be a break-through (8), particulary in the areas where the air pollution due to vehicle emission is to be avoided. However, if L.P.G. are to serve as competitive fuel, the performance of the devices utilising these gases should be efficient. Although the recent researches at the Ethyl Corporation of the U.S.A. could prove that L.P.G. or propane can be improved in their resistance to knock by introducing the knock-suppressors which, however, makes the fuel uneconomical for ordinary use (55) as well as hazardous. The nature of autoignition of propane is, therefore, studied to provide a better understanding of its knocking behaviour and to attempt to predict the onset

of such limits which could be of great help for the engine designers.

In view of the fact that in practice mixture strengths of the order of 55 - 65% of stoichiometric value are adopted in dual-fuel engine, autoignition of only lower region of peninsula as described by Klat (51), has been considered. It is also pointed out that under knocking conditions of engine operation, the autoigniting end-charge may well be lower than this range of mixture strength since some of the main gaseous fuel charge may take part in the compression-ignition of the pilot fuel, thus rendering it leaner than what is inducted.

An examination of gross rates of combustion heat-release due to autoignition of propane, as displayed in Figs. (A2.21 and B2.1), indicates that under the operating conditions adopted this hydrocarbon undergoes a single stage combustion; whereas, during slow oxidation under low temperature autoignition, it is reported to exhibit two stages (94). This could most probably be due to higher intake temperatures together with higher compression ratios employed to obtain incipient autoignition, both of which tend to reduce the influence of first stage combustion as shall be discussed later. The rate of pressure rise diagram displayed during propane autoignition trials also did not exhibit any multistage combustion (see Plate B1.8) as was apparant during autoignition of n-Heptane shown in the same plate. It is evident, when compared with normal dual-fuel combustion processes, that the rate of heat release in autoignition is significantly high, suggesting indirectly that abnormally high rates of pressure rise are associated with knocking combustion, mainly because the combustion heat release is contributed by the autoignition of the end-charge. The peak of heat release attained within 5^{o}C.A. $\simeq$ 1 m s is an evidence of the rapidity of autoignition reactions. The monotonic increase of rate of heat release indicates that the motored autoignition, if once set in, envelops the whole charge unlike the spark-ignition combustion where the flame develops progressively, thereby burning the charge gradually. This

is why, because of the freedom from flame initiating source, such as a spark, more stabilised conditions were obtainable under incipient autoignition as compared to spark-ignition (see Plates B1.7a - 7d) where the cyclic dispersion is sensitive to the initial development of the flame front around the spark gap and its subsequent progress to enflame the rest of the charge. It is interesting to recall that during dual-fuel engine operation under light knocking combustion, it was noticed that the cyclic dispersion was less as compared to lean-mixture conditions. However, persistant operation under such conditions tended to advance the point of ignition and, if the conditions are conducive, result into violent knock. The reduction of cyclic dispersion, otherwise imminent under lean and normal combustion in dual-fuel engines, during knocking cycle is thought to be conditioned by the influence of the auto-igniting end-charge.

It has already been shown, e.g. in Table (A4.1), that of all the other modes of combustion considered, autoignition of propane in a motored engine is of shorter duration. It was perhaps the rapidity and short-lived but high intensity autoignition phenomena that prompted some of the investigators to infer that knock is due to flame acceleration. However, with the advent of ultra high-speed photography (65, 70), improved sampling techniques (16), supported by chromotographic analyses (1, 2) and many other indirect evidences as to the effectiveness in knock suppression through gaseous charge rather than the pilot igniting charge (22), it is now believed that knock is due to the autoignition of the end-charge.

The temperature at the onset of autoignition of propane under various mixture strengths and intake temperatures is found to be of the same order-of-magnitude. It can be noticed that with comparatively lesser intake temperatures, compression ratios had to be increased, thereby bringing about, in effect, the same temperature level around T.D.C. for autoignition to take place. The ignition temperature versus mixture strength plot in Fig. B2.11 illustrates this view pertaining to autoignition of propane.

B3.1-2 n-heptane as a fuel

The autoignition behaviour of n-heptane was studied for the following reasons:

(i) it is a pure hydrocarbon which could easily be carburetted into the engine cylinder to form an effectively homogeneous mixture in the earlier part of the cycle;

(ii) the overall ignition behaviour of n-heptane can be considered to be representative of commerical diesel fuel which has a similar cetane number; and

(iii) its relatively well-known multistage ignition characteristics can provide an indirect check as to the effectiveness of the present heat release and macro-kinetic analyses of its influence in the autoignition of its blends with methane and propane.

The two-stage autoignition of n-heptane is evident from the rate of pressure (see Plate B1.8b) and also from computed gross rates of heat release, as shown in Fig. (B2.4). The variation of reaction rates as deduced from the rates of gross heat release and plotted in Fig. (B2.4) over the whole process of autoignition can be looked on as built up of two distinct stages, corresponding to the higher compression ratios (10:1 or above) employed in the present investigation. The first stage is an outcome of the 'invisible' reactions (as they remain unrecorded by the pressure pick-up and other instruments such as photo-multipliers) taking place during the early part of compression. Then, the first stage sets in and adds noticeable combustion energy to the system consequent temperature rise over and above the compression temperature change (see Fig. B2.7b). The first stage usually prevails for about 15^{o}C.A. $\simeq$ 3 m s (at 900 r.p.m.). It is normally referred to as 'cool flame' stage because it does not emit light similar to that of 'hot' flames and its thermal contribution is comparatively low. It might well be pointed out that there is a correspondence between the duration of first stage signified by the present heat-

release rates and the light emission noted by Levedahl (57), Malmberg et al. (66) and Cornelius and Caplan (15). The variation of rate of pressure rise and rate of heat release is, therefore, somewhat analogous to light emission intensity recorded by the above workers. The first stage attains the peak in less than half the total duration, while it recedes thereafter in spite of the increase in pressure and temperature brought about partly by the piston movement and partly by the earlier part of the first stage heating itself. There exists a negative temperature coefficient which is connected with reduced concentration of active intermediate substances. Finally, the second stage follows and this is characterised by significant liberation of combustion energy and also, as will be shown later, to have higher positive activation energy. The duration between the two peaks of heat release, as shown by B and D, is of kinetic significance. Summarised in Table (B2.3) is $(\theta_D - \theta_B)$, i.e. the duration lapsed between the second stage attains its peak following that of the first. It can be seen that the addition of gaseous fuels lengthens this duration.

The start of staged ignition in the present analysis is reckoned to be when

$$\frac{d^2q}{d\theta^2} > 0,$$

as shown by points A and C in Fig. (B2.4), while the peak rates of heat release are easily discernible. These computed parameters can be taken to characterise the combustion stages through the corresponding pressure rise (Δp), temperature rise (ΔT), cumulative heat release (Q) and peak values of rates of heat release. It is rather meaningless to refer to ignition lags in terms of degrees crank angle with reference to T.D.C., as these will be conditioned by the point of the cycle at which ignition begins and the compression ratio being employed. However, it is to be noted that the duration of significant rate of heat release due to first or second stage combustion can also be considered as a characterising parameter. Likewise, a relative term $\Delta\tau$, as being the difference of the

ignition lags of the two stages, can effectively be interpreted as the duration of first stage. In this investigation, high compression ratios were repeatedly employed to minimise the role of residuals and to reduce cyclic dispersion.

Figs. (B2.5 and B2.5a) typically show the relative significance of the two stages of combustion under incipient autoignition as the mixture strength of inducted n-heptane is increased gradually. It can be seen that the heat release during the first stage increases with an increase in mixture strength, although compression ratios had to be varied to suit incipient autoignition. Similarly, the heat released during the second stage is dependent on the overall mixture strength and the heat released during first stage. Other important parameters have been tabulated in Table (B2.1).

The reasons for adopting carbon dioxide have already been described in the preceding chapters. As can be seen, the increase of CO_2 in the intake delayed the first stage and subsequently the second stage. The rates of heat release in both the stages are reduced. The reduction in the temperature as a result of carbon dioxide addition would contribute significantly to the delay of the first stage because of the strong dependence of the latter on temperature. Figs.(B2.7a - 7c) depict the effect of compression ratio on the extent of first stage combustion. As reported by other workers (Yantovski, Voinov), it can be seen that the increase in compression ratio was accompanied by a decrease in the combustion heat release with a consequent reduction in Δp, ΔT and the duration of first stage. For almost all the mixture strengths employed (ϕ = 0.3, 0.5, 0.8, 1.0), the two-stage autoignition retained its characteristics. Under richer mixture conditions the second stage ensued earlier, thus reducing τ_2. The rates of heat were released in proportion to the increase in mixture strength and remained correspondingly higher during the intermediate period between the first and second stage.

B3.1-3 Propane - n-heptane mixtures as a fuel

Figs. (B2.8) to (B2.10) are typical records for the detailed analysis of the effects of propane addition to a fixed quantity of n-heptane induced per unit time. Fig. (B2.9a), the re-plotted first stage of Fig. (B2.9), shows that the addition of propane exercises some inhibiting influence on the observed first stage combustion; while propane appears to take part readily in the second stage. This addition, as shown in Fig. (B2.10b) brings down the temperature level and may well exercise kinetic influence on the primary chain propagating steps (2). This is evidenced when the diluting effect of CO_2 on the first stage is compared with that exercised by propane addition. Propane appears to suppress and delay the first stage reaction more than CO_2 under comparable temperature level. A striking similarity is noticeable between the auto-ignition behaviour of these n-heptane-propane mixtures and the combustion processes in dual-fuel engines wherein the ignition of pilot diesel fuel encounters an inordinate delay during the initial stage of combustion in the presence of gaseous fuel. It is noted that under conditions when the first stage combustion is suppressed significantly (see Fig. (B2.9), cycle 6), sporadic auto-ignition ensues. This indicates that under such conditions, the thermochemical effect of propane is excessive, thereby rendering the second stage delay too long before the reaction is slowed down by piston travel. It, in turn, demonstrates the dependence of the burning of the gaseous fuel on the staged combustion even when the system is essentially homogeneous.

Fig. (B2.11) records the ignition temperature versus mixture strength of the n-heptane-propane blends. It is to be noted that for all the cases of incipient autoignition considered, the tendency to autoignite in a narrow band was exhibited rendering the two-stage auto-ignition boundaries clearly definable. The corresponding ignition temperatures of various mixtures of propane, when autoignited on its own with air in the same engine, are shown in the same figure. It is significant to note that

the first stage combustion of the admixture of propane and n-heptane appears to bring about almost identical conditions responsible for the autoignition of the former.

B3.1-4 Methane-n-heptane mixtures as a fuel

Methane was blended on the same lines as described above, with n-heptane over a wide range of mixture strengths to obtain incipient autoignition. The resulting behaviour of methane could then be studied and compared, in general, with that of propane. Figs. (B2.12 to B2.14) represent typical heat-release analyses of a range of mixture strengths involving concentrations of methane and heptane at a constant compression ratio. It is apparent that methane, similar to propane, exercises inhibitive influence on the first stage combustion. The superior knock resistance characteristics of methane over propane are readily noticeable. Higher methane concentrations in the blend with n-heptane could easily be handled at higher compression ratios without reaching violent autoignition boundaries.

A comparative study of the autoignition of methane and propane blends with n-heptane shows that with methane blends higher rates of combustion heat are released during both the stages under similar conditions. With methane blends we encounter higher Δp, ΔT, and Q during the first stage. The present investigation with gaseous fuels indicated that relatively higher pressure rise during the first stage combustion of the methane-n-heptane binary mixtures, compared to that with propane-n-heptane, resulted in a shorter ignition delay for the second stage. This is in keeping with the observation that in the multistage combustion of liquid hydrocarbon fuels the ignition lag of the second stage is in an inverse relation with the observed pressure rise during the preceding stage (23), indicating that it is mainly a temperature effect. This behaviour of methane and propane in binary mixtures with n-heptane is akin to the trends found in dual-fuel engines where the overall ignition delay with methane is lower than that for propane(51).

Table (B2.3) summarises some of the main parameters of the first stage combustion. The comparative higher rates of heat release, higher Δp and ΔT and shorter duration of the first stage are noticeable with methane blends. It is also apparent that the addition of either propane or methane invariably decreases the maximum rate of heat release and cumulative heat release during the first stage.

The first stage combustion was not delayed significantly with increased methane concentrations in the charge and is probably mainly because the addition of methane entails a smaller temperature reduction at around T.D.C., as compared to propane. The ignition lag for the first stage (τ_1) being dependent on temperature, therefore remains comparatively less affected. Plots of the ignition boundaries of methane-n-heptane blends appear in Fig. (B2.16). It is evident that the autoignition of methane as influenced by n-heptane in the admixture, is strikingly similar to that of propane, shown in Fig. (B2.11).

B3.2 Discussion on Overall Combustion Kinetics

While introducing the method of derivation of overall chemical kinetic data, it was noted that our knowledge as to the details of chemical reactions involving the oxidation of a hydrocarbon, is very scanty. In most situations we are aware of the resultant behaviour of the system, even though we are totally unaware of the intermediate paths traced by the system to reach that level of completeness. Chemical kinetics signify the rates of combustion processes which are of a chemical nature. In engine development there are some instances, for example the MAN 'M' system of combustion, when use was made of kinetic principles for controlling the combustion rates by allowing a controlled quantity of fuel in the charge to burn. The studies of ignition lags made clear their temperature and pressure dependence. Various correlations for τ as a fn(T,p) exist in the literature which correspond to particular operating conditions and fuel properties. The main difficulty in prescribing such correlations was

the bifurcation of the physical and chemical parts of the ignition delay, which tend to overlap one another under different design and operating conditions of the engines.

The heat-release analyses clearly confirm that kinetics do play an important role in the autoignition behaviour of n-heptane, propane, methane and their blends in engines. The mode of pressure development during the first stage of combustion under comparable temperatures can vary depending on the blend used. The heat analyses, therefore, have been extended to derive overall effective chemical kinetic data for the blends over a temperature range. Only those experimental records were selected for analysis where combustion was achieved on or around the T.D.C. position. Thus, marginal autoigniting cycles, which were irregular and sporadic, were eliminated. This approach resulted in reproducible experimental records. Normally the range of compression ratios employed was limited by the increased effect of residuals at low compression ratios. The extent of heating the intake charge was such that regular autoignition was obtained. During the trials of methane, propane and n-heptane blends it was found extremely difficult to obtain the second stage combustion at T.D.C. position, as it very much depended on the extent of first stage combustion. Under these circumstances, a latitude of 5^{o}C.A. before or after T.D.C. position was provided, while the reproducibility of records was regarded an essential criterion.

The results from a series of tests involving propane-air mixtures over a range of mixture strengths, initial temperature and compression ratio were analysed following the procedure as detailed in Chapter B2. Purely for the purpose of the demonstration of the utility of this approach and for simplicity, a second-order reaction was assumed, i.e. a = b = 1 in equation (1) of Chapter B2. Fig. (B2.17) presents a superimposed record of the data derived from a range of autoigniting cycles of propane-air mixtures. It can be seen that the experimental points obtained, despite the wide variation of initial conditions employed, do lie in a well-defined narrow band. Moreover,

there seem to be two distinct temperature zones; namely, below and above 1000°K. Such a tendency is fairly well-known for many common fuels (89). The two activation energy values derived from the slopes of the two parts of the curve are 8 K-Cal/mol. for higher temperature range and 60 K-Cal/mol. for the lower temperature range. The latter value compares favourably with 64 K-Cal/mol. carefully derived by Miller (69) for propane. It is interesting to note that fitting a single straight line through experimental points can yield values for $\overline{E}$ ranging from 8 to 60 K-Cal/mol., depending on the number of experimental points and the temperature range selected. This may partly explain the wide variation of activation energy values, $\overline{E}$, reported in the literature for propane.

Fig. (B2.19) is the plot of normalised reaction rate versus 1/T on the simplified basis of a second-order reaction for the autoignition processes of n-heptane. The well-known two-stage autoignition behaviour is characterised in this figure by what appear to be four different dominant regions for different regimes of temperature. Four corresponding activation energies are thus possible. A remarkable similarity can be found between the present motored-engine test values of $E_1 = 27$, $E_2 = -20$ and $E_3 = 38$ K-Cal/mole and those obtained by Voinov (99, 100) with a rapid compression machine under comparable temperature and pressure range. Fig. (B2.20) shows superimposed records of different autoignition trials for a narrow range of lean mixture strengths displaying some slight scatter when a second-order reaction is assumed. Similar data for richer mixtures of n-heptane diluted with CO_2 indicate that the activation energies for both the stages of autoignition remain essentially the same, suggesting that they follow the same pattern over a wide range of mixture strength. However, there is evidence that the reaction rate constant (K) is somewhat influenced by the extent of CO_2 addition, indicating the limitation of the assumption that a second-order reaction can adequately represent the reaction. The values of activation energy found graphically have been summarised in Tables (B2.1) and

(B2.2). The normalised reaction rates versus inverse of absolute temperature shown in Figs. (B2.21) and (B2.22) indicate that the values $E_1 = 27$, $E_2 = -20$ and $E_3 = 38$, hold also for the wide range of mixture strength with slight changes in E_3.

An examination of Fig. (B2.23) to Fig. (B2.29) reveals that addition of propane to the autoignition of n-heptane brings about relatively less change in the values of $\overline{E}_1$ and $\overline{E}_2$, while $\overline{E}_3$ is significantly increased. Yantovski reports small variations in the values of $\overline{E}_1$ with the change of iso-octane concentration in blends with n-heptane (109). However, the studies of combustion processes beyond the negative $\overline{E}$ (i.e. E_2) were not covered by that investigator. Agreement is also found in the reduced rise of pressure during first stage as the propane was added progressively. Notable rapid increase in $\overline{E}_3$, which presents the second stage combustion, is indicative of the difficulty in autoigniting the blends with propane as a dominant fraction. Fig. (B2.36) illustrates this. A similar retardation has been noted by other workers (71). Voinov and Skorodelov (99, 100) appear to be silent about such high values of $\overline{E}_3$ obtained for the autoignition of di-isobutylene which has Research Octane No. more than 100, similar to that of propane and methane employed in the present investigation. It yet remains to be seen as to whether there exists any correlation between the composition of the blend and $\overline{E}_3$ over a wider temperature range. Realising the limitations imposed by simplifying assumptions discussed in Section B2.2 and difficulties in obtaining the slope of the experimental points reliably, it was attempted to find any significant change affected by a small variation of the reaction orders (a) and (b). It was found that the slope, and hence values of $\overline{E}$, are comparatively insensitive to such a change.

The addition of methane also brings about small changes in $\overline{E}_1$, while $\overline{E}_2$ and $\overline{E}_3$ are significantly affected. There is a tendency to increase in the negative values of $\overline{E}_2$ as methane addition is increased progressively. This indicates a different pattern of reduction in the concen-

tration of active intermediate substances which are formed by the first stage, with increase in temperature. Figs. (B2.30) to (B2.35) illustrate the variations in all the three values of $\overline{E}_1$, $\overline{E}_2$ and $\overline{E}_3$. As shown in Fig. (B2.36), the values of $\overline{E}_3$ tend to increase with increased proportion of methane in the blend. Indeed an increase in methane beyond the molar ratio

$$n_{CH_4}/n_{C_7H_{16}} \simeq 5$$

entailed either sporadic autoignition or total ignition failures. The unusually high values of $\overline{E}_3$ responsible for the second stage explain this.

B3.3 Conclusions

An examination of a large number of heat-release records of the autoignition of propane-air mixtures over a range of lean mixture strengths (stoic ratio 0.27 to 0.44) and intake temperatures of 106°, 122° and 149°C suggests that:

(1) Under the higher temperatures and pressures adopted, propane appears to undergo a single main stage of autoingition. The precombustion reactions could neither be observed through rates of pressure records nor from the computed rates of heat release. Higher rates of combustion heat release, although of shorter duartion as compared to normal combustion processes in dual-fuel engines, are associated with autoignition, explaining our earlier finding that the knocking dual-fuel engine cycles exhibit higher rates of combustion heat release (42);

(2) The temperatures at which autoignition of propane sets in over a range of mixture strength are of the same order-of-magnitude. They are around 850°K.

Analysis of rates of heat release during autoignition of n-heptane and its blends with propane and methane threw light on the mechanism of dual-fuel engine

combustion processes in general and particularly those under knocking. Present analysis explained the following with regard to dual-fuel combustion phenomena:

(1) Motored-engine technique offers an excellent method for the analysis of chemical processes in dual-fuel combustion phenomena;

(2) Whilst the analysis of autoignition behaviour of n-heptane confirmed the accuracy of the present approach in bringing out in detail hitherto rather ill-defined thermo-chemical parameters related to multi-stage reactions, it confirmed that chemical kinetics do play an important role in the combustion of a gaseous fuel in the presence of another hydrocarbon of ignition character similar to that of diesel fuel;

(3) The ignition boundaries of methane-n-heptane and propane-n-heptane blends are strikingly similar and their upper boundary belonging to the second stage ignition corresponds to the temperature level required for the autoignition of propane and methane with air. This suggests the possibility of pilot fuel vapour conditioned autoignition of the end-charge and hence the knock in dual-fuel engines;

(4) Propane and methane are invariably found to exercise inhibiting influence on the precombustion reactions by delaying their incidence in the cycle. The analysis suggests that this is brought about by way of reducing the temperature in the cycle to which the ignition lag of these reactions is sensitive.

It has been demonstrated that the relatively simple procedure of deriving chemical combustion kinetic data from heat-release analyses of autoignition reactions in a motored engine, is capable of providing reasonably acceptable values for the gross kinetic data of common fuels over a range of temperatures and pressures similar to that found in practical combustion systems.

P A R T C

C H A P T E R C1

GENERAL DISCUSSION AND CONCLUSIONS

C1.0 Introduction

After having examined the combustion processes in dual-fuel engines and the nature of these processes experimentally in a fired as well as a motored engine, we shall now discuss the possibility of presenting them in a simplified model. At first the utility of such an exercise is outlined and then the past efforts in presenting a mathematical model are critically examined; their limitations and simplifying assumptions are discussed. In the light of the evidence gathered, a qualitative model is presented.

The presentation of a model pertaining to complex combustion processes such as in dual-fuel engines, is desirable for the following reasons:

(i) it enables information to be presented in a simplified way;

(ii) it generalises most of the data even though obtained empirically;

(iii) it economises the efforts and rationalises the attempts of the designers in basing their design on some sound basis; and

(iv) it renders the empirical data correlatable whereby extra- or interpolation is possible to extend its applicability to systems of allied nature.

The requirements of a successful model to be formulated mathematically are:

(i) the underlying processes be adequately understood;

(ii) minimum number of simplifying assumptions, which otherwise limit the utility of such an exercise, be adopted; and

(iii) sufficient data should be available to testify such formulation.

C1.1 Dual-fuel Combustion Phenomena in Engines

We can, for ease of reference, divide the dual-fuel engine combustion phenomena into two categories: firstly, those associated with normal engine operation and secondly, those which are responsible for limiting performance under knocking and part-load conditions. In the following discussion an attempt is made to gather the experimental evidence of the present and other investigations in order to shed more light on the nature of their mechanisms.

C1.1-1 'Normal' combustion processes

In dual-fuel engines the initiating source of combustion is pilot fuel. Various studies on the quality and quantity of pilot fuel have found the following:

(i) the ignition quality, i.e. Cetane Number of the pilot fuel, is comparatively insignificant in effecting any improvements in the cycle efficiency. Whilst the poor ignition quality may give rise to ignition failure, its increase does neither increase the useful output nor extend the knock-limit (51).

The effect of a knock suppressor introduced with the pilot fuel has comparatively less effect than when introduced with the gaseous charge (22).

(ii) Whereas lesser quantities of pilot fuel are desirable from the standpoint of economy, the onset of knock can be averted by increasing the pilot rate. This, in effect, increases the ignition source, which was indicated in the form of an increase in heat release in the earlier stage (chapter A4). Some gaseous charge is therefore involved in the pilot burning phase because of enlargement of the ignition zone while the rest of the charge burns progressively without the formation of the end-charge.

(iii) Increase in pilot quantity brings about more stability in combustion by improving cyclic dispersion as the initiating source is too strong to

be influenced by the physical processes such as mixing and quenching.

(iv) Increase in pilot rate improves the part-load performance by increased utilisation of rather weak gaseous charge which otherwise would have survived combustion, and appeared in the exhaust.

From the foregoing, it can be seen that the pilot fuel, although it contributes to the overall combustion processes, exercises a leading role. The inherent cyclic dispersion in dual-fuel engines, which lies in between that for diesel and gas engines (54), may well be attributed to the heterogenity of the initial combustion of pilot fuel. In large-bore engines the pilot fuel is still more important. For, in such cases, it is not only imperative that the initiating source should be capable of enflaming most of the charge, rendering the end less liable to ignite on its own, but the utilisation of lean mixtures requires effective mixing processes without combustion instability.

It is perhaps pertinent to trace the history of events in the dual-fuel engine cylinder. The pilot fuel injected through conventional means disintegrates primarily due to atomisation by the injector. Further disintegration takes place due to turbulence. The leading tip of the pilot spray encounters relatively hotter environment brought about by compression of air and premixed gaseous fuel. Unlike diesel engine, since the pilot fuel is relatively small, effective vapourisation therefore can be expected. Thus, with similar compression ratios and design of the combustion chamber for diesel and dual-fuel system, the physical processes of pilot fuel disintegration proceed more towards completion in the case of the dual-fuel engine. However, in this case, the pilot fuel vapour encounters premixed gaseous fuel and air. Ignition is delayed because the presence of the gaseous fuel in both quality and quantity exercises influence on the ignition processes. It has been shown in Chapter B2 that pre-combustion reactions, together with the main combustion, are delayed because of chemical inhibition of the gaseous

fuel. In this respect, the observations of this investigation are in agreement with those of Moore and Lewis (72) and Klat (51). The centre of ignition should essentially be in the vapour zone as near to the droplet surface the temperature is that of its boiling point and the atmosphere is depleted of oxygen in comparison to the case when air alone was present. The reactions leading to ignition can therefore be expected to take place in the vapour phase. The extent of homogenity of liquid fuel vapour and the gaseous fuels depends on how the gaseous fuel is introduced. In the event of no substantial chemical reaction, the vapour tends to assume main charge temperature. Ignition will ensue in the regions where during the process of vapour mixing with the fuel, the reaction rate is greatest. Kinetically, the process of ignition will be governed by the relative concentration of the pilot fuel vapour and gaseous fuel, the temperature attained and the concentration of oxygen in that region. If any of these participants do not exist in that region, ignition may not ensue. It will be recalled that sporadic combustion was observed when, under dual-fuel trials, the pilot fuel was reduced gradually in an attempt to establish the minimum possible pilot fuelling rate. In the course of auto-ignition trials, it was observed that dominance of gaseous fuel also gives rise to sporadic combustion leading to ignition failure.

In this investigation it has already been shown that noticeable precombustion reactions are associated with the autoignition of the fuels. Thus, for the compression ignition to be established, it is desirable to provide suitable environment for the precombustion reactions to develop. Under conditions of lean mixture for ignition to take place and leading to subsequent combustion processes, it is necessary that the pilot injection timings be advanced so as to increase the residence time and hence the activity of partial oxidation reactions preceding main combustion phase.

Other proposed suggestions for improving the part-load performance of dual-fuel engines (72, 74, 75) are

either to increase the pilot rate or to preheat the intake charge. Whereas the increase in pilot quantity extends the initial combustion zone as was manifested by the increase in heat release rates, the charge preheat gives rise to higher compression temperatures, thus encouraging the precombustion reactions, whereby consuming most of the gaseous fuel which would otherwise escape unreacted.

C1.1-2 'Knocking' combustion processes

In Chapter B3 the mechanism of 'knock' has been discussed at length. In dual-fuel engines knock is encountered with relatively rich mixtures (70% of chemically correct mixtures or above). Knock could be observed due to its audibility, sharpness in pressure rise and, under severe conditions, high frequency pressure oscillations during expansion stroke. The heat release diagram of knocking (see Fig. A2.15) shows marked changes. It is now believed, and the experimental evidence gathered so far supports this, that knock is due to the autoignition of the charge located away from the initial combustion zone. This inflammable charge is usually referred to as 'end-charge' because of its remoteness from the ignition source. In dual-fuel engines the end-charge mainly consists of the gaseous fuel. In small bore engines it may well contain traces of pilot fuel vapour, as the pilot fuel spray can reach the end-zones. The quantity and quality of the gaseous fuel is the determining factor for the onset of knock. If the gaseous fuel is resistant to autoignition then the combustion initiating from the pilot fuel develops progressively and enflames the charge. However, if the end-charge is easily autoignitable, it will ignite before the arrival of the proper flame front from the initiating source. Under such cases, excessive rates of heat release in rapid succession have been found in the present investigation. The autoignition studies have demonstrated that excessive rates of heat release are associated with this mode of combustion.

That the origin of knock is the autoignition of the end-charge is supported by the insignificant part

played by the pilot fuel unless it is increased beyond economic limits. The knock suppressors introduced through pilot are not so effective as compared to when they are blended with gaseous charge. The results of the present investigation have borne out that particularly in the event of the presence of heavier hydrocarbon vapour, the auto-ignition of propane and methane does take place under comparable operating engine conditions, suggesting that autoignition reactions are conditioned by the pre-combustion processes.

The injection timings of the pilot fuel affects the residence time, hence influencing the preignition activities in general. Advancing injection under rich mixture conditions should be inducive to knock. Turbulence in the mixture depends on the design of the engine and its running speed. Whereas with increased turbulence effective mixing is desirably effected in part-load performance, it has little effect in avoiding knock if once it sets in (43).

Intake temperature has a decisive influence on knocking performance. Increased intake temperature may well be the outcome of supercharging with ineffective inter-cooling, unusually temperate atmosphere, such as in tropical countries, and mixing of exhaust gases with the intake charge during scavenging. It has been fairly well established (47, 51) that the logarithmic knock limited output varies linearly with the inverse of intake temper-ature for most of the common gaseous fuels.

C1.2 Consideration of a Simplified Model

Before embarking on a study of the possibility of constructing a qualitative model on the basis of the understanding developed through trials on dual-fuel and motored engines, it is considered relevant to examine past attempts; their underlying assumptions and limitations.

The importance of ignition delay has long been recognised. For it exercises a controlling role in the development of combustion processes. Most of the analytical approaches (35, 51, 61), broadly speaking,

attempted to characterise the events occurring during the ignition delay as being precursor to knock. For example, Livengood and Wu (35), in an attempt to correlate the ignition delay data, obtained from rapid compression machines with engine knock, assumed an equivalent aggregate reaction to have the same end result as that under knocking. They developed a concept of a critical value for the concentration of active chain carriers which in turn provided the limits of integration of the reaction rates. The functional relation between the reaction products and the critical concentration of active species, when approached to same order of magnitude, autoignition hence knock was considered to set it. They demonstrated a correlation with experimental results for the case reported. There is, however, no mention of the extent of agreement to be expected with the approximate computed data.

Karim's analytical approach (35) to knocking in dual-fuel engines is based on the application of elementary chemical kinetics. Setting out with an overall bi-molecular global model of second order, he argues that for a fixed quantity of pilot fuel, timing of injection and engine speed, the rate of temperature rise after pilot burning (dT/dt) remains constant. The limiting condition of knock is shown to be when

$$W_f \, e^{\frac{-E}{RTig}} \simeq \text{Const} \quad ,$$

where W_f is the amount of fuel induced per unit time, E is the effective overall activation energy, R is the universal gas constant and Tig is the ignition temperature. It is implied that the effective compression ratio, the density of the mixture (constant volume combustion) and the mixture properties during compression are unchanged.

Arguing that the power developed is proportional to release of combustion energy which in turn is dependent on the amount of fuel inducted, it is shown that:

$$(HP)_{knock} \propto Q$$

$$(HP)_{knock} \propto W_f$$

$$\log(BMEP)_{knock} = \text{const} + \frac{E}{R\ Tig}$$

$$\log(\text{BMEP})_{\text{knock}} = \overline{A} + \frac{\overline{B}}{T_o}$$

where $\overline{A}$ and $\overline{B}$ are constants depending on the engine operating conditions and fuel used. Klat (51) and Rogers (47) ascribed experimentally the values of $\overline{A}$ and $\overline{B}$ by observing the brake mean effective pressure (B.M.E.P.) at knock in a dual-fuel engine.

Recently, Annand and Abayazid (4) have reported some difficulties in the application of such a simplified model to correspond to supercharged motored engine on the point of autoignition. Such difficulties are understandable if we examine the assumptions in the formulation of the model. For example, the assumption of constant volume heat release necessarily implies that the autoignition takes place at or close to T.D.C., whereas under marginal autoignition conditions (i.e. a cycle out of a few hundred autoigniting cycles), the point of ignition may well lie in expansion stroke.

In the present investigation it has been shown that the kinetic data derived for the autoignition reactions of n-heptane and propane, assuming a bimolecular reaction scheme, is of the order of magnitude as referred to in the literature. The temperature rise during precombustion reactions, remaining the same (see Fig. B2.11 and Fig. B2.16), supports the view that the initiating source in the dual-fuel combustion can be conceived as an 'effective pilot'. Such a concept is useful in the determination of the ignition temperature of the rest of charge which is the final temperature at the completion of the 'pilot' burning phase. The concept of 'effective pilot' in dual-fuel engine combustion is considered to be useful. It is not only helpful in the construction of a model, but it also offers a useful guide as to the minimum requirements for the ignition of the second stage of the dual-fuel combustion processes.

We shall now endeavour to see whether, on the strength of the evidence gathered so far, it is possible to formulate a qualitative model and to show what further information is required to quantify it.

It has already been shown that the knowledge of rates of burning of the fuel in the combustion cycle of an engine can effectively be utilised in the prediction of pressure development and hence the engine performance (see Section A2.2-2 and Fig. A2.18), in general, and particularly under knocking conditions. Shown in Fig. C.1.5 is the predicted pressure development during autoignition of propane. The rates of burning have first been calculated with the generalised overall chemical kinetic data as shown in Section B2.2-2, while the rest of the procedure, in essence, remains as what has been described in Section A2.2. The dual-fuel combustion processes in an engine can be suggested to be made up of:

1. Under 'normal' combustion

(i) compression ignition of the diesel fuel together with some of the gaseous fuel in the fringes of the pattern as shown by the autoignition of n-heptane and is shown in Fig. C1.1 . It is pointed out here that the characteristic pre-mixed burning of the pilot fuel is to be expected because of delayed ignition in the presence of gaseous fuel;

(ii) combustion of premixed gaseous fuel following pilot fuel combustion. It may be approximated to follow a pattern of progressive inflammation.

Now, for the compression ignition of pilot fuel, we ought to know the point of ignition and the rate-law it follows. As a first approximation, the presence of the gaseous fuel may be neglected and ignition delay data available can be adopted. With this simplifying assumption, the chemical kinetic data obtained in a motored engine are useful in calculating the reaction rate. The bulk of the gaseous fuel then follows the combustion of pilot fuel. The point of ignition of the gaseous charge may as a gross approximation, be taken as concurrent with that of pilot fuel, or at some later stage. The rates of heat release so calculated are shown in Fig. C1.1. Fig. C.1.2 combines the two parts in accordance with both the above assumptions. Apparently, the first approximation

that the ignition of the gaseous fuel charge starts with that of pilot fuel does not give an acceptable synthesised diagram. On the other hand, it is interesting to note that the synthesised heat release diagram (curve 2, Fig. C1.2) corresponds to that of typical heat release records as computed from pressure development (see, for example, Fig. A2.4). The present state of our knowledge is far from being complete in providing us the exact mechanisms of the compression-ignition of premixed gaseous fuel preceded by the compression-ignition of a heavier hydrocarbon.

2. Under knocking combustion

It has been previously pointed out in various contexts that the ignition of pilot is unaffected by knocking. Therefore, the compression ignition of the pilot fuel, as shown in Fig. C1.1, can be taken to hold under knocking conditions. It may be recalled, however, that there occurs slight advance in the combustion processes due to excessive rates of heat release. It can be postulated that the combustion of the gaseous fuel charge following the pilot fuel combustion, in this case, follows the pattern observed due to autoignition. It is also known that this stage sets in earlier than the progressive inflammation encountered during normal combustion, Thus, shown in Fig.C1.3 is the qualitative representation of gaseous phase of combustion, while in Fig. C1.4 both the stages have been added to establish the net effect which resembles the experimentally analysed heat release records presented in Section A2.3-1.

Another approach in synthesising the heat release of dual-fuel combustion processes could well be on the lines as suggested by Lyn (62) and Gee and Karim (27) for diesel engine combustion. The estimation of first stage combustion, due mainly to pilot fuel in a dual-fuel engine, can at first be looked into as consisting of a multitude of droplets burning in air. The triangular rate law, as adopted by Lyn , may be assumed to hold. However, the presence of gaseous fuel imposes many complications. While the knowledge of droplet burning in a combustible atmosphere is too discrete, the application of such an

oversimplified model for dual-fuel combustion would not be more than a hypothetical exercise.

The preliminary attempts as suggested in the preceding lines for the synthesis of heat release in dual-fuel engines, do raise the following questions:

(i) What quantity of gaseous fuel is entrained in the pilot fuel spray and to what extent does it take part in the first stage of combustion? In other words, the exact definition of 'effective pilot combustion';

(ii) When exactly does the inflammation or auto-ignition of the gaseous charge take place, i.e. it is necessary to have reliable quantitative data corresponding to blended fuels combustion.

C1.3 Recommendations for Future Work

In order to provide quantitative basis for the construction of a model, it is necessary that the solutions to the above questions be arrived at.

High-speed photographic studies may well reveal the relative importance of the two-staged combustion in a dual-fuel engine as indicated by the present heat release analysis. As an alternative, contemporary sampling techniques to probe the combustion products analysis during the course of combustion is thought to be revealing and will provide quantitative information as to the progress of combustion. Such data may be valuable to refine the approximations adopted in the computer programme related to the progress of combustion.

The computer programme presently developed can be further exploited in the following directions:

(i) Computations can be effected for the heat release analysis of large bore dual-fuel engines so as to check the correspondence between the processes in such engines and those presently observed in a relatively small laboratory engine.

(ii) The thermodynamic and transport properties of gaseous fuels and their mixtures can be computed

with due provision of dissociation at the elevated temperatures as prevelant in engines. For ease in data handling, reference charts can be plotted with the aid of computer. Such information is highly desirable in cycle analysis of internal combustion engines utilising fuels of different composition, depending on the source of availability.

The procedure of determining overall chemical combustion kinetic data is fairly well established. Use can be made of such a procedure in the areas where there is dearth of this useful information.

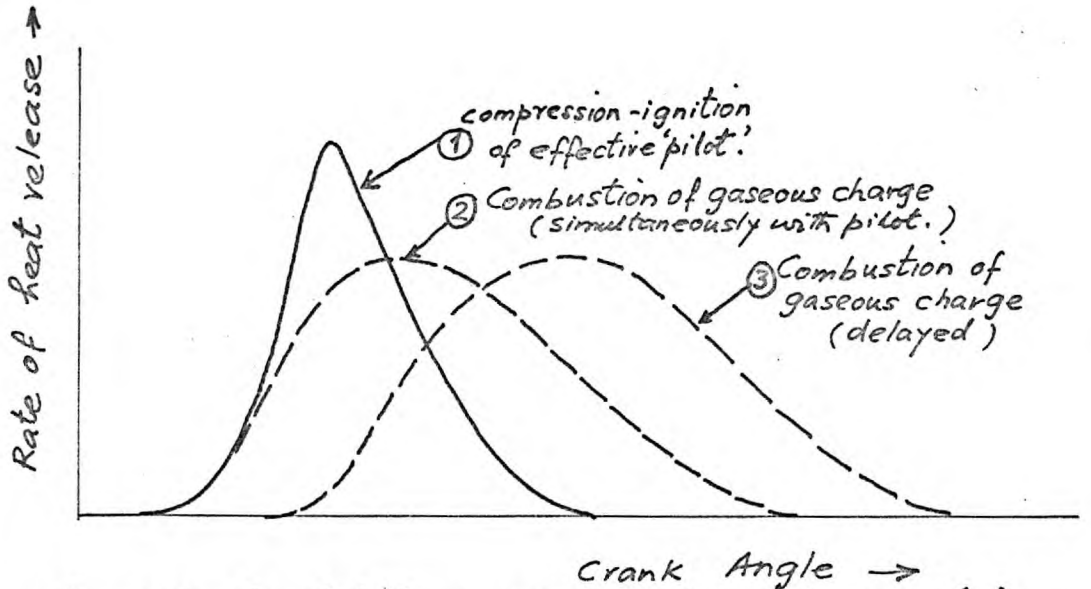


Fig. C1.1 Qualitative presentation of effective pilot and gaseous charge combustion under 'Normal' combustion.

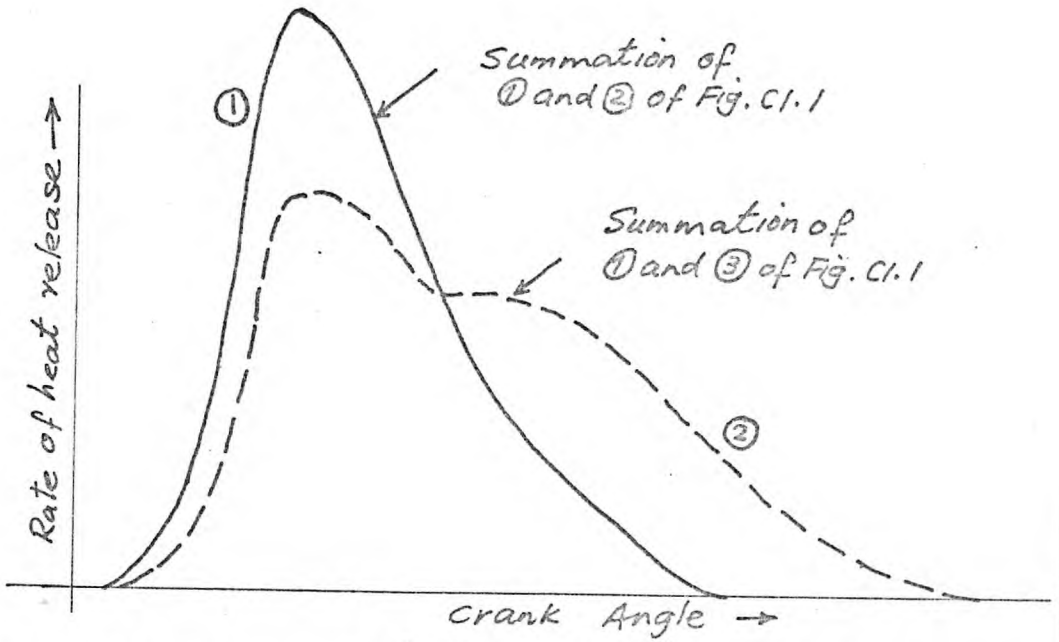


Fig. C1.2 Summation of qualitative rates of heat release in a dual-fuel engine

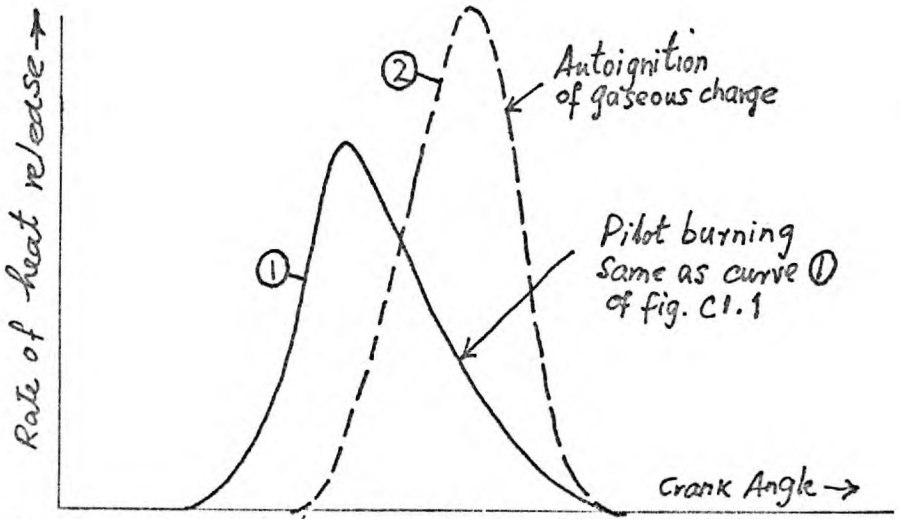


Fig. C1.3 pilot burning and gaseous fuel autoignition

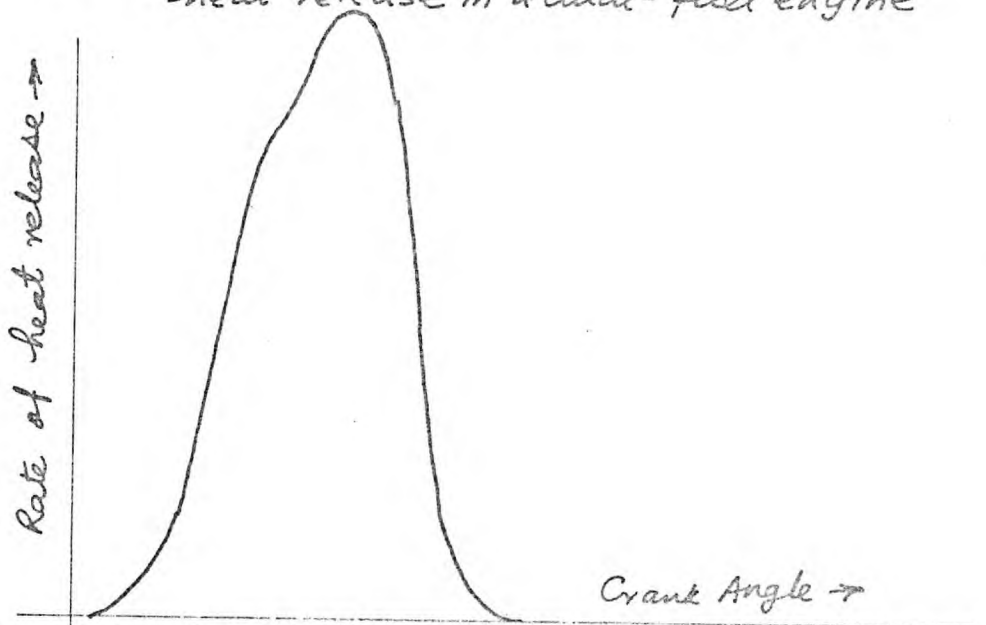


Fig. C1.4 Summation of phase ① and ② of Fig. C1.3

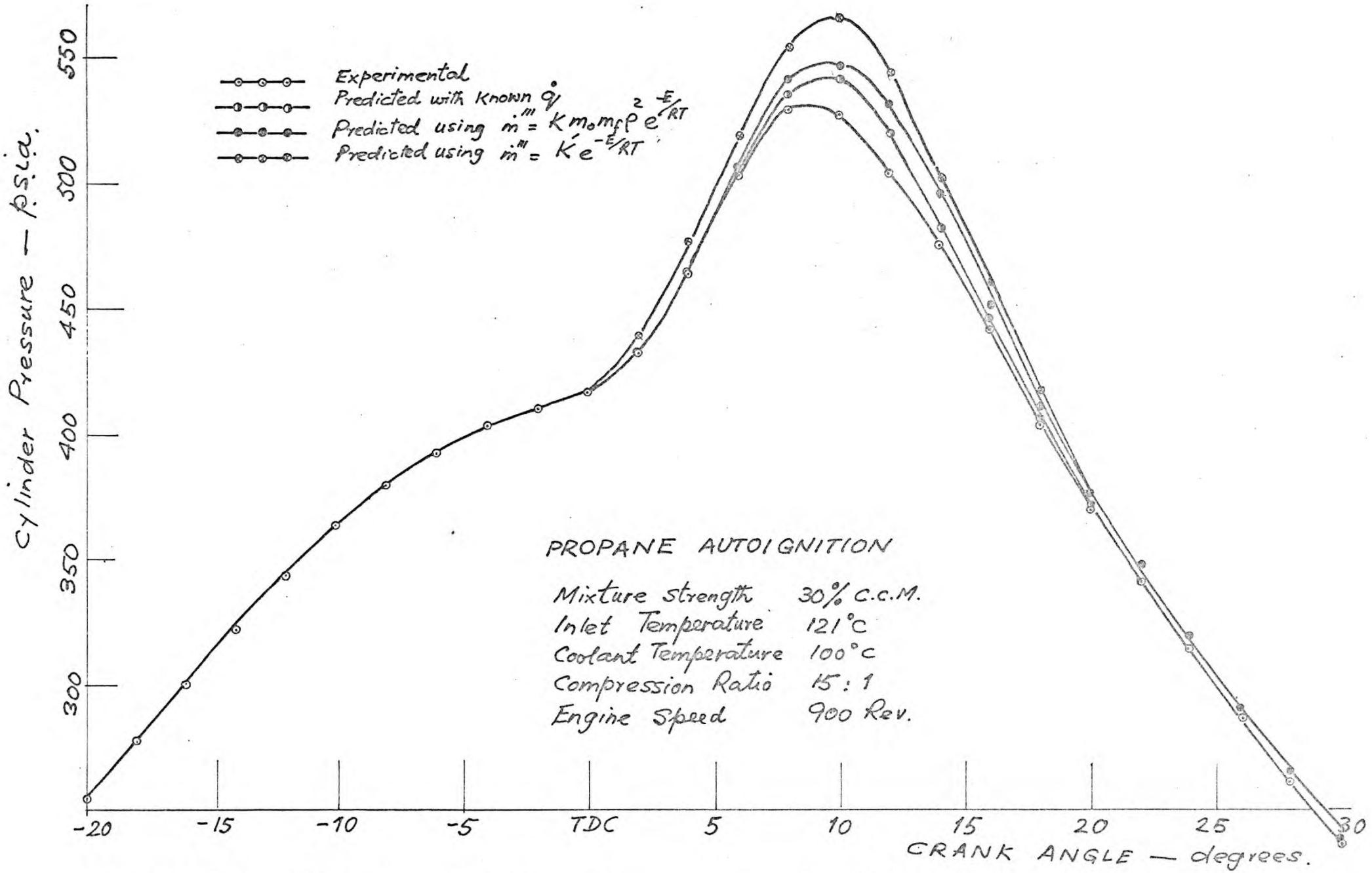


Fig. (C1.5) Comparison of various methods of pressure prediction with known rate of heat release, reaction rate constants and Activation Energy.

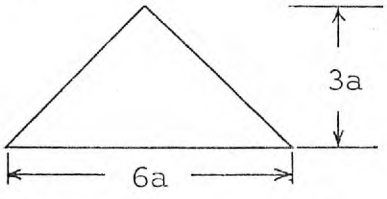
A P P E N D I X I

THEORY OF VISCOUS FLOW AIR METER

It can be shown that the pressure drop across a triangular passage of right-angled triangle with height (3a) and base (6a) under laminar air flow conditions is:

$$\Delta p = \frac{c\,\mu\,V}{g\,a^2} \times \ell \text{ , where}$$

Δp = pressure drop
c = a constant
μ = viscosity of air
V = velocity
ℓ = length of the passage
a = length parameter as shown in the figure



$$Q = A\,V$$

$$= 9 \times a^2 \times n \times \frac{\Delta p\, g\, a^2}{c\,\mu\,\ell}$$

$$= \frac{9g\,a^4\,n}{c\,\mu\,\ell} \times \Delta p$$

where n is the number of passages.

$$Q \propto \Delta p$$

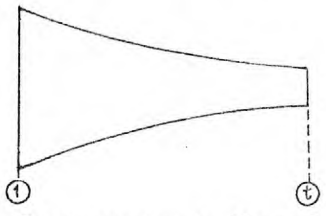
provided due corrections for the change in viscosity be made due to change in ambient temperatures.

The constant of proportionality is evaluated by calibration.

A P P E N D I X II

THEORY OF CHOKED NOZZLE FLOW

As mentioned in the text earlier, in the choked nozzle the flow of a gas is linearly dependent on the ratio of $P_1/\sqrt{T_1}$. We shall now prove such relationship.



Convergent Nozzle.

According to equation of continuity, the mass flow rate at any cross section is

$$\dot{m} = c\rho AV \qquad (1)$$

Since for a choked nozzle critical conditions exist at the throat, i.e. the velocity of gas at the throat corresponds to the velocity of sound in the gas under those conditions, equation (1) can be rewritten as

$$\dot{m} = c\ \rho_t\ A_t V_t \qquad (2)$$

$$= c\ \frac{P_t}{RT_t} \cdot A_t\ \sqrt{\gamma g_o RT_t}\ , \text{ where}$$

$V_t = \sqrt{\gamma g_o RT_t}$ is the velocity of sound.

$$\dot{m} = \frac{\gamma g_o}{R}\ \frac{cP_t\ A_t}{\sqrt{T_t}} \qquad (3)$$

Since under critical flow the conditions at the throat and that at the inlet are related as under:

$$P_t = \left(\frac{2}{\gamma+1}\right)^{\frac{\gamma}{\gamma-1}} P_1 \qquad (4)$$

$$T_t = \left(\frac{2}{\gamma+1}\right) T_1 \qquad (5)$$

Substituting (4) and (5) in equation (3), we get:

$$\dot{m} = c \left(\frac{\gamma g_o}{R}\right)^{\frac{1}{2}} \frac{A_t P_1}{\sqrt{T_1}} \left(\frac{2}{\gamma+1}\right)^{\frac{\gamma+1}{2(\gamma-1)}}$$

$$\dot{m} = K \frac{P_1}{\sqrt{T_1}} \quad , \quad \text{where}$$

$$K = c\, A_t \left[\left(\frac{\gamma g_o}{R}\right) \left(\frac{2}{\gamma+1}\right)^{\frac{\gamma+1}{\gamma-1}}\right]^{\frac{1}{2}}$$

The proportionality of flow rate with $\frac{P_1}{\sqrt{T_1}}$ was checked by way of calibration as shown in Chapter A2.

A P P E N D I X III

TYPICAL COMPOSITION OF FUELS AND DILUENT USED

1. Methane

(a) Composition

CH_4	97.8% (by volume)
CO_2	1.06%
N_2	0.91%
O_2	0.24

(b) Density .0457 lb/cft

(c) Lower Calorific Value 11450 Chu/lb

(d) Fuel/Air Stoichiometric Ratio .05952

Supplied by the British Oxygen Company Ltd.

2. Propane

(a) Composition

C_3H_8	9.47% (by volume)
C_2H_6	3.1%
C_4H_{10}	2.2%

(b) Density .1225 lb/cft

(c) Lower Calorific Value 11100 Chu/lb

(d) Fuel/Air Stoichiometric Ratio .06369

Supplied by the British Oxygen Company Ltd.

3. n-Heptane

(a) Composition

$n\text{-}C_7H_{16}$	99.9%
$Iso\text{-}C_7H_{16}$	0.1%

(b) Lower Calorific Value 10700 Chu/lb

(c) Fuel/Air Stoichiometric Ratio .0661

Supplied by Esso Petroleum Ltd.,
Conforming to IP standards.

4. Carbon dioxide

(a) Composition

Air	300 - 3000 p.p.m.
Water	20 p.p.m.
S	0.1 p.p.m.
CO	traces

(b) Density .1225 lb/cft

Supplied by Distillers Co. Ltd.,
Conforming to commercial grade.

A P P E N D I X IV

DERIVATION OF RATE OF HEAT RELEASE EQUATION (DIFFERENTIAL FORM)

The following are the assumptions which formed the basis of heat release evaluation:

(i) The cylinder charge is homogeneous, such that the entire charge is assumed to have one temperature at a given instant.

(ii) The energy released as a result of combustion corresponds to that of the entire charge at all stages.

(iii) The process of combustion remains steady for a finite length of time justifying the application of the 1st low of thermodynamics, i.e.:

$$\Delta(\text{Energy released}) + \Delta(\text{Heat transfer})_{in} = \Delta(\text{Heat transfer})_{out} + \Delta(\text{Work out}) + \Delta(\text{Increase in internal energy of charge}) \quad (1)$$

If $\dot{q}$ is the net rate of heat release due to combustion giving pressure rise at approximately constant volume,

$$\dot{q}\Delta\theta = \Delta(\text{Energy released} + \text{Heat in} - \text{Heat out}) \quad (2)$$

If the cylinder charge is assumed to be an ideal gas and the energy content is solely its internal energy, then equations (1) and (2) may lead to the following relationship:

$$\dot{q}\Delta\theta = \frac{P\Delta V}{J} + m\,\overline{Cv}\,\Delta T \quad (3)$$

Since $$\overline{Cv} = \frac{R}{(\bar{\gamma}-1)} \quad (4)$$

and $$PV = mJRT$$

or $$\frac{P\Delta V + V\Delta P}{J} = mR\Delta T \quad (5)$$

assuming that the mass and the gas constant do not vary.

Substituting (4) and (5) in (3) we get

$$\dot{q}\Delta\theta = \frac{P\Delta V}{J} + \frac{P\Delta V + V\Delta P}{J(\gamma-1)}$$

$$= \frac{(\bar{\gamma}-1)\ P\Delta V + P\Delta V + V\Delta P}{J(\bar{\gamma}-1)}$$

$$\dot{q}\Delta\theta = \frac{\gamma P\Delta V + V\Delta P}{J(\bar{\gamma}-1)}$$

Under steady conditions the time derivative becomes as follows.

$$\dot{q} = \frac{1}{J(\gamma-1)} \left(\gamma\ P\ \frac{dV}{d\theta} + V\ \frac{dP}{d\theta}\right) \qquad (6)$$

$$\dot{q}_g = \dot{q} + Q_{HT} \times \text{Area} \qquad (7)$$

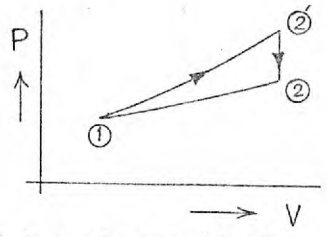
The equations (6) and (7) formed the basis of our investigations. In the above equations basing on P and V, the values of $\frac{dV}{d\theta}$, $\frac{dP}{d\theta}$, $\overline{\gamma}$ were evaluated separately at every degree of crank rotation.

The variation of $\overline{\gamma}$ w.r.t. temperature was computed on the basis of variation of $\overline{C}p$ and $\overline{C}v$.

A P P E N D I X V

DERIVATION OF RATE OF HEAT RELEASE EQUATION (FINITE DIFFERENCE FORM)

With reference to Fig. (1) the p-V path traced by the process 1-2 can be looked on as made up of 1-2' as adiabatic and 2'-2 as constant volume heat addition or otherwise.



It can be shown that

$$\Delta q_{1-2} = \frac{1}{\gamma-1} \left(\frac{p_2 V_2^{\gamma} - p_1 V_1^{\gamma}}{V_2^{\gamma-1}}\right) \qquad (1)$$

Since $V_2 = V_1 + \Delta V$

$p_2 = p_1 + \Delta p$

Then, on substitution, equation (1) becomes

$$\Delta q_{1-2} = \frac{V_2^{1-\gamma}}{\gamma-1} \{(p_1 + \Delta p)(V_1 + \Delta V)^{\gamma} - p_1 V_1^{\gamma}\}$$

$$= \frac{V_2^{1-\gamma}}{\gamma-1} \{(p_1 + \Delta p)\left[V_1^{\gamma}\left(1 + \frac{\Delta V}{V_1}\right)^{\gamma}\right] - p_1 V_1^{\gamma}\}$$

Using Taylor's truncated series for expansion:

$$\Delta q_{1-2} = \frac{V_2^{1-\gamma}}{\gamma-1} \{(p_1 + \Delta p)\left[V_1^{\gamma}\left(1 + \gamma \frac{\Delta V}{V_1}\right)\right] - p_1 V_1^{\gamma}\}$$

$$= \frac{V_2^{1-\gamma}}{\gamma-1} \cdot V_1^{\gamma} \left[p_1 + \Delta p + \frac{\gamma \Delta V\, p_1}{V_1} + \gamma \frac{\Delta p \Delta V}{V_1} - p_1 V_1^{\gamma}\right]$$

$$= \left(\frac{V_1^{\gamma-1}}{V_2}\right) \frac{1}{\gamma-1} \left[p_1 V_1 + \gamma p_1 \Delta V + V_1 \Delta p\right] - p_1 V_1$$

$$\Delta q_{1-2} = \left(\frac{V_1}{V_2}\right)^{\gamma-1} \frac{1}{\gamma-1} [\gamma\, p_1 \Delta V + V_1\, \Delta p]$$

Now,
$$\left(\frac{V_1}{V_2}\right)^{\gamma} = \left(\frac{V_1 + \Delta V - \Delta V}{V_1 + \Delta V}\right)^{\gamma-1}$$

$$= \left(1 - \frac{\Delta V}{V_1 + \Delta V}\right)^{\gamma-1}$$

$$= 1 - (\gamma-1)\left(\frac{\Delta V}{V_1 + \Delta V}\right)$$

$$\Delta q_{1-2} = \left[1 - (\gamma-1)\frac{\Delta V}{V_1 + \Delta V}\right] \left[\frac{\gamma\, p_1\, \Delta V + V_1\, \Delta p}{\gamma - 1}\right]$$

cf. $\dot{q} = \dfrac{\gamma p dV + V dp}{\gamma - 1}$ Appendix IV,

which is the exact differential form, ignoring the term

$$\left[(\gamma-1)\frac{\Delta V}{V_1 + \Delta V}\right] ,$$

which is negligible for small increments of ΔV.

A P P E N D I X VI

THE COMPUTER PROGRAMME

1. A List of Some Fortran Symbols

The following is a list of some important variables which constitute the majority of arguments in either the MAIN programme or the Subroutines.

Fortran Symbol	Description	Units
A	Calibrated scale values of cylinder pressure above datum pressure	
AA(1)	No. of moles of CO_2 after first approximation	lb moles
AFR	Air-fuel ratio by mass	
AM	Reaction rate	lb/^{o}C.A.
AMASS	Mass of the cylinder charge	lb/stroke
AR	Momentary area for heat transfer	ft^2
AT	Convective component of heat transfer	Chu/^{o}C.A.
AX	Piston displacement	ft
B	Reference scavenging pressure	psia
BB(1)	No. of moles of H_2O after first approximation	lb moles
BORE	Engine cylinder bore	in
C1	Reaction rate parameter	
CC	Diesel oil flow rate	cm^3/s
CET	Diesel fuel (characterised as cetane) rate	lb/stroke
CETM	Diesel fuel rate	lb moles/ stroke
CFG1, CFG2 ..	Gas and air flow rates	ft^3/s
CH4	Methane flow rate	lb/stroke
CH4M	No. of moles of methane	lb mole/ stroke
CONM	Thermal conductivity of mixture	Chu/s ft degC

Fortran Symbol	Description	Units
CONP	Thermal conductivity of products	Chu/s ft degC
COEF 1,2,3	Constants a, b and c for Annand's correlation	
CPM	Specific heat of mixutre at constant pressure	Chu/lb. mole deg C
CPPR	Specific heat of products at constant pressure	
CR	Compression ratio	
CROW	Piston and cylinder head area	ft^2
DEN	Density of diesel fuel	gm/cm^3
DP	$dP/d\theta$	psi/degC.A.
DV	$dV/d\theta$	ft^3/degC.A.
E	Overall apparent activation energy	K Cal/mol.
FRAC	Fraction of fuel burnt	
G	Specific heat ratio of cylinder charge ($\overline{\gamma}$)	
H	Crank rotation	degC.A.
HT	Heat flux by Eichelberg's formula	Chu/degC.A.
HTIN	Heat input	Chu/stroke
HHT	Heat flux by Annand's correlation	Chu/degC.A.
K	No. of step	
KPCO2,KPH20	Equilibrium constant for dissociation of CO_2 and H_2O, respectively	$atm^{\frac{1}{2}}$
M1, M2 ...	Index, integer numbers	
MM	No. of the set of input data	
NSTR	No. of strokes/working cycle	
P	Cylinder gas pressure	psia
PIG	Point of ignition	$^oC.A.$

Fortran Symbol	Description	Units
PIJE	Point of injection ends	^{o}C.A.
PIJS	Point of injection starts	^{o}C.A.
Q	Gross rate of heat release	Chu/degC.A.
QQ	Net rate of heat release	Chu/degC.A.
TQ	Cumulative heat release	Chu/stroke
R	n_{CO}/n_{CO_2}	
RAT	Ratio of residuals to intake charge	
RATIO	Connecting rod to crank throw ratio	
RES	Amount of residuals	lb/stroke
REV	Engine speed	rev/min
RHO	Density of charge	lb/ft^3
RM	Charge mean gas constant	ft lb/lb degC
RT	Radiative component of heat transfer	Chu/^{o}C.A.
S	n_{H_2}/n_{H_2O}	
STR	% chemically correct mixture	
SUMM	Molar summation of mixture	lb mole/stroke
SUMP	" " " products	lb mole/stroke
T	Cylinder gas temperature	^{o}K
TC	Coolant outlet temperature	^{o}K
TO	Intake temperature	^{o}K
TP	Piston crown temperature	^{o}K
TW	Cylinder wall temperature	^{o}K
V	Cylinder volume	ft^3
VISM	Viscosity of mixture	lb/ft sec
VISP	Viscosity of products	lb/ft sec
VP	Velocity of piston	ft/s
X	Inverse of temperature	$^{o}K^{-1}$

2. A List of Subroutines

All the subroutines employed in the computer programme are enlisted here together with their respective nomenclature and function.

Name of the Subroutine		Function called for
1.	MAIN	(i) Reads out input data. (ii) Transfers the data into computable form. (iii) Controls all the subroutines. (iv) Writes out output as pertinent to every cycle.
2.	SMOOTH	(i) Smooths the data scatter of pressure variation from degree to degree of crank rotation. Iteration of smoothing procedure can be effected, if desired.
3.	VOLUME	(i) Computes the areas for heat transfer with the following sub-divisions: (i) Area of the cylinder liner as as available with piston travel, (ii) Area of piston crown and cylinder head. (ii) Computes instantaneous cylinder volume.
4.	DISSN	Accounts for dissociation of the products as follows: (i) Defines the equilibrium constants of dissociation as a polynominal of temperature. (ii) Computes the concentration of (CO) and (H_2) from the known concentration of CO_2 and H_2) in the products and the level of temperature attained at a particular instant.
5.	SPECHT	(i) Defines the specific heat at constant pressure as a poly-nominal function in temperature for each constituent of reactants and products. (ii) Computes the specific heat ratio ($\overline{\gamma}$). (iii) Computes the heating value of fuel mixture as a function of temper-ature.

Name of the Subroutine		Function called for
6.	HTTR	Computes the instantaneous heat flux from Annand's and Eichelberg's formulae.
7.	PRGRAD	Computes the rates of pressure rise by empirical differentiation of pressure data.
8.	SIMP	Integrates the gross rates of heat release by Simpson's rule.
9.	FINRAT	Computes the fraction of the fuel burnt up to a given instant with the known configuration of cumulative heat release.
10.	KINTIC	(i) Computes the reaction rates. (ii) Reaction rate parameter is computed as a function of: (a) Rate of burning of fuel, (b) Density variation, (c) Concentration of oxygen and fuel at a given instant. (iii) Writes out the Naperian logarithmic reaction rates as against inverse of temperature.
11.	RESID	Computes the amount of residuals entrained in the cylinder with a knowledge of: (a) Scavenging pressure variation, (b) Intake temperature, (c) Cylinder volume, (d) Exhaust temperature.

3. List of Input Data

The following list is appended which formed a proforma framed for data acquisition from the engine manufacturers. This scheme could not however be pursued due to the pressing nature of other parts of the problem. It is hoped that it would serve to explain the nature of data required for an elaborate heat release analysis.

1. Type of operation, i.e. Diesel/Dual-fuel/Gas.
2. No. of cylinders.
3. No. of strokes/working stroke.

4. Speed.

5. Bore. 5a. Compression ratio.

6. Stroke.

7. Connecting rod - Crank throw ratio.

8. Timings with reference to crank rotation:

(1) Injection starts,
(ii) Duration of injection,
(iii) Ignition timing (if spark ignited),
(iv) Valve timings.

9. Fuel injection system:

(i) Direct or indirect,
(ii) Atomisation pressure,
(iii) Gas injection timings, if any.

10. Flow measurements

(i) Diesel fuel consumption,
(ii) Air consumption,
(iii) Gaseous fuel consumption.

11. Fuel analysis

A. Diesel fuel

(i) Density,
(ii) Calorific value (a) lower, (b) higher,
(iii) Chemical structure, if known,
(iv) Additives, if any,
(v) Viscosity.

B. Gaseous fuel

(i) Composition of fuel, if not 100% pure,
(ii) Calorific value (a) lower, (b) higher,
(iii) Source of availability.

12. Atmospheric data

(i) Ambient pressure,
(ii) Ambient temperature,
(iii) Relative humidity, if known.

13. Boost pressure, if supercharged.

14. Intake temperature, if preheated or supercharged.

15. Coolant details:

(i) Type, i.e. air/water,
(ii) Coolant outlet temperature.

16. Exhaust gas analysis:

(i) Temperature,
(ii) Smoke density,
(iii) Composition.

17. Type of combustion chamber.

18. Is the inlet valve shrouded?

19. Oscillograms (preferably in the form of film):

    (i) Cylinder pressure. Preferably for the whole cycle duration, i.e. 720°C.A. Few consecutive cycles to assess cyclic dispersion, calibration scale.
    (ii) Injector lift.
    (iii) Crank rotation in degrees, or position of T.D.C. and B.D.C. if self-generated time base is adopted.
    (iv) Pressure-time derivative (for qualitative analysis).
    (v) Pressure transducer calibration.
    (vi) Datum line of reference pressure.

20. Electronic equipment details:

    (i) Type of transducer and amplifier,
    (ii) Type of oscilloscope,
    (iii) Whether transducer compensated for flame sensitivity and tranverse vibrations,
    (iv) Linearity of pick-up for wide pressure range.

21. B.M.E.P.

22. It is appreciable if three load conditions traces, viz. light load[1], full load[2] and knocking[3] are considered.

---

(1) Light load may be taken as that corresponding to very weak mixture strength - perhaps just sufficient for the engine to overcome frictional losses.

(2) Full load is the one the engine is rated for.

(3) If we exceed the mixture strength over the full load, the knock may ensue. It is preferable not to reach violent knock, as it entails pressure fluctuations rendering the data analysis void of certainty.

```
$EXECUTE        IBJOB
$IBJOB          MAP
$IBFTC MAIN
       REAL P(150),H(150),T(150),Q(150),TQ(150),DP(150),G(150),
      1RM(150),RRM(150),V(150),DV(150),A(150),AR(150),DELH(150),QQT(150)
      2AM(150),HT(150),HHT(150)
       COMMON/AB/AIRM,CH4M,CETM,PIG,AMASS,PROM,HEPTM,NF
       COMMON/CA/BORE,STROKE,RATIO,CROW,REV,PO,CR,VOLM
       COMMON/CONC/AA(1),BB(1),DD(1),EE(1),FF(1),AN2,O2,FRAC(150),CO2
       COMMON/LOSS/COEF1,COEF2,COEF3,PRAN,M1,TC,DELT1,DELT2,HTR(150),PBD
      1,PP(150),AHT(150)
       COMMON/REY/AX(150),ZZ(150)
       COMMON/RES/PROP,HEPTP,RAT
       COMMON/HEAT/QQ(150)
C      TEMPERATURE RISE OF THE TRANSDUCER OVER AMBIANT IS COMPENSATED. *
       READ(5,6)N,NC
       READ (5,8) (H(K),K=1,N)
       READ(5,17) COEF1,COEF2,COEF3,PRAN,TC,DELT1,DELT2
       READ(5,12) BORE,STROKE,RATIO,NSTR
       READ(5,16) M1,M2,M3
       MM=1
2      NF=0
       M2=1
       READ (5,7) (A(K),K=1,N)
9      FORMAT(5F6.5,7F6.2)
       READ(5,9)CFG1,CFG2,CFG3,CFG4,CC,CFG5,X,PO,SCALE,TO,HEAD,DIFF
       READ(5,22) PIJS,PIJE,PIG,GRAT
22     FORMAT(4F10.3)
       WRITE(6,100)
       AMIC=4.5/(X 1.0)-0.5
       AMIC=AMIC-0.045
       CR=4.5/(0.5 AMIC)+1.
       REV=900.
       PBDC=PO*0.491+HEAD/(12.*2.30)-5.*463.*DIFF/(460.*425.)
       TO=(TO-273.)*100./91.+273.
       WRITE(6,89)
       IF(SCALE.EQ.6.)  CAL=100./430.
       IF(SCALE.EQ.0.05)  CAL=300./1534.
       IF(SCALE.EQ.0.1)  CAL=700./1780.
       TEXH=523.
       DO 11 JJ=1,N
11     P(JJ)=A(JJ)*CAL+PBDC
       CALL  SMOOTH(P,N)
       CALL        VOLUME(H,V,DV,AR,N,VOLM)
       CALL  PRGRAD(DP,P,N)
       CET=0.
       PP(1)=P(1)
       SUM=0.
       CH4=CFG1*2./REV
       PRO=CFG2*2./REV
       AIR=CFG3*2./REV
       CH4M=CH4/16.
       PROM=PRO/44.
       AIRM=AIR/28.97
       HEPT=CC/450.
       HEPTM=HEPT/100.2
       CO2=CFG5*2./REV
       AMASS=CH4+PRO+HEPT+AIR+(CFG4+CFG5)*2./REV
       AN2=AIR*0.768+CFG4*2./REV
```

```
      O2=AIR*0.232
      AFR=AIR/(CH4+PRO+HEPT)
      ABC=PROM/HEPTM
      STR=(17.5*CH4+15.69*PRO+15.15*HEPT)/AIR*100.
      WRITE(6,888)CFG1,CFG2,CFG3,CC,PIG,TO,CR,AFR,STR
888   FORMAT(1H0,10X,8HMETHANE=,F8.6,4X,8HPROPANE=,F8.6,4X,4HAIR=,F8.6,
     1X,8HHEPTANE=,F8.6,4X,18HPOINT OF IGNITION=,F5.1,/,10X,18HINLET TE
     2PERATURE=,F6.1,2X,18HCOMPRESSION RATIO=,F7.3,2X,15HAIR-FUEL RATIO
     3,F6.2,2X,17HMIXTURE STRENGTH=,F7.3)
      HTIN=(PRO*19929./1.8 CH4*21500./1.8+HEPT*10640.)*10.**3
      RIN=AN2*100./AMASS
      RNF=AN2/(AN2+CH4+PRO HEPT)*100.
      PRHR=HEPT*10640./(PRO*11050.)
      RCO2F=CO2/(CO2+CH4+PRO+HEPT)
      RCO2IN=CO2*100./AMASS
      WRITE(6,999) HTIN,RNF,RIN,PRHR,RCO2F,RCO2IN
999   FORMAT(1H0,11HHEAT INPUT=,F8.3,2X,15H N2-FUEL RATIO=,F6.2,2X,17H
     12-INTAKE RATIO=,F6.2,2X,12H HEAT-RATIO=,F6.2,2X,9HCO2-FUEL=,F6.2,
     21X,7HCO2-IN=,F6.2)
50    DO 88 K=1,N
      IF(NF.EQ.3)  GO TO  40
      IF(NF.EQ.0) GO TO 31
      IF(NF.EQ.1.AND.H(K).LT.PIG) GO TO 88
      IF(NF.EQ.1.AND.H(K).LT.PIG)  GO  TO  88
      IF(NF.EQ.2.AND.H(K).LT.PIG)  GO  TO  101
      IF(NF.EQ.2.AND.H(K).GE.PIG)  GO  TO  1000
31    IF(H(K).GE.PIG)  GO TO 33
      SUMM=CH4M+PROM+HEPTM O2/32.+AN2/28.161 CO2/44.
40    RRM(K)=1.98726*SUMM
      RM(K)=RRM(K)*1400./AMASS
      GO TO 59
33    IF(NF.EQ.0)  FRAC(K)=1.
      IF(NF.EQ.3) GO  TO  44
      AA(1)=(CH4M 3.*PROM+7.*HEPTM)*FRAC(K)+CO2/44.
      BB(1)=(2.*CH4M+4.*PROM+8.*HEPTM)*FRAC(K)
      DD(1)=O2/32.-(2.*CH4M+5.*PROM+11.*HEPTM)*FRAC(K)
      SUMP=AA(1)+BB(1)+DD(1)+AN2/28.161+(PROM+CH4M+CETM)*(1.-FRAC(K))
44    RRM(K)=1.98726*SUMP
      RM(K)=RRM(K)*1400./AMASS
59    T(K)=144.*P(K)*V(K)/(1400.*RRM(K))
      IF(H(K).LE.PIG) GO TO 60
      IF(T(K).LT.1500.)  GO  TO  60
      CALL        DISSN(T,P,K,PO,PIG,SUMP)
60    CALL        SPECHT(T,SUMM,SUMP,K,H,CPPR,CPMM,G,DELH)
      IF(K.EQ.1) GO TO 20
      IF(NF.GE.1)  GO  TO  20
      PP(K)=PP(K-1)*(V(K-1)/V(K))**G(K)
C     THE  EQUATION  OF  HEAT  RELEASE
20    QQ(K)=(G(K)*P(K)*DV(K)+V(K)*DP(K))*144.*10.**3/(1400.*(G(K)-1.))
      CALL        HTTR(AT,RT,HT,HHT,AR,CPPR,CPMM,K,H,P,T,SUMM,SUMP,V)
      Q(K)=QQ(K)+HHT(K)
      CALL   SIMP(TQ,Q,K)
      IF(NF.EQ.3.AND.H(K).LT.PIG)  GO  TO 101
      IF(NF-1)88,88,1000
1000  IF(Q(K).LE..75) GO TO 101
      WTF=(HEPT+PRO+CH4)/(CH4M+PROM+HEPTM)
      AM(K)=-Q(K)*WTF/(DELH(K)*1000.)
      SUM=SUM+AM(K)
      AMB=SUM
```

```
      FRAC(K)=AMB/(PRO+HEPT+CH4)
      HEPTB=AMB/(1.+ABC)
      PROB=HEPTB*ABC
      CO2M=(3.*PROB+7.*44./100.2*HEPTB)/44.  CO2/44.
      H2OM=(18./11.*PROB+144./100.2*HEPTB)/18.
      O2MB=(40./11.*PROB+11.*32./100.2*HEPTB)/32.
      O2M=O2/32.-O2MB
      PROP=PRO*(1.-FRAC(K))/44.
      HEPTP=HEPT*(1.-FRAC(K))/100.2
      SUMP=CO2M+H2OM+O2M+PROP+HEPTP+AN2/28.161
      WT=AMASS/SUMP
      R=1.98726*1400./WT
      T(K)=144.*P(K)*V(K)/(AMASS*R)
      IF(T(K).GE.1500.) CALL  DISSN(T,P,K,PO,PIG,SUMP)
      CALL        SPECHT(T,SUMM,SUMP,K,H,CPPR,CPMM,G,DELH)
      QQT(K)=(G(K)*P(K)*DV(K)+V(K)*DP(K))*144.*10.**3/(1400.*(G(K)-1.))
      X=ABS(QQT(K)-QQ(K))*100./QQ(K)
      CALL        HTTR(AT,RT,HT,HHT,AR,CPPR,CPMM,K,H,P,T,SUMM,SUMP,V)
      Q(K)=QQT(K) HHT(K)
C
101   WRITE(6,30)H(K),P(K),T(K),PP(K),QQ(K),QQT(K),Q(K),TQ(K),DP(K),H(K
     1),HT(K),HHT(K),AHT(K),HTR(K),G(K),SUMM,SUMP
30    FORMAT(1H ,F5.1,3F7.1,3F6.2,2F7.1,F5.1,5F6.3,2E11.4)
88    CONTINUE
      M2=M2+1
      IF(M2.GT.2) GO TO 3000
      CALL        FINRAT(TQ,N,FRAC,PIG,H)
3000   NF=NF+1
C
      IF(NF.EQ.2)  WRITE(6,90)
90    FORMAT(1H0,25X,70H COMPUTATIONS OF HEAT RELEASE INCORPORATING FIN
     1TE RATES OF COMBUSTION)
      IF(NF.LE.2) GO TO 50
C
      WRITE(6,500)
500   FORMAT(1H1,30X,60H DERIVATION OF KINETIC DATA FROM THE HEAT RELEA
     1E ANALYSIS.,/)
      CALL        KIN TIC(AM,H,T,Q,V,N)
      IF(NF.EQ.3) CALL RESID(PBDC,VOLM,TEXH,TO,CPMM,CPPR,SUMM,SUMP,P,T,
     1MASS,PO,R)
      SUM=0.
      MM=MM+1
      DO 121 K=1,N
121   QQT(K)=0.
      SUMM=0.
      SUMP=0.
      IF(MM.LE.NC) GO TO 2
6     FORMAT(2I3)
7     FORMAT(10F7.3)
8     FORMAT(10F7.1)
12    FORMAT(3F10.5,I1)
16    FORMAT(3I3)
17    FORMAT(7F10.5)
89    FORMAT(1H0,20X,82H COMPUTATIONS OF HEAT RELEASE IN AUTOIGNITION O
     1 GASEOUS FUELS IN A MOTORED ENGINE)
99    FORMAT(1H0,40X,6H PIJS=,F6.2,4X,6H PIJE=,F6.2,4X,5H PIG=,F6.2)
100   FORMAT(1H1)
      STOP
      END
```

```
$IBFTC VOLM
      SUBROUTINE VOLUME(H,V,DV,AR,N,VOLM)
      DIMENSION AR(60),H(60),V(60),DV(60)
      COMMON/CA/BORE,STROKE,RATIO,CROW,REV,PO,CR,VOLM
      COMMON/REY/AX(150),ZZ(150)
      AREA=3.1416*BORE*BORE/(4.*144.)
      CROW=2.*AREA
      OMEGA=2.*3.1416*REV/60.
      RADIUS=STROKE/24.
      DO 8 K=1,N
      THETA=H(K)*3.1416/180.
      U=SIN(THETA)*SIN(THETA)
      WW=COS(THETA)
      CV=AREA*STROKE/(12.*(CR-1.))
      AX(K)=STROKE*(RATIO+1.-SQRT(RATIO*RATIO-U)-WW)/24. +CV/AREA
      ZZ(K)=OMEGA*RADIUS*(SIN(THETA)+SIN(2.*THETA)/(2.*SQRT(RATIO**2-U)
     1)
      V(K)=AREA*AX(K)
      DV(K)=AREA*(SIN(2.*THETA)/(2.*SQRT(RATIO*RATIO-U))+SIN(THETA))*3.
     1416*STROKE/(2.*12.*180.)
8     AR(K)=3.1416*BORE*AX(K)/12.
      VOLM=CV+AREA*STROKE/12.
      RETURN
      END
```

```
$IBFTC SMTH
      SUBROUTINE SMOOTH(P,N)
      DIMENSION X(150),P(150),Y(150)
C     SMOOTHING OF  DATA  SCATTER  BY  FINITE  DIFFERENCES
      II=0
91    N1=N-1
      DO150 I=1,N1
150   X(I)=P(I+1) P(I)
      DO 60 J=1,N1
      IF(J.EQ.1) GO TO 60
      Y(J)=X(J)-X(J-1)
60    CONTINUE
      N2=N-2
      DO 70 L1=2,N2
70    Y(L1)=Y(L1+1)-Y(L1)
      Z=Y(2)
      W=Y(N2)
      DO 80 M1=3,N2
      X(M1)=(Y(M1)-Y(M1-1))*3./35.
80    P(M1)=P(M1) X(M1)
      P(1)=P(1)+Z/5.+X(3)
      P(2)=P(2)-0.4*Z-X(3)*5./3.
      P(N 1)=P(N-1)+0.4*W-X(N-2)*5./3.
      P(N)=P(N)-0.2*W+X(N-2)
      II=II+1
      IF (II.LT.5 )  GO  TO  91
      RETURN
      END
```

```
$IBFTC SPHT
      SUBROUTINE SPECHT(T,SUMM,SUMP,K,H,CPPR,CPMM,G,DELH)
      DIMENSION G(150),T(150),H(150),DELH(150)
      COMMON/AB/AIRM,CH4M,CETM,PIG,AMASS,PROM,HEPTM,NF
      COMMON/CONC/AA(1),BB(1),DD(1),EE(1),FF(1),AN2,O2,FRAC(150),CO2
      IF (H(K).LT.PIG) GO  TO  55
      M =1
      CPCO2=0.6039775+.1208784E-01*T(K)-.6892165E-05*T(K)**2+.1978687E-
     18*T(K)**3-.2758421E-12*T(K)**4+.1483168E-16*T(K)**5
      CPH2O=.69876E01+.2855784E-02*T(K)+.408244 E-06*T(K)**2-.4530978E-
     29*T(K)**3+.9097223E-13*T(K)**4-.5813041E-17*T(K)**5
      CPN2=.6170795E01+.2272505E-02*T(K)-.7181618E-06*T(K)**2+.1037995E
     309*T(K)**3-.5571979E 14*T(K)**4
      CPO2=.6014893E01+.3832211E-02*T(K)-.2106804E-05*T(K)**2+.6449786E
     4 09*T(K)**3 .9553103E-13*T(K)**4+.5355434E-17*T(K)**5
      CPH2=0.703464E01-0.7481993E-03*T(K)+0.1414508E-06*T(K)**2-0.52323
     59E-09*T(K)**3+0.81761E-13*T(K)**4-0.4673767E-17*T(K)**5
      CPCO=0.6133285E01+0.2539359E 02*T(K)-0.883906E-06*T(K)**2+0.13996
     67E-09*T(K)**3-0.8205784E-14*T(K)**4
      CPCH4=    .3741979E01 .1448081E-01*T(K) .3963176E 05*T(K)**2-.7442
     562E 08*T(K)**3+.2758348E-11*T(K)**4-.3280506E-15*T(K)**5
      CPCET=(0.388+0.00045*(1.8*(T(K)-273.)+32.))/0.7768
      CPRO=-0.966 72.9*T(K)/10.**3 37.55*T(K)*T(K)/10.**6+7.58*T(K)**3/
     60.**9
      CPHEPT=13.03+110.08*T(K)/10.**3-31.9*T(K)*T(K)/10.**6
      D=CPCO2*AA(M)+CPH2O*BB(M)+CPO2*DD(M)+CPH2*FF(M)+CPCO*EE(M) CPN2*A
     72/28.161+(CPRO*PROM+CPCH4*CH4M+CPHEPT*HEPTM)*(1. FRAC(K))
      CPP=D/SUMP
      CPPR=D/AMASS
      G(K)=CPP/(CPP-1.98726)
      T(K 1)=2.*T(K)-T(K-1)
      CM=((5.*PROM+11.*HEPTM)*(CPO2+CPN2*.79/.21)+CPRO*PROM+CPHEPT*HEPT
     1)/(PROM+HEPTM)
      CP=(CPCO2*(3.*PROM+7.*HEPTM) CPH2O*(3.*PROM+8.*HEPTM)+CPN2*(5.*PR
     2M+11.*HEPTM)*0.79/0.21)/(PROM+HEPTM)
      DELH(K)=-(19929.*PROM*44./1.8+10640.*HEPTM*100.2)/(HEPTM+PROM)
     1-CP*(T(K+1) 298.)+CM*(T(K)-298.)
30    RETURN
55    CPCH4=    .3741979E01 .1448081E-01*T(K) .3963176E 05*T(K)**2-.7442
     162E 08*T(K)**3+.2758348E-11*T(K)**4-.3280506E-15*T(K)**5
      CPN2=.6170795E01+.2272505E-02*T(K)-.7181618E-06*T(K)**2+.1037995E
     309*T(K)**3-.5571979E 14*T(K)**4
      CPO2=.6014893E01+.3832211E-02*T(K)-.2106804E-05*T(K)**2+.6449786E
     4 09*T(K)**3 .9553103E-13*T(K)**4+.5355434E-17*T(K)**5
      CPCET=(0.388+0.00045*(1.8*(T(K)-273.)+32.))/0.7768
      CPRO=-0.966 72.9*T(K)/10.**3 37.55*T(K)*T(K)/10.**6+7.58*T(K)**3/
     30.**9
      CPHEPT=13.03+110.08*T(K)/10.**3-31.9*T(K)*T(K)/10.**6
      C=CPCH4*CH4M+CPRO*PROM+CPHEPT*HEPTM+CPN2*AN2/28.161+CPO2*O2/32.
     1+CPCO2*CO2/44.
      CPM=C/SUMM
      CPMM=C/AMASS
5     G(K)=CPM/(CPM-1.98726)
C
20    RETURN
      END
```

```
$IBFTC TRAN
      SUBROUTINE HTTR(AT,RT,HT,HHT,AR,CPPR,CPMM,K,H,P,T,SUMM,SUMP,V)
      DIMENSION AR(150),H(150),V(150),P(150),TT(150),T(150)
      DIMENSION HT(150),HHT(150)
      COMMON/AB/AIRM,CH4M,CETM,PIG,AMASS,PROM,HEPTM,NF
      COMMON/CA/BORE,STROKE,RATIO,CROW,REV,PO,CR,VOLM
      COMMON/CONC/AA(1),BB(1),DD(1),EE(1),FF(1),AN2,O2,FRAC(150),CO2
      COMMON/LOSS/COEF1,COEF2,COEF3,PRAN,M1,TC,DELT1,DELT2,HTR(150),PBD
     1,PP(150),AHT(150)
      COMMON/REY/AX(150),ZZ(150)
      COMMON/HEAT/QQ(150)
      VP=(2.*STROKE*REV/(60.*12.))**0.3333
C
      TT(K)=T(K)**0.645/10.**7
      VOSCH=110.*(P(K)/14.22)**0.8/((BORE*0.3048/12.)**0.2*T(K)**0.53)
      Z=2.*STROKE*REV*0.3048/(60.*12.)
      B=PO*0.491
      TP=TC+DELT1
      TW=TC+DELT2
      DT=T(K)-TW
      DT1=T(K)-TP
      RHO=AMASS/V(K)
      IF(H(K).LT.PIG)  GO  TO  33
      XCO2=AA(1)/SUMP
      XH2O=BB(1)/SUMP
      XO2=DD(1)/SUMP
      XAN2=AN2/(28.161*SUMP)
      XPRO=PROM*(1.-FRAC(K))/SUMP
      XCH4=CH4M*(1.-FRAC(K))/SUMP
      XHEPT=HEPTM*(1.-FRAC(K))/SUMP
      X5=XCO2*6.63
      X6=XH2O*4.24
      X7=XAN2*5.29
      X8=XO2*5.65
      X9=XCO*5.29
      X10=XCH2*1.414
      X11=XH2*1.414
      X12=XPRO*6.63
      X13=XCH4*4.
      X14=XHEPT*10.1
      VISCO2=3.*TT(K)
      VISH2O=2.19*TT(K)
      VISN2=3.07*TT(K)
      VISH2=1.54*TT(K)
      VISCO=3.*TT(K)
      VISCH4=2.25*TT(K)
      VISHEP=0.89*TT(K)
      VISPRO=1.5*TT(K)
      VISP=(X5*VISCO2+X6*VISH2O+X7*VISN2+X8*VISO2+X9*VISCO+X10*VISH2+X1
     1*VISH2+X12*VISPRO+X13*VISCH4 X14*VISHEP)/(X5+X6+X7+X8+X9+ X10+X11
     2X12 X13+X14)
      REY= ABS(RHO*ZZ(K)*AX(K)/VISP)
      CONP=CPPR*VISP/PRAN
C     ANNAND'S CORRELATION
      AT=COEF1*CONP*(REY**COEF2)*2.*(AR(K)*DT+CROW*DT1)*1000./(BORE*REV
      RT=COEF3*((T(K)**4-TW**4)*AR(K)+(T(K)**4-TP**4)*CROW)/(6.*REV*10.
     1*9)
      HT(K)=AT+RT
      REY1=RHO*11.25*BORE/(12.*VISP)
```

```
      AT1=0.26*CONP*(REY1**.750)*2.*(AR(K)*DT+CROW*DT1)*1000./(BORE*REV
      AHT(K)=AT1+RT
      WHT=WOSCH*(2.28*Z+3.24*PBDC*V(K)*(P(K) PP(K))/(202.*VOLM*TO*1000.
     1)**0.8
      HTR(K)=WHT*0.0571*(AR(K)*DT+CROW*DT1)/(6.*REV)
      IF(M1.EQ.0) GO TO 22
      HHT(K)=8.06*VP*SQRT(P(K)*T(K)/B)*(AR(K)*DT+CROW*DT1)/(6.*REV*10.
     1**2)
22    RETURN
33    VISCH4=2.25*TT(K)
      VISCO2=3.*TT(K)
      VISN2=3.07*TT(K)
      VISO2=3.75*TT(K)
      VISHEP=0.89*TT(K)
      VISPRO=1.5*TT(K)
      XCH4=CH4M/SUMM
      XPRO=PROM/SUMM
      XN2=AN2/(28.161*SUMM)
      XO2=O2/(32.*SUMM)
      XHEPT=HEPTM/SUMM
      XCO2=CO2/(44.*SUMM)
      X1=XCH4*4.
      X2=XN2*5.29
      X3=XHEPT*10.1
      X4=XPRO*6.63
      X5=XO2*5.65
      X6=XCO2*5.29
      VISM=(X1*VISCH4+X2*VISN2+X3*VISHEP+X4*VISPRO+X5*VISO2+X6*VISCO2)/
     1(X1 X2+X3+X4+X5+X6)
      REY=ABS(RHO*ZZ(K)*AX(K)/VISM)
      CONM=CPMM*VISM/PRAN
      HT(K)=COEF1*CONM*(REY**COEF2)*DT*(AR(K)+CROW)*1000./(6.*REV*AX(K)
      REY1=RHO*11.25*BORE/(12.*VISM)
      AHT(K)=0.26*CONM*(REY1**.750)*DT*2.*(AR(K)+CROW)*1000./(BORE*REV)
      IF(M1.EQ.0) GO TO 44
      HHT(K)=8.06*VP*SQRT(P(K)*T(K)/B)*(AR(K)*DT+CROW*DT1)/(6.*REV*10.
     1**2)
      WHT=WOSCH*2.28*Z
      HTR(K)=WHT*0.0571*(AR(K)+CROW)*DT/(6.*REV)
44    RETURN
      END
```

```
$IBFTC DISN
      SUBROUTINE DISSN(T,P,K,PO,PIG,SUMP)
      REAL  KP1,KP2,KP3,KP4,KPCO2,KPH2O,T(150),P(150)
      COMMON/CONC/AA(1),BB(1),DD(1),EE(1),FF(1),AN2,O2,FRAC(150),CO2
C     COMPUTATIONS OF DISSOCIATION OF PRODUCTS
      B=0.491*PO
      KP1=-(-.153E01*ALOG(T(K))+.4247E-03*T(K)+(.3953E 08*T(K)**2)-(.10
     1583E-10*T(K)**3)+(.14336E-14*T(K)**4)-(.64025E-19*T(K)**5) .47035
     21+.28664E05/T(K))*.425
      KPH2O=10.**KP1
      KP2=      .59272*ALOG(T(K))-.14358E-02*T(K)+.57245E-06*T(K)**2-.15
     326E 09*T(K)**3+.21033E-13*T(K)**4-.12041E-17*T(K)**5-.29E01+.4740
     41E05/T(K)
      KP3=      .215319E01*ALOG(T(K))-.33569E 02*T(K)+.98802E-06*T(K)**2
     5.21389E-09*T(K)**3+.26565E-13*T(K)**4-.1408E-17*T(K)**5-.1873E01+
     6.1368417E05/T(K)
      KP4=(KP3-KP2)*0.425
      KPCO2=10.0**KP4
      R=AA(1)*0.05
      S=BB(1)*0.05
      IF(DD(1).LE.0.)  GO  TO  20
      EE(1)=AA(1)*KPCO2*SQRT(     SUMP*B/(P(K)*DD(1)))
      FF(1)=BB(1)*KPH2O*SQRT(     SUMP*B/(P(K)*DD(1)))
20    CONTINUE
      SUMP=AA(1)+BB(1)+DD(1)+AN2/28.161
      RETURN
      END
```

```
$IBFTC GRAD
      SUBROUTINE PRGRAD(DP,P,N)
      DIMENSION P(60),DP(60)
      DO 20 K=1,N
      IF(K-2) 15,16,14
14    IF(K-(N-1)) 17,18,19
15    DP(K)=(-21.*P(1) +13.*P(2)+17.*P(3)-9.*P(4))/20.
      GO TO 20
16    DP(K)=(-11.*P(1)+3.*P(2)+7.*P(3)+P(4))/20.
      GO  TO  20
17    DP(K)=(-2.*P(K-2)-P(K-1)+P(K 1)+2.*P(K 2))/10.
      GO TO 20
18    DP(K)=-(-11.*P(N)+3.*P(N-1)+17.*P(N-2) 9.*P(N-3))/20.
      GO TO 20
19    DP(K)=-(-21.*P(N)+13.*P(N-1) 17.*P(N-2)-9.*P(N-3))/20.
20    CONTINUE
      RETURN
      END
```

```
$IBFTC SIMS
      SUBROUTINE SIMP(TQ,Q,K)
      DIMENSION TQ(60),Q(60)
C     SUMMATION OF GROSS RATES OF HEAT RELEASE BY SIMPSONS, RULE
      L=K/2
      L=2*L
      IF(L.EQ.K) GO TO 67
      IF(K-3) 67,61,62
61    TQ(K)=0.33333*(Q(1)+4.*Q(2)+Q(3))
      GO TO 88
62    IF(K-5) 67,63,64
63    TQ(K)=0.33333*(Q(1)+4.*(Q(2) Q(4))+2.*Q(3)+Q(5))
      GO  TO  88
64    SUM4=0.0
      SUM2=0.0
      KK=K-1
      LL=K-2
      DO 65 I=2,KK,2
65    SUM4=SUM4+Q(I)
      DO 66I= 3,LL,2
66    SUM2=SUM2+Q(I)
      TQ(K)=0.333*(Q(I)+Q(K)+4.*SUM4+2.*SUM2)
      GO TO 88
67    TQ(K)=0.0
88    RETURN
      END
```

```
$IBFTC FINT
      SUBROUTINE FINRAT(TQ,N,FRAC,PIG,H)
      DIMENSION FRAC(60),TQ(60),H(60)
      PP=PIG+1.
      N1=N-1
      DO 300 K=1,N
      IF(H(K).GT.PP) GO TO 100
      FRAC(K)=0.0
      IF(H(K)-PIG)300,200,200
200   IF(TQ(K).EQ.0.) GO TO 300
      TQI=TQ(K)
300    CONTINUE
100   DO 400 K=2,N1
      IF(H(K)-PIG) 400,400,500
500   IF(TQ(K).NE.0.) GO TO 111
      TQ(K)=(TQ(K 1)+TQ(K+1))/2.
111   FRAC(K)=(TQ(K)-TQI)/(TQ(N-1) TQI)
      IF(FRAC(K).GT.1.) FRAC(K)=1.
400   CONTINUE
      RETURN
      END
```

```
$IBFTC KITC
      SUBROUTINE KIN TIC(AM,H,T,Q,V,N)
      DIMENSION H(150),T(150),Q(150),V(150),AM(150),AMF(150),FAMF(150)
     1 AMFF(150),AMO2FF(150),FMO2(150),D(150),FFAMF(150),YY(150),C1(150
     2,B(150),A1(150,4),E(150),X(150),Y(150),C(150),
     3 AMO2F(150),O2FF(150),FO2FF(150)
      COMMON/AB/AIRM,CH4M,CETM,PIG,AMASS,PROM,HEPTM
      COMMON/RES/PROP,HEPTP,RAT
      COMMON/CONC/AA(1),BB(1),DD(1),EE(1),FF(1),AN2,O2,FRAC(150),CO2
      AMO2FI=AIRM*28.97*0.23+DD(1)*RAT
      AMFI=PROM*44.+HEPTM*100.2+CH4M*16.+(HEPTP+PROP+CH4P)*RAT
      SUM=0.
      WRITE(6,100)
100   FORMAT(1H0,97H H(K)   T(K)   FRAC(K) FAMF FFAMF O2FF FO2FF    AMF(K)
     1    AMO2F(K)    AMFI        AMO2FI                    )
      RATIO1=CH4M*16./(HEPTM*100.2)
      RATIO=PROM*44./(HEPTM*100.2)
      DO 20 K=1,N
      IF(AM(K).LE.0.) GO TO 20
      IF(H(K).LT.PIG) GO TO 20
      IF(Q(K).LE..75) GO  TO  20
      SUM=SUM+AM(K)
      AMB=SUM
      AMF(K)=AMFI  AMB
      IF(AMF(K).LE.0.) AMF(K)=.001*AMFI
      FAMF(K)=AMF(K)/AMFI
      AMFF(K)=AMF(K)/V(K)
      HEPTB=AMB/(1.+RATIO)
      CH4B=HEPTB*RATIO1
      PROB=HEPTB*RATIO
      AMO2=HEPTB*88./25.+PROB*40./11.+4.*CH4B
      AMO2F(K)=AMO2FI-AMO2
      AMO2FF(K)=AMO2F(K)/V(K)
      FFAMF(K)=1.  FAMF(K)
      O2FF(K)=AMO2F(K)/AMO2FI
      FO2FF(K)=1.  O2FF(K)
      B(K)=1./(1.98726*T(K))
      A1(K,1)=ALOG(AMO2FF(K))
      A1(K,2)=ALOG(AMFF(K))
      A1(K,3)=-B(K)
      A1(K,4)=ALOG(T(K))/2.
      YY(K)=ALOG(AM(K)/V(K))
60    WRITE(6,10)H(K),T(K),FRAC(K),FAMF(K),FFAMF(K),O2FF(K),FO2FF(K),AM
     1(K),AMO2F(K),AMFI,AMO2FI
10    FORMAT(1H ,F5.1,1X,F7.2,5(1X,F5.3),4E10.3)
20    CONTINUE
      WRITE(6,200)
200   FORMAT(1H0,86HH(K)       E(K)          C1(K)      X(K)      AM(K)
     1    T(K)      M  BK              AK      )
      M=1
      N1=N-1
      DO 30 K=1,N1
      IF(H(K).LT.PIG) GO TO 30
      IF(Q(K).LE..75)  GO  TO  30
      M=M 1
      A1(K,1)=A1(K,1)-A1(K 1,1)
      A1(K,2)=A1(K,2)-A1(K 1,2)
      A1(K,3)=A1(K,3)-A1(K 1,3)
      A1(K,4)=A1(K,4)-A1(K 1,4)
```

```
      YY(K)=YY(K) YY(K+1)
      YY(K)=YY(K) A1(K,1)-A1(K,2)
      E(K)=YY(K)/A1(K,3)
50    CONTINUE
      C1(K)=ALOG((AM(K)/V(K))/(AMFF(K)*AMO2FF(K)))
      X(K)=B(K)*1.98726*10.**3
      Y(K)=C1(K)
      BK= E(K)/(1.98726*T(K))
      IF(ABS(BK).GE.88.)  GO  TO  300
      AK=AM(K)/(V(K)*AMO2FF(K)*AMFF(K)*EXP(BK))
300   WRITE(6,40)H(K),E(K),C1(K),X(K),AM(K),T(K),M,BK,AK
40    FORMAT(1H ,F5.1,2X,E12.4,2(2X,F7.3),1X,E12.4,2X,F9.3,2X,I2,2E12.4
30    CONTINUE
      RETURN
      END
```

```
$IBFTC RESIDUE
      SUBROUTINE RESID(PBDC,VOLM,TEXH,TO,CPMM,CPPR,SUMM,SUMP,P,T,AMASS,
     1PO,R)
      COMMON/CONC/AA(2),BB(1),DD(1),EE(1),FF(1),AN2,O2,FRAC(150),CO2
      DIMENSION T(150),P(150)
      COMMON/RES/PROP,HEPTP,RAT
      A=144.*PBDC*VOLM/R
      RES=(A-AMASS*TO)*0.242/(CPPR*TEXH)
      RAT=RES/AMASS
      SUMM=SUMM+RAT*SUMP
      SUMP=SUMP*(1.+RAT)
      AA(1)=AA(1)*(1.+RAT)
      BB(1)=BB(1)*(1.+RAT)
      DD(1)=DD(1)*(1.+RAT)
      AN2=AN2*(1. RAT)
      AMASS=AMASS*(1.+RAT)
      WRITE(6,1)     RAT,TEXH,PBDC
1     FORMAT(1H0,50X,10HRESIDUALS=,E12.4,2F10.2)
      WRITE(6,2)
2     FORMAT(1H0,25X,61HCOMPUTATIONS OF HEAT RELEASE RATES ACCOUNTING F
     1R   RESIDUALS)
      RETURN
      END
```

A P P E N D I X VII

THEORY OF SMOOTHING OF DATA SCATTER

As we referred the pressure variations to per degree crank rotation, it can be assumed that the second derivative $d^2P/d\theta^2$ does not change essentially during the course of a few measurements (53). In particular we want to combine every measurement with its two neighbours to the left and two to the right. Thus we have five points of measurement under consideration, which we assume to lie on a parabola of second order defined as follows:

$$P = a + b\theta + c\theta^2 \qquad (1)$$

In equation (1) the coefficients a, b and c need adjustment to our data. As three coefficients cannot be adjusted to a data of five, we use the principle of least squares, which suggests that for general conformity of actual and observed values, the sum of the squares of their residuals should be a minimum. Thus if s is such a sum, we have:

$$s = \sum_{\theta=1}^{\theta=5} (P - P')^2 \qquad (2)$$

where P and P' are the actual and measured pressures, respectively.

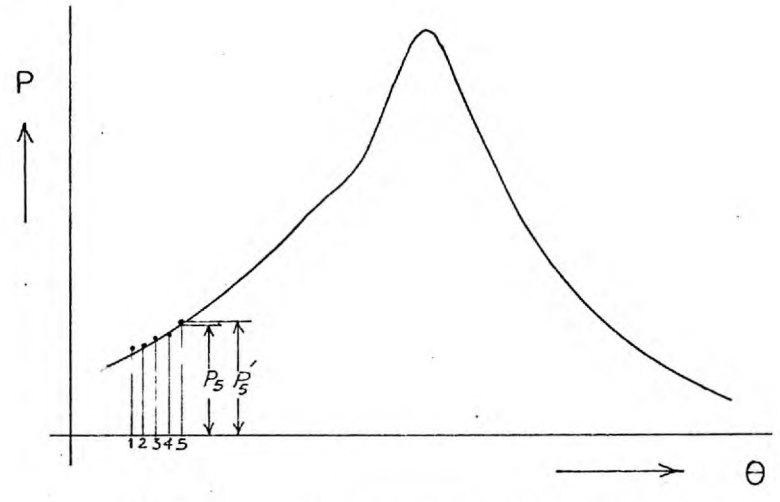


Fig. Pressure-Time Record.

Now the sum of equation (2) to be $\min^m$:

$$\frac{ds}{da} = \frac{ds}{db} = \frac{ds}{dc} = 0 \quad .$$

Applying first and last condition, i.e. $\frac{ds}{da} = \frac{ds}{dc} = 0$, we get the following two 'normal equations':

$$5a + 10c - \sum_{\theta=1}^{\theta=5} P' = 0 \qquad (3)$$

$$10a + 34c = \sum_{\theta=1}^{\theta=5} K^2 P' = 0 \qquad (4)$$

Where in equation (4) $K = \theta_2 - \theta_1 = \theta_4 - \theta_3 = 1$.

Since the parabola passes through the point of consideration such that from equation (1)

$$P'_3 = a \text{ for } \theta_3 = 0. \qquad (5)$$

Solution of equations (3), (4) and (5) for 'a' gives:

$$\begin{aligned} 70a &= -6P'_1 + 24P'_2 + 34P'_3 + 24P'_4 - 6P'_5 \\ &= 70P'_3 - 6(P'_1 - 4P'_2 + 6P'_3 - 4P'_4 + P'_5) \\ &= 70P'_3 - 6\delta^4 P'_3 \end{aligned}$$

where $\delta^4 P'_3$ denotes the fourth central difference of the zero line. Thus,

$$P_3 = a = P'_3 - \frac{3}{35}\delta^4 P'_3$$

Thus similar procedure can be carried out for P_3 to P_{n-2}. But the same treatment does not hold good for P_1, P_2, P_{n-1}, P_n which do not either have two neighbours upstream or downstream. For the first two points we also have the third value P'_3. Simple reasoning could lead to the following relations:

$$P_2 = P'_2 - \frac{2}{5}\delta^3 + \frac{1}{7}\delta^4$$

$$P_1 = P'_1 + \frac{1}{5}\delta^3 - \frac{3}{35}\delta^4 \quad ,$$

where δ^3 and δ^4 refer to the nearest available central differences. Similar reasoning shall apply to P_{n-1} and P_n.

$$P_n = P'_n - \frac{1}{5}\delta^3 + \frac{3}{35}\delta^4$$

$$P_{n-1} = P'_{n-1} + \frac{2}{5}\delta^3 - \frac{1}{7}\delta^4 \quad .$$

A P P E N D I X VIII

THE SIMPSON'S RULE OF INTEGRATION FOR EVALUATING CUMULATIVE HEAT RELEASE

The Simpson's rule suggests that the curve whose guadrature is required can better be approximated to follow a parabola for three consecutive points. This method is a better approximation than the trapezoidal rule, particularly for the quadrature of a curve with equal intervals. It can be shown that the area bounded by three consecutive ordinates under the curve is as follows:

$$Q_{1-3} = \frac{1}{3} (\dot{q}_1 + 4\dot{q}_2 + \dot{q}_3)$$

We, therefore, separate the odd and even ordinates and apply them with different weights. However, except the initial and last four values of the rates of heat release, we can improve the approximation by employing five consecutive values for quadrature, thus:

$$Q_{1-5} = \frac{1}{3} (\dot{q}_1 + 4(\dot{q}_2 + \dot{q}_4) + 2\dot{q}_3 + \dot{q}_5) \quad .$$

A P P E N D I X IX

EVALUATION OF COMPOSITION OF PRODUCTS

The complete combustion of pilot oil and methane charge can be represented as:

$$wC_{16}H_{34}+xCH_4+yO_2+zN_2 = aCO_2+bH_2O+CN_2+dO_2 \quad (1)$$

where, w, x, y and z are known by measurements.

If CO_2 and H_2O are assumed to dissociate as follows:

$$CO_2 = CO + \tfrac{1}{2}O_2 \quad (2)$$

$$H_2O = H_2 + \tfrac{1}{2}O_2 \quad (3)$$

the quantities of CO_2, H_2O and O_2 are estimated from equation (1) on the basis of mass balance

$$m_{CO_2} = a = 16w + x \quad (4)$$

$$m_{H_2O} = b = 2x + 17w \quad (5)$$

$$m_{O_2} = d = y - a - \frac{b}{2} \quad (6)$$

After evaluating the quantities of CO_2, H_2O and O_2 after combustion with gross approximations, as shown above, we revert to finding the dissociated products as follows:

$$\text{Let } K_1 = \frac{(CO)(O_2)^{\frac{1}{2}}}{(CO_2)} \cdot \left(\frac{p}{\Sigma m}\right)^{\frac{1}{2}} \quad (7)$$

$$K_2 = \frac{(H_2)(O_2)^{\frac{1}{2}}}{(H_2O)} \cdot \left(\frac{p}{\Sigma m}\right)^{\frac{1}{2}} \quad (8)$$

where K_1 and K_2 are equilibrium constants of dissociation for CO_2 and H_2O, respectively.

Since in J.A.N.A.F. Tables (31) we get only the equilibirum constant of formation, K_1 was calculated indirectly as follows:

$$\text{Let } K_3 = \frac{(C)(O_2)}{(CO_2)}$$

$$\text{and } K_4 = \frac{(C)(O_2)^{\frac{1}{2}}}{(CO)}$$

$$K_1 = \frac{K_3}{K_4} \cdot \left(\frac{p}{\Sigma m}\right)^{\frac{1}{2}} = \frac{(CO)(O_2)^{\frac{1}{2}}}{(CO_2)} \cdot \left(\frac{p}{\Sigma m}\right)^{\frac{1}{2}} \quad ;$$

similarly, for the reaction $H_2 + \frac{1}{2}O_2 \rightarrow H_2O$,

$$K_5 = \frac{(H_2O)}{(H_2)(O_2)^{\frac{1}{2}}}$$

and K_5 has been defined as polynominal if temperature is as follows:

$$\ell n(K_5) = \frac{a}{R} \ell n\, T + \frac{b}{2R} T + \frac{c}{6R} T^2 + \frac{d}{12R} T^3 + \frac{e}{20R} T^4 + \frac{f}{30R} T^5 - \frac{1}{R} - \frac{\Delta H_o}{RT}$$

$$\ell n(K_2) = -\left(\frac{a}{R} \ell nT + \frac{b}{2R} T + \frac{c}{6R} T^2 + \frac{d}{12R} T^3 + \frac{e}{20R} T^4 + \frac{f}{30R} T^5 - \frac{1}{r} - \frac{\Delta H_o}{R} \cdot \frac{1}{T}\right)$$

$$= -x \text{ (say)} \quad .$$

In computer programme, in order to facilitate computations, K_2 has been defined as follows:

$$K_2 = e^{-x} = 10^{-0.425x} \quad .$$

After evaluating the dissociation constants the concentrations of (CO), (H_2) and (O_2) have been found as follows:

$$(CO) = \frac{K_1 \cdot m_{CO_2}}{m_{O_2}^{\frac{1}{2}}} \left(\frac{\Sigma m}{P}\right)^{\frac{1}{2}}$$

Similarly, $$(H_2) = \frac{K_2 \cdot m_{H_2O}}{m_{O_2}^{\frac{1}{2}}} \left(\frac{\Sigma m}{P}\right)^{\frac{1}{2}}$$

It was found that the concentrations of (H_2) and (CO) were negligible at temperatures below $1600^{o}K$.

A P P E N D I X X

EVALUATION OF $\frac{dP}{d\theta}$ by EMPIRICAL DIFFERENTIATION

The least squares method for minimising the differences of the derivative has been adopted. As mentioned in Appendix VII instead of evaluating corrected value of function at $\theta = 0$, we are now interested in the coefficient b. The condition of minimum differences gives the following general formulae for a series of P corresponding to $\theta = 1$ to n.

$$\left(\frac{dP}{d\theta}\right)_{\theta = 3} = \frac{-2P_1 - P_2 + P_4 + 2P_5}{10}$$

$$\left(\frac{dP}{d\theta}\right)_{\theta = n-2} = \frac{-2P_{n-4} - P_{n-3} + P_{n-1} + 2P_n}{10}$$

The formulae of the first two and last two derivatives which do not have either downstream or upstream neighbours, are:

$$\left(\frac{dP}{d\theta}\right)_{\theta = 1} = \frac{-21xP_1 + 13P_2 + 17P_3 - 9P_4}{20}$$

$$\left(\frac{dP}{d\theta}\right)_{\theta = 2} = \frac{-11P_1 + 3P_2 + 7P_3 + P_4}{20}$$

$$\left(\frac{dP}{d\theta}\right)_{\theta = n-1} = \frac{-11P_n + 3P_{n-1} + P_{n+1} + 2P_{n+2}}{20}$$

$$\left(\frac{dP}{d\theta}\right)_{\theta = n} = \frac{-21P_n + 13P_{n-1} + 17P_{n-2} - 9P_{n-3}}{20}$$

A P P E N D I X XI

LIST OF SYMBOLS

a, b	Order of reaction
c	Constant
$\overline{Cp}$, $\overline{Cv}$	Mean specific heats at constant pressure and volume corresponding to charge temperature
D	Engine bore
$\overline{E}$	Overall activation energy of chemical reaction
f	Fraction of fuel burnt
h	Step-length in computations
ΔH_T	Heat of combustion of fuel at temperature T with reference to Standard temperature
J	Mechanical equivalent of heat
k	Conductivity of the charge
K	Reaction rate constant
m	Mass of the charge
m_f	Relative mass of the fuel to the charge
$\dot{m}'''$	Rate of reaction per unit volume and time
M	Molecular weight
n	Molar concentration
Nu	Nusselt number
p	Cylinder gas pressure
$dp/d\theta$	Rate of pressure change
Δp	Rise of pressure across a finite interval
$\dot{q}$	Net rate of heat release
$\dot{q}_g$	Gross rate of heat release
Q	Cumulative heat release
$\dot{Q}''_{HT}$	Rate of heat transfer per unit area and time
R	Universal gas constant
Re	Reynolds number
T	Cylinder gas temperature
Tw	Cylinder wall temperature
V	Cylinder volume
$dv/d\theta$	Rate of change of cylinder volume
Vp	Mean piston speed

ρ	Charge density
$\overline{\gamma}$	Specific heat ratio
θ	Crank angle
μ	Viscosity
ϵ	Percentage error
τ	Ignition lag
$\Delta\tau$	Duration of first stage combustion

Subscripts

j	Combustion product
θ	Crank angle
b	Burnt fraction of the fuel
f	Fuel
ox	Oxygen
o	Initial conditions at the beginning of compression
1, 2	First and second stages of combustion

Abbreviations

B.H.P.	Brake Horse Power
B.M.E.P.	Brake Mean Effective Pressure
C.F.R.	Cooperative Fuel Research
K.L.B.M.E.P.	Knock Limited Brake Mean Effective Pressure
L.P.G.	Liquified Petroleum Gases
L.N.G.	Liquified Natural Gas
T.D.C.	Top Dead Centre

A P P E N D I X XII

REFERENCES

1. AFFLECK, W.S. and FISH, A. (1968)
"Knock: flame acceleration on spontaneous ignition?" Combustion and Flame, Vol. 12, No. 3, p. 243.

2. AFFLECK, W.S. and FISH, A. (1967)
"Two-stage ignition under engine conditions parallel that at low pressures." Eleventh Symposium (international) on combustion, p. 1003. The Combustion Institute: Pittsburg.

3. AFFLECK, W.S. and THOMAS, A. (1969)
"An opposed piston rapid compression machine for preflame reaction studies." Proc. I. Mech. E., Vol. 183.

4. ANNAND, W.J.D. and ABAYAZID, O.M. (1967)
"Self-ignition of propane-air mixtures in a supercharged, motored reciprocating enge." Proc. I. Mech. E., (1966-67) Vol. 181, Part 1, No. 20, p. 467.

5. ANNAND, W.J.D. (1963)
"Heat transfer in the cylinders of reciprocating internal combustion engines." Proc. I. Mech. E., Vol. 177, No. 36, p. 973.

6. "A.S.T.M. Manual for rating motor fuels by Motor and Research Methods." (1960)
Pub: American Soc. of Testing Materials, Philadelphia Pa., U.S.A.

7. "Methods for the Measurement of Fluid Flow in Pipes." B.S. 1042: Part 1: 1964. Pub: British Standards Institution, London.

8. ANON.(1969)
"Diesel buses converted to dual-fuel." The Engineer, Vol. 227, No. 5894, Jan. 1969, p. 41.

9. ANON. (1968)
"Dual-fuel engines: competitive power." Engineering, Vol. 206, No.5356, p. 900.

10. AZZOUZ, D. (1966)
"Some studies of combustion processes in dual-fuel engines." M.Sc. (Eng.) Thesis, London University.

11. BALL, G.A. (1955)
"Photographic studies of cool flames and knock in an engine." Fifth Symposium (International) on Combustion, p. 366, Reinhold: New York.

12. BECK, N.J., SIMON, K.C., OYEHARA, O.A., WINANS, J.G. and MYERS, P.S. (1955)
"Temperature measurement from iodine absorption spectrum." Fifth Symposium (International) on Combustion, p. 412. Reinhold: New York.

13. BOYCE, T.R. (1969)
"The pre-ignition processes in compression - ignition engines." Ph.D. Thesis, London University.

14. BOYER, R.L. (1949)
"New diesels burn gas or oil." S.A.E. Journal, Vol. 57, May 1949, p. 47.

15. CORNELIUS, W. and CAPLAN, J.D. (1952)
"Some effects of fuel structure, tetraethyl lead, and engine deposits on precombustion reactions in a fired engine." S.A.E. Quart. Trans., Vol. 6, No. 3, p. 488.

16. DOWNS, D. and WHEELER, R.W. (1952)
"Recent developments in "knock" research." Proc. I. Mech. E. (A.D.) 1951-52, Part III, pp. 89-99.

17. DOWNS, D., STREET, J.C. and WHEELER, R.W. (1953)
"Cool flame formation in a motored engine." Fuel, Vol. 32, p. 279.

18. EGERTON, A.C. (1957)
"Methane and its combustion." Melchett Lecture for 1956, J. Inst. Fuel, Vol. 30, p. 3.

19. EICHELBERG, G. (1939)
"Some new investigations of old combustion engine problems." Engineering, Vol. 148, p. 3870, 3871; 463, 682, 547, 603 and Vol. 149, p. 297.

20. ELLIOT, M.A. and DAVIS, R.M. (1951)
"Dual-fuel combustion in diesel engines." Ind. and Eng. Chem., Vol. 43, 1951, p. 2854.

21. ELLIOT, M.A. (1949)
"Combustion of diesel fuel." S.A.E. Quart. Tr. Vol. 3, No. 3, p. 490.

22. FELT, A.E. and STEELE,JR., W.A. (1962)
"Combustion control in dual-fuel engines." S.A.E. Trans., Vol. 70, p. 644.

23. FISH, A., READ, I.A., AFFLECK, W.S. and HASKELL, W.W. (1969)
"The controlling role of cool flames in two stage ignition." Combustion and Flame, Vol. 13, No. 1, p. 39.

24. FRISTROM, R.M. and WESTENBERG, A.A. (1965)
"Flame Structures". McGraw Hill Book Co.

25. GARNER, F.H., GRIGG, G.H., MORTON, F. and REID, W.D. (1956)
"Preflame reactions in diesel engines - Part III." J. Inst. Pet., Vol. 42, No. 387, p. 69.

26. GARNER, F.H., MORTON, F. and SAUNBY, J.B. (1961)
"Preflame reactions in diesel engines - Part V. A study of temperature, pressure and ignition delay." J. Inst. Pet., Vol. 47, No. 450, p. 175.

27. GEE, D.E. and KARIM, G.A. (1966)
"Heat release in a compression - ignition engine." The Engineer, Sept. 1966, p. 473.

28. GOUDIE, G.O. (1969)
Private communication regarding heat release analyses of 'M' system of combustion.

29. HASKELL, W.W. and BAME, J.L. (1966)
"Engine knock - an end-gas explosion." S.A.E. Paper No. 650506.

30. HOPKINS, V.H.F., TALBOT, R.J. and WHITEHOUSE, N.D. (1962)
"The development of dual-fuel engines for powers above 1500 B.H.P." Proc. Sixth C.I.M.A.C. Congress, Copenhagen.

31. "J.A.N.A.F. Thermochemical Tables" (1965)
Published by U.S. Dept. of Commerce - National Bureau of Standards: Washington, D.C., U.S.A.

32. JOST, W.(1946)
"Explosion and combustion processes in gases." (In German). Translated into English by H.O. Croft, McGraw Hill Book Co., New York and London.

33. JOST, W. (1963)
"Knock reactions." Ninth Symp. (International) on Combustion, p. 1013, Academic Press.

34. KAKIMOTO, H. (1962)
Contribution to the discussion on "Multifuel Engine Practice" by J.S. MEURER. S.A.E. Vol. 70, p. 729.

35. KARIM, G.A. (1966)
"An analytical approach to the uncontrolled combustion phenomena in dual-fuel engines." J. Inst. Fuel, Dec. 1964, p. 530.

36. KARIM, G.A. (1968-1969)
Private communications.

37. KARIM, G.A. (1968)
"The ignition of a premixed fuel and air charge by pilot fuel spray injection with reference to dual-fuel combustion." S.A.E. Paper No. 680768.

38. KARIM, G.A. and KLAT, S.R. (1966)
"The knock and autoignition characteristics of some gaseous fuels and their mixtures." J. Inst. Fuel, March 1966, p. 109.

39. KARIM, G.A. and KHAN, M.O. (1969)
"The determination of gross chemical kinetic data for the combustion of common fuels using a motored piston engine." J. Inst. Fuel, Vol. 42, No. 340, p. 340.

40. KARIM, G.A., KHAN, M.O. and MOORE, N.P.W. (1970)
"Gross chemical kinetics from motored engines." A paper in the press for S.A.E. Annual Meeting, Detroit, Jan. 1970.

41. KARIM, G.A. (1968)
"Combustion in dual-fuel engines - A status report." Proc. of Eighth C.I.M.A.C. Congress, Brussels.

42. KARIM, G.A. and KHAN, M.O. (1968)
"Examination of effective rates of heat release in a dual-fuel engine." J . Mech. Engg. Sc., Vol. 10, No. 1, p. 13.

43. KARIM, G.A., KLAT, S.R. and MOORE, N.P.W. (1967)
"Knock in dual-fuel engines." Proc. I. Mech. E., Vol. 181, Part I, No. 20, p. 453.

44. KARIM, G.A. and KLAT, S.R. (1965)
"The measurement of the mass flow rate of different gases using a choked nozzle." Lab Practice, Vol. 15, No. 2, p. 184.

45. KARIM, G.A., MOORE, N.P.W. (1963)
"The simultaneous production of sythensis gas and power in a compression - ignition engine." J. Inst. Fuel, Vol. 36, p. 98.

46. KARIM, G.A. and KHAN, M.O. (1967)
"A generalised computer programme for the determination of rates of heat release a d heat transfer in reciprocating engines." Imperial College, Dept. of Mech. Eng. Tech. Note No. C/TN/4, Dec. 1967.

47. KARIM, G.A. and ROGERS, A.J. (1967)
"Comparative studies of propane and butane as dual-fuel engine fuels." J. Inst. Fuel, Nov. 1967, p. 513.

48. KATZ, D.L. (ed.) (1959)
"Handbook of Natural Gas Engineering." McGraw Hill Book Co., New York.

49. KHAN, M.O. (1966)
"Some further studies of combustion processes in dual-fuel engines." M.Sc.(Eng.) Thesis, London Univ.

50. KHAN, M.O. (1967)
Discussion to two papers on knock and self-ignition in I.C. engines. Proc. I. Mech. E., Vol. 181, Part I No. 20, p. 478.

51. KLAT, S.R. (1965)
"Combustion mechanisms in dual-fuel engines." Ph.D. Thesis, London University.

52. KRIEGER, R.B. and BORMAN, G.L. (1966)
"The computations of apparent heat release for internal combustion engines." A.S.M.E. Paper No. 66-WA/DGP-4, Nov. 1966.

53. LANCZOS, C. (1957)
"Applied Analysis." Sir Isaac Pitman and Sons Ltd., London.

54. LAND, M.L. (1967)
"Performance and operation of spark-ignited gas engines." Proc. I. Mech. E., Vol. 181, Part I. (Nominated lecture).

55. LEIKER, M. (1967)
"Gas and dual-fuel engines in today's power industry." (In German). MTZ Vol. 28, Dec. 1967, No. 12, pp. 487 - 492.

56. LEIKER, M. (1965)
"Gas engines and dual-fuel engines and gaseous fuels." (In German). MTZ Vol. 26, May 1965, No. 5, pp. 195 - 212.

57. LEVEDAHL, W.J. (1965)
"Multistage autoignition of engine fuels." Fifth Symposium (International) on Combustion, p. 372. Reinhold: New York.

58. LEWIS, B. and VON ELBE, G.J. (1961)
"Combustion, Flames and Explosion of Gases." Academic Press.

59. LICHTY, L.C. (1967)
"Combustion Engine Processes." Revised 6th Ed., McGraw Hill Book Co.

60. LIVENGOOD, J.L., TAYLOR, C.F. and WU, P.C. (1958)
"Measurement of gas temperature in an engine by velocity of sound method." S.A.E. Trans., Vol. 66, p. 683.

61. LIVENGOOD, J.C. and WU, P.C. (1955)
"Correlation of autoignition phenomena in internal combustion engines and rapid compression machines." Fifth Symposium (International) on Combustion, p.347, Reinhold: New York.

62. LYN, W.T. (1962)
"Study of burning rate and nature of combustion in a diesel engine." Ninth Symposium (International) on Combustion, p. 1069.

63. LYN, W.T. and AUSTEN, A.E.W. (1960)
"Calculations of the effects of rate of heat release on the shape of cylinder pressure diagrams and cycle efficiency." Proc. I. Mech. E. (A.D.), No. 1, 1960 - 1961, pp. 34 - 63.

64. MA, A.S.C. and MOORE, N.P.W. (1966)
"Autoignition and knock characteristics of benzine-n-heptane air mixtures." Combustion and Flame, Vol. 10, No. 3, p. 245.

65. MALE, T. (1949)
"Photographs at 500,000 frames per second of combustion and detonation in a reciprocating engine." Third Symposium (International) on Combustion, p. 721, Williams and Wilkins: Baltimore.

66. MALMBERG, E.W., SMITH, M.L., BIGLER, J.E. and BOBBIT, J.A. (1955)
"A study of cool flames and associated reactions in an engine." Fifth Symposium (International) on Combustion, p. 385. Reinhold: New York.

67. McAULAY, K.J. (1966)
"Development and evaluation of the simulation of the compression - ignition engine." S.A.E. paper 650451.

68. MILKINS, E.E. (1967)
"Heat transfer from a rapidly compressed gas." M.Sc. (Eng.) Thesis, London, University, Nov. 1967.

69. MILLER, R.E. (1959)
"Some factors governing the ignition delay of a gaseous fuel." Seventh Symposium (International) on Combustion, Butterworths and Co., London, p. 417.

70. MILLER, C.D. (1947)
"Roles of detonation waves and autoignition in spark-ignition engine knock as shown by photographs taken at 40,000 and 200,000 frames per second." S.A.E. Quart. Trans., Vol. 1, Jan. 1947.

71. MINKOFF, G.J. and TIPPER, C.F.H. (1962)
"Chemistry of Combustion Reactions." Butterworth & Co. (Publishers) Ltd., London, 1962.

72. MOORE, N.P.W. and LEWIS, J.D. (1953)
"An investigation of combustion in dual-fuel engines." Proc. Quatrième Congrés International du Chauffage Industriel, Group 1, Section 12, Paper 45.

73. MOORE, N.P.W. and ROY, B.N. (1959)
"Studies of autoignition and knock with propane as an engine fuel." Combustion and Flame, Vol. 3, No. 4, p. 421.

74. MOORE, N.P.W. and MITCHELL, R.W.S. (1955)
"Combustion in dual-fuel engines." Proc. of the Joint Conf. on Combustion, I. Mech. E./A.S.M.E., p. 300.

75. MOORE, N.P.W. and SIMONSON, J.R. (1955)
"The oxidation of weak methane - air mixtures at high temperatures." Fifth Symp. (International) on Combustion, p. 458, Reinhold: New York.

76. MOORE, N.P.W. and LYN, W.T. (1951)
"Combustion of weak mixtures of methane and propane by pilot oil ignition in a compression - ignition engine." Fuel, 1951, Vol, 30, p. 158.

77. NG, H.L. (1963)
"Investigation of the ignition of hydrocarbon-air mixtures in an adiabatic compression machine." Ph.D. Thesis, London University.

78. NUSSELT, W. (1914)
"Abstract of early Nusselt heat transfer papers." A.S.M.E. Journal 36, pp. 098 - 0101.

79. OBERT, E.F. (1968)
"Internal Combustion Engines." 3rd Ed. International Text Book Co., Scranton, Pa.

80. OVERBYE, V.D., BENNETHUS, J.E., UYEHARA, O.A. and MYERS, P.S. (1961)
"Unsteady heat transfer in engines." S.A.E. Trans., Vol. 69, p. 461.

81. PAHNKE, A.J., COHEN, P.M. and STURGIS, B.M. (1954)
"Preflame oxidation of hydrocarbons in a motored engine." Ind. Engg. Chem., Vol. 46, No. 5, pp. 1024 - 1029.

82. PASTELL, D.L. (1950)
"Precombustion reactions in a motored engine." S.A.E. Quart. Trans., Vol. 4, No. 4, pp. 571-587.

83. PATTERSON, D.J. and VAN WYLEN, G. (1964)
"A digital computer simulation for spark-ignited engine cycles." S.A.E., Progress in Technology, Vol. 7, p. 82.

84. RASSWEILER, G.M. and WITHROW, L. (1938)
"Absorption spectra of gaseous charges in a gasoline engine." Ind. and Eng. Chem., Vol. 25, p. 923.

85. SCHEUERMEYER, M., STEIGERWALD, H. (1943)
"The measurement of the ignition lag of compressed fuel and air mixtures for the purpose of investigating the tendency to knocking." M.T.Z., Vol. 8, No. 9, 1943. (In German).

86. SCHWEITZER, P.H. (1926)
"The tangent method of analysis for indicator cards of internal combustion engines." Pennsylvania State University Engineering Experiment Station, Bulletin 35.

87. SHIPINSKI, J., UYEHARA, O.A. and MYERS, P.S. (1968)
"Experimental correlation between rate-of-injection and rate-of-heat-release in a diesel engine." A.S.M.E. 68-DGP-11, May 1968.

88. SITKIE, G. (1962)
"Contribution to the theory of heat transfer in the internal combustion engine." (in German) Konstruktion, 14, 67, p. 17. (B.I.C.E.R.A. English translation No. 63/T2, July 1963).

89. SOKOLIK, A.S. (1960)
"Self-ignition, flame and detonation in gases." (In Russian). Translated in English by N. Kaner (1963).

90. SPIERS, H.M. (Ed.), (1962)
"Technical data on Fuel." Published by The British National Committee, World Power Conference, London.

91. STEINBERG, M. and KASKAN, W.E. (1955)
"The ignition of combustible mixtures by shock waves." Fifth symposium (International) on Combustion, p. 664, Reinhold, New York.

92. TAYLOR, C.F., TAYLOR,E.S., LIVENGOOD, J.C., RUSSELL, W.A. and LEARY, W.A. (1950)
"Ignition of fuels by rapid compression." S.A.E. Quart. Trans. Vol. 4, No. 2., pp. 232-274.

93. TOPPING, J. (1962)
"Errors of observation and their treatment." 3rd. Ed. Chapman and Hall Ltd.

94. TOWNEND, D.T.A. and CHAMBERLAIN, E.A.C. (1936)
"The influence of pressure on the spontaneous ignition of inflammable gas-air mixtures. IV - Methane-, Ethane-, and propane-air mixtures." Proc. Roy. Soc. A., Vol. 154, p. 95.

95. TOWNEND, D.T.A., COHEN, L.L. and MANDLEKAR, M.R. (1934)
"The influence of pressure on the spontaneous ignition of inflammable gas-air mixtures. III - Hexane- and Iso-butane-air mixtures." Proc. Roy. Soc. A., Vol. 146, p. 113.

96. TSAO, K.C., MYERS, P.S. and UYEHARA, O.A. (1962)
"Gas temperatures during compression in motored and fixed diesel engines." S.A.E. Trans., Vol. 70, pp. 136-145.

97. TSAO, K.C. and WU, S.M. (1966)
"On the mathematical model of motored compression temperature." S.A.E. Paper No. 650453.

98. VOINOV, A.N., SKORODELOV, D.I. and SOKOLOV, F.P. (1964) "Temperature and pressure dependence of retarded ignition of hydrocarbon-air mixtures during adiabatic compression." Kinetikia-i-kataliz, Vol. 5, No. 3. pp. 388-398. (In Russian).

99. VOINOV, A.N. and SKORODELOV, D.I. (1967) "Study on the development of preflame processes and ignition of hydrocarbons of various structures. - (i) Induction periods of ignition and cold flames as functions of compression temperature and pressure." Kinetika-i-Kataliz, Vol. 8, No. 2, pp. 252-260. (In Russian).

100. VOINOV, A.N. and SKORODELOV, D.I. (1967) "A study of the characteristics of the development of pre-ignition processes and the combustion of hydrocarbons of different structure. - (ii) The intensity of the cool-flame stage." Kinetika-i-Kataliz, Vol. 8, No. 3, pp. 493-505.

101. WALCUTT, C., MASON, J.M. and RIFKIN, E.B. (1954) "Effect of preflame oxidation reactions on engine knock." Ind. and Eng. Chem., Vol. 46, p. 1029.

102. WALCUTT, C. and RIFKIN, E.G. (1951) "Precombustion reactions in an engine." Ind. Engg. Chem., Vol. 43, No. 12, pp. 2844-2849.

103. WATSON, H.C.W. (1968) "Experimental and analytical studies of the compression -ignition of fuel-oxidant mixtures." Ph.D. Thesis, London University, June 1968.

104. WHITEHOUSE, N.D., STOTTER, A., GOUDIE, G.O. and PRENTICE, B.W. (1962) "Method of predicting some aspects of performance of a diesel engine using a digital computer." Proc. I. Mech. E. Vol. 176, No. 9, p. 195-217.

105. WITZKY, J.E. and CLARK JR., J.M. (1968) "Stratification and combustion in reciprocating engines." A.S.M.E. Paper 68-DGP-4.

106. YANTOVSKII, S.A. (1964) "Two-stage combustion of explosive mixtures - (i) The temperature zones of ignition in heptane-air mixtures at pressures over 1 atm." Kinetika-i-Kataliz, Vol. 5, No. 1, pp. 34-39 (In Russian).

107. YANTOVSKII, S.A. (1964) "Two-stage combustion of explosive mixtures. - (ii) Intensity of the first- and second-phase ignition of heptane with air at pressures higher than atmospheric." Kinetika-i-Kataliz, Vol. 5, No. 3, pp. 399-406 (In Russian).

108. YANTOVSKII, S.A. (1966)
"Two-stage combustion of explosive mixtures. - (iii) Kinetic zones of autoignition of iso-octane-air mixtures under high pressures." Kinetika-i-Kataliz, Vol. 7, No. 1, pp. 21-26. (In Russian).

109. YANTOVSKII, S.A. (1967)
"Two-stage combustion of explosive mixtures. - (iv) Rate of pressure rise during the cold flame stage of combustion of binary iso-octane-n-Heptane mixtures in air." Kinetika-i-Kataliz, Vol. 8, No. 3, pp. 506-511. (In Russian).

A P P E N D I X XIII

PUBLICATIONS

1. KARIM, G.A., KHAN, M.O. and MOORE, N.P.W. (1970)
"Gross Chemical Kinetics from Motored Piston Engines". Paper No. 700060 in the press for SAE Annual Meeting, Detroit, Jan. 1970.

2. KARIM, G.A. and KHAN, M.O. (1969)
"The determination of gross chemical kinetic data for the combustion of common fuels using a motored piston engine." J. Inst. Fuel, Vol.42, No. 340, p. 340.

3. KARIM, G.A. and KHAN, M.O. (1968)
"Examination of effective rates of combustion heat release in a dual-fuel engine." J. Mech. Eng. Sc., Vol. 10, No. 1, p. 13.

Reprinted from the JOURNAL OF THE INSTITUTE OF FUEL, *May*, 1969.

G. A. KARIM, Ph.D., D.I.C., C.Eng., M.I.Mech.E.,* and M. O. KHAN, M.Sc.(Eng.), D.I.C., G.I.Mech.E., A.M.Inst.F.†

The determination of gross chemical kinetic data for the combustion of common fuels using a motored-piston engine

The authors describe a method of obtaining gross kinetic data of the combustion of common fuels on the basis of combustion heat release pattern derived from a knowledge of initial conditions of the reacting charge and its pressure and density-time variations in a motored auto-igniting engine. The procedure adopted is largely dependent on the accurate provision of these input data and on the detailed knowledge of the thermodynamic and transport properties of the working system. The computer programme developed for the purpose incorporated iterative smoothing of experimental data scatter and accounted for dissociation, variability of thermodynamic and transport properties of the working system, and for heat loss to the surrounding walls. The apparatus and the experimental, analytical, and computational techniques developed, are described. An illustration is then presented for the kinetic data of the combustion of propane in air.

1. Nomenclature

$\bar{C}_p$	Specific heat of charge at constant pressure
E	Activation energy of a chemical reaction
H_T	Heat of combustion of fuel at temperature T
i	Oxygen to fuel stoichiometric mass ratio
J	Mechanical equivalent of heat
K	Reaction rate constant
m	Mass of the charge
m_f	Relative mass of the charge
m_f'''	Fuel conversion rate per unit time and volume of the mixture
p	Cylinder charge pressure
$\dot{q}$	Rate of net heat release per unit time
$\dot{Q}_{HT}'''$	Rate of heat transfer per unit area and time
R	Universal gas constant
Re	Reynolds Number
V	Cylinder volume
ρ	Charge density
$\bar{\gamma}$	Specific heats ratio $\left(\frac{\bar{C}_p}{\bar{C}_v}\right)$
θ	Crank rotation

Subscripts

b	Burnt fraction
f	Fuel
o	Initial conditions at the beginning of compression
ox	Oxygen

2. Introduction

In most practical combustion systems it is seldom that only physical processes exercise overall control and hence any attempt to present the combustion processes entirely on thermodynamic bases has only limited application. Therefore, in order to provide a rational basis for the prediction of the gross behaviour of a combustion system, kinetic data are needed. Only in a few instances of practical engineering importance does the reaction process proceed in a single step from fuel and oxidant to combustion products. The conversion of reactants into the products proceeds usually through a number of intermediate steps. Our present knowledge of chemical kinetics does not permit us to present a reliable detailed kinetic scheme for the reaction of common fuels and a resort to overall-chemical kinetics is inevitable at this stage, excepting a few cases such as hydrogen–oxygen mixtures. The overall reaction rate may be represented adequately for some of the common hydro-carbons by the following form of single step reaction:

$$\dot{m}_f''' = K(m_f)^a\,(m_o)^b\,\rho^{(a+b)}\,e^{-E/RT} \quad . \quad . \quad (1)$$

This simplified rate ($\dot{m}_f'''$) implies that it is a function of the concentrations of fuel (m_f) and oxygen (m_o) and an exponential relationship with respect to temperature (T) which is commonly known as being of the Arrhenius form. The extent of agreement of actual experimental results with this assumption will be expected to apply only over a limited range of operating conditions. The success of overall mechanisms suggests that it is a reaction step that controls the overall conversion rate and at the same time bears some quantitative relationship to the major constituents. Such a controlling step does vary from one fuel to another and depends on the temperature and concentration ranges.

Most of the established methods for deriving kinetic data experimentally, such as optical studies of flames, shock-tubes, steady-flow reactors, and well-stirred reactors deal with the combustion processes in situations far removed from that prevailing in actual devices, such as the internal-combustion engine. Moreover, the available overall kinetic data in the literature exhibit considerable quantitative variation thus rendering their application full of uncertainty. The present paper describes the use of a motored engine for the determination of relatively reliable kinetic data as a function of temperature for a range of fuel-air mixtures involving common fuels. The apparatus used and the experimental and analytical techniques developed are relatively simple, but require the use of fast computers.

3. Apparatus

A C.F.R. variable-compression ratio engine was modified so that gaseous fuels could be introduced and metered accurately using chocked-nozzle meters. The air flow was measured using a viscous-flow meter. Fig. 1 shows a schematic diagram of the layout of the apparatus employed.

The engine was motored at a constant speed of 900 r.p.m. and the jacket water temperature was maintained at 100°C. The mixture strength was controlled mainly by varying the fuel supply while the mixture temperature was adjusted, so that auto-ignition can take place at/or around the point of maximum piston travel without the provision of a deliberate source of ignition.

The accurate measurements of pressure development inside the cylinder during the compression, combustion and expansion stages is essential for a reliable analysis and a piezo-electric pressure transducer was used for this purpose. It was flush-mounted into the combustion chamber and a silicon asbestos disc was used as a shield for the elimination of inaccuracies caused by the sensitivity of the diaphragm to hot combustion products. The

*Formerly Department of Mechanical Engineering, Imperial College; now Department of Mechanical Engineering, The University of Calgary, Calgary, Alberta, Canada.
†Department of Mechanical Engineering, Imperial College of Science and Technology, London.

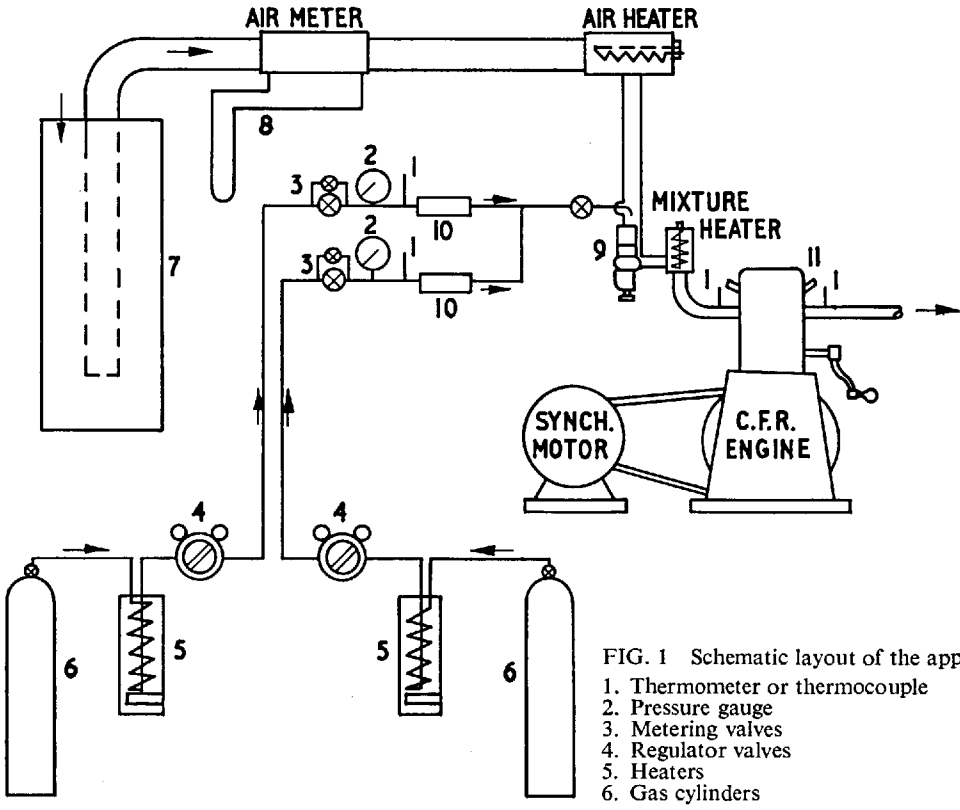


FIG. 1 Schematic layout of the apparatus employed.

1. Thermometer or thermocouple
2. Pressure gauge
3. Metering valves
4. Regulator valves
5. Heaters
6. Gas cylinders
7. Air tank
8. Manometer
9. Carburettor
10. Choked nozzle meter
11. Pressure transducer

transducer used was specially compensated for transverse vibrations. This proved to be of particular value when dealing with auto-ignition and the consequent structural vibrations which otherwise impose inaccuracies on the transducer. The linearity of the transducer was found to be exceptionally good over a wide range after both static and dynamic calibrations *in situ*. Extreme care was exercised by reading the magnified pressure records by a specially made digitalizer.

4. The calculation of effective rates of combustion heat release from pressure-time development records

It is possible, from the observation of the pressure-time development of reacting homogeneous charge in a cylinder controlled by a moving piston, for the overall effective reaction rate of the system to be calculated.[1] Normally, the charge density–time variation is controlled by the engine assembly. The problem of determining the gross heat release was idealized to the extent that the cylinder charge was assumed to be homogeneous. Moreover, the energy as a result of combustion was assumed to be released throughout the entire charge at all stages of the working cycle. The application of the first law of thermodynamics to the cylinder charge over an infinitesimally small increment of time, as shown in Appendix 1, led to the following working equation:

$$\dot{q} = \frac{\bar{\gamma}P}{J(\bar{\gamma}-1)}\frac{dV}{d\theta} + \frac{V}{J(\bar{\gamma}-1)}\frac{dP}{d\theta} \quad . \qquad (2)$$

where $\dot{q}$ is the net heat release rate, P cylinder pressure, V cylinder volume, θ crank angle, t time and $\bar{\gamma}$ is the ratio of specific heats of the charge at time t.

An account for any heat loss or gain to the system per unit area could be made with reference to a generalized correlation for heat transfer proposed by Annand,[2] following a survey of heat transfer literature, of the type:

$$\dot{Q}_{HT}'' = a\frac{k}{D}(\bar{R}e)^b(T - Tw) + c(T^4 - Rw^4) \qquad (3)$$

where a, b and c are constants, $\bar{R}e$ Reynolds number, T absolute charge temperature, T_w is the corresponding temperature of the wall, k thermal conductivity and D is the engine bore. It is normally up to the user to decide, from a knowledge of the relative importance of the radiative to convective heat transfer components and of the design of his engine, the appropriate values for these constants.

Another widely used correlation for the estimation of heat transfer is that due to Eichelberg,[2] which is the following:

$$\dot{Q}_{HT}''' = 8{\cdot}06 \times 10^{-5}(V_p)^{\frac{1}{3}}(PT)^{\frac{1}{2}}(T - T_w) \qquad (4)$$

where V_p is mean piston speed in ft/s and P is the pressure in atmospheres. This empirically-based formulation was adopted by many workers despite its short comings mainly because of its simple form.

When an account for heat transfer is made, the gross-heat release rate may be determined from a knowledge of θ, V, $\frac{dv}{d\theta}$ together with an assumed knowledge of the corresponding variation of the effective thermodynamic and transport properties of the charge.

With this in mind the following simplifying assumptions were incorporated in the computer programme developed for the solution of the problem:

(i) Purely for the evaluation of the thermodynamic properties of the system, the assumption was made that the extent of conversion of reactants to products at any instant was directly proportional to the energy released by combustion thus far.

(ii) The reaction was homogeneous with no effective temperature or pressure gradients within the charge.

(iii) The effects of leakage and residuals, unless otherwise stated, were negligible.

(iv) The charge behaves as an ideal gas.

(v) The rate of heat transfer when accounted for, followed either Eichelberg's or Annand's formulations. The working surface temperatures were known and remained unaltered throughout the cycle.

(vi) The reactants and products were assumed to be in

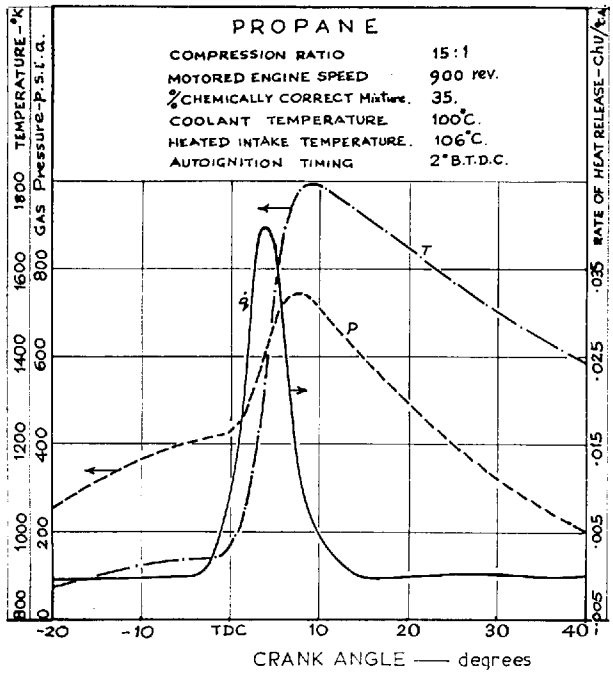


FIG. 2 Variation of effective rate of heat release, mean gas temperature and pressure during the cycle.

an equilibrium state corresponding to the instantaneous temperature and pressure of the system.

(vii) The presence of residuals were accounted for, if found necessary.

A computer programme embodying ten subroutines was developed in Fortran IV for an IBM 7094 Computer,[1] to carry out the necessary calculations. A subroutine was provided for the smoothing of experimental cylinder pressure input data. Then smoothing of data was found to be necessary in view of the errors involved in the processing of pressure-time records and the sensitivity of the calculated heat release rate to any variations in the pressure values.

The mean cylinder charge temperature was calculated on the basis of the smoothed pressure values and cylinder volume employing the ideal gas relationship. When combustion was taking place, the cylinder charge was assumed initially for a small increment of crank angle rotation, to be the products of complete combustion. This assumption is then modified iteratively to account for dissociation and variable specific heats[2] employing special subroutines. The extent of consideration of dissociation could be varied depending on the accuracy required and the temperature of the charge. Dissociation could be ignored, for example, when the molar fraction of the dissociated species fell well below a certain specified percentage of their respective parent products. This procedure could be improved upon, if need be, by the facility of repeating the calculations on the assumption of finite rate of conversion of the reactants to products in a manner depending on the reaction rate. This later procedure may be a little lengthy but was desirable in applications where heat was released gradually over a wide range of crank rotation, such as with slow reacting mixtures.

The net heat release over the small increment of crank angle $\Delta\theta$, was calculated using equation (1) and thermodynamic properties defined as polynominals in temperature based on data reported in the JANAF tables.[3] The associated heat transfer was then calculated by a subroutine based on Annand's formulation of equation (3).

Facilities were provided for the computation of the transport properties of the cylinder charge for any temperature together with the computation of heat transfer coefficient, if need be, on the basis of Eichelberg's formulation of equation (4). The extent of heat transfer was then calculated taking into consideration the working temperature of the cylinder head and liner and that of the piston together with their respective areas.

The gross heat release was then found by the summation of the net heat release rate and that of heat loss. The cumulative heat release was computed by progressive numerical integration employing Simpson's rule.

An iterative execution of the above calculations over consecutive small increments of crank angle rotation was then carried out. Fig. 2 shows a typical variation of the rate of heat release due to auto-ignition reactions and the calculated mean charge temperature derived on the basis of the observed pressure-time variation.

5. The derivation of overall combustion kinetics from the effective rates of combustion heat release

In view of the absence of any deliberate source of ignition and the operation with turbulent homogeneous mixtures it can be justifiably assumed that throughout the pre-ignition and post-ignition processes there are no temperature and pressure gradients within the charge. On this basis the gross reaction rate ($\dot{m}_f'''$) over any small increment of time Δt can be derived from the gross volumetric heat release values $\dot{q}'''$ according to the following relationship:

$$\dot{m}_f''' = \frac{\Delta q'''}{\Delta H_T} \quad . \quad . \quad . \quad (5)$$

where H_T is the heating values of the fuel at conditions corresponding to that at the temperature under consideration.

On this basis the instantaneous relative concentration of the fuel and oxidant will then be given by the following respective relationships:

$$m_f = m_{f,o} - \int_o^t \frac{\dot{m}_f'''}{\rho}\, dt \quad . \quad . \quad (6)$$

$$m_{ox} = m_{ox,o} - i \int_o^t \frac{\dot{m}_f'''}{\rho}\, dt \quad . \quad . \quad (7)$$

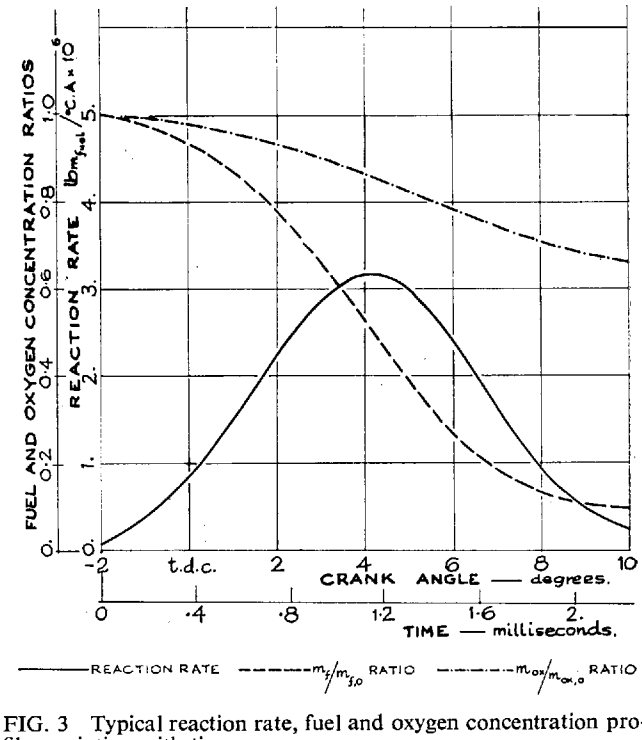


FIG. 3 Typical reaction rate, fuel and oxygen concentration profiles variation with time.

where $m_{f,o}$ and $m_{ox,o}$ are the initial mass concentrations of fuel and oxygen respectively.

Evidently the known instantaneous reaction rate values, concentration of fuel and oxygen, density and temperature could enable one, in theory, to find the statistical derivation of the best values of K, a, b and E, of equation (1), which satisfy the set of experimental data observed. This procedure, however, can be simplified by determining the K and E values for the reaction with assumed reaction order. Fig. 3 shows a typical set of derived data based on the heat release data of Fig. 2.

6. Some experimental results and discussion

When selecting experimental records for analysis only the records of cycles where combustion was achieved on or around the T.D.C. position were selected. Thus marginal auto-igniting cycles, which were irregular and sporadic, were eliminated. This approach resulted in reproducible experimental records. Normally the range of compression ratios employed was limited by the increased effect of residuals at low compression ratios. The extent of heating of the intake charge was such that regular auto-ignition was obtained.

The results from a series of tests involving propane–air mixtures over a range of mixture strength, initial temperature and compression ratio were analysed on the above basis. Purely for the purpose of the demonstration of the utility of this approach and for simplicity, a second order reaction was assumed, i.e. $a = b = 1$ in equation (1). Fig. 4 presents a superimposed record of the data derived from a range of auto-igniting cycles of propane–air mixtures. It can be seen that the experimental points obtained, despite the wide variation of initial conditions employed, do lie in a well-defined narrow band. Moreover, there seem to be two distinct temperature zones, namely, below and above 1 000°K. Such a tendency is fairly well known for many common fuels.[4] The two activation energy values derived from the slopes of the two parts of the curve are 8·0 K-cal/mole for the higher temperature range and 60·0 K-cal/mole for the lower temperature range. The latter value compares favourably with 64 K-cal/mole carefully derived by Miller[5] for propane. It is interesting to note that fitting a single straight line through experimental points can yield values for $\bar{E}$ ranging from 8 to 60 K-cal/mole, depending on the number of experimental points and the temperature range selected. This may partly explain the wide variation of activation energy values, $\bar{E}$, reported in the literature for propane.

The values as derived from Fig. 4 are relatively insensitive to errors in the measurement of the initial dynamic pressure at the beginning of compression or to the neglect of the variation of thermodynamic properties with temperature. Moreover, it has also been observed that a slight variation in the indices (a) or (b) of equation (1) does not alter the general tendency of the slope as shown in Fig. 4. Thus the procedure described can provide reasonably accurate values for the gross kinetic data of common fuels over a range of temperature and pressure similar to that in practical combustion systems.

7. Acknowledgment

One of the authors (M. O. Khan) thanks the Burmah Oil Company for a scholarship given to him while carrying out this investigation.

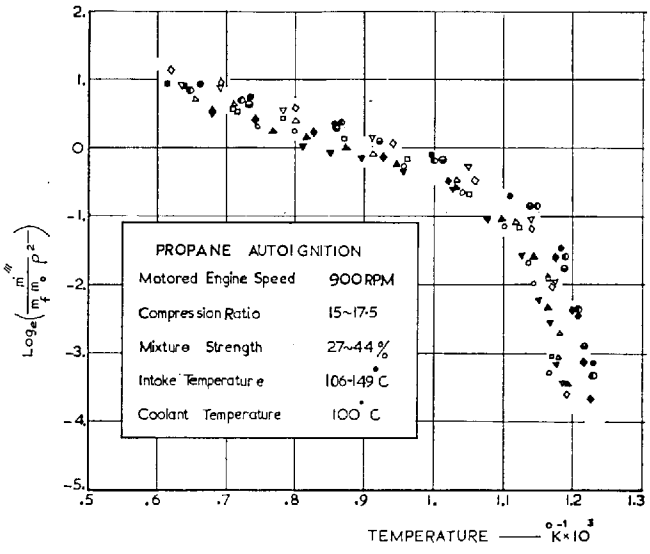


FIG. 4 Superimposed plots of normalized reaction rates plotted against the inverse of absolute temperature.

8. References

1. KARIM, G. A., and KHAN, M. O. A generalized computer programme for the determination of rate of heat release and heat transfer in reciprocating engines. Imperial College, Department of Mechanical Engineering Technical Note No. C/TN/4. Dec. 1967.
2. ANNAND, W. J. D. Heat transfer in the cylinders of reciprocating internal combustion engines. *Proc. Instn mech Engrs*, 1963, **177** (No. 36), 973.
3. J.A.N.A.F. Thermo-Chemical data tables. U.S. Dept. of Commerce, Washington, D.C., 1964.
4. SOKOLIK, A. S. Self-ignition, flame and detonation in gases. Translation into English from Russian by N. Kaner. Israel Program for Scientific Translation, Jerusalem, 1963.
5. MILLER, R. E. Some factors governing ignition delay of a gaseous fuel. VII Symposium on Combustion, 417, 1959.

Appendix 1. Derivation of rate of heat release equation

As the gaseous fuel is introduced with air in the motored engine the charge can be assumed to be homogeneous and with the combustion energy released throughout the charge. The application of the first law of thermodynamics to the system comprising the charge over a small increment of time Δt corresponding to a crank angle change $\Delta\theta$:

$$\Delta \text{ (energy released)} + \Delta \text{ (heat transfer in)} = \Delta \text{ (heat transfer out)} + \Delta \text{ (work out)} + \Delta \text{ (internal energy of the system)} \quad . \quad (7)$$

If ($\dot{q}$) is the net rate of heat release due to combustion then equation (1) becomes:

$$\dot{q}\Delta t = \text{(energy released)} + \text{(heat in} - \text{heat out)} \quad (8)$$

If the cylinder charge is assumed to be an ideal gas and the energy of the system is in the form of internal energy, then:

$$\dot{q}\Delta t = \frac{P\Delta V}{J} + m\bar{C}_v\,\Delta T \quad . \quad . \quad (9)$$

In the limit equation (9) becomes:

$$\dot{q} = \left(\frac{\bar{\gamma}P}{J(\bar{\gamma}-1)}\frac{dV}{d\theta} + \frac{V}{J(\bar{\gamma}-1)}\frac{dP}{d\theta}\right)\frac{d\theta}{dt} \quad . \quad (10)$$

(*Paper received* 19*th June*, 1968.)

Printed in England by Stephen Austin and Sons Ltd., Hertford.

EXAMINATION OF EFFECTIVE RATES OF COMBUSTION HEAT RELEASE IN A DUAL-FUEL ENGINE

By G. A. Karim*† and M. O. Khan*

The combustion processes in a dual-fuel engine are examined through the computation and analysis of effective rates of heat release. Methane was adopted as the primary fuel and the effect of deliberately introducing carbon dioxide along with the methane was also examined to simulate operation on methane sources containing carbon dioxide as a major contaminant. An examination of the various heat release records suggests that dual-fuel combustion generally appears to undergo two distinct phases. The first phase is associated mainly with the consumption of the pilot and some associated gaseous fuel, while the second phase is dependent on the concentrations and the quality of the gaseous fuel employed. Under light audible knock, the first phase gets prolonged and persists over a much longer period than under knock-free combustion. The rates of burning are excessively high and project well over the second phase. This is indirectly indicative of the auto-ignition nature of knock and the simultaneous rapid burning of the pilot together with a very substantial fraction of the gaseous charge.

INTRODUCTION

ANY EMPHASIS on the efficient utilization of gaseous fuels, whether from natural or industrial sources for power production in relatively small units, will focus attention on the dual-fuel engine and the limitations imposed by the associated combustion phenomena. These problems are mainly due to the poor utilization of the gaseous fuel at light load together with that of the loss of combustion control, commonly termed as the onset of knock which imposes a ceiling to the useful output of these engines.

Under dual-fuel operation the primary fuel is normally gaseous at atmospheric temperatures and pressures, and in four-stroke engines is usually inducted with the engine air charge. During the compression stroke at some point near to top-dead-centre position, a small charge of liquid fuel is injected through the conventional diesel fuel system to act as a source of ignition for the main charge.

Power output is controlled by changing the amount of the primary gaseous fuel added to the air, whilst the quantity of the pilot charge per injection is usually fixed for a given engine regardless of the engine output and normally contributes to less than 10 per cent of the total heat release at full load. Engines of this type are usually capable of operating in this manner or purely on the diesel principle. Such a system is assuming a particular significance with the increased exploitation of natural gas reserves in various parts of the globe and the prospects of increased availability of natural gas from sources located in and around the North Sea.

Although the nature of the limitations in such devices at light load associated with the use of lean gaseous fuel mixtures, and that of knock in the richer ones, has been the subject of several investigations, it is fair to say that the exact nature of the combustion processes in such a relatively complex system is far from being completely understood. With this in mind a continuing extensive study spanning a few years at Imperial College has been carried out. The present paper briefly summarizes the work undertaken as a part of this programme to examine the combustion processes in a dual-fuel engine through the computation and analysis of effective rates of heat release. This analysis infers that a gross characterization of the combustion process can be made by a consideration of the rate of energy release which manifests itself as a pressure change, with the assumption that such energy is released throughout the charge. This technique is relatively well known and has been successfully adopted in the study of combustion processes in diesel engines. Original studies by Austen and Lyn (1)‡ and later by Gee and Karim (2) have demonstrated that heat-release analysis is one of the most effective means of interpreting

The MS. of this paper was first received at the Institution on 28th February 1967 and in its revised form, as accepted by the Council for publication, on 6th June 1967. 33

* *Mechanical Engineering Department, Imperial College of Science and Technology, London.*
† *Associate Member of the Institution.*

‡ *References are given in Appendix 2.*

indirectly the combustion processes in compression-ignition engines. No efforts, however, seem to have been directed in the past towards employing such an analysis to the more complex combustion processes of the dual-fuel type.

The present work was undertaken making use of the technique of heat-release analysis to establish better understanding and solutions to the problems related to dual-fuel combustion. Methane was adopted as the primary fuel in view of its extensive abundance in natural gas resources, its comparatively high caloric value on mass basis, among other common fuels, and the large information available about its combustion characteristics in general and in dual-fuel engines in particular. The effect of deliberately introducing carbon dioxide along with methane was also examined to simulate operation on methane sources containing carbon dioxide as a major contaminant, as commonly is the case with sludge gas.

The rational computations of rates of heat release entail the evaluation of the thermodynamic properties of the reactants and their products with proper assessment of the effects of dissociation, the instantaneous pressure and volume of the cylinder and their variations with respect to time. Such elaborate calculations could effectively be undertaken only with the help of a high-speed digital computer. For this investigation a high-speed IBM 7090 digital computer was used.

Notation

$\bar{C}_p, \bar{C}_v$	Mean specific heats at constant pressure and volume correspondingly of the charge under conditions relating to T.
J	Mechanical equivalent of heat.
m	Mass of the charge.
p	Cylinder pressure.
$\dot{q}$	The net rate of heat release due to combustion per unit time.
T	Charge mean absolute temperature.
t	Time.
v	Cylinder volume.
$\bar{\gamma}$	$\bar{C}_p/\bar{C}_v$.
θ	Crank angle, degrees.

APPARATUS

The engine used was a single-cylinder direct-injection type of $4\frac{1}{8}$-in bore and 6-in stroke. The engine was coupled to an electric dynamometer which permitted the engine to be motored to assess mechanical losses. A special fuel pump was fitted for this investigation capable of metering accurately very small quantities of pilot fuel and of varying the point of injection whenever required.

The air drawn in by the engine was metered by a viscous-flow air meter, while the gaseous fuels were metered by choked nozzles, and were added to the inlet air at the throat of a mixing venturi located upstream of the inlet valve. The high-pressure gas supply, after passing through a pressure regulator, was led to the engine through a system of control valves and expanded through the choked nozzles for flow rate measurement. Two metering circuits were provided. One of these was used for the measurement of carbon-dioxide flow rate.

Engine cylinder pressure development was indicated by a piezoelectric transducer, while the movement of the injector needle was established by a photoelectric transducer. Signals at known crank angle intervals were generated by an electromagnetic transducer close to the engine flywheel. These signals were displayed on a Tektronix oscilloscope and particular attention was paid to the reduction of sources of error in the measurement of pressure. Moreover, in order to find out a mean cycle for analysis, five separate records were obtained at random. Such records indicated very little combustion irregularity. Knocking was reckoned by virtue of its audibility in the form of engine roughness, which was also manifested by the presence of high-frequency oscillations on the pressure traces as indicated by Karim and co-workers (3).

CALCULATION OF THE EFFECTIVE RATES OF HEAT RELEASE FROM PRESSURE–TIME DEVELOPMENT RECORDS

Due to the complex and relatively unknown nature of the combustion processes in a dual-fuel engine, the problem of determining the gross heat-release rate was idealized to the extent that the cylinder charge was assumed to be homogeneous. Moreover, the energy was assumed to be released as a result of combustion throughout the entire charge at all stages of the working cycle. The application of the first law of thermodynamics to the cylinder charge over an infinitesimally small increment of time will lead, as shown in Appendix 1, to the following equation:

$$\dot{q} = \left\{ \frac{\bar{\gamma}}{\bar{\gamma}-1} \frac{P}{J} \frac{\mathrm{d}V}{\mathrm{d}\theta} + \frac{V}{\bar{\gamma}-1} \frac{1}{J} \frac{\mathrm{d}P}{\mathrm{d}\theta} \right\} \frac{\mathrm{d}\theta}{\mathrm{d}t}$$

where $\dot{q}$ is the net heat-release rate.

Should an account for any heat loss or gain to the system be made then the gross heat-release rate may be determined from a knowledge of P, V, $\mathrm{d}V/\mathrm{d}\theta$, $\mathrm{d}P/\mathrm{d}\theta$, and $\mathrm{d}\theta/\mathrm{d}t$ together with an appropriate knowledge as to the corresponding variation of the effective thermodynamic properties of the charge. With this in mind the following simplifying assumptions were incorporated in the computer program used for this investigation:

(1) Purely for evaluation of the thermodynamic properties of the system, combustion was assumed to take place simultaneously after a significant pressure rise from the normal compression curve.

(2) The reaction was homogeneous with no effective temperature, concentration or pressure gradients within the charge.

(3) The effects of leakage and residual gases were neglected.

(4) The charge behaves as an ideal gas throughout the process.

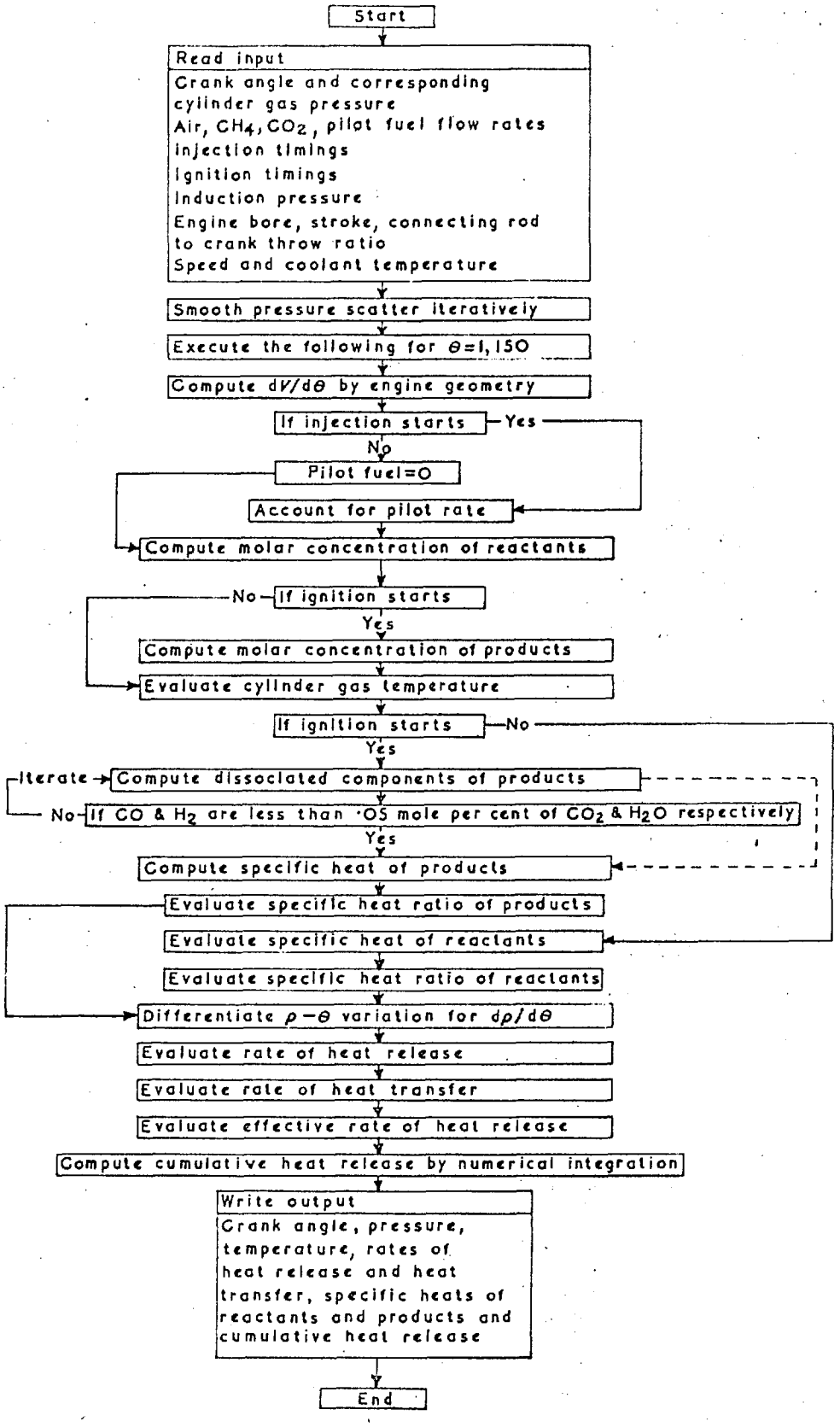


Fig. 1. *Schematic procedure adopted in the digital calculation of a dual-fuel engine cycle*

(5) The rate of heat transfer, when accounted for, follows the Eichelberg formula (5), and that the cylinder wall temperature remained constant throughout the working cycle.

Fig. 1 shows schematically the procedure adopted in the digital calculation of a dual-fuel engine cycle which is also workable for a diesel cycle. In fact the computer program developed treats the diesel cycle as a special case of the dual-fuel operation. The calculations are based on the observed pressure-development history during a working cycle. The analysis of pressure variation with respect to each degree of crank rotation was carried out after projecting the 35 mm camera records on a calibrated screen. These values were then smoothed out after subsequent replotting to reduce the extent of any imminent scatter. The data thus obtained were then smoothed further by computer methods incorporating the principle of fourth differences. This procedure was resorted to to ensure satisfactory smoothing because of the extreme sensitivity of heat-release values to any pressure variations particularly with small heat-release values. Moreover, extreme care was taken to ensure maximum accuracy of pressure measurements by a suitable choice of transducer and electronic equipment.

The thermodynamic properties required for the calculations such as C_p and K_p were computed on the basis of their temperature dependence and in accordance with JANAF thermo-chemical data (4).

EXPERIMENTAL RESULTS

A very large number of pressure–time development records were obtained over a wide range of operating conditions of the dual-fuel engine. These records were then processed and analysed using computer methods in the manner outlined earlier. Fig. 2 is a typical example of the diagrams constructed directly from computer results. These were the cylinder pressure, the rate of pressure rise, the rate of heat release, cumulative heat release and cylinder gas temperature. These values were calculated with reference to each degree of crank rotation, over a normal range of 150° of crank rotation and the charge drawn in per cycle. Figs 3 and 4 show a cross-section of superimposed rate of heat-release diagrams obtained with two ranges of pilot fuel for different concentrations of the primary fuel methane in the intake mixture under constant pilot injection timing and engine speed. The concentrations of the primary gas covered the wide range from the case when just sufficient power is produced to overcome the motoring losses to that when knock was detected.

Fig. 5 presents the cumulative heat release of the rates shown in Fig. 3, while Figs 6 and 7 present the heat-release rate development records for a given feed concentration of methane when employing a range of pilot fuelling rates. Figs 8 and 9 depict the effects of carbon dioxide addition to the methane covering a wide range of carbon dioxide addition from pure methane operation under knocking conditions to that of almost 50 per cent of the methane used and where it can be readily seen that under knocking conditions the presence of carbon dioxide smooths operation appreciably.

The introduction of carbon dioxide in the intake charge under normal operating conditions generally protracted the delay period and reduced the overall rate of burning and power output. For the same mixture strength it usually produced exhaust gas temperatures higher than that obtained with no such addition denoting much slower combustion. The presence of carbon dioxide with fuel will normally affect the final products of combustion mainly through the water–gas shift reaction.

DISCUSSION

The small negative heat release that can be observed on all the records prior to ignition can be the direct consequence of the inadequacy of the Eichelberg formulation (5) to account fully for the heat losses during the last stages of compression. We found, however, that other heat loss formulation such as that of Annand (5) produced only a slight improvement to an extent that it was considered unnecessary to depart from the simple Eichelberg formulation in the present analysis. Moreover, the relative contribution to the apparent heat release of the processes of pilot fuel evaporation and the pre-ignition processes cannot be adequately established. Such uncertainties are to be expected in an overall analysis of this nature (1).

In contrast to 'pure' diesel combustion, the pilot when injected in a dual-fuel engine normally undergoes more delayed ignition. This is believed to be mainly due to the influence of the gaseous fuel present in the charge (3). A protracted delay should enable the pilot injection to be completed with substantial evaporation and mixing of the pilot vapour with the gaseous fuel charge, before ignition begins. Once ignition commences some of the gaseous fuel present in the vicinity of the multiple ignition sources will inevitably be involved. It will make a substantial contribution to the initial part of the heat release if the charge is rich enough to be beyond the effective lower flammability limit of the mixture.

An examination of the various heat release records, of which Figs 2–6 represent a typical cross-section, suggests that dual-fuel combustion generally appears to undergo two distinct phases. The first phase is associated mainly with the consumption of the pilot and some associated gaseous fuel, while the second phase is almost entirely dependent on the concentration and the quality of the gaseous fuel employed.

It can be seen, for example, from Fig. 3 that for a given pilot fuelling rate, the initial rate of heat release remains almost the same as the gaseous fuel concentration is increased. This similarity of the initial rates of heat release tends to keep close together the cumulative heat-release diagrams around the t.d.c. point and marked changes become apparent only over the later part of the cycle. As the main fuelling rate was increased further, there occurred

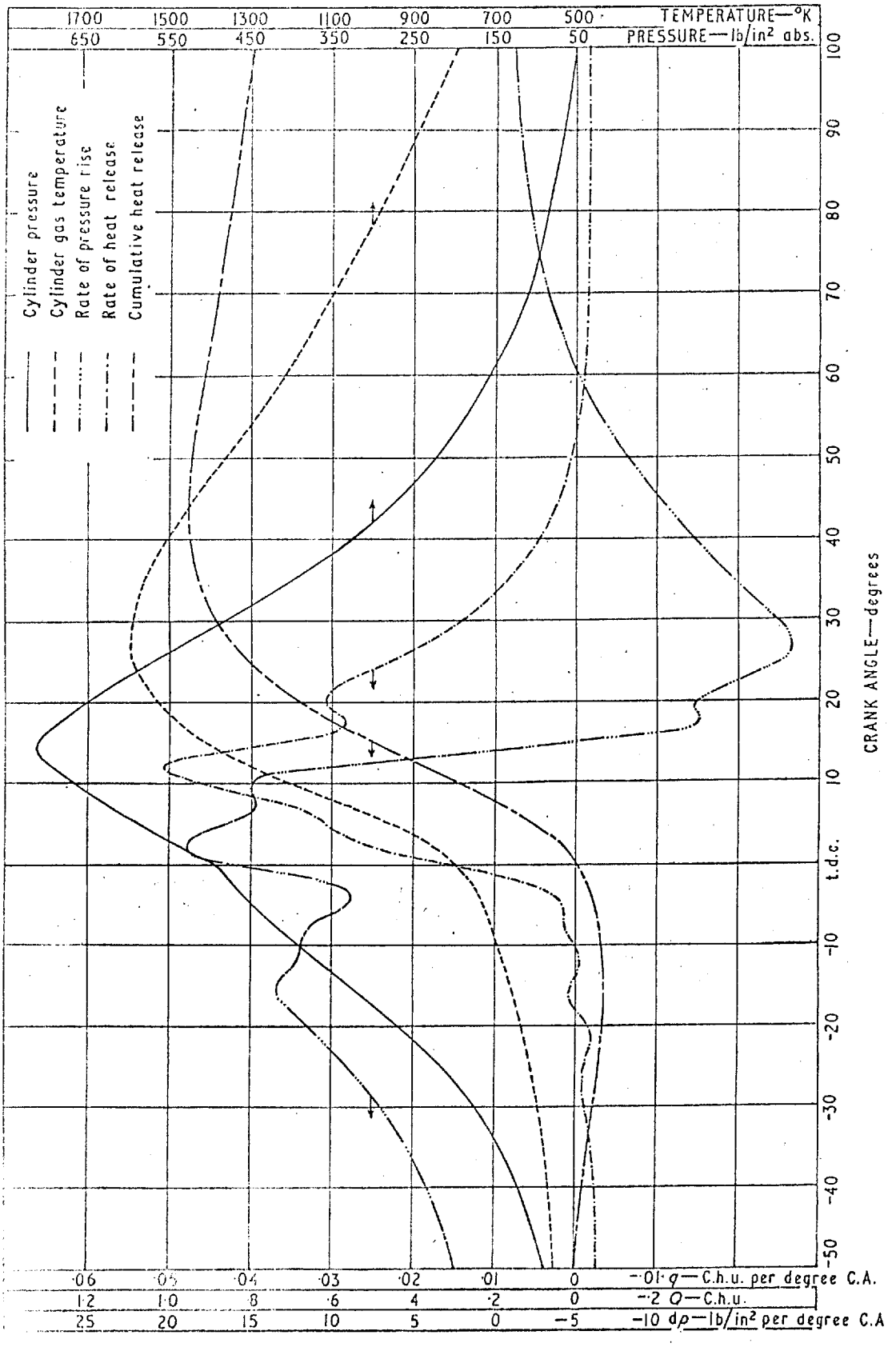
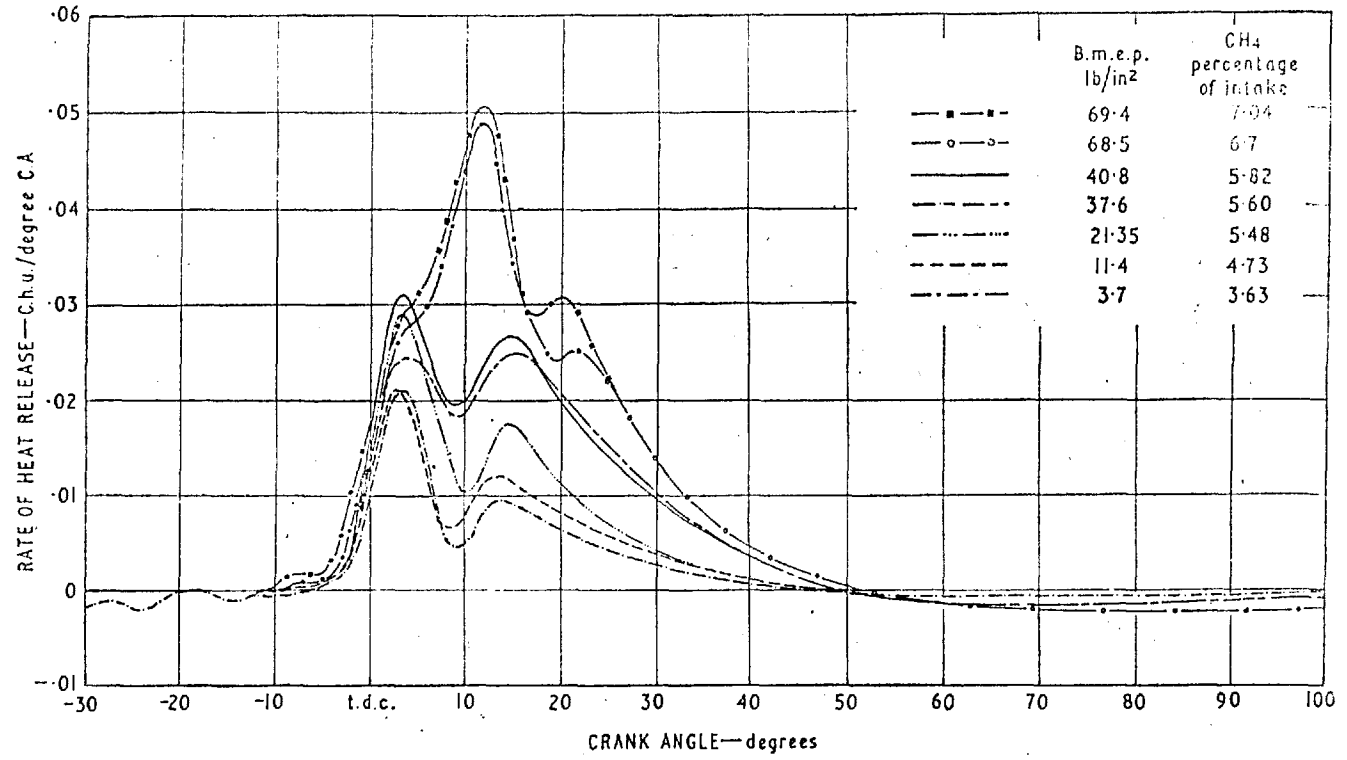


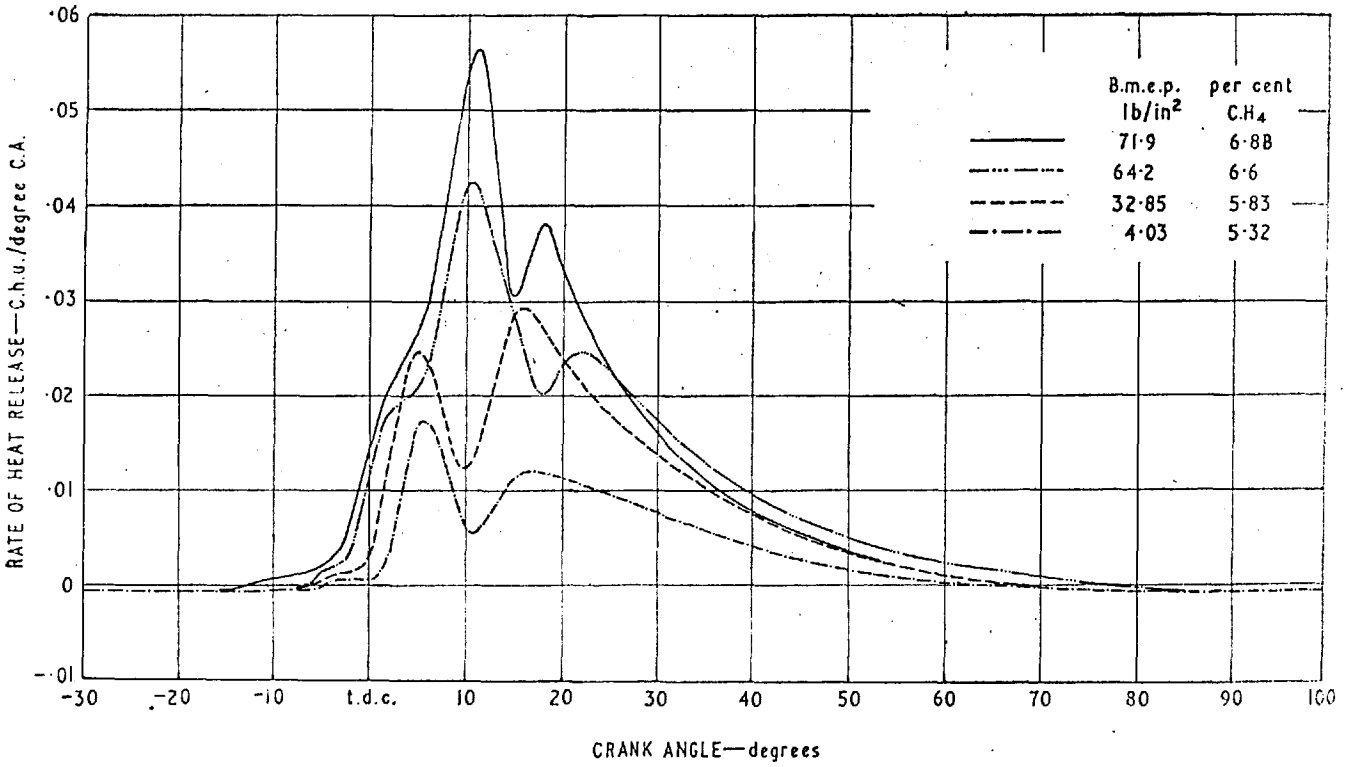
Fig. 2. *Typical output plots from the IBM 7090 computer*

Percentage CH_4 in intake 7·04; percentage chemically correct mixture 77·5; b.m.e.p. 69·4 lb/in²; speed 1000 rev/min; pilot fuel 0·5 lb/h; injection timing 20° before top dead centre; coolant outlet temperature 70°C.



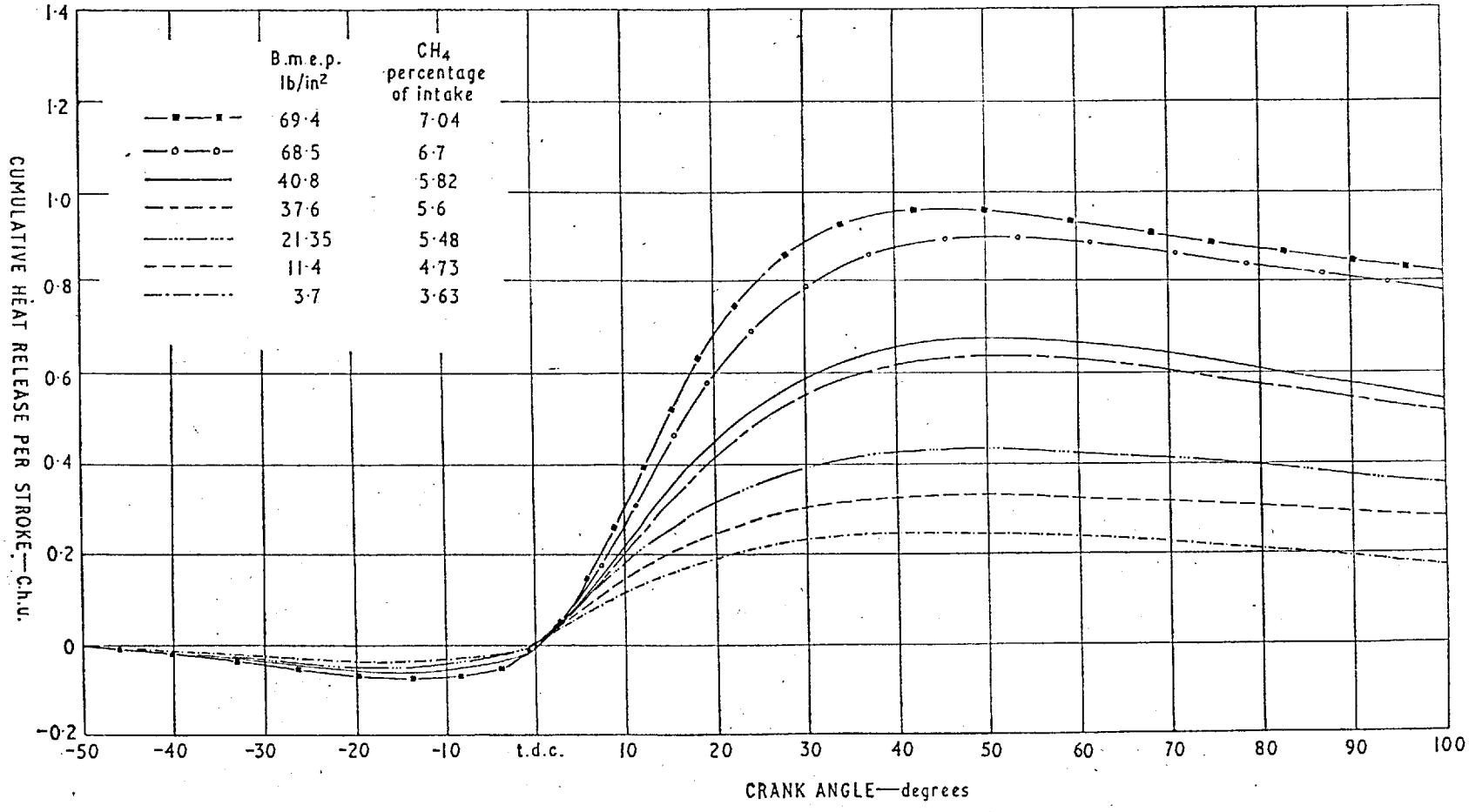
Pilot fuel 0·5 lb/h; injection timing 20° before top dead centre; injection duration 11° C.A.; speed 1000 rev/min; coolant outlet temperature 70°C.

Fig. 3. *Analysis of heat release variations for a dual-fuel engine: effects of varying gaseous fuel concentrations with 0·5 lb/h pilot quantity*



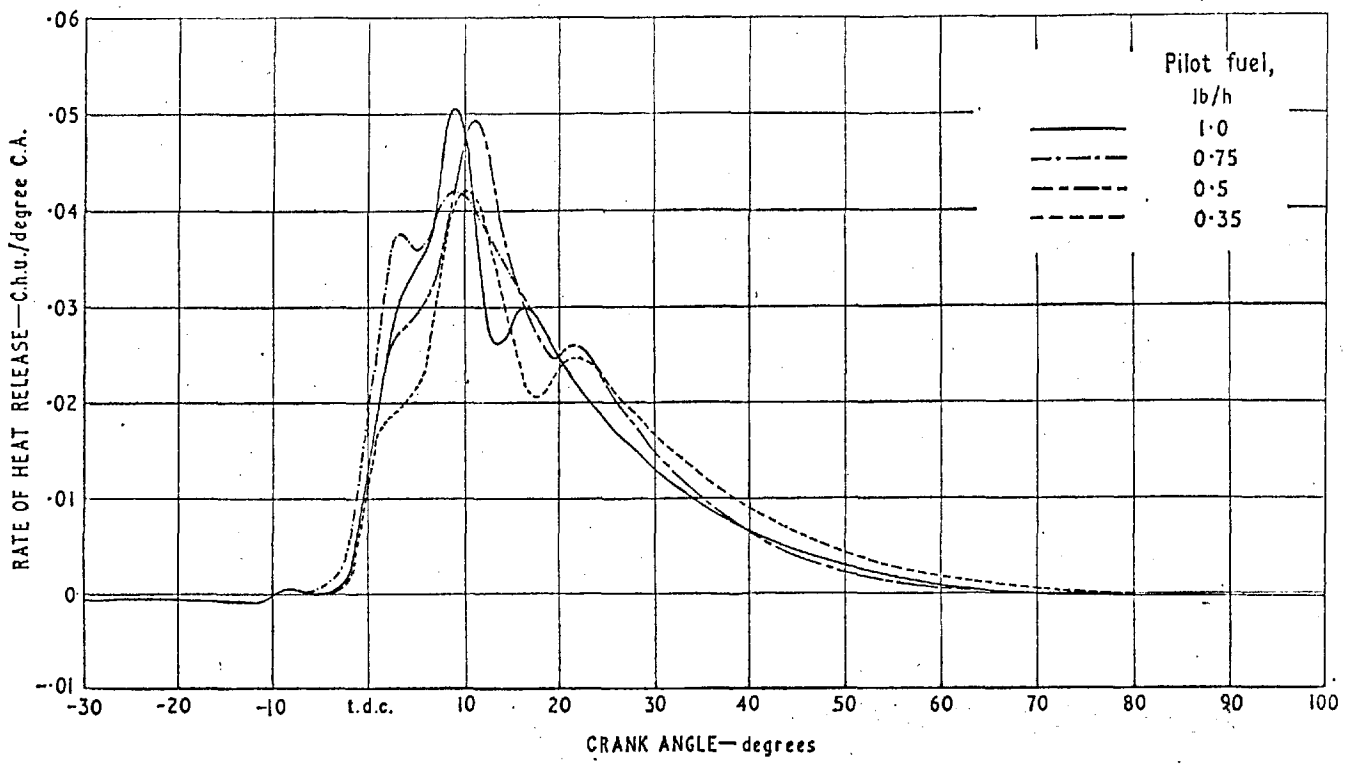
Pilot fuel 0·35 lb/h; injection timing 20° before top dead centre; injection duration 20° C.A.; speed 1000 rev/min; coolant outlet temperature 70°C.

Fig. 4. *Analysis of heat release variations for a dual-fuel engine: effects of varying gaseous fuel concentrations with 0·35 lb/h pilot quantity*



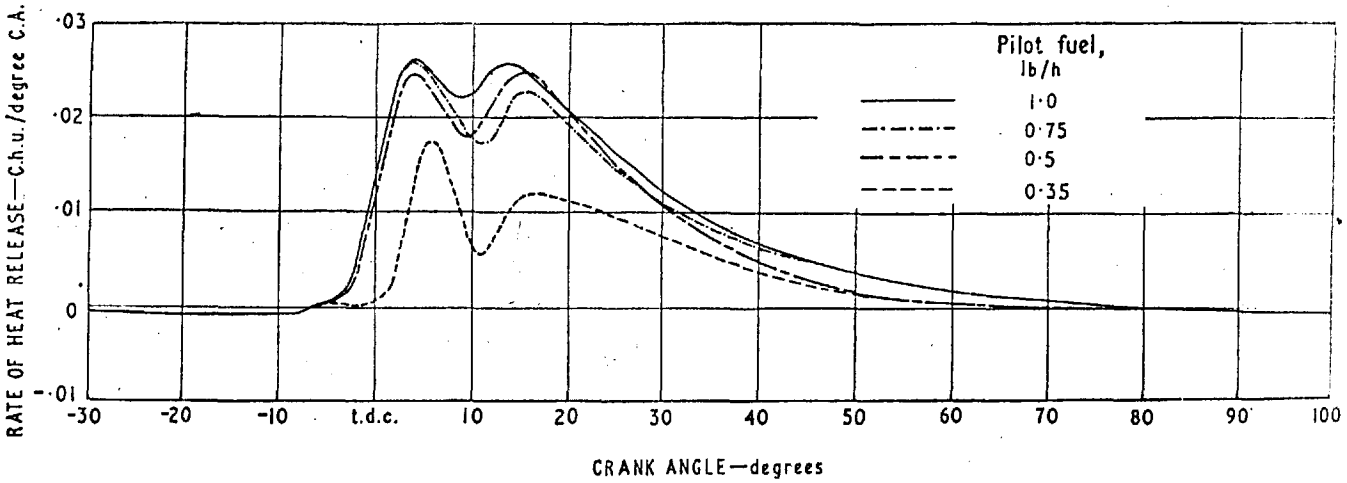
Pilot fuel 0·5 lb/h; injection timing 20° before top dead centre; injection duration 11° C.A.; speed 1000 rev/min; coolant outlet temperature 70°C.

Fig. 5. *Cumulative heat release records: effects of varying gaseous fuel concentrations with 0·5 lb/h pilot quantity*



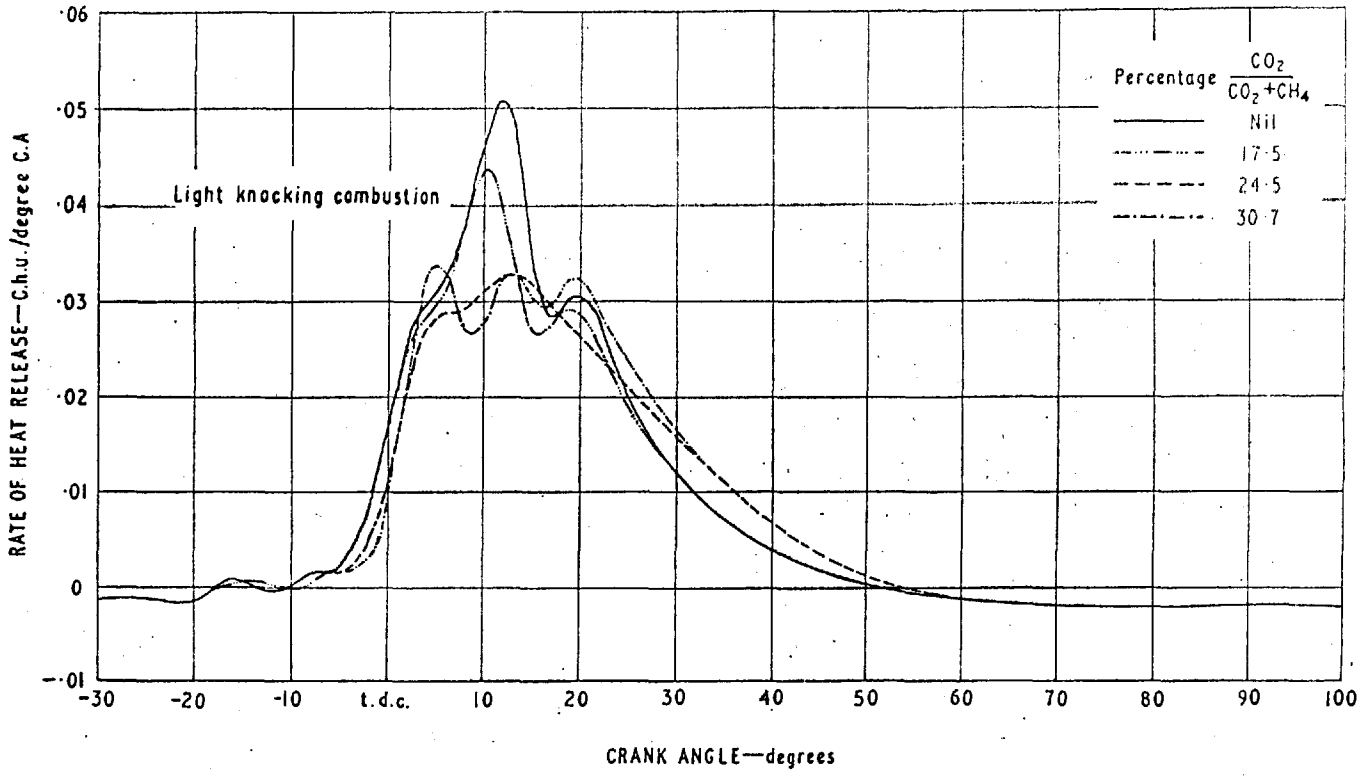
Percentage CH_4 in intake 6·74; injection timing 20° before top dead centre; speed 1000 rev/min; coolant outlet temperature 70°C.

Fig. 6. *Analysis of heat release variations for a dual-fuel engine: effects of varying pilot fuel quantity with a constant methane concentration in the intake charge*



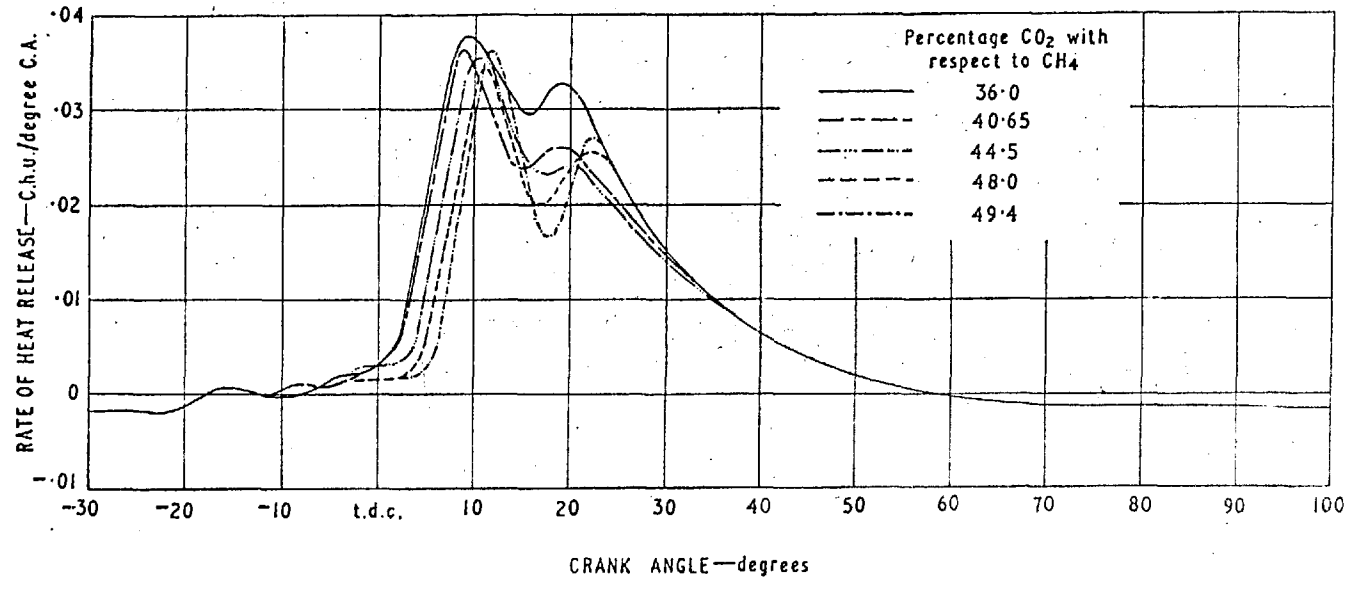
Injection timing 20° before top dead centre; percentage CH_4 in intake 5·65; speed 1000 rev/min.

Fig. 7. *Analysis of heat release variations for a dual-fuel engine: effects of varying pilot fuel quantity with a constant methane concentration in the intake charge*



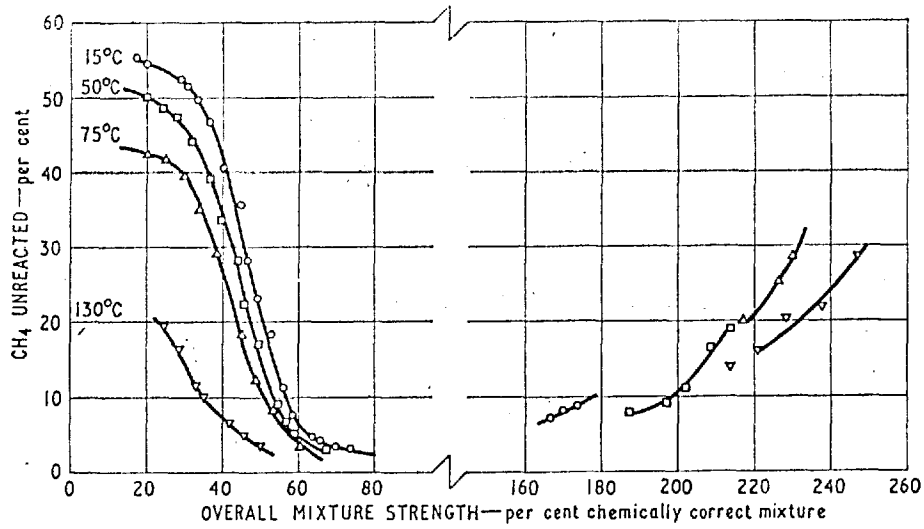
Average mixture strength 78·8 per cent; percentage CH_4 in intake 7·1; pilot fuel 0·5 lb/h; speed 1000 rev/min; injection timing 20° before top dead centre.

Fig. 8. *Analysis of heat release variations for a dual-fuel engine: effects of varying CO_2 concentrations in the intake for a constant average charge mixture strength and a constant pilot quantity*



Percentage chemically correct mixture 78·4; percentage CH_4 in intake 7·1; pilot fuel 0·5 lb/h; injection timing 20° before top dead centre; speed 1000 rev/min.

Fig. 9. *Analysis of heat release variations for a dual-fuel engine: effects of varying CO_2 concentrations in the intake for a constant average charge mixture strength and a constant pilot quantity*



Pilot fuel quantity 0·5 lb/h; injection timing 18° before top dead centre.

Fig. 10. *Percentage of unreacted methane as a function of overall mixture strength for different intake charge temperatures*

a proportionate increase in the heat release during the first phase indicating that a larger proportion of the charge was involved. When the pilot fuel is increased, however, for a constant addition of gaseous fuel, the initial rates of heat release show a marked difference accordingly. It is interesting to note that under relatively lean mixtures the heat release during the first phase corresponds approximately to the heat value of the pilot fuel itself, confirming that the first phase is associated primarily with pilot combustion. It can also be seen from Fig. 5 that, even under rather lean mixture conditions, the first phase shows the tendency to project over the second as the pilot is increased. When the premixed gaseous fuel mixture is rich enough, the increased pilot fuelling rate will incorporate in the combustion a substantial amount of the gaseous charge which would eventually give rise to a considerable increase in the rate of heat release and may lead to knock.

The ignition characteristics of the pilot fuel are pronouncedly affected by the gaseous charge under small pilot fuelling rates. This is clear in Fig. 4, where a reduction of the gaseous fuel in the charge shows substantial delay in the initial release of heat. The ignition delay was observed to diminish slightly with richer gaseous fuel concentrations suggesting that the gaseous fuel takes an active part in the pre-ignition reactions of the pilot itself.

Under the conditions of light audible knock, the initial rates of combustion remain the same except that the first stage of combustion becomes prolonged and persists over a much longer period than the knock-free combustion. The rates of burning are excessively high and project well over the second phase. This is indirectly indicative of the autoignition nature of knock (3) and the simultaneous rapid burning of the pilot together with a very substantial fraction of the gaseous charge.

The second phase of dual-fuel combustion with normal knock-free operation is indicative of a much slower burning. Under lean mixture strengths and with a relatively small pilot it separates out from the first phase indicating unfavourable conditions for the rapid consumption of the gaseous fuel which contributes only marginally to the heat released. A substantial percentage of the fuel as shown in Fig. 10 will appear in the exhaust having undergone no change.(6).

The analyses of heat release rates with carbon dioxide addition indicated that although the initial rates of burning remained substantially the same, the peaks of the heat release rates of both the stages and the total heat released were reduced. The flame was thus restricted to pass through the charge rendering an increased amount of the fuel to escape without being fully consumed.

The knocking intensity was found to be reduced with the increased addition of carbon dioxide. For the case presented in Fig. 8, knock was found to persist until a concentration of about 25 per cent carbon dioxide was reached in the fuel. Under these conditions the two phases of combustion merged together thus exhibiting a more progressive burning and producing a heat release rate variation with time in a way not unlike that of the familiar spark-ignition engine.

It has been demonstrated that the approach of heat release analysis, when adopted with the aid of high-speed computer techniques, can offer a useful means for the interpretation of the overall nature of some of the complex combustion phenomena in dual-fuel engines. The evidence obtained is in general agreement with and supplements the relatively limited experimental evidence available as to the nature of the combustion processes in these devices (3) (7).

CONCLUSIONS

An examination of various heat release records suggests that the dual-fuel combustion generally appears to undergo two distinct phases. The first phase is associated mainly with the consumption of the pilot liquid fuel together with a part of the gaseous fuel, depending on the concentration of the latter in the main charge. The second phase, which tends to be much slower, is dependent mainly on the concentrations and quality of the gaseous fuel employed. The heat release analyses of lean mixture operation indicate in conformity with other experimental evidence that the comparatively inefficient combustion under such conditions is due mainly to the inability of the gaseous charge to supplement effectively the heat release of the first phase. The use of larger pilots or higher initial temperatures can reduce this tendency.

Under light audible knock the two phases of combustion merge together and produce excessive rates of heat release which persist over a much longer period than that under knock-free operation. This is indirectly indicative of the auto-ignition nature of knock and the simultaneous burning of the pilot together with a substantial fraction of the gaseous charge.

ACKNOWLEDGEMENT

One of the authors (M.O.K.) thanks the Burmah Oil Co. for a scholarship which was given to him while carrying out this investigation.

APPENDIX 1

DERIVATION OF RATE OF HEAT-RELEASE EQUATION

Considering the cylinder charge to be homogeneous and with the combustion energy released throughout the entire charge, the application of the first law of thermodynamics to the system comprising the charge over a small increment of time Δt, corresponding to a crank angle charge $\Delta\theta$:

$$\Delta(\text{energy released}) + \Delta(\text{heat transfer in}) = \Delta(\text{heat transfer out}) + \Delta(\text{work out}) + \Delta(\text{internal energy of the system}) \quad (1)$$

If $(\dot{q})$ is the net rate of heat release due to combustion, then equation (1) becomes:

$$\dot{q}\,\Delta t = \Delta[(\text{energy released}) + (\text{heat in}) - (\text{heat out})] \quad (2)$$

If the cylinder charge is assumed to be an ideal gas and the energy of the system is in the form of internal energy, then:

$$\dot{q}\,\Delta t = \frac{P\,\Delta V}{J} + mC_v\,\Delta T \quad . \quad . \quad . \quad . \quad (3)$$

Equation (3) may be written as

$$\dot{q}\,\Delta t = \frac{\bar{\gamma}P\,\Delta V + V\,\Delta P}{J(\bar{\gamma}-1)} \quad . \quad . \quad . \quad . \quad (4)$$

In the limit equation (4) becomes:

$$\dot{q} = \left\{\frac{\bar{\gamma}P}{J(\bar{\gamma}-1)}\frac{\mathrm{d}V}{\mathrm{d}\theta} + \frac{V}{J(\bar{\gamma}-1)}\frac{\mathrm{d}P}{\mathrm{d}\theta}\right\}\frac{\mathrm{d}\theta}{\mathrm{d}t}$$

The computer program

A generalized program equally workable for diesel or dual-fuel operation was devised, for IBM 7090 in Fortran IV, which required the following information as input:

(1) Engine dimensions such as bore, stroke, and connecting rod to crank throw ratio.

(2) Temperature and pressure of the cylinder contents at the start of compression.

(3) The manually smoothed values of cylinder gas pressures and the corresponding crank rotation in degrees.

(4) The flow rates of air, gaseous fuel, pilot fuel, and CO_2 introduced per stroke.

(5) The cylinder walls' temperature.

(6) The pilot fuel injection timings and the starting point of combustion. The rate of injection of pilot fuel into the cylinder was distributed equally per degree of crank rotation over the period of injection, and the thermodynamic properties were modified accordingly. The pilot fuel was assumed to be adequately represented by cetane.

The computer was required to execute the following steps:

(1) Iterative smoothing of the pressure–time development input data on the principle of fourth differences.

(2) Cylinder volume and its rate of change with respect to crank angle as dictated by the geometric configuration of the engine.

(3) Differentiation of pressure–crank angle input data for the rate of pressure change.

(4) Evaluation of cylinder gas temperature employing ideal gas relationship.

(5) Estimation of mean thermodynamic properties of cylinder contents on the basis of their temperature dependence, in conformity with JANAF thermo-chemical data (4).

(6) Accounting for dissociated components and iterative modification of their parent species thereafter in accordance with a digital procedure established by Edson *et al.* (8).

(7) Application of first law of thermodynamics as per this section of this Appendix and evaluation of effective rates of heat release.

(8) Calculation of rates of heat transfer in accordance with Eichelberg's formula or other correlations (5).

(9) Calculation of gross rates of heat release after accounting for heat transfer.

(10) Summation of rates of heat release to evaluate cumulative heat release.

All the above steps, shown schematically in Fig. 1, were executed by the computer within 0·2 min for a complete cycle.

APPENDIX 2

REFERENCES

(1) AUSTEN, A. E. W. and LYN, W. T. 'Relation between fuel injection and heat release in a direct-injection engine and the nature of combustion processes', *Proc. Auto. Div. Instn mech. Engrs* 1960–61 (No. 1), 47.

(2) GEE, D. E. and KARIM, G. A. 'Heat release in a compression-ignition engine', *Engineer, Lond.* 1966 (September).

(3) KARIM, G. A., KLAT, S. R. and MOORE, N. P. W. 'Knock in dual-fuel engines', *Proc. Instn mech. Engrs* 1966–67 181 (Pt 1, No. 20), 453.

(4) 'JANAF thermo-chemical data tables', U.S. Department of Commerce, Washington, D.C., 1964.

(5) ANNAND, W. J. 'Heat transfer in the cylinders of reciprocating internal cumbustion engines', *Proc. Instn mech. Engrs* 1963 177 (No. 36), 973.

(6) AZZOUZ, D. 'Some studies of combustion processes in dual-fuel engines', M.Sc. thesis, London University, 1965.

(7) MOORE, N. P. W. and MITCHELL, R. W. S. 'Combustion in dual-fuel engines', *Proc. Joint Conf. Combustion* 1955, 300 (Instn Mech. Engrs, London, and Am. Soc. Mech. Engrs, New York).

(8) EDSON, M. H. 'The influence of compression ratio and dissociation on ideal Otto cycle engine thermal efficiency', *Progress in Technology* 1964 7 (Soc. Automot. Engrs).